# CHANGES IN BURST AND SPIKE PROPAGATION ASSOCIATED WITH GAP JUNCTION FORMATION IN MYOMETRIUM AT PARTURITION

BY

© STEVEN MICHAEL MILLER, B.Sc., M.Sc.

A Thesis

Submitted to the School of Graduate Studies

in Partial Fulfilment of the Requirements

for the Degree

Doctor of Philosophy

McMaster University

November, 1986

# BURST AND SPIKE PROPAGATION IN MYOMETRIUM

DOCTOR OF PHILOSOPHY (1986) McMASTER UNIVERSITY

(Medical Sciences) Hamilton, Ontario

TITLE: Changes in Burst and Spike Propagation Associated With Gap Junction Formation in Myometrium at Parturition

AUTHOR: Steven Michael Miller, B.Sc. (University of Washington)

M.Sc. (University of British Columbia)

SUPERVISOR: Professor Robert E. Garfield

NUMBER OF PAGES: xiv, 306

## ABSTRACT

The factors regulating the uterus in the maintenance of pregnancy and the onset of labour are two important and unresolved problems in uterine physiology. At term, specialized cell-to-cell contacts, gap junctions, appear between the uterine smooth muscle cells. These structures are thought to allow direct passage of ions and small molecules between cells, thus their formation between uterine smooth muscle cells at term may promote propagation of electrical activity and development of contractile synchrony in the uterine wall, necessary for expulsion of the fetus(es). The objective of this thesis was to examine the possible functional role of gap junction formation in the myometrium at parturition. The hypothesis that gap junction formation results in improved electrical coupling at parturition was tested by measuring the spread of electrical excitation (which gives an indirect measure of cell-to-cell electrical coupling) in the myometrium before (i.e. at preterm) and after (i.e. at delivery) in situ gap junction formation. Some of the tissues used for these experiments were examined by thin section electron microscopy for the presence of gap junctions.

Spontaneous burst discharges propagated over the entire recording distance of 15 mm in the longitudinal axis of the myometrium at both preterm and at parturition. Burst activity at both times showed some of the characteristics of a system of coupled relaxation oscillators. However, individual spikes within the bursts propagated further and with

higher velocity in this axis at parturition as compared to at preterm. In the transverse axis of the myometrium, both bursts and individual spikes within bursts propagated over longer distances at parturition than before. Propagation in this axis at parturition appeared to require an intact or undamaged circular muscle layer.

Analysis of the propagation of spikes evoked by electrical stimulation confirmed that spike propagation was improved (e.g. higher velocity and longer distance of spread) in both the longitudinal and transverse axes of the myometrium at parturition.

Electron microscopy studies confirmed that gap junctions were present in large numbers between uterine smooth muscle cells during parturition and were absent or present in very small numbers at preterm. Thus, improved propagation of electrical discharges was associated with an increase in gap junction contact between myometrial cells. These results are consistent with the hypothesis that gap junction formation at term results in improved electrical coupling of uterine smooth muscle cells.

## Acknowledgements

I am grateful to my supervisor, Dr. Bob Garfield, and co-supervisor, Dr. Ed Daniel, for suggesting this work, and for their guidance and encouragement. I thank the other members of my advisory committee, Dr. Grant Smith and Dr. Jan Huizinga, for their advice.

Dr. S.N. Reddy developed the computer programs that I used for signal analysis, and he also suggested some of the experiments, and offered some good advice.

James Yu was helpful at many times with the "electronics", and he also showed me the finer points of computers.

To Vic Kachura, your help in preparing slides and prints for the various meetings and conferences (always done at the last possible moment), is appreciated. Thanks for being a good friend over the years.

Debbie Merrett and Elizabeth Welsh helped with the sectioning of tissues and quantification for gap junctions. Deb, your considerable skill in printing thesis figures was very helpful and is greatly appreciated.

Finally, to Joy and Megan, thanks for giving up all those evenings and weekends that I needed to complete this degree. Joy, I am grateful for your efforts at home and at work which enabled me to realize my ambition.

TABLE OF CONTENTS

## LIST OF TABLES

## LIST OF FIGURES

## KNOWLEDGE

"To know that we know what we know, and that we do not know what we do not know, that is true knowledge".

-Confucius-

# CHAPTER 1

## General Introduction and Review of the Literature

## GENERAL INTRODUCTION

The onset and progress of labour is promoted by electrical and mechanical synchrony in the uterine wall. How this synchronous activity is generated at term, and conversely how it is suppressed before term, are two of the most important and controversial questions of uterine physiology (Mosler, 1968; Csapo, 1981). Propagation of action potentials from pacemaker to nonpacemaker areas is widely held to be the basis of synchronous uterine activity. Garfield and Daniel and associates (see Garfield et al., 1977; 1978) recently discovered a morphological change in the uterine smooth muscle cells at the end of gestation that may be involved in the synchronization of uterine contractions, and hence be essential for normal labour and delivery. They noted the presence of gap junction contacts between uterine smooth muscle cells only immediately before, during and immediately after delivery (and their absence at any other time in pregnancy). Gap junctions are generally thought to provide low-resistance pathways to current flow between many cell types and their presence in the myometrium at term should promote action potential propagation and hence labour. Conversely, their absence at preterm should restrain propagation and thus prevent synchronous uterine activity and labour. Recent studies (Sims et al., 1982; Cole et al., 1985) have shown an improved cell-to-cell coupling associated with increased gap junction number in rat myometrium at parturition. However, there have been no detailed studies on whether action potential propagation in the pregnant uterus is improved at delivery when gap junctions develop, despite the significance of this information regarding the control of uterine function.

The objectives for this thesis were to assess the propagation of action potentials and action potential bursts in the longitudinal and circular axes of the rat myometrium, before (e.g. at preterm) and after (e.g. at delivery) gap junction formation, to help determine the role of gap junctions in synchronizing uterine contractions at parturition. This study should also help elucidate the structural basis (i.e. gap junctions or other structures) for electrical coupling within and between the muscle layers of the myometrium. Furthermore, by comparing propagation in the myometrium at preterm (gestation day 17), when plasma progesterone levels are high, and during delivery, when progesterone levels are low, important information about the nature of the so-called "progesterone block" of impulse propagation (see Csapo, 1962; 1971) can be obtained.

## REVIEW OF THE LITERATURE

### A) General Anatomy of the Uterus and Ultrastructure of the Myometrium

#### General Anatomy

The rat possesses a duplex type of uterus, meaning that the uterus is composed of two separated tubes or horns which, although fused externally at the cervical end, open independently into the vagina via two separate cervical canals (Mossman, 1977). Each uterine horn is a tubular organ whose wall is composed of three coats: 1) an inner mucosa, the endometrium, lining the uterine cavity, 2) a surrounding muscle coat, the myometrium, and 3) a thin external serous coat, the serosa (Ham and Cormack, 1979). The endometrium consists mainly of columnar epithelium (a single layer of which lines the uterine lumen),

an underlying connective tissue stroma which is continuous with the myometrium, and various coiled tubular glands which are embedded in the stroma and open into the uterine lumen. The myometrium consists of two distinct smooth muscle layers with vascular zones in between: an outer longitudinal layer and inner circular layer, whose muscle fibers are arranged respectively, parallel to or concentrically around the long axis of the uterus (Finn and Porter, 1975). Contraction of the longitudinal muscle would thus tend to shorten the uterus while contraction of the circular layer would constrict the uterine lumen. In some regions of the myometrium, the longitudinal and circular fibers may intertwine (Finn and Porter, 1975; Garfield, 1979). This arrangement would allow spread of contractions from one muscle layer to the other.

Structure of the Myometrium

The longitudinal and circular layers of the myometrium are composed of smooth muscle cells embedded in a connective tissue network and arranged into bundles of approximately 10 to 50 partially overlapping cells, their orientation being in the direction of the bundle's long axis (Melton and Saldivar, 1964; Burnstock, 1970; Garfield and Daniel, 1974; Garfield and Somlyo, 1985). Based on studies in other smooth muscles, it is estimated that each cell within the bundle is surrounded by 10 to 12 others (Burnstock, 1970). Collagen fibrils, elastic fibers and fibroblasts constitute the connective tissue network supporting the smooth muscle cells (Silva, 1967). Between the muscle bundles there exists a similar connective tissue network, containing in addition, macrophages, mast cells, lymphocytes, blood vessels and nerves (Silva, 1967; Csapo, 1981).

Muscle bundles are inter-connected: those of the longitudinal myometrium interlace to form a network while those of the circular myometrium appear less clearly arranged (Silva, 1967; Garfield and Somlyo, 1985).

Transmission of force along the length of the muscle results from transmission of tension (generated by individual muscle cells) from cell to cell (within a bundle and/or between connecting bundles) and from cell to the connective tissue stroma (Gabella, 1979; 1984a).

The individual uterine smooth muscle cells are the physiological units of contractile function (Csapo, 1971; Marshall, 1974). They are small, spindle-shaped cells of dimensions 2-10 $\mu$m wide and 50-800 $\mu$m long, these dimensions varying with the functional state of the uterus (Marshall, 1974; Finn and Porter, 1975). During pregnancy the myometrial muscle cells increase both in number and size, the largest cells being observed at term when they may become 3-5 times as long as at the time of implantation (Abe, 1970; Shoenberg, 1977). The combined actions of the steroid hormones estrogen and progesterone, and chronic stretch are thought to be the regulating factors (Carsten, 1968; Marshall, 1974). In the rat uterus hyperplasia is thought to occur very early in pregnancy (before implantation of the blastocyst), the cells subsequently increasing in size but not absolute number as pregnancy progresses (Marshall, 1974; Hamoir, 1977). However, measurement of the DNA content in rat myometrium in more recent studies suggested an equal contribution of both hyperplasia and hypertrophy to the growth of the myometrium during pregnancy (Afting and Elce, 1978).

Innervation of the Myometrium

The rat uterus receives a dual adrenergic and cholinergic innervation entering the uterine wall directly or along the uterine arteries and veins to positions in the connective tissue between the inner and outer muscle layers (Adham and Schenk, 1969; Marshall, 1970; Bell, 1972; Papka et al., 1985). Branches from these nerve trunks form plexuses in the myometrium and endometrium from

which fibers then arise to innervate bundles of uterine smooth muscle as well as smooth muscle in the walls of blood vessels (Silva, 1967; Adham and Schenk, 1969; Papka et al., 1985). Using histofluorescence and acetylcholinesterase histochemical techniques, it has been shown that in pregnant and nonpregnant rat uterus the adrenergic fibers predominantly innervate blood vessels while the cholinergic fibers innervate both uterine smooth muscle and blood vessels (Hervonen et al., 1973; Singh et al., 1985). This finding is in agreement with an earlier study of myometrial nerves in the rat in which nerves were classified as either adrenergic or cholinergic according to the types (i.e. granular versus agranular) of intra-axonal vesicles (Silva, 1967) but disagrees with the studies of Adham and Schenk (1969) and Papka et al. (1985) who found an equal density of adrenergic and cholinergic nerves to the nonvascular smooth muscle in the rat myometrium. All of the above results must be accepted with caution, however, as acetylcholinesterase reactivity can be present in noradrenergic as well as cholinergic neurons (Wallace, 1981), and it is certain that nerve types cannot be identified ultrastructurally by the appearance (granular versus agranular) of their intra-axonal vesicles (Gabella, 1981). The density of adrenergic and cholinergic innervation varies in different parts of the rat uterus, the utero-tubal junction and cervical end being more richly innervated than the uterine body (Adham and Schenk, 1969; Bell, 1972; Marshall, 1973; Singh et al., 1985). In addition to adrenergic and cholinergic nerve fibers, peptidergic (viz. vasoactive intestinal polypeptide, substance P, neuropeptide Y and gastrin-releasing peptide) nerves have recently been found in the nonpregnant rat uterus (Larsson et al., 1977; Alm et al., 1980; Ottesen et al., 1981; Stjernquist et al., 1983; 1986; Gu et al., 1984; Papka et al., 1985). Their

distribution, like that of the adrenergic and cholinergic nerves, is to the vascular and nonvascular smooth musculature of the myometrium, except for gastrin-releasing peptide (GRP) nerve fibers which are exclusively associated with the nonvascular smooth muscle. They (with the exception of GRP) are also similarly more numerous in the cervix than in the uterine horns (but see Papka et al., 1985).

Concerning the nerve-muscle relationship, there is a low density of nerves to myometrial smooth muscle cells as compared to richly innervated smooth muscles such as rat vas deferens and urinary bladder. In the latter, each muscle cell is closely related to a nerve axon whereas in the myometrium nerve fibers are related to groups or bundles of muscle cells (Silva, 1967; Adham and Schenk, 1969; Marshall, 1970; 1973). Few detailed studies have been concerned with the ultrastructure of the nerve fiber-muscle cell relationship in the myometrium (Marshall, 1981). However, Silva (1967) studied this relationship in nonpregnant and pregnant rat myometrium and found bundles of nonmyelinated nerves situated at varying distances (the closest at about 1000 nm) from myometrial muscle cells while others lay free in the connective tissue between muscle bundles. Although the anatomical ends or terminal varicosities of the axons occasionally come into close apposition (approx. 20 nm in rat myometrium) to the uterine smooth muscle cells (Silva, 1967), the cell membranes of neither have the specialized structure found at the motor end plates of skeletal muscle (Marshall, 1970; 1973; Garfield and Somlyo, 1985). During the latter half of pregnancy, in response to hormones and chronic stretch, the adrenergic and cholinergic nerve endings in the uterine corpus (but not the utero-tubal junction or cervical end) degenerate resulting in a functional denervation of

the myometrium (Sjoberg, 1968; Thorbert, 1979; Marshall, 1981; Thorburn et al., 1984; Arkinstall and Jones, 1985; Singh et al., 1985; Sigger et al., 1986). Although not studied in detail in the pregnant rat uterus, peptidergic (vasoactive intestinal polypeptide and neuropeptide Y) nerves decrease in number during pregnancy, at least in the human (Ottesen et al., 1982) and guinea pig (Fried et al., 1985) uterus.

The exact role of nerves in uterine function is not fully understood in the rat or any other species (Marshall, 1973; 1981; Ottesen et al., 1981), but it has been suggested that they might control myometrial contractility, blood flow, secretion or sensation (Alm et al., 1980; Ottesen et al., 1981; Garfield and Somlyo, 1985). While it is unlikely that autonomic nerves affect impulse propagation in the myometrium (Finn and Porter, 1975; Thorburn et al., 1984), they may play a physiological role in local nervous control of uterine contractility (Marshall, 1981; Ottesen et al., 1981; Singh et al., 1985).

Ultrastructure of Myometrial Smooth Muscle Cells

Ultrastructurally, the uterine smooth muscle cell is similar to other smooth muscle types (Finn and Porter, 1975; Shoenberg, 1977) and contains a single elongated nucleus (usually located centrally) as well as myofilaments, microtubules and various organelles in the cytoplasm. The myofilaments are arranged into bundles (fibrils) running parallel (Gabella, 1979) or obliquely (Shoenberg, 1977) to the cell axis and include thick (myosin) and thin (actin) contractile filaments as well as intermediate (desmin) filaments, the latter perhaps providing a supporting framework for the contractile filaments (Shoenberg, 1977; Gabella, 1981). In uterine smooth muscle the content of the contractile filaments is influenced by ovarian hormones and chronic stretch

(Csapo, 1971). During pregnancy, for example, the actomyosin concentration (mg per gram muscle) of the uterus increases by approximately two-fold at term allowing an increased working capacity of the myometrium (Csapo, 1950; Michael and Schofield, 1969; Csapo, 1971; Hamoir, 1977). This increase in contractile protein, combined with an increase in muscle length (due to increasing stretch on the uterus) allows the uterus to develop maximum tension at term (Marshall, 1974). The organelles in the cytoplasm include mitochondria, golgi apparatus, lysosomes and sarcoplasmic reticulum. The latter is organized into a network of tubules and sacs consisting of both granular (rough) and agranular (smooth) reticulum in continuity which, at specialized regions (junctional sarcoplasmic reticulum), makes frequent close contact with the plasma membrane (Garfield and Somlyo, 1985). Surrounding the cytoplasm is a plasma membrane with numerous goblet-shaped invaginations called surface vesicles or caveolae. These are grouped in rows, two to four caveolae wide, parallel to the cell's long axis and account for about 30% of the cell surface area in some smooth muscles (Gabella, 1981; 1984b). However, their function in smooth muscle is obscure (Gabella, 1979; 1984b). Also prominent in the plasma membrane, (occupying 30-50 % of the cell surface in the middle portions of the cell) are dense bands which alternate with the longitudinal rows of caveolae (Gabella, 1979; 1981; 1984b). These electron-dense regions on the cytoplasmic side of the membrane, (which can extend for 1-2 $\mu$m along the cell length in visceral smooth muscle), are believed to be anchorage sites for the thin and perhaps intermediate filaments (Shoenberg, 1977; Gabella, 1979; 1981; 1984b). Their arrangement along the muscle cell surface allows for extensive cell shortening during contraction and for changes in shape of the cell profile (e.g. increased cellular diameter) to accomodate the

volume displaced by cell shortening (Fay et al., 1976; Gabella, 1979). Wherever dense bands are absent, protrusions of the membrane occur. A basal lamina (about 20 nm thick) coats the entire plasma membrane surface except at the level of the gap junctions and where stromal collagen fibrils or elastic fibers abut on the plasma membrane (Gabella, 1981; 1984b). Its function may be to provide a mechanical link for force transmission between the myofilaments and connective tissue stroma, via the plasma membrane (Gabella, 1984a; 1984b).

Cell-to-Cell Contacts Between Myometrial Smooth Muscle Cells

Over most of their surface, the smooth muscle cells within the muscle bundles comprising the contractile coats of most hollow organs are separated from their neighbours by a basement membrane-filled space of greater than 50 to 100 nm (Burnstock, 1970; Gabella, 1981). However, at selected points neighbouring smooth muscle cells come into closer apposition forming specialized contacts. In rat uterine smooth muscle four different types of cell-to-cell contacts have been described on the basis of their appearance in thin section electron micrographs: 1) intermediate contacts, 2) close contacts or simple appositions, 3) interdigitations and 4) nexuses or gap junctions (Bergman, 1968; Garfield and Daniel, 1974; Garfield et al., 1977, 1978; Garfield, 1985).

Intermediate contacts are areas where the plasma membranes of apposing cells run parallel, separated by an intercellular space of approximately 20-100 nm (Gabella, 1984b; Garfield, 1985). They are further characterized by a granular appearing central dense line in the intercellular space and an increased density in the subadjacent cytoplasms (Henderson, 1975; Gabella, 1984b). In late pregnant rat uterus these contacts are 0.3 to 0.5 $\mu$m in width and extremely long (5-10 $\mu$m), and are found more frequently in the longitudinal than in the circular muscle layer (Garfield and Daniel, 1974).

Regions in which the plasma membranes of adjacent cells run parallel separated by a space of approximately 10 nm and having no membrane specialization are called close contacts or simple appositions (Henderson, 1975). These contacts, approximately 0.5 μm in width with an intercellular space of 10 to 30 nm, are present in about equal numbers in the longitudinal and circular muscles of late pregnant rat uterus (Garfield and Daniel, 1974).

Interdigitations are projections of one cell into an invagination of another cell and usually end in a close contact but sometimes in a gap junction. They are more common in contracted as compared to relaxed tissues (Garfield and Daniel, 1974; Henderson, 1975; Garfield, 1985).

Gap junctions or nexuses, often seen on protrusions between smooth muscle cells, at the ends of interdigitations and sometimes on cytoplasmic extensions between the same cell (reflexive gap junction), are points of very close contact (2-3 nm space or gap) and specialized structure between apposing plasma membranes (Henderson, 1975; Gabella, 1984b; Garfield, 1985). In thin section electron micrographs they appear as five or seven lined structures or, when examined using freeze-fracture electron microscopy, as irregular rounded areas containing a few to hundreds of membrane particles (Henderson, 1975; Gabella, 1984b; Garfield, 1985). Extensive structural and biochemical studies of gap junctions in both excitable and nonexcitable tissues (vertebrate and invertebrate) revealed the following generalities which are also assumed for uterine and other smooth muscles (Henderson, 1975; Gabella, 1981; 1984b; Loewenstein, 1981; Larsen, 1983; Garfield, 1985; Revel et al., 1985). Gap junctions consist of discoid aggregations of two or three to many thousands of 6-10 nm particles spaced in varying patterns at center-to-center distances of

7-14 nm. Each particle (connexon) consists of 6 protein subunits (connexins), molecular weight of 26,000 to 30,000 per subunit, arranged in a circle around a central channel (1.5-2.0 nm in diameter).' The particles span the entire plasma membrane and protrude into the gap to abut with complementary particles on the juxtaposed membrane, forming aqueous channels (insulated from the extracellular space) connecting the cytoplasms of cells sharing junctions. They thus provide direct pathways for intercellular flow of ions and larger molecules (up to 1200 daltons) between cells. Recent results show that gap junctions isolated from term-pregnant rat uteri are structurally and biochemically similar to gap junctions from rat heart and liver (Zervos et al., 1985).

In pregnant rat myometrium, few or no gap junctions are present between smooth muscle cells until right before, during and just after parturition when they appear in relatively large numbers and approximately equal amounts in both longitudinal and circular muscle layers (Garfield et al., 1977; 1978; Puri and Garfield, 1982; Sims et al., 1982; Wathes and Porter, 1982; Saito et al., 1985). Gap junction size and the percentage of the membrane surface area occupied by gap junctions are also much greater at these times. Values of about 200 to 300 nm (Garfield et al., 1977, 1978; Puri and Garfield, 1982; Wathes and Porter, 1982; MacKenzie and Garfield, 1985; Saito et al., 1985) and 0.2 to 0.4 % of the plasma membrane area (Garfield et al., 1978; Puri and Garfield, 1982; Sims et al., 1982; MacKenzie and Garfield, 1985) have been reported for respectively, the mean size and fractional area occupied by gap junctions in parturient rat uterus. It has been estimated that a single uterine smooth muscle cell at term has approximately 250 to 1000 gap junctions (Garfield et al., 1978; Garfield, 1985). Steroid hormones (estrogen and progesterone), prostaglandins and uterine

distension (stretch) are factors regulating gap junction formation in rat myometrium (Garfield et al., 1978; 1980a,b; 1982; Puri and Garfield, 1982; Wathes and Porter, 1982; MacKenzie et al., 1983; MacKenzie and Garfield, 1985).

## B) Electrophysiology of Uterine Smooth Muscle

The most recent comprehensive review of uterine electrophysiology was written by Kao (1977a) and dealt exclusively with the longitudinal muscle whose electrical properties were also assumed for the circular muscle. Since then, detailed studies of the circular muscle have revealed some marked differences in electrical properties compared to the longitudinal muscle (Osa and Fujino, 1978; Anderson et al., 1981; Bengtsson et al., 1984b). The following is a selective account of the *in vitro* electrical properties of longitudinal and circular smooth muscle of the rat uterus. These properties cannot be assumed to apply to the uteri of all species, as recent studies on the electrophysiology of the circular muscle from pregnant sheep myometrium have revealed some marked differences as compared to the rat myometrium (Parkington, 1985).

### Resting Membrane Potential

Uterine smooth muscle from the longitudinal or circular layer spontaneously generates electrical discharges between periods of quiescence. During the silent period, the membrane potential reaches a maximum value ("resting" membrane potential) that varies from about 40 to 70 mV (inside negative) (Abe, 1970). In the longitudinal muscle during pregnancy, the membrane potential increases from a nonpregnant level of 30 to 40 mV, reaching a maximum (60 to 70 mV) at midpregnancy, and then declining to approximately 50 mV at

term (Casteels and Kuriyama, 1965; Kuriyama and Suzuki, 1976a; Kanda and Kuriyama, 1980). Permeability changes of the membrane to $K^+$ ions during pregnancy (caused by changes in the levels of estrogen and progesterone, and stretch) are the likely cause of the membrane potential changes (Casteels and Kuriyama, 1965; Marshall, 1974; Kao, 1977a; Kanda and Kuriyama, 1980; Mironneau et al., 1981). The membrane potential of the circular muscle, while consistently lower than that of the longitudinal muscle, follows a similar decline during the middle to late stages of gestation, except at term when there is an abrupt transient increase in membrane potential which subsequently declines during delivery (Anderson et al., 1981; Kishikawa, 1981; Bengtsson et al., 1984b). In terms of regional differences, muscle cells at placental sites have a consistently higher membrane potential (up to 7 mV on gestation days 17 to 19) than those from nonplacental regions, until delivery when they are the same (Thiersch et al., 1959; Kuriyama, 1961; Casteels and Kuriyama, 1965; Abe, 1970; Kanda and Kuriyama, 1980).

Spontaneous Electrical Activity

The spontaneous electrical discharges in longitudinal muscle from nonpregnant, pregnant and postpartum uteri consist of intermittent bursts of spike-shaped action potentials (Kuriyama, 1961; Csapo, 1962; Marshall, 1962; Ohkawa, 1975; Kuriyama and Suzuki, 1976a; Kanda and Kuriyama, 1980). In contrast, discharges of the circular muscle consist of single plateau-type (i.e. spike followed by a slow, sustained depolarization) action potentials in nonpregnant, early and midpregnant uteri, changing to repetitive spike-shaped action potentials superimposed on a plateau that gradually diminishes in amplitude towards term, to spike bursts at delivery (Osa and Fujino, 1978;

Anderson et al., 1981; Kishikawa, 1981; Osa and Ogasawara, 1983; Bengtsson et al., 1984b). Uterine volume (chronic stretch) and ovarian hormones (principally estrogen), through their effect on the resting membrane potential, contribute to the change in action potential shape (Kawarabayashi and Marshall, 1981).

During the progress of gestation, the spontaneous discharge frequencies of the longitudinal versus circular muscle change in a reciprocal fashion. Thus, preterm the discharge frequency in the longitudinal muscle is less than in the circular muscle, the activity increasing in the former but decreasing in the latter until immediately before delivery when they are the same (Anderson et al., 1981; Bengtsson et al., 1984a; 1984b). Throughout gestation, except at term, placental regions are electrically less active than nonplacental regions (Kanda and Kuriyama, 1980). In longitudinal muscle, the spike discharge frequency is highest at midterm and then declines towards term (Thiersch et al., 1959; Kuriyama, 1961; Kuriyama and Suzuki, 1976a; Anderson et al., 1981; Kishikawa, 1981). When spikes appear in the circular muscle at term they are discharged at a frequency lower than that in the longitudinal layer (Anderson et al., 1981).

As in other excitable tissues, the action potential in uterine smooth muscle results from voltage- and time-dependent changes in membrane ionic permeabilities (Anderson, 1978). In longitudinal (Abe, 1971; Anderson et al., 1971; Mironneau, 1973; Vassort, 1981; Mironneau et al., 1982; 1984b) and circular muscles ( Kawarabayashi and Osa, 1976; Osa and Kawarabayashi, 1977; Bengtsson et al., 1984a; Chamley and Parkington, 1984) the depolarizing phase of the spike is due to an inward current carried mainly by $Ca^{2+}$ ions but also by $Na^{+}$ ions (Anderson, 1969; Anderson et al., 1971; Kao and McCullough, 1975) although their exact contributions remain uncertain (Abe, 1970; Kao, 1977b; Anderson, 1978;

Kuriyama, 1981; Tomita, 1981). The outward current causing repolarization (studied in detail in longitudinal and assumed for circular muscles) is carried by $K^+$ ions and consists of a fast (voltage-dependent) and slow ($Ca^{2+}$-activated) component (Kao and McCullough, 1975; Mironneau and Savineau, 1980; Mironneau et al., 1981; 1984b). In preterm circular muscle, the plateau-type action potential is likely due to a combined effect of a sustained inward $Ca^{2+}$ or $Na^+$ current and a decrease in the voltage-sensitive outward current (Osa and Kawarabayashi, 1977; Kawarabayashi, 1978; Bengtsson et al., 1984b; Chamley and Parkington, 1984).

Origin of Pacemaker Activity

Spontaneous electrical activity in uterine smooth muscle arises from pacemaker cells (pacesetters) which can be identified from nonpacemakers (pacefollowers or propagating cells) by the occurrence or absence, respectively, of a characteristic pacemaker potential (Kuriyama, 1961; Kuriyama and Csapo, 1961; Marshall, 1962; Kao, 1977a). The resting membrane potential of pacemaker cells is significantly lower than that of nonpacemakers and in contrast, remains constant throughout pregnancy (Lodge and Sproat, 1981). Pacemaker regions are about 2 mm by 4 mm in size (Marshall, 1959; Daniel and Lodge, 1973; Lodge and Sproat, 1981) and have no discrete anatomical location, i.e. each myometrial cell is capable of becoming a pacemaker and thus pacemaker sites can shift from one area to another (Daniel, 1960; Kuriyama and Csapo, 1961; Marshall, 1962; Osa et al., 1983). The development of new pacemaker activities is associated with membrane depolarization, although depolarization alone is not sufficient to initiate pacemaker activity (Tomita, 1970; Kao, 1977a; Lodge and Sproat, 1981).

It has not been definitely resolved as to whether the uterus *in situ* has a localized pacemaker (Marshall, 1974; Osa et al., 1983). The ovarian and cervical ends of the late pregnant rat uterus were found to contract

independently and asynchronously, while at delivery contractions were claimed to originate at the ovarian end (Fuchs, 1973; 1978). Similar claims regarding the location of pacemaker activity at the uterine tubal end during delivery have been made for the uteri of the cat, rabbit, monkey and human (Daniel, 1960; see Marshall, 1974; Wolfs and van Leeuwen, 1979; Osa et al., 1983). However, detailed in vivo recordings of electrical activity at multiple sites along the uterus during pregnancy or at delivery in several species have not revealed a constant, localized pacemaker from which excitation spreads (rabbit: Kao, 1959; Csapo and Takeda, 1965; rat: de Paiva and Csapo, 1973; human: Wolfs and van Leeuwen, 1979; sheep: Thorburn et al., 1984).

Pacemaker activity in longitudinal rat myometrium is characterized by subthreshold oscillations in membrane potential of two types (Kuriyama, 1961; Reiner and Marshall, 1975; Anderson and Ramon, 1976; Kao, 1977a; Tomita, 1981): 1) pacesetter potential (also called slow pacemaker potential, oscillatory local potential or slow wave depolarization), varying in amplitude from 3 to 20 mV with a period of 10 seconds to minutes, generates a burst of spike discharges and 2) prepotential, having an amplitude of 2 to 7 mv and period of 800 to 1200 msec, triggers an individual action potential within a spike burst. Thus, the frequencies of the pacesetter and prepotential set respectively, the burst discharge frequency and spike frequency. The pacesetter and prepotential pacemaker potentials are functionally related in that the slow pacemaker depolarizes the membrane to threshold for prepotential pacemaker activity (the latter triggering a spike ), maintains this depolarization to allow repetitive spiking and modulates the rate (slope) of prepotential depolarization and hence spike discharge frequency (Marshall, 1959; Kuriyama, 1961; Reiner and Marshall,

1975; Anderson and Ramon, 1976). Conversely, spiking is terminated when the slow pacemaker potential repolarizes the membrane below the threshold for prepotential pacemaker activity.

The ionic mechanisms responsible for the pacesetter potential and prepotential in uterine smooth muscle are largely unknown (Reiner and Marshall, 1975; Anderson, 1978). However, at least part of the inward current is carried by $Ca^{2+}$ ions (Reiner and Marshall, 1975; see review of Prosser and Mangel, 1982). The membrane depolarization of the pacesetter potential is associated with an increase in membrane resistance, presumably due to a decrease in $K^+$ ion conductance (Kuriyama and Suzuki, 1976a; Anderson and Ramon, 1976). Thus, intracellular $Ca^{2+}$ levels may mediate pacesetter activity by regulating $K^+$ ion permeability (Reiner and Marshall, 1975; Kuriyama and Suzuki, 1976a). According to this scheme, $K^+$ ion permeability is reduced (membrane depolarized) when $Ca^{2+}$ ions are extruded from the cell by a metabolically driven $Ca^{2+}$-pump (Tomita and Watanabe, 1973). Further depolarization results from an influx of $Na^+$ or $Ca^{2+}$ ions, or a combination of both, into the cell (through voltage-dependent channels not associated with spike generation) when $K^+$ conductance is low (Tomita, 1981; Prosser and Mangel, 1982). Subsequently, a rise in intracellular $Ca^{2+}$ (resulting from the $Ca^{2+}$ influx and a decrease in $Ca^{2+}$ pump activity) increases $K^+$ ion conductance and repolarizes the membrane (Prosser and Mangel, 1982). Prepotentials, on the other hand, probably result from activation of a time- and voltage-dependent $Ca^{2+}$ conductance (Prosser and Mangel, 1982). However, the intrinsic mechanisms generating the oscillations of the $Ca^{2+}$-pump postulated by this model are unkown (Anderson, 1978; Tomita et al., 1985).

Interaction Between Longitudinal and Circular Layers

Several in vitro studies provide evidence for electrical coupling between the longitudinal and circular muscles in late pregnant mouse (Osa, 1974) and midpregnant rat (Ohkawa, 1975; Osa and Katase, 1975) uteri: 1) electrical or mechanical activity of one muscle layer occurs in synchrony with that of the other layer and 2) electrical stimulation of the long axis of the longitudinal layer produces a membrane response in the circular layer and vice versa. However, the kind of electrical interaction is not established. The marked differences in electrical properties (e.g. membrane potential, action potential and strength-duration relationship) as well as frequency of spontaneous electrical activity (see above) mitigates against an extensive electrotonic interaction between the muscle layers during most of gestation, except perhaps just before and during delivery (Osa and Katase, 1975; Bengtsson et al., 1984b). On the other hand, coupling may be via capacitative or electric field effects (see Sperelakis, 1979; Sperelakis et al., 1983). However, any mode of electrical coupling requires either that muscle cells from one muscle layer are contiguous with those of the other layer or that the layers be connected via some other type of excitable cell. While muscle cells from the two layers may sometimes come into close contact (Garfield, 1979), most of the space between the muscle layers is occupied by nerves, blood vessels and connective tissue (Finn and Porter, 1975), an arrangement which would not favour extensive electrical interaction. Mediation of the inter-layer interaction by intrinsic nerves can probably be excluded as tetrodotoxin doesn't block the interaction (Osa, 1974; Ohkawa, 1975). Mechanical interference can also be excluded as a means of transmission since the electrical interaction is not affected by suppressing the mechanical activity by cadmium treatment (Osa and Katase, 1975). Cells

possessing membrane activity of an intermediary type (i.e. with characteristics of both longitudinal and circular muscle cells) were found by Osa and Katase (1975) when they advanced a microelectrode (from either the serosal or endometrial surface) through uterine strips from midpregnant rats. These may represent smooth muscle cells in bundles interconnecting the longitudinal and circular layers (Osa and Katase, 1975; see "General Anatomy of the Uterus", above), although little is known about the morphological basis for the inter-layer coupling. There have been no studies of possible gestational changes in electrical coupling between longitudinal and circular muscle layers of the myometrium.

C) Transmission of Electrical Activity

Transmission is properly used in electrophysiological terms to describe the spread of excitation from cell to cell through a junction or synapse, while propagation (conduction) is used when excitation spreads within the same cell (Tomita, 1970). In this and the following chapters, the term propagation (or conduction) will be used to describe the transmission of excitation through the myometrium, since this tissue behaves as a single cell (syncitium) in many respects (see reviews of Tomita, 1970; 1975).

Propagation of electrical activity in uterine as well as other visceral smooth muscles (which is necessary to synchronize the electrical and contractile activities of many individual muscle cells to produce a coordinated contraction), is brought about by local circuit current flow between active and resting regions of the tissue (Prosser, 1962; Barr and Dewey, 1968; Tomita, 1970;

Daniel and Lodge, 1973). Whereas the individual smooth muscle cell is the electrical unit of excitation, the functional unit of conduction is believed to be a bundle of smooth muscle cells of approximately 100-200 $\mu$m diameter and several millimeters in length (Burnstock and Prosser, 1960; Melton and Saldivar, 1964; Csapo, 1971; Marshall, 1974). It is assumed that the individual cells within the bundle, and at points where bundles overlap, are electrically coupled through low-resistance pathways to form a multicellular electrical syncitium (Tomita, 1970; 1975; Anderson, 1978). This assumption is based on the many studies showing that small strips or bundles of uterine (rat: Abe, 1970; 1971; Daniel and Lodge, 1973; Kuriyama and Suzuki, 1976a; Kawarabayashi, 1978; Zelcer and Daniel, 1979; Kanda and Kuriyama, 1980; Sims et al., 1982; Chamley and Parkington, 1984; mouse: Osa, 1974; sheep: Thorburn et al., 1984; Parkington, 1985) as well as other smooth muscle types (Tomita, 1970; 1975; Creed, 1979) show cable-like (core-conductor) properties, analogous to those of nerve and skeletal muscle fibers (Marshall, 1974; Tomita, 1970; 1975), when part of the tissue is polarized with large external electrodes (Abe and Tomita, 1968). In other words, the spatial decay of the electrotonic potential recorded along the muscle bundles is exponential and the value of the length constant is much larger than the length of a single muscle cell (Tomita, 1975; Creed, 1979). However, Sperelakis (1969) has questioned the validity of the length constant (determined by extracellular application of current) as a measure of cell-to-cell coupling. He suggests that in a bundle of parallel-packed fibers, the voltage decay measured intracellularly along the bundle is due primarily to current flow in the extracellular space within the bundle and not within the cells (Sperelakis and Picone, 1986). In any event, electrical activity (e.g. action potentials

triggered in pacemaker cells) can propagate away from its site of origin by current flow (its spatial distribution governed partly by the tissue's cable properties) between the active source and adjacent electrically-coupled membrane regions. The organization of uterine smooth muscle into branching bundles of electrically coupled cells therefore provides the basis for considering the myometrium a functional syncytium (Anderson, 1978). However, despite its superficial resemblance to core conductors, the current flow through such a syncytium with its three dimensional inter-cellular connections is likely complex (Nagai and Prosser, 1963; Daniel and Lodge, 1973; Tomita, 1970; 1975), and the geometrical factor of branching may produce some complications in spike propagation. For example, spike propagation along a bundle may be blocked at a branching point due to a low safety factor, or the action potential shape distorted at a junction point where spikes conducted along different bundles converge (Tomita, 1970; 1975). Furthermore, impulses may travel at different velocities over distinct pathways (Melton and Saldivar, 1964; 1965; 1967; Tomita, 1970). The linea uteri (a specialized bundle of longitudinal muscle located along the uterine midline) may be the prime conduction pathway allowing rapid spread of action potentials along the uterine horn and perhaps also between the two uterine horns (Melton and Saldivar, 1967).

An action potential generated in a single pacemaker cell within a bundle will not propagate because the local circuit current spreads in three dimensions to surrounding inter-connected cells and thus becomes too weak to excite them (Tomita, 1970; 1975; Holman and Neild, 1979). However, if excitation is generated simultaneously in many cells at one region of the bundle (so that there is no transverse current flow between them) the local circuit current

spreads in the longitudinal direction only and the spike can propagate along the bundle (Tomita, 1970; 1975). The mechanism(s) causing synchronization of the many cells comprising the pacemaker region is unknown (Tomita, 1970; Holman and Neild, 1979), although it is probably related to the transmission of the pacesetter potential between neighbouring pacemaker cells (Tomita, 1970; Marshall, 1974; Creed, 1979).

Conduction Velocity

Conduction velocity of action potentials (measured in the longitudinal direction) in uterine smooth muscle studied in vitro varies between species and as a function of gestational state within a given species (Abe, 1970; Daniel and Lodge, 1973). In the rat uterus, mean conduction velocities of 1.25 to 10.5 cm/sec for nonpregnant and hormone-treated ovariectomized animals (Melton, 1956; Daniel, 1960; Melton and Saldivar, 1964; 1965; 1967; 1970; Saldivar and Melton, 1966) and 7 to 33 cm/sec for pregnant animals (Daniel, 1960; Kanda and Kuriyama, 1980) have been obtained for spontaneous and evoked action potentials. During the progress of gestation in the rat longitudinal myometrium, the conduction velocity of evoked spikes increases in both nonplacental and placental regions (Kanda and Kuriyama, 1980). However, the conduction velocity of the uterus is different depending on the direction. In the pregnant mouse uterus for example, longitudinal conduction velocity is higher in the cervical than in the ovarian direction (Kuriyama, 1961). It is claimed that longitudinal conduction velocity is the same in both directions in the nonpregnant rat myometrium (Melton and Saldivar, 1964), although this has not been extensively studied. In addition, conduction velocity between two cells in the same or in different bundles is higher in the longitudinal than in the transverse direction

in the uterus (Goto et al., 1961; Kuriyama, 1961; Osa, 1974). Similar results concerning propagation velocities in longitudinal as compared to transverse axes have been obtained in other visceral smooth muscles (Burnstock and Prosser, 1960; Nagai and Prosser, 1963; Barr and Dewey, 1968; Holman and Neild, 1979). In midpregnant rat uteri, spike bursts recorded from the longitudinal myometrium are conducted with higher velocity in the longitudinal as compared to the circular axis (Ohkawa, 1975) and in late pregnant rat uterus individual spikes comprising spontaneous spike bursts, recorded simultaneously from two different muscle cells in the longitudinal muscle, have longer inter-electrode time shifts (i.e. slower conduction velocities) in the transverse than in the longitudinal direction (Landa et al., 1959). Zelcer and Daniel (1979) have also shown that the transverse spread of passive current in the longitudinal muscle of the myometrium from midpregnant or delivering rats was smaller (i.e. length constant smaller) than that in the longitudinal direction. These higher propagation velocities and length constants in the longitudinal as compared to the tangential direction of the cell axis are probably directly related to the much lower internal resistance in the long axis of the cells that arises from the smaller number of cell junctions per unit length. In addition to directional conduction velocity differences, regional differences exist. For example, throughout gestation in pregnant rat uterus longitudinal conduction velocity is consistently higher, and at midgestation the length constant larger, in nonplacental than in placental regions (Kanda and Kuriyama, 1980). It is probable that the circular layer of the rat myometrium at midterm has a slower conduction velocity than the longitudinal layer since the length constant of the circular layer is smaller than that of the longitudinal layer (Abe, 1971;

Kawarabayashi, 1978). In the pregnant mouse myometrium, the length constant is shorter and conduction velocity slower in the circular than in the longitudinal layer (Osa, 1974).

Conduction Distance

The extent of conduction (i.e. the distance travelled by the same action potential) in the uterus has been studied in some detail in nonpregnant and pregnant rat uterus. Conduction distances of less than 1 to 2 mm for ovariectomized, nonpregnant (Melton and Saldivar, 1964), 6 to 37 mm for nonpregnant estrogen- and estrogen-plus progesterone-treated (Melton, 1956; Daniel, 1960; Melton and Saldivar, 1964; 1965; 1967) and 14.4 mm for early pregnant (Daniel, 1960) animals have been reported. However, the velocity and extent of uterine conduction during pregnancy has not been adequately studied in any animal species, despite the importance of such information in understanding the mechanism underlying the synchronization of uterine smooth muscle cell activity at parturition (Csapo, 1971; 1981).

Cell-to-Cell Coupling During Pregnancy

Gestational changes in the degree of current spread (cell-to-cell coupling) in uterine smooth muscle have been assessed by measurement of passive electrical (i.e. cable) properties. In circular (Thorburn et al., 1984; Parkington, 1985) and longitudinal (Sims et al., 1982) smooth muscle from sheep and rat uteri, respectively, the length constants and membrane time constants were higher at term than at preterm indicating an enhanced cell-to-cell coupling at term. Others (Abe, 1971; Daniel and Lodge, 1973; Kuriyama and Suzuki, 1976a; Daniel and Zelcer, 1979) studying longitudinal rat myometrium found no such gestational changes. However, with the exception of the study of Sims et al. (1982) the

tissues used for electrical coupling measurements in rat myometrium were not examined for the presence of gap junctions which may have developed in vitro in the preterm tissues before or during electrical recording (Garfield et al., 1980a; Garfield, 1985) and contributed to the electrical coupling (see below). Another factor, the degree of stretch (if not properly controlled) will likely influence the measured length constant (Tomita, 1975; Zelcer and Daniel, 1979; Sims et al., 1982). Using a different method to assess electrical coupling in the rat myometrium, Sims et al. (1982) found a lower junctional resistance (i.e. increased coupling) during delivery than before term or postpartum.

Conduction velocity (v) in a core-conductor can be calculated from the relation $v = S \lambda/\tau$ , where S is a safety factor depending on both the excitability of the muscle cell membrane and the action potential amplitude, $\lambda$ is the length constant and $\tau$ is the membrane time constant (Holman, 1968). Thus, changes in passive or active membrane properties during gestation may affect action potential conduction velocity. It would be useful, therefore, to correlate action potential conduction velocities with passive cable properties in both longitudinal and circular muscle to determine which factors influence spike propagation in the uterus (Daniel and Lodge, 1973). Recently this relation was studied in frog skeletal muscle fibers and the time constant (principally the surface membrane capacitance) was the main membrane constant which determined conduction velocity (Homma et al., 1983).

Structural Basis of Cell-to-Cell Coupling

Electrical interaction between uterine smooth muscle cells is usually assumed to imply the existence of inter-cellular low resistance pathways for current flow (but see Sperelakis et al., 1983). It is generally believed that the

gap junction or nexus represents the structural basis for electrical coupling in smooth muscle (Barr et al., 1968; Dewey and Barr, 1968; Gabella, 1981; Garfield, 1985) and other tissues (Loewenstein, 1981; Bennett et al., 1984). The development of gap junctions at term in the longitudinal myometrium of the pregnant rat is related to improved electrical coupling in this tissue (Sims et al., 1982). However, relatively good coupling between uterine smooth muscle cells exist before term (Abe, 1971; Daniel and Lodge, 1973; Osa, 1974; Kuriyama and Suzuki, 1976a; Kawarabayashi, 1978; Zelcer and Daniel, 1979; Kanda and Kuriyama, 1980; Sims et al., 1982; Thorburn et al., 1984; Parkington, 1985) and in nonpregnant myometrium (Kuriyama and Suzuki, 1976a; Chamley and Parkington, 1984) where presumably few or no gap junctions are present (but gap junction measurements were only made in the study of Sims et al., 1982; and see "Anatomy and Ultrastructure of the Uterus", above; Dahl and Berger, 1978; Garfield et al., 1979; Zervos et al., 1985), or in other smooth muscle tissues where gap junctions have not been detected (Daniel et al., 1976; Gabella, 1981; Garfield, 1985). This implies the existence of alternate ways (other than local circuit current flow through low-resistance connections between cells) for current spread through the syncytium (Daniel et al., 1976; Zelcer and Daniel, 1979). For example, Sperelakis and associates (Sperelakis and Mann, 1977; Sperelakis et al., 1983) have postulated a model of electrical coupling ("electric field coupling") that allows electrical transmission between adjoining cells without the requirement of low-resistance cell-to-cell connections. According to this model, electrical current spreads by way of the extracellular space in regions of close (approx. 20 nm) contact ("junctional cleft") between adjacent cells. Alternately, electrical transmission may be by way of capacitative current flow

("capacitative coupling") in regions of close contact between muscle cells, as proposed for electrical coupling in myocardial cells (Sperelakis, 1979). Interdigitations, close or simple apposition contacts, or intermediate contacts between uterine muscle cells (see "Cell-to-Cell Contacts", above) may provide these regions of close contact (Zelcer and Daniel, 1979; Marshall, 1981). In summary, while it is unlikely that gap junctions are the only route for current spread between uterine (or other) smooth muscle cells, their presence in large numbers at term is likely to improve myometrial electrical coupling. Thus, gap junctions may be sufficient but not necessary for cell-to-cell electrical coupling in the uterus (Daniel et al., 1976; Sims et al., 1982; Garfield, 1985).

D) Electromechanical Coupling

Contractile activity in uterine smooth muscle is initiated by a rise in the intracellular concentration of free ionized $Ca^{2+}$ to approximately $10^{-5}$ M from a resting level of about $10^{-7}$ M (Daniel et al., 1983). The source of this activator $Ca^{2+}$ is extracellular (i.e. $Ca^{2+}$ ions which flow into the cell down their electrochemical gradient in response to a change in membrane permeability) or intracellular (i.e. $Ca^{2+}$ ions released from intracellular storage sites) or a combination of both (Mironneau, 1973; 1976a; Marshall, 1974; Grosset and Mironneau, 1977; Kuriyama, 1981; Daniel et al., 1983; Mironneau et al., 1984a,b). Conversely, a reduction of intracellular free $Ca^{2+}$ (either as a result of efflux into the extracellular space or re-uptake into intracellular storage sites) terminates contraction (Marshall, 1974; Kuriyama, 1981; Daniel et al., 1983).

In longitudinal and circular muscles of pregnant rat myometrium, the inward $Ca^{2+}$ current (through voltage-dependent transmembrane $Ca^{2+}$ channels)

during a single action potential initiates a twitch contraction (Mironneau, 1973; Kawarabayashi and Osa, 1976; Bengtsson et al., 1984b). When action potentials are repetitively discharged (e.g. in spike bursts) the contraction amplitude is increased because: a) the intracellular level of free $Ca^{2+}$ is increased and b) the increments in tension triggered by individual spikes can summate (Kuriyama and Csapo, 1961; Mironneau, 1973; Reiner and Marshall, 1975; Kao, 1977a). When action potentials are discharged at a rate higher than about 1 c/s, a fused tetanic type contraction is generated (Kuriyama and Csapo, 1961; Mironneau, 1973). Thus, the frequency and duration of spike frequency can control the contraction height and duration, respectively (Marshall, 1974). In this way, the frequency of pacemaker discharge (pacesetter and prepotential) determines, respectively the rate and intensity of uterine contractions (Marshall, 1973; Kao, 1977a). However, increases in contractile force in the longitudinal muscle may be achieved by a more or less synchronous stimulation of large areas of the myometrium (i.e. increased cell-to-cell coupling), as apposed to a faster rate of stimulation of individual cells (Kao, 1977a). This is supported by the recent observation that between late pregnancy and delivery the amplitude of spontaneous contractions increases in the longitudinal myometrium despite a decrease in spike frequency and a lack of change in the ability of the muscle to contract (Anderson et al., 1981; Bengtsson et al., 1984a,b; Izumi, 1985). However, part of the increase in contractile force may be due to increases in the $Ca^{2+}$-sensitivity of the contractile proteins and $Ca^{2+}$ release from intracellular storage sites, during the progress of gestation (see Izumi, 1985).

In the circular muscle at midterm, contractions are weaker than in the longitudinal muscle, but as pregnancy progresses they increase in strength until at term when they are of similar strength (or just slightly weaker) than

contractions in the longitudinal layer (Osa and Katase, 1975; Anderson et al., 1981; Bengtsson et al., 1984b; Izumi, 1985). These changes are not due to changes in the ability of the circular muscle to contract (see above) but rather mainly to changes in membrane electrical events (i.e. stronger contractions generated by spike bursts at term than by single, plateau-type action potentials at midterm) and cell-to-cell coupling (Osa and Katase, 1975; Anderson et al., 1981; Bengtsson et al., 1984a,b; Thorburn et al. 1984). The differences in magnitude between longitudinal and circular muscles at midterm may also be explained by differences in membrane electrical events, cell-to-cell coupling and perhaps intracellular $Ca^{2+}$ release (Kawarabayashi, 1978; Bengtsson et al., 1984a,b; Izumi, 1985).

An important, but unresolved problem is how the contractile activities of the longitudinal and circular muscles participate in the performance of delivery (Chow and Marshall, 1981; Osa et al., 1983). It is thus not known whether the intrauterine pressure measurements in vivo represent the activity of the longitudinal or circular muscle layer or both (Osa et al., 1983). However, Mosler (1968) reported for the isolated nonpregnant rat uterine horn that contraction of the longitudinal muscle alone has little affect on the intrauterine pressure.

## E) Mechanisms of Parturition

Parturition is the process of expulsion of the uterine contents (i.e. delivery of the fetus) by forceful and coordinated uterine contractions. In situ recording of uterine electrical activity, intrauterine pressure (IUP), or

simultaneous recording of both shows that labour is associated with a transition from local, asynchronic electrical activity (and hence irregular, low amplitude IUP cycles) to synchronic electrical activity (and hence regular, high amplitude IUP cycles) in rat (de Paiva and Csapo, 1973; Fuchs, 1973; 1985; see Wolfs and van Leeuwen, 1979) and other species (Csapo and Takeda, 1965; Fuchs, 1973; 1985; Wolfs and van Leeuwen, 1979; Thorburn et al., 1984). Thus, forceful and coordinated uterine contractions result from the synchronous contractile activities of large numbers of uterine smooth muscle cells (Liggins, 1979; Csapo, 1981), which in turn results from propagation of electrical excitation between individual smooth muscle cells (Csapo, 1971; see "Electromechanical Coupling", above). So in discussing parturition, two processes must be addressed: 1) activation of individual uterine smooth muscle cells and 2) conduction of this activity throughout the uterus to produce a synchronized contraction. Some earlier reviews on the control (initiation) of parturition (Finn and Porter, 1975; Csapo, 1977; 1981; Fuchs, 1978; Liggins, 1979; Thorburn and Challis, 1979; Challis, 1984) advance several theories which differ in details (e.g. identity of inhibitors or stimulants) but not end result (i.e. forceful and coordinated contractions). Whether parturition is caused by release from inhibition or by stimulation (Liggins, 1979) or a combination of both (Thorburn et al., 1984) is debatable, as is the relative importance of maternal as opposed to fetal factors (Liggins, 1973; Challis, 1984). The following is an account of some possible regulatory factors (e.g. progesterone, estrogen, uterine volume, prostaglandins, oxytocin, relaxin, nerves and gap junctions) that probably control the activation or synchronization of uterine contractions in the rat. It is likely that parturition occurs as a result of a complex interaction of these and perhaps

other yet unknown factors, and that the same basic mechanisms, although modified in many ways, control parturition in other species (Marshall, 1974; Thorburn et al., 1977; Liggins, 1979; Mitchell, 1984).

Progesterone

The inhibitory action of progesterone during pregnancy (and its withdrawal just before parturition ) is the basis for the well-known (but controversial) "progesterone-block" hypothesis (Csapo, 1961), later called the "brake model" (Csapo, 1971) and then the "see-saw" theory of parturition (Csapo, 1977). Accordingly, progesterone inhibits ("blocks") uterine excitation, conduction and pharmacological reactivity and thus inhibits uterine contractility to maintain pregnancy (Csapo and Takeda, 1965; Fuchs, 1973; but see Saldivar and Melton, 1966). When progesterone levels decline and the block is removed, the uterus is able to fully respond to endogenous stimulants, such as uterine distension, estrogen, oxytocin and prostaglandins, and pregnancy is terminated (Csapo, 1977). In the rat, ovarian (corpus luteum) progesterone production dominates the pregnant uterus but there is a also a significant placental progesterone production during late pregnancy (Csapo and Wiest, 1969). Plasma or tissue progesterone levels decline significantly (progesterone withdrawal) at about gestation day 19 (Csapo and Wiest, 1969; Wiest, 1970; Fuchs, 1978; Kishikawa, 1981; Puri and Garfield, 1982; Saito et al., 1985) while progesterone nuclear receptors start to decline at about gestation day 15 (Saito et al., 1985).

The exact mechanism of progesterone's blocking action is unknown and there are many discrepancies between it's in vivo (i.e. treatment before excising tissue) and in vitro (i.e. treatment after excising tissue) actions

(Saldivar and Melton, 1966; Fuchs, 1973; Finn and Porter, 1975; Kao, 1977a; Osa and Ogasawara, 1984). This is likely because: 1) *in vitro* experiments do not completely reproduce the *in situ* conditions or 2) the *in situ* hormonal influence may change when the myometrium is excised and then studied *in vitro* (Abe, 1970). Progesterone treatment *in situ* may affect uterine excitability or conduction by increasing (hyperpolarizing) the resting membrane potential and thus the threshold for excitation (Marshall, 1959; 1962; Daniel, 1960; Csapo, 1961; 1962; Kuriyama, 1961; Kuriyama and Csapo, 1961; Talo and Csapo, 1970; Kuriyama and Suzuki, 1976a; Bengtsson, 1982). However, it is not certain whether progesterone actually affects the resting membrane potential in uterine smooth muscle, because factors such as stretch (see below), time of removal of uterus from the animal and measurement of membrane potential, solvent used for dissolving the hormone *in vitro* and cell sampling bias may not have been adequately controlled (Kao and Nishiyama, 1964; Carsten, 1968; Marshall, 1974; Kao, 1977a). On the other hand, the higher resting membrane potential, decreased spontaneous electrical activity and slower conduction velocity in placental than in nonplacental regions of the myometrium (see "Electrophysiology of Uterine Smooth Muscle", above) support the idea of a local blocking effect of progesterone (Csapo, 1961; 1969). However, it cannot be definitely concluded that those properties of the placental region are due solely to the action of progesterone (Abe, 1970; see Finn and Porter, 1975; Kanda and Kuriyama, 1980).

It is possible that progesterone blocks conduction by a different mechanism, namely by decreasing electrical coupling between myometrial cells (Ichikawa and Bortoff, 1970). For example, progesterone treatment increases junctional resistance (and hence decreases electrical coupling) in estrogen-

primed rabbit myometrium (Ichikawa and Bortoff, 1970; Bortoff and Gilloteaux, 1980). This effect, (also likely to occur in rat myometrium), may be due to the inhibition of gap junction formation by progesterone because: 1) gap junctions develop after progesterone levels decline in rat and other species (Puri and Garfield, 1982; Garfield, 1985; Saito et al., 1985), 2) progesterone treatment inhibits gap junction formation in rat myometrium (Garfield et al., 1982; MacKenzie and Garfield, 1985) and 3) junctional resistance is higher in preterm pregnant rat myometrium (when gap junctions are absent or present in only small numbers) than at delivery when gap junctions develop (Sims et al., 1982).

Csapo (1971, 1977) suggested that progesterone inhibits uterine excitability and pharmacological reactivity by stabilizing a pool of membrane-bound "activator-calcium" whose release is required for electro- or pharmaco-mechanical coupling during pregnancy. However, Bengtsson et al. (1984a) studying rat myometrium found no change between late pregnancy and term in the in vitro $Ca^{2+}$ sensitivity or dependence of longitudinal and circular muscle contractions. It is more likely that pharmacological reactivity is regulated by agonist receptor concentrations in the membrane which may in turn be inhibited by progesterone (i.e. estrogen-regulated receptor synthesis may be inhibited by progesterone; see Saito et al., 1985).

Estrogen

In the pregnant rat, plasma amd uterine tissue concentrations of estrogen (largely of ovarian origin) increase markedly during the final 24 to 48 hours before delivery and peak at the time of parturition (Csapo, 1971; Soloff et al., 1979; Thorburn and Challis, 1979; Kishikawa, 1981; Puri and Garfield, 1982; Saito et al., 1985). Because of its well known excitatory effects on uterine

contractility (Bozler, 1941) it seems probable that estrogen plays a role in the initiation of parturition (Csapo, 1971). For example, myometrial electrical activity of the rat and other species is highly sensitive to estrogen deprivation, i.e. estrogen administration to nonpregnant or spayed rats increases the uterine smooth muscle cell resting membrane potential into a range where excitability is improved and action potential discharge (spontaneous or drug-induced) is readily initiated, and enhances impulse propagation (Bozler, 1941; Melton, 1956; Marshall, 1959; Kuriyama, 1961; Melton and Saldivar, 1964; Casteels and Kuriyama, 1965; Kuriyama and Suzuki, 1976a; Ogasawara et al., 1980; and see reviews of Daniel and Lodge, 1973; Marshall, 1973; Kao, 1977a; Fuchs, 1978). As well, the absence of estrogen in the circular muscle of the late pregnant rat myometrium prevents both the decline in resting membrane potential and transition from plateau-type action potential to repetitive spiking (Kawarabayashi and Marshall, 1981). Gap junction formation in the myometrium is also induced by estrogen, which may partly be the basis for the increased cell-to-cell coupling (length constant) in estrogen-dominated (Kuriyama and Suzuki, 1976a) or parturient (Sims et al., 1982) rat myometrium (see "Transmission of Electrical Activity", above; and "Gap Junctions", below). At late pregnancy estrogen may also enhance uterine contractility through its stimulation of uterine prostaglandin production (see Thorburn and Challis, 1979; Williams, 1983) and actomyosin formation (see Michael and Schofield, 1969; Csapo, 1971; 1981).

Estrogen also enhances the pharmacologic response of the uterus (Csapo, 1971; Kuriyama and Suzuki, 1976b; Kao, 1977a; Fuchs, 1978) by modulating both the resting membrane potential and the number of agonist (oxytocin: Alexandrova and Soloff, 1980; Fuchs, 1983; relaxin: Mercado-Simmen et al., 1982) receptors in the myometrium (Marshall, 1973; Saito et al., 1985).

Relaxin

Relaxin, a polypeptide hormone secreted by the corpora lutea during pregnancy in the rat and other species may be important for inhibiting uterine contractility in late pregnancy when progesterone levels decline (see Porter, 1979 for historical review; Chamley and Parkington, 1984; Weiss, 1984; Downing and Sherwood, 1985b). Relaxin is not detected in pregnant rat serum until gestation day 10 and then its concentration increases markedly and remains at high levels during the last 9 or 10 days of pregnancy (see Sherwood et al., 1980 for details; Porter, 1982). On the other hand, rat myometrial relaxin receptor concentration increases to its highest level on gestation day 17 and then steeply declines towards term (Mercado-Simmen et al., 1982), suggesting that the high circulating relaxin levels may have little significance as far as the uterine muscle is concerned (Porter, 1982). In other words, the myometrium may become increasingly refractory to relaxin as parturition approaches.

While relaxin administration diminishes or completely inhibits spontaneous myometrial contractility in nonpregnant (Porter et al., 1979; Bradshaw et al., 1981; Cheah and Sherwood, 1981) and pregnant (Downing and Sherwood, 1985b) rat *in vivo*, as well as uterine strips studied *in vitro* (Bradshaw et al., 1981; Sarosi et al., 1983; Chamley and Parkington, 1984), its exact mechanism of action is uncertain. Chamley and Parkington (1984) found that relaxin inhibits uterine circular muscle contractility by abolishing the plateau component of the action potential. Thus, when the plateau component in circular uterine muscle disappears near term (see "Electrophysiology of Uterine Smooth Muscle", above) relaxin has only a transient inhibitory effect. Similarly, relaxin only transiently inhibits (or has no effect) on uterine longitudinal

muscle ( which lacks a plateau-type action potential). Alternately, relaxin may diminish rat uterine contractile activity (at the contractile filament level) by decreasing myosin light chain phosphorylation (Nishikori et al., 1982).

The precise role of relaxin in maintaining uterine quiescence (and hence pregnancy) in the rat or any other species is uncertain (Porter, 1982; Weiss, 1984). Porter (1979) suggested that preterm, relaxin restrains spontaneous and $PGF_{2\alpha}$-driven uterine activity but leaves the uterus responsive to oxytocin. This view is supported by the recent in vitro studies of Chamley and Parkington (1984), at least in the circular muscle, and by the results which show that relaxin inhibits prostaglandin (prostacyclin) release in late pregnant rat myometrium (Williams and El-Tahir, 1982). It is perplexing that relaxin doesn't affect longitudinal muscle contractions (Chamley and Parkington, 1984). What then is the role of the increasing longitudinal muscle activity (see Anderson et al., 1981) towards term? It has also been suggested that relaxin enhances the in vivo uterotonic action of oxytocin by improving myometrial coordination (Porter, 1979; Downing et al., 1980; Bradshaw et al., 1981; Downing and Sherwood, 1985a,b). However, the in vitro data (for both longitudinal and circular muscles) is contradictory (see Chamley and Parkington, 1984). Perhaps relaxin's more significant role in controlling parturition is to induce cervical ripening (Bradshaw et al., 1981; Downing and Sherwood, 1985c).

Oxytocin

The neurohypophyseal hormone oxytocin is a potent uterine stimulant which initiates contractions in quiescent uteri or increases contractile frequency and force in active uteri (Fuchs, 1973; 1978; 1983; 1985; Marshall, 1974; Kao, 1977a). When administered in vivo (Csapo and Takeda, 1965; Csapo,

1969; 1971; Fuchs, 1973; 1978) or in vitro (see Marshall, 1974; Kao, 1977a and Anderson, 1978 for literature reviews; Ohkawa, 1975; Kuriyama and Suzuki, 1976b; Chamley and Parkington, 1984), oxytocin produces those effects primarily by increasing the duration and repetition frequency of spike burst discharges, increasing the spike discharge frequency within individual bursts and perhaps also by improving electrical conduction (see "Electromechanical Coupling", above).

The ionic basis of oxytocin's enhancement of membrane electrical activity is disputed, i.e. increase in $Ca^{2+}$ (Marshall, 1974) as opposed to $Na^{+}$ (Kao, 1977a) current. However, voltage-clamp studies on pregnant rat longitudinal myometrium show that oxytocin selectively potentiates the inward $Ca^{2+}$ current (Mironneau, 1976b). As well as stimulating $Ca^{2+}$ entry into the cell at the plasma membrane, oxytocin might raise intracellular $Ca^{2+}$ (and thus enhance uterine contractility) by mobilizing $Ca^{2+}$ from intracellular stores (Schild, 1964; Sakai et al., 1981; Batra, 1985) or by inhibiting active $Ca^{2+}$ extrusion from the cell (Soloff and Sweet, 1982; Popescu et al., 1985; Soloff, 1985).

In term pregnant rat, serum oxytocin levels (as detected using a highly sensitive and specific radioimmunoassay of serial samples taken during parturition) remain unchanged until just before expulsion of the first fetus when they increase markedly, remain elevated during delivery and then decrease after expulsion of the last fetus (Higuchi et al., 1985). Peak concentrations of oxytocin, coincident with delivery of the first or second fetus, have also recently been shown in serial blood samples obtained just before and during parturition in the rabbit (O'Byrne et al., 1986). Uterine sensitivity to oxytocin

increases as gestation progresses and reaches maximal levels shortly before or at parturition (Csapo, 1971; Fuchs, 1973; 1978; 1985; Kuriyama and Suzuki, 1976b; Chan, 1983). There is some evidence that the circular muscle of the rat myometrium behaves differently than the longitudinal muscle with respect to gestational changes in oxytocin sensitivity (Ohkawa, 1975; Crankshaw, 1985).

Marshall (1974) discusses the relationship between uterine resting membrane potential and oxytocin sensitivity. When membrane potentials are highest (at midterm) the uterus exhibits a reduced sensitivity to oxytocin. The fall in membrane potential towards the end of gestation lowers the threshold for spike discharge and hence facilitates oxytocin's stimulatory effect. Paradoxically, however, sensitivity of the muscle cell membrane to oxytocin is higher in placental as compared to that in nonplacental regions at any state of gestation (Kanda and Kuriyama, 1980) even when the membrane potential of the former region is higher (see "Electrophysiology of Uterine Smooth Muscle", above). Prostaglandins enhance oxytocin sensitivity in the term pregnant rat uterus (Williams et al., 1979; Chan, 1983), perhaps by depolarizing the muscle membrane (Williams et al., 1979), although the exact mechanism is not known.

Oxytocin receptors increase in number (but not affinity for oxytocin) just prior to parturition in rat myometrium (i.e. measured in fractions containing both longitudinal and circular smooth muscle cell membranes) and, when gestation is terminated prematurely or is prolonged, myometrial oxytocin receptor concentration rises prematurely or is delayed, respectively (Soloff, 1985). While the uterine oxytocin sensitivity is well correlated with the change in receptor concentration (Soloff et al., 1979; Alexandrova and Soloff, 1980; Fuchs, 1983; but see Crankshaw, 1985), additional factors such as the level of the membrane

potential (see above) or electrical coupling between smooth muscle cells (see "Gap Junctions", below) may also be important (Soloff, 1985). Crankshaw (1985) has suggested that changes in coupling between receptor occupation and oxytocin action, as opposed to an increase in oxytocin receptor number, are more important in determining the intensity of the uterine response to oxytocin during gestation. Ovarian hormones, stretch, or a combination of both are involved in the regulation of rat uterine oxytocin receptors: e.g. estrogen or estrogen in combination with uterine stretch, increases receptor number while progesterone inhibits the estrogen-induced increase (Soloff et al., 1979; Alexandrova and Soloff, 1980; 1985; Fuchs, 1983; 1985).

While the similarity between normal parturition and that induced by oxytocin, the increase in serum oxytocin levels and myometrial oxytocin receptors during parturition, and the maximal uterine sensitivity to oxytocin just prior to delivery suggest oxytocin's involvement in parturition, its relative importance is uncertain (Fuchs, 1973; 1978; 1983; Marshall, 1974).

Prostaglandins

The evidence suggesting a role for prostaglandins in parturition in the rat and other species is extensive (Aiken, 1972; Csapo, 1977; 1981; Fowler, 1977; Fuchs, 1978; Thorburn and Challis, 1979; Novy and Liggins, 1980; Anderson et al., 1981; Phillips and Poyser, 1981; Dubin et al., 1982; Puri and Garfield, 1982; Chan, 1983; Mitchell, 1984). In brief the evidence is as follows: 1) prostaglandins (administered *in vivo* or *in vitro*) markedly stimulate uterine contractility and enhance uterine sensitivity to other uterotonic agents (e.g. oxytocin), 2) prostaglandin production by uterine and intrauterine tissues increases as pregnancy proceeds (but which tissue is the major prostaglandin

source is controversial), 3) parturition is delayed or accelerated by agents which block prostaglandin synthesis or metabolism, respectively (but see Anderson et al., 1981) and 4) in vivo administration of prostaglandins induces parturition (but not in the rat, see Fuchs, 1973; 1978). However, it is undecided whether prostaglandins enhance uterine contractility or excitability in situ by their direct action on the myometrium (see below) or indirectly via the ovaries, i.e. causing luteal regression and subsequent decrease in plasma progesterone levels (Fuchs, 1973; 1978; Anderson et al., 1981).

Concerning their direct action on the myometrium, prostaglandins ($PGF_{2\alpha}$, $PGE_1$ and $PGE_2$) increase the electrical and mechanical activity of uterine smooth muscle in vitro. Depending on the amount, prostaglandins cause an increase in frequency of phasic contractions or an increase in tonic tension upon which phasic contractions are superimposed (Kuriyama and Suzuki, 1976b; Reiner and Marshall, 1976; Chamley and Parkington, 1984). Underlying the phasic contractile change is a slow membrane depolarization (caused by an inward $Na^+$ current: Reiner and Marshall, 1976 , $Ca^{2+}$ current unchanged, Grosset and Mironneau, 1977) that initiates or increases the frequency of spike burst discharges, whereas the increased resting (tonic) tension is likely due to prostaglandin-stimulated intracellular $Ca^{2+}$ release (Paton and Daniel, 1967; Reiner and Marshall, 1976; Grosset and Mironneau, 1977; Anderson, 1978; Villar et al., 1985) and perhaps inhibition of active $Ca^{2+}$ extrusion from the cell (see Popescu et al., 1985). The sensitivity of the isolated longitudinal rat myometrium to exogenous prostaglandins increases during the last stage of gestation (Reiner and Marshall, 1976; Kuriyama and Suzuki, 1976b), but surprisingly there is no difference in prostaglandin sensitivity in nonplacental as compared to placental regions (Kanda and Kuriyama, 1980).

Prostaglandins may also enhance uterine contractility (i.e. synchronize contractile activities) and hence initiate labour by stimulating gap junction formation (Garfield et al., 1980a; Puri and Garfield, 1982). However, in the late or term pregnant rat exogenous prostaglandin administration does not usually induce synchronous contractile activity or labour (Fuchs, 1973; 1978). An earlier study (de Paiva and Csapo, 1973) showed that synchronous uterine electrical acitivity (but not labour) developed 24 hours after prostaglandin administration in late pregnant rats, but a prostaglandin-induced progesterone withdrawal was suggested as the underlying basis for the electrical change. More detailed studies of the in situ relationships between gap junction formation, electrical conduction and prostaglandins are needed. For example, while the relative uterotonic potencies of the different prostaglandins have been studied for the pregnant rat (Phillips and Poyser, 1981), little is known about their relative potencies in stimulating gap junction formation (Garfield et al., 1980a, b; Puri and Garfield, 1982; MacKenzie et al., 1983). However, regulation of gap junction formation by prostaglandins is complex, as studies by Garfield and associates (Garfield et al., 1980a,b; MacKenzie et al., 1983) suggest that some prostaglandins may stimulate (e.g. thromboxanes and possibly endoperoxides) while other others inhibit (e.g. prostacyclin) gap junction development (Garfield, 1985).

In summary, prostaglandins are potent uterine stimulants but their exact role in parturition is difficult to assess. This is because they have a wide range of biological activities and can therefore influence parturition in a number of ways including: 1) direct stimulation of the myometrium, 2) modulating oxytocin release and sensitivity, 3) inhibition of progesterone synthesis in the

corpus luteum or placenta, 4) mediating cervical ripening and 5) regulating uteroplacental blood flow (Novy and Liggins, 1980; Fuchs, 1983).

Uterine Volume (Stretch)

The growing uterine contents during pregnancy impose a sustained stretch upon the uterine smooth muscle which alters its electrical properties (Csapo, 1971). For example, stretch lowers the membrane potential and threshold for excitation thus increasing the membrane activity, i.e. action potential and burst discharge frequencies, in rat and rabbit myometrium (Kuriyama, 1961; Marshall, 1962; Kao, 1977a). However, stretch does not alter membrane potential nor membrane activity in the progesterone-dominated rat myometrium (Marshall, 1962). Conduction velocity is increased by uterine distension (perhaps by stimulating gap junction formation; see below), thus synchronizing contractile activity (Daniel, 1960; Csapo et al., 1963; Fuchs, 1973). Chronic stretch is also required for the transition in action potential from plateau-type to repetitive spiking, in the circular muscle near term (Kawarabayashi and Marshall, 1981). Csapo (1977; 1981) also suggests that stretch activates uterine prostaglandin release and uterine actomyosin formation (Csapo, 1971).

These results suggest that the growing uterine contents (by activating the myometrium and increasing electrical conduction) facilitate their own expulsion (Csapo, 1971).

Nerves

The role (if any) of autonomic nerves in parturition has not been clarified (Marshall, 1973; Fuchs, 1978; Thorbert, 1979; Arkinstall and Jones, 1985; Sigger, 1986). In the longitudinal myometrium of the pregnant rat uterus, the neurotransmitter norepinephrine (which is the major catecholamine during

pregnancy; see Arkinstall and Jones, 1985) is inhibitory at midgestation and at term (Kawarabayashi and Osa, 1976; Chow and Marshall, 1981). The circular muscle, in contrast, shows a different response, i.e. excitation at preterm and inhibition at term (Kawarabayashi and Osa, 1976; Osa and Watanabe, 1978; Chow and Marshall, 1981; Kishikawa, 1981). It is thus possible that the adrenergic nerves, until they degenerate in late pregnancy, have a tonic inhibitory effect on longitudinal muscle and excitatory effect on circular muscle contractions. However, the uterine body of the rat has a notably poor adrenergic innervation (Marshall, 1970; Hervonen et al., 1973). On the other hand, acetylcholine is excitatory on the myometrium (both longitudinal and circular muscle layers) at all stages of gestation (Marshall, 1973; Kao, 1977a; Bengtsson et al., 1984b; Izumi, 1985). However, it is perplexing why the cholinergic nerves should degenerate in the uterine body in late pregnancy (see "Innervation of the Myometrium", above) if they played a role in initiating parturition. It has been suggested that adrenergic or cholinergic nerves may function to initiate pacemaker activity at the utero-tubal junction (where they remain intact) during the late stages of pregnancy and at parturition (Thorbert, 1979; Singh et al., 1985). However, adrenergic nerves may not be involved in the initiation of parturition, at least in the rat, since sympathetic denervation of the utero-tubal junctions and upper uterine horn at midgestation does not affect the time of onset or duration of parturition (Roche et al., 1985).

Regarding the motor effects of the peptidergic nerves, substance P (SP) and gastrin-releasing peptide (GRP) increase both the frequency and amplitude of uterine smooth muscle contractions, while vasoactive intestinal polypeptide (VIP) has an inhibitory effect on both the spontaneous and SP-

stimulated contractions of the nonpregnant uteri of rats and other species (Ottesen, 1981; Ottesen et al., 1981; 1982; 1983; Stjernquist et al., 1986). Neuropeptide Y, on the other hand, inhibits neurally (e.g. cholinergic nerves) evoked but not spontaneous contractions of the nonpregnant rat uterus (Stjernquist et al., 1983). The effects of peptidergic nerves on the motility of the pregnant rat uterus have not been studied, however it is likely that their effects are weak, especially in late pregnancy when the nerve distribution is sparse (Ottesen, 1981; Ottesen et al., 1981). For example in the human uterus, as the number of VIP-containing nerve fibers decreases during pregnancy, their inhibitory effect on spontaneous uterine contractions diminishes (Ottesen et al., 1982).

Gap Junctions

Strong and coordinated uterine contractions, a prerequisite for successful parturition (Fuchs, 1978; 1985; Csapo, 1981), likely result from the spread of electrical current through the myometrium so that many smooth muscle cells are simultaneously activated (see "Electromechanical Coupling", above). Extensive studies by Garfield and associates (Demianczuk et al., 1984; and see review of Garfield, 1985) and others (Dahl and Berger, 1978; Wathes and Porter, 1982; Saito et al., 1985) on gap junction development in uteri of rat and other species (human, baboon, sheep, rabbit, guinea pig, and mice) support the concept that formation of gap junction (i.e. low-resistance) contacts between myometrial smooth muscle cells is the structural basis for the synchronized contractile activity of the uterus during parturition. The evidence can be summarized as follows: 1) gap junctions are absent or present in low frequency in nonpregnant or in pregnant (but preterm) myometrium, 2) myometrial gap junctions increase in

number at the end of term, are present in increased frequency and size during parturition (or when labour occurs prematurely) and disappear within 24 hours after parturition, 3) when normal or premature labour is prevented experimentally, gap junctions are present in reduced number, 4) synchronous electrical and contractile activities (recorded in situ) appear in the myometria of various species at a time when gap junctions are present, 5) improved myometrial electrical coupling is correlated with the development of increased gap junctional area (measured in vitro in rat uterus: Sims et al., 1982; and in vivo in sheep uterus: Verhoeff et al., 1985) and 6) the role of gap junctions in inter-cellular electrical coupling of smooth muscle and other excitable tissues is widely acknowledged (see reviews of: Barr and Dewey, 1968; Loewenstein, 1981; De Mello, 1982).

i) Control of Gap Junction Formation

The mechanisms responsible for controlling gap junction formation in the rat myometrium during parturition have not yet been fully established. However, it is likely that changes in the steroid hormones and prostaglandins preceding parturition are responsible for the regulation of myometrial gap junctions in the rat and other species (see Garfield, 1985 for a comprehensive review). For example, in the pregnant rat, a pronounced increase in serum and tissue estrogen concentrations and a withdrawal of progesterone occur just prior to parturition (see "Estrogen" and "Progesterone", above). Myometrial gap junctions increase markedly just before delivery, coinciding with the change in steroid hormone levels (Garfield et al., 1978; 1982; Puri and Garfield, 1982; Saito et al., 1985) suggesting that estrogen may stimulate while progesterone may inhibit gap junction formation. Supporting this idea are studies showing that:

1) estrogen treatment of immature or mature nonpregnant rats, ovariectomized preterm pregnant or postpartum rats, and *in vitro* estrogen treatment of myometrial tissues from immature nonpregnant or midterm pregnant rats stimulates gap junction formation (Bergman, 1968; Garfield et al., 1980a; 1982; Merk et al., 1980; Wathes and Porter, 1982; MacKenzie et al., 1983; MacKenzie and Garfield, 1985) and 2) progesterone treatment prevents or diminishes this estrogen-stimulated gap junction formation *in vivo* or *in vitro*, respectively (Garfield et al., 1982; MacKenzie and Garfield, 1985). Also, in term pregnant rats, gap junction formation is inhibited by progesterone treatment (Garfield et al., 1978). Other factors, such as uterine distension or prostaglandins which increase during pregnancy, may modulate the gap junction regulating effects of the steroid hormones (Wathes and Porter, 1982; and see below).

Protein synthesis is essential for gap junction formation in the rat myometrium (Garfield et al., 1980b), thus the steroid hormones may regulate gap junction formation by regulating the synthesis of the connexon proteins comprising the junctions' molecular structure (see Garfield, 1985). Accordingly, estrogen, which is well known to stimulate uterine protein synthesis (Segal et al., 1977), may regulate gap junction formation by stimulating the synthesis (i.e. DNA transcription) of mRNA specific for the gap junction protein (see Dahl et al., 1980). The high circulating levels of progesterone until late pregnancy, on the other hand, may inhibit this genomic expression and hence inhibit estrogen-stimulated synthesis of the gap junction proteins (Saito et al., 1985).

Once the monomeric gap junction proteins (connexins) are synthesized in the cytoplasm, they are inserted into the plasma membrane, assembled into gap junction particles (see "Cell-to-Cell Contacts Between Uterine Smooth Muscle

Cells", above), and the particles then aggregated to form a gap junction plaque (Dahl and Berger, 1978; Hertzberg, 1980; and see Garfield, 1985). Presumably this same sequence of events occurs on the juxtaposed plasma membranes of adjacent smooth muscle cells so that the particles can align to form cell-to-cell channels. The control of the above steps in the assembly of the gap junction structure is poorly understood (see Braun et al., 1984). However, the observation that the mean size of myometrial gap junctions in estrogen-treated nonpregnant rat uteri was less than the mean gap junction size in untreated delivering animals (MacKenzie and Garfield, 1985) suggests that factors other than the steroid hormones may be involved in the aggregation of junction particles. A possible role of the prostaglandins in the control of gap junction formation is suggested by the well-known increase in uterine prostaglandin synthesis before and during labour in rat and other species (see "Prostaglandins", above) and in pregnant rats induced to deliver prematurely (Garfield et al., 1982). Studies by Garfield and associates (Garfield et al., 1980a,b; MacKenzie et al., 1983; MacKenzie and Garfield, 1985) show that prostaglandins directly influence gap junction formation in the rat myometrium: some prostaglandins (e.g. thromboxanes and possibly endoperoxides or leukotrienes) stimulate while others (e.g. prostacyclin) inhibit gap junction formation. Garfield (see Figure 16 in Garfield, 1985) proposed that prostaglandins may act to crosslink the gap junction particles or alter plasma membrane fluidity, thus regulating particle aggregation into gap junction structures. Prostaglandins may also control the number of cytoplasmic estrogen receptors and thus directly control the estrogen-stimulation of gap junction protein synthesis (MacKenzie et al., 1983).

ii) Control of Gap Junction Conductance

There is considerable evidence suggesting that gap junctions once formed can exist in either an open or closed state (see review of Spray and Bennett, 1985). In other words, the opening or closing (i.e. permeability) of the intercellular channels (pores) of the gap junction particles may be controlled (and hence cell-to-cell communication regulated) by agents which bind to the connexon proteins and alter their conformation. Calcium ions are well known to cause structural and hence functional changes in gap junctions in other tissues (see Spray and Bennett, 1985) and recent results suggest that myometrial gap junctions behave similarly (Cole and Garfield, 1985). Thus, agents (e.g. oxytocin, prostaglandin) that alter intracellular $Ca^{2+}$ might affect gap junction function by altering the pore size of the junctions. Intracellular levels of cAMP and $H^+$ ions which also regulate junctional permeabiltity in other cell systems are likely to affect myometrial gap junction permeability as well (De Mello, 1983; Cole and Garfield, 1985; Spray and Bennett, 1985). However, unlike in some other cell systems, direct measurements of intracellular $Ca^{2+}$, pH or cAMP levels and gap junction permeability have not been made in uterine smooth muscle. While nexuses in embryonic tissues also exhibit voltage-dependent gating, those from fully differentiated tissues (including cardiac muscle and presumably smooth muscle) are not sensitive to voltage gradients across them (Spray and Bennett, 1985; Weingart, 1986).

Garfield (1985) suggested that gap junctions might be the sites for oxytocin binding in the rat myometrium as the increases in oxytocin receptor numbers and gap junctions occur more or less simultaneously, and both are likely regulated by the same mechanisms (Fuchs, 1985; Garfield, 1985; Soloff, 1985).

Oxytocin might thus directly alter junctional permeability by binding to the connexon proteins and causing a conformational change (Garfield, 1985). However, oxytocin does not alter propagation or synchronization of uterine contractions measured *in vivo* in the term pregnant rat (Fuchs, 1978). Paradoxically, oxytocin sensitivity is higher in placental regions of the pregnant rat myometrium, at all stages of gestation, while cell-to-cell coupling (i.e. length constant and conduction velocity) shows the opposite relation (Kanda and Kuriyama, 1980).

Concerning their role in parturition, gap junction formation at term (induced by a cascade of events such as decreased synthesis of progesterone, increased synthesis of estrogen or prostaglandins, and uterine distension) helps to convert the myometrium into a well-coupled syncytium such that excitation (triggered by oxytocin, prostaglandins, uterine distension, or some unknown factor) can readily propagate to inactive distant cells resulting in synchronous contractile activity of widely separated uterine regions (Garfield et al., 1978; Csapo, 1981; Fuchs, 1985). However, more studies of gap junctions in relation to electrical coupling of myometrial smooth muscle cells (both *in vivo* and *in vitro*) in rat and other species are needed to support this claim. The studies described in this thesis will help our understanding of the functional role of gap junction formation in the initiation of parturition.

# CHAPTER 2

## Changes in Burst Propagation Associated With the Formation of Gap Junctions in the Myometrium at Parturition

## INTRODUCTION

Coordinated uterine contractions at term, necessary for effective expulsion of the fetus, and hence termination of pregnancy, require conduction of excitation (i.e. intercellular communication) amongst the multitude of smooth muscle cells comprising the uterine wall. While the considerable evidence obtained from *in vivo* recordings of uterine electrical activity at multiple sites along the uteri of rats (de Paiva and Csapo, 1973) and other species (Csapo and Takeda, 1965; Taverne et al., 1979a; Wolfs and van Leeuwen, 1979; Verhoeff et al., 1985) shows an increase in the extent or velocity of conduction of spontaneous electrical activity (but see Germain et al., 1982; Harding et al., 1982), these studies provide little direct evidence that the bursts of activity are necessarily propagated events (Thorburn et al., 1984). Also, while these studies may show a qualitative change in electrical conduction, they do not provide quantitative data on the extent or velocity of conduction or show whether the conduction change during pregnancy is in the longitudinal or circular (or both) axes. These problems are due in part to the relatively large distances (3 to 30 cm or more) between recording sites, making it likely that: 1) the electrical activity is originating at points between the electrodes but giving the appearance that it is conducted from one electrode to the next and 2) the conduction pathway between electrodes is not straight. More reliable information on electrical conduction in the uterus can be obtained using an array of closely spaced recording electrodes on muscle strips excised from the uterus. However, detailed quantitative measurements of the spread of

spontaneous electrical excitation in strips of pregnant uteri have been made in only a few studies. For example, Daniel and associates (Daniel and Singh, 1958; Daniel, 1960; Daniel and Renner, 1960) studied the spread of spontaneous electrical activity in large strips of the uteri from pregnant rats, cats, rabbits and humans, using two glass pore external electrodes placed at fixed distances parallel to the long axes of the uteri. Landa et al. (1959) using 2 microelectrodes, and Ohkawa (1975) using 2 glass pore external electrodes, studied the propagation of spontaneous electrical activity in both the longitudinal and transverse axes of uterine strips from late pregnant and midpregnant rats, respectively. No information is available, however, comparing the conduction of spontaneous electrical activity at term with that in late pregnancy, despite the considerable importance of such information in understanding the basis of the improvement in coordination of uterine contractile activity during labour (Csapo, 1981).

Previous studies suggested that gap junctions, which form in large numbers between uterine smooth muscle cells immediately prior to delivery (see Chapter 1) are instrumental in mediating myometrial intercellular communication. Thus, formation of gap junctions in the longitudinal rat myometrium at term is associated with an increased electrical (Sims et al., 1982) and metabolic (Cole et al., 1985) coupling. However, no information has been available about the functional consequences of gap junction formation which also occurs in the circular muscle at this time (see Chapter 1). In addition, only limited information is available about the interaction between the longitudinal and circular muscle layers, despite the likely importance of such an interaction for developing uterine wall tension at parturition. For example, while several

studies of pregnant mouse and rat uteri show that electrical or mechanical activity can spread from one layer to the other (Osa, 1974; Ohkawa, 1975; Osa and Katase, 1975), there is no information concerning the possible improvement of coupling between the longitudinal and circular layers at parturition. This, despite the likelihood that at parturition, electrical activity must spread extensively in both the longitudinal and transverse axes of the uterus to produce a coordinated contraction (Mosler, 1968).

In this study, spontaneous electrical activity was simultaneously recorded from several spots on the surface of relatively large pieces of the uterine wall, using an array of external, blunt glass pore electrodes, to provide information on the patterns of excitability and intercellular communication (i.e. electrical coupling) in the longitudinal and circular (transverse) axes of the late pregnant and parturient rat myometrium (see Kao, 1977a). Surface electrodes give recordings of the voltage drop produced by the flow of current in the interstitial fluid, not that in the cell membrane itself (Kao, 1977a), and they enable reproducible recording to be carried out for long periods of time, with little damage to the tissue (Daniel, 1960). The amplitudes of the recorded action potentials are usually less than a millivolt or so, due to shunting of the extracellular current through the low-resistance interstitial fluid, hence in order to "see" the electrical activity clearly, the backgroud "noise" must be carefully reduced (Kao, 1977a). Because of the relatively large diameter of the electrode pore (200 to 300 $\mu$m), the activities of many single cells are being recorded. If the activities of the cells under the electrode are asynchronous, then the recored signal may be of reduced amplitude or complex shape (or both). Single-cell recordings with intracellular microelectrodes, on the other hand,

have higher amplitudes and provide quantitative information about voltage changes in the cell membrane. They do not, however, provide adequate information about cellular interactions unless multiple microelectrodes are used (Kao, 1977a). This would be technically difficult, as the small size of the uterine smooth muscle cells and their spontaneous contractions make it difficult to keep even one microelectrode inside a single cell for longer than a few minutes (Marshall, 1973).

Comparison of the spread of spontaneous electrical excitation (spike bursts) in the longitudinal and transverse axes of the rat myometrium at delivery (many GJs) and five days before (few if any GJs) will help to determine the functional significance of gap junction formation in the longitudinal and circular muscle layers. Gap junction frequency was measured in some of the preterm and delivering tissues (both before and after the recording experiments), to strengthen the association between myometrial electrical coupling and gap junction formation. In the following chapter, the propagation of individual spikes was studied.

## MATERIALS AND METHODS

### A) Tissue Preparation

Timed pregnant white Wistar rats (Charles River) arrived at our animal quarters at days 12 or 15 of their pregnancies, were caged individually in a constant-temperature room with a light-dark (L:D) cycle of 12L:12D and fed a standard commercial diet, until they were used for experiments at delivery (day 22) or 5 days before (day 17). Most of the pregnant rats delivered their

fetuses between 700 and 1500 hrs on day 22, as timed from the day of breeding. The average litter size (n=63 deliveries) was 8.3 $\pm$ 1.7 pups (mean $\pm$ SD) and the median number was 9 pups per litter.

To obtain tissue for experimentation, animals were stunned by a blow to the head and then sacrificed by cervical dislocation. In the case of delivering rats, the animals were sacrificed after the delivery of one or two pups. The uterine horns were then carefully removed and placed for dissection in a glass tray filled with warm (37 °C) Krebs-bicarbonate solution, bubbled with a gas mixture of 95% $O_2$-5% $CO_2$. The Krebs-bicarbonate (Krebs) solution, which was used in all experiments, contained (mM): NaCl 115.5; KCl 4.6; $CaCl_2$ 2.5; $MgSO_4$ 1.16; $NaH_2PO_4$ 1.2; $NaHCO_3$ 21.9; glucose 11.1. When bubbled with 95% $O_2$-5% $CO_2$, this solution had a pH of 7.3-7.4 at 37 °C. The *in situ* length of the uterus was maintained after removal from the animal by pinning the uterine horns at their ovarian and cervical ends, to the Sylgard floor of the dissecting tray. The uterus was then opened lengthwise, along the side of mesenteric attachment, and the fetuses and placentae gently removed. The emptied uterine horn was then pinned out (endometrial side up), in the shape of a flat sheet, to the Sylgard bottom of the dissection tray. The width of the sheet was made equal to the *in situ* circumference of the uterine horn that was measured with a piece of thread placed around the uterus (over a fetus), before removing the uterus from the animal. The circumferences (means $\pm$ SD) were 4.66 $\pm$ .30 and 5.54 $\pm$ .40 cm, respectively (n=30 measurements: i.e. 5 animals per gestational state x 2 uterine horns per animal x 3 measurements per uterine horn). From this flat sheet of muscle, uterine strips of approximate dimensions 3 cm long by .5 to 1 cm wide, were cut from nonplacental regions over the fetal compartments in the

following ways: 1) longitudinal strip; longitudinal axis of the strip parallel to the longitudinal direction of the uterine horn and 2) circular strip; long axis of the strip tangential to the long axis of the uterine horn. These strips were either used immediately (i.e. within .5 hr) or left pinned out in the dissecting tray filled with oxygenated Krebs solution at room temperature (20-22 °C) for up to two hours before being transferred to the electrical recording chamber.

B) Electrical Recording

Muscle strips were transferred to a plexiglass organ bath (see Figure 1A) whose recording chamber of 30 ml capacity was perfused with pre-oxygenated, pre-warmed Krebs solution at a constant flow rate of about 10 ml/min. Bath temperature was regulated to 37 $\pm$ 1 °C and monitored by a mercury-filled glass thermometer placed in the solution at the corner of the recording chamber. The bath solution was constantly bubbled with 95% $O_2$-5% $CO_2$. Uterine strips were pinned out (i.e. along their ends and sides), serosal side up and at their in situ length, to the Sylgard floor of the recording chamber. All strips were equilibrated for at least 20 min before recordings were made.

Electrical activity was monitored with extracellular glass pore surface electrodes that were made by fire-polishing 4 cm segments of borosilicate glass capillary tubing (1.0-1.5 mm inside diameter; 2 mm outside diameter) to reduce the tip diameters to pore sizes of 200-300 $\mu$m. The electrodes were filled by capillary action with the Krebs solution of the bath and then platinum or chlorided-silver wires were inserted. Six such electrodes were aligned vertically in an electrode holder which fixed their relative positions in a straight line (see Figure 1B). Inter-electrode distances (measured between the centers of the pores of adjacent electrodes) were set at

3 mm. The electrode array was advanced to press lightly against the muscle surface, parallel to the long axis of the uterine strip, by means of the coarse adjustment of a microscope base to which the holder was attached. Unipolar electrical recordings of the cells beneath the electrode pores were made in volume, with reference to a chlorided-silver electrode placed in one corner of the recording chamber. Using this arrangement, relative positivity of the electrical signal at the recording electrode was indicated by an upwards deflection. These action potentials, of triphasic shape, were displayed through AC amplifiers (Beckman AC/DC input coupler, 9806A) on a six-channel ink-writing chart recorder (Beckman Type RP Dynograph). With a time constant of 1 second and high-frequency filtration, the band-pass was between .16 and 22 Hz, thereby eliminating any baseline drift due to muscle surface movement, without appreciably distorting the configuration of the action potentials. Recordings were displayed on the polygraph at a paper speed of 1 mm/sec and were simultaneously stored on FM tape by feeding the dynograph outputs into an eight-channel tape recorder (Hewlett-Packard, model 3968A, tape speed 4.75 cm/sec). At this tape speed, the band-pass was DC to 625 Hz.

C) Analysis of Spontaneous Activity

Recordings of spontaneous myogenic electrical activity were made simultaneously from six electrodes, uniformly spaced at 3 mm apart along the tissue, for a minimum of 15 min. The records were analyzed for 1) the frequencies of burst discharges, 2) burst durations and 3) the spike frequencies within bursts, as follows. The (instantaneous) burst discharge frequency was determined, for each consecutive burst at a given recording site, by measuring the inter-burst intervals and taking their reciprocals. The inter-burst interval

(i.e. the time interval from the beginning of the positive deflection of the first spike in a burst to the beginning of the positive deflection of the first spike in the following burst), was measured manually using a plastic ruler on the original chart records made at a paper speed of 1 mm/sec (see Figure 2A). These measurements were accurate to within about 1 mm (i.e. 1 sec) which was less than 4% of the smallest interval (i.e. 31 sec) between consecutive bursts. The burst frequencies from three adjacent electrode sites were averaged to give a mean value for each strip.

Burst durations and spike frequencies within bursts were measured, for three sets of spike bursts (viz. bursts simultaneously recorded at six electrode sites; selected as described below), on a computer using digitizer and computer programs, as described in Chapter 3. Burst durations (lengths) were calculated as the time intervals between the peaks of the first and last spikes comprising the bursts, while spike frequencies were calculated by measuring the inter-spike intervals and taking their reciprocals (see Figure 2B and Figure 2, Chapter 3). To obtain an unbiased selection of bursts for analysis, each set of bursts from the original chart recording of an experiment were numbered as integers (i.e. 1, 2, 3, etc.), starting from the beginning of the record. Numbers (i.e. sets of bursts) were then randomly selected using a table of random numbers. If a set of bursts so chosen represented a poor quality recording, then another random number was selected until a "good" recording was found. For a selected set of bursts, burst duration and spike frequency measurements from three adjacent electrodes were averaged to give a mean value. Electrode sites that represented the best quality of recording were chosen for analysis.

D) Analysis of Burst Propagation

Spontaneous activity was recorded (see above) for a minimum of 15-20 min. For each uterine strip, the electrical activity was analyzed for 1) the presence of entrainment (i.e. the more-or-less simultaneous occurence of burst discharges at adjacent recording sites), 2) the distance over which bursts were entrained (i.e. the distance between electrodes over which bursts spread) and 3) the "excitable" region, as outlined below. Visual analysis of the original chart records (paper speed, 1 mm/sec) revealed the presence or absence of entrainment as well as the distances over which bursts were entrained. To determine the distance over which spike bursts recorded at adjacent electrodes showed the same number of spikes at the onset of bursts (we have termed this distance the "excitable region"), fast speed (25 mm/sec) chart records were obtained by playback from tape. At this paper speed, the individual spikes comprising the spike bursts (and hence the "excitable regions") were revealed. Three sets of spike bursts (i.e. simultaneously recorded at the six electrode sites along the tissue) from each strip were selected for the "excitable" region analysis (see above).

To examine the interactions between spike bursts recorded at different sites along the tissue, the six recording electrodes in some strips were arranged in pairs, each pair being 6 mm apart while electrodes comprising the pair were 3 mm apart. After recording the electrical activity for about 10 min or so, cuts through the entire thickness of the strip between electrode pairs were made with a scalpel without disturbing the electrodes. Before cutting, a row of pins was placed across the strip, on either side where the cut was made, to prevent shortening of the partitioned strip and isolated segments. Comparison of the records from the intact strip prior to cutting with those from

the isolated segments of the partitioned strips, revealed any change in burst frequency or entrainment. In some circular strips, with the electrodes arranged as above, cuts in the circular muscle were made from the underside of the strip, without disturbing the electrodes. This was accomplished by mounting the circular strips, serosal side up and at their in situ length, on 5 mm thick Sylgard blocks (1.5 x 4.0 cm) which had a 12 mm razor blade embedded such that the blade edge protruded about 1 mm above the block surface. These blocks were then secured with pins to the floor of the recording chamber. Cuts in the circular muscle were thus made by gently pressing (using a blunt-ended plexiglass rod) on the serosal surface of the portion of the strip that lay over the razor blade. Analysis of the records from before and after cutting revealed any change in burst propagation.

E) Electron Microscopy

Samples of longitudinal and circular uterine strips were taken prior to (i.e. within 10 min after the uterus was removed from the animal) and following completion of the experiments, and then prepared for electron microscopy as follows. Tissues (.5 x 1 cm) were pinned to dental wax and immediately placed in fixative (2% glutaradehyde + 4.5% sucrose + 1.2 mM $CaCl_2$ in 75 mM cacodylate buffer, pH 7.4) for a minimum of 2 hrs at room temperature. Following fixation, tissues were removed from the dental wax, cut into small pieces (2 mm x 5 mm) and washed in 100 mM cacodylate buffer (pH 7.4), containing 6% sucrose and 1.25 mM $CaCl_2$. Tissues were next placed in fresh washing buffer, stored for 1 to 7 days at 4 °C and then postfixed for 90 min in 50 mM cacodylate buffer (pH 7.4), containing 2% osmium tetroxide. All tissues were then stained en bloc with saturated uranyl acetate for 60 min, dehydrated in a

series of graded ethanols and embedded in molds with Spurr resin. Thin sections of tissue were cut, in transverse orientation to their long axes, using a diamond knife (Dupont) on a Reichert-Jung ultramicratome (Ultracut) and then mounted on 200 mesh grids. After brief staining (2 min) with lead citrate, the sections were examined at 60 kV using a Philips 300 or 301 electron microscope.

F) Quantification of Gap Junctions

To quantitate the number of gap junctions in the tissues, 18-22 non-overlapping photographs were taken at 4,200 X (Philips 301 microscope) or 3,630 X (Philips 300) magnification and enlarged 8 or 9.3 times to final print magnifications of 33,600 X and 33,760 X, respectively. Gap junctions were identified as membrane structures with either 5 or 7 lines at some point along their length, when examined with a small (5 X) magnifying glass. The length of each gap junction was measured in mm, using a scale on the magnifying glass. The total length of myometrial plasma membranes was estimated, using a transparent grid superimposed over the photos to count the number of intersects of the grid with the plasma membrane, according to the following formula (Garfield et al., 1980a):

$$B = \pi/2 \times I/L \times A \times CF$$

where B is the total length of myometrial cell plasma membrane; I is the average number of grid intersects with the plasma membrane, from two estimates taken at right angles to one another; L is the total length of probe lines on the grid (68.56 cm, i.e. 21 lines of 3.26 cm length); A is the area of the photograph covered by the grid system (392.03 $cm^2$); CF is the correction factor for magnification. Using these measurements, the following were calculated for all photographs: 1) the number of gap junctions, 2) the mean length of the gap

junctions, 3) the total length of myometrial plasma membranes, 4) the mean number (frequency) of gap junctions per 1000 $\mu$m length of myometrial plasma membrane and 5) the fractional area of gap junctions (calculated by dividing the gap junctional area, i.e. twice the total length of gap junction membrane, by the total length of myometrial plasma membrane).

G) Statistical Analysis

For the morphological data, all results are expressed as mean values $\pm$ SD. A Wilcoxon Rank Sum Test was used to compare these values. For the electrophysiological measurements, all results are mean values $\pm$ SE. A one-way analysis of variance was used to compare these data.

## RESULTS

### General Ultrastructural Features of the Rat Myometrium

The uterus is a hollow tubular organ whose wall is composed of three layers: 1) the innermost endometrium, 2) the myometrium in the middle and 3) the outermost serosa (Figure 3). The myometrium consists of an outer longitudinal layer, which is shown in transverse section and an inner circular layer, which is shown in longitudinal section in Figure 3. The longitudinal and circular muscle layers are composed of interlacing bundles of smooth muscle fibers (Figure 4A). An electronmicrograph of a cross-section through a bundle shows that the bundles are comprised of many loosely-packed smooth muscle cells (Figure 4B). Surrounding the bundle are fibroblasts and collagen fibers.

### Gap Junctions in the Myometrium From Preterm and Delivering Rats

No gap junctions were observed between uterine smooth muscle cells in the longitudinal myometria fixed immediately after removal of the uterus from

rats on gestation day 17 (Figure 5; Table I). In contrast, longitudinal myometrial tissues fixed immediately after removal from delivering rats, had large numbers of gap junctions between smooth muscle cells (Figure 6, Table I). The mean frequency of gap junctions (7.46 gap junctions/1000 $\mu$m), their mean size (165 nm) and the mean fractional area of plasma membrane occupied by gap junctions (.245%) in these tissues are comparable to values previously reported in the literature (Garfield et al., 1977; and see "Cell-to-Cell Contacts Between Myometrial Smooth Muscle Cells", Chapter 1).

In some preterm myometrial strips fixed after completion of electrical recording, a few small gap junctions were observed between smooth muscle cells in the longitudinal or circular layers (Figure 7, Table I). These presumably developed in vitro during the course of the experiment. However, they were 9-12 times less frequent than in delivering tissues fixed after completion of electrical recordings (Table I). In addition, the mean fractional area of plasma membrane occupied by gap junctions in these preterm tissues was about 20 times less than that in the delivering tissues, due to the smaller size and lower frequency of gap junctions in the preterm tissues. Thus, even though a few gap junctions developed in vitro in the preterm strips, their frequency, size and fractional area were significantly less ($p < .05$) than in delivering tissues (Table I).

Spontaneous Electrical Activity

Spontaneous electrical activity was recorded extracellularly (using glass-pore surface electrodes) placed on the longitudinal muscle surface of uterine strips excised from pregnant rats at delivery and 5 days before. At both stages of gestation, the activity consisted of bursts of action potentials

separated by quiescent periods (Figures 8,9,10,11,12 ). Although not studied in detail, tetrodotoxin (TTX) added to the muscle bath (1 $\mu$g/ml) did not affect these features. All uterine strips were spontaneously active throughout the duration of the experiments, except for some preterm tissues which became quiescent after 10 to 15 minutes in the recording chamber. Activity in these strips could be restored by lowering the bath temperature to about 33 °C or by the addition of acetylcholine (1 $\mu$g/ml) or oxytocin ($10^{-3}$ U/ml) to the bathing fluid, indicating that they were capable of response. On the other hand, addition of TTX to a concentration of 1 $\mu$g/ml, or scorpion venom to a concentration of 5 $\mu$g/ml, did not restore the activity. Some preterm uterine strips became quiescent within a similar time period when TTX (1 $\mu$g/ml) was present since the beginning of the experiment. Lowering the bath temperature or adding acetylcholine (1 $\mu$g/ml) restored the activity. These results suggest that the spontaneous activity was a myogenic and not a neurogenic phenomenon.

As studied in detail in longitudinal uterine strips only, the frequency of burst discharges increased significantly ($p < .001$) from .45 $\pm$ .06 cycles/min on gestation day 17, to 1.19 $\pm$ .12 cycles/min at delivery (Figure 8). Burst durations were significantly longer ($p < .001$) preterm (32.20 $\pm$ 7.93 sec) than at term (21.52 $\pm$ 4.38 sec). Individual spikes comprising the bursts (see Figure 10) discharged at a higher ($p < .001$) frequency on day 17 of pregnancy (3.99 $\pm$ .59 cycles/sec) than at delivery (1.49 $\pm$ .33 cycles/sec). These characteristics of spontaneous electrical activity are summarized in Table II.

Burst Entrainment Distance

To examine the spread of electrical activity (i.e. spike bursts) in the longitudinal and transverse axes of the myometrium, spontaneous burst discharges were recorded at multiple sites, along the longitudinal axes of

longitudinal and circular cut tissues (mounted with the serosal surface exposed), using an array of six uniformly spaced electrodes (inter-electrode distance, 3 mm). Thus, in the longitudinal strips the electrodes were aligned along the long axes of the longitudinal fibers, while in the circular strips they were aligned in the direction of the circular muscle fibers. In the longitudinal strips, both preterm and at delivery, bursts were entrained over the entire recording distance of 15 mm, as evidenced by the occurence of the burst discharges at similar, overlapping times along the tissue (Figures 9 and 10; Table III). These distances may be only the lower limit of the actual spread because the activity may have propagated further than the most distal or proximal electrodes (see below). Burst activities in these strips, from either stage of gestation, were initiated at either the ovarian, cervical or middle portions of the strips. In some strips, the site of origin of this pacemaker was not always constant throughout the duration of the experiment, i.e. pacemaker activity could shift from one portion of the strip to another. These features, as well as the entrainment distances (see Figures 13A, 14A) were not affected by the presence of TTX (1 $\mu$g/ml) in the bathing fluid.

In the circular uterine strips from preterm animals, on the other hand, bursts were entrained over distances that ranged from 0 mm to 15 mm (median distance, 6 mm). Within all circular strips, the entrainment distances were variable as shown in Figure 11. In this record, entrainment distances of 3 mm and 6 mm are seen. The mean entrainment distance in 63 sets of bursts recorded from 7 circular strips (6 preterm animals) was 5.01 $\pm$ 4.02 mm. At delivery, in contrast, all bursts from 7 circular strips (7 animals) were entrained over the 15 mm recording distance (Figure 12; Table III). Thus at

preterm, the mean distance over which bursts were entrained in the longitudinal axis was almost 3 times longer ($p < .001$) than that in the transverse axis, while at delivery the entrainment distances ($15 \pm 0$ mm) in the longitudinal and transverse axes were similar (Figures 9, 10, 11 and 12; Table III). The 15 mm distance of entrainment in the transverse axis at delivery, may be only the limit of actual spread because the bursts may have propagated further than the most distal or proximal electrodes (see below). In 3 preterm circular strips where TTX (1 $\mu$g/ml) was added to the bathing fluid before the start of recording, the mean entrainment distance ($4.71 \pm 4.22$ mm) was not significantly different ($p = .7$) from the mean distance ($5.01 \pm 4.02$ mm) in strips where TTX was not added (Figures 11 and 13B). In the recording shown in figure 13B, variable entrainment distances of 0 mm, 3 mm and 9 mm within a single strip can be seen. Similarly, in the transverse axis at delivery, the mean distance over which bursts were entrained was the same ($15 \pm 0$ mm) in the presence or absence of 1 $\mu$g/ml of TTX (Figures 12, 14B). Entrainment of bursts in the longitudinal and transverse axes from the same uterine horn of a preterm pregnant rat is shown in Figure 13, while Figure 14 shows entrainment in both axes of a uterine horn from a delivering rat.

"Excitable" Region

Although spike bursts were entrained over the entire recording distance of 15 mm in preterm longitudinal strips, their spikes were not usually completely coordinated throughout the entire burst duration. In other words, the beginnings of bursts recorded at adjacent electrode sites usually had different numbers of spikes. This phenomenon can be seen in Figure 15 for example, which shows a fast speed (10 mm/sec) trace of the beginnings and ends

of a set of spike bursts recorded simultaneously at six sites in the long axis of a preterm longitudinal uterine strip. While the spike bursts at electrodes "5" and "6" were coordinated at the onset of bursting, the initial spikes comprising the bursts were conducted over only a limited area of the muscle. For example, at electrode "5", the first spikes gradually approached but did not pass beyond electrode "4" (i.e. increasing positive deflections without a negative phase; see arrows). Subsequently (i.e. by the time of discharge of the fifth spike), the spikes appeared to spread beyond electrode "4", i.e. they acquired a negative phase (Daniel, 1960). Similarly, the initial triphasic spikes in electrode "4" were conducted into, but not past the region under electrode "3", and the first spike at electrode "2" was not conducted past electrode "1" (see arrows in Figure 15). The term "excitable" region was used to describe that distance over which the beginnings of spike bursts recorded at adjacent electrode sites showed coordination of spike discharge (i.e. equal numbers of spikes). Thus, for this set of bursts which spread over a 15 mm distance, the "excitable" region was only 3 mm. Over 5 seconds elapsed since the beginning of the burst at electrode "6" to the beginning of the burst at electrode "1". In contrast to the beginnings of the bursts, spike discharges at their ends were coordinated (Figure 15B). Of 30 sets of bursts used for analysis of the length of the "excitable" region (see below), 18 were coordinated at the burst ends. Within a given preterm longitudinal strip, the length of the "excitable" region was variable, as shown in Figures 16 and 17. Values ranging from 0 mm to 15 mm could be obtained from a single strip (Figures 16 and 17). For 30 sets of spike bursts from 10 preterm longitudinal strips (5 uterine horns from 5 animals), the mean length of the "excitable" region was $6.10 \pm 3.48$ mm (Table IV). Most of the

values ranged from 3 mm to 9 mm (median value, 6 mm). Only 2 sets of bursts (from 2 uterine horns) had "excitable" regions of 15 mm. One of these sets of bursts is shown in Figure 17. Although the bursts in this recording are coordinated at their beginnings (Figure 17A), the ends were not (Figure 17B). Short "excitable" regions were also observed in the 3 preterm uterine strips that were treated with 1 $\mu$g/ml TTX (Figure 18). The mean length of the "excitable" region in 15 sets of bursts from those strips (6.40 $\pm$ 3.56 mm) was not significantly different ($p = .8$) from the mean length (6.10 $\pm$ 3.48 mm) in the untreated strips.

In longitudinal uterine strips from delivering animals, in contrast, nearly all bursts recorded at adjacent electrode sites showed equal numbers of spikes throughout their bursts (Figure 19). For 30 sets of bursts from 10 longitudinal strips from 5 uterine horns (5 delivering animals), only 3 sets (from the same uterine strip) had "excitable" regions that were shorter than 15 mm, namely 12 mm. An example of one of these sets of bursts is shown in Figure 20. In this record, only the first spike comprising the bursts at electrode sites "2" to "6" did not appear to be conducted past electrode "1" (see arrow). The initial spikes recorded at electrodes "1" and "2" differ markedly in shape and amplitude (i.e. slower rate of rise and smaller amplitude) from those subsequently recorded during the burst. This may indicate that initially the number of active cells under those electrodes was small, or that the activities were asynchronic, while as bursting continued the number of active cells increased and their activities became more synchronic. Such a situation could arise if electrodes "1" and "2" were over branching points in a bundle and would therefore not necessarily indicate a failure of conduction. The mean length of

the "excitable" region in the delivering longitudinal strips (14.80 $\pm$ .76 mm) was significantly ($p < .001$) greater than that at preterm (Table IV). In three delivering longitudinal uterine strips that were treated with TTX (1 $\mu$g/ml), the mean length of the "excitable" region (15 $\pm$ 0 mm) was similar to that in the untreated strips (Figure 21).

The length of the "excitable" region was studied in detail in several circular uterine strips from animals at both stages of gestation. The shapes of the spikes recorded in these preterm and parturient tissues were sometimes of complex shape and variable amplitude, making the assessment of the "excitable" region difficult. However, in 6 preterm circular strips from 5 uterine horns (5 animals) fast speed (10 mm/sec) traces of 24 burst sets (4 per strip) revealed that the mean length of the "excitable" regions was 3.00 $\pm$ 1.77 mm (Figures 22 and 23; Table IV). In these strips, the lengths of the "excitable" regions ranged from 0 mm to 6 mm (median length, 3 mm). For example, a set of bursts which spread over a 15 mm distance, but with an "excitable" region of only 3 mm, is shown in Figure 23. In 2 preterm circular strips that were treated with 1 $\mu$g/ml of TTX, the "excitable" regions were also < 3 mm (Figure 24). In 5 circular strips from 4 delivering animals (4 uterine horns), the mean length of the "excitable" regions of 20 sets of bursts (4 per strip) was 6.60 $\pm$ 1.23 mm (Figure 25; Table IV). In all of these strips, the lengths of the "excitable" regions were either 6 mm or 9 mm (median length, 6 mm). The "excitable" regions were also 6 mm in several sets of bursts from 2 delivering circular strips that were pretreated with 1 $\mu$g/ml TTX (Figure 26). Thus, the mean length of the "excitable" region in the transverse axis is more than 2 times greater ($p < .001$) at delivery than at preterm.

## Mechanism of Burst Propagation

### A. Longitudinal Axis

To prove that burst discharges recorded at adjacent electrode sites in longitudinal uterine strips were propagated between electrode sites, spontaneous activity was recorded before and after isolation of electrode sites by cutting through the strip, as follows. Six electrodes, placed in 3 pairs, each pair separated by a distance of 6 mm, were placed along the long axis of the strip. Electrodes comprising each pair were spaced at 3 mm apart. With that electrode arrangement, a scalpel could be fit in the 6 mm space between electrode pairs and tissue cut, without lifting the electrodes off the tissue. Prior to cutting, two rows of pins were placed across the strip on either side of the line where the cut was made. This prevented the cut ends of the isolated segments from contracting down and thus changing the length of the segment. The result of such a procedure, using a longitudinal uterine strip from a delivering rat, is shown in Figure 27. In the intact strip, prior to cutting, bursts were entrained over the 21 mm recording distance and the burst frequency, measured for about 10 minutes, was 1.56 $\pm$ .21 cycles/min (Figure 27A). The ovarian end of the strip, near electrodes "1" and "2", had phase lead . The strip was then partitioned between electrodes "4" and "5" and the spontaneous activity in the isolated segment containing electrodes "5" and "6" immediately became out of phase, decreased in frequency to about .84 $\pm$ .14 cycles/min and thus lagged behind that in the intact portion of the strip (Figure 27B). In the intact portion of the strip containing electrodes "1-4", the bursts were still entrained with phase lead maintained by the ovarian end of the strip. However, over the next 10 minutes the burst frequency decreased to about 1.28 $\pm$ .12

cycles/min, and during this time the driving pacemaker shifted to a location near electrode "3" (Figure 27C). A second cut was then made through the strip between electrodes "2" and "3". Almost immediately the burst activity in the segment containing electrodes "1" and "2" became out of phase, decreased in frequency to about .86 ± .04 cycles/min, and thus lagged behind that in the segment containing electrodes "3" and "4" (Figure 27D). The spontaneous burst activity in the latter segment decreased in frequency to about .98 ± .08 cycles/min for the duration of the experiment (Figure 27E). Thus, when electrode sites were entrained in the intact uterine strip, the electrical acitivities in those sites with lower intrinsic frequencies were pulled up by those sites having a higher intrinsic frequency. This type of experiment was repeated in another strip from the same uterine horn and in 3 other uterine strips from 3 delivering rats. Of the 5 tissues studied, 3 had ovarian lead while 2 showed cervical phase lead, in the intact strip. In all of these strips, the "intrinsic" discharge frequencies of the isolated segments were always about 15–40% less than those in the corresponding intact strips, and the highest discharge frequency was always retained by the portion of the strip which had phase lead prior to cutting. However, the highest residual frequency was always less than the regular frequency in the intact strip.

Uncoupling of burst activities between electrode pairs as a result of partitioning an intact strip, was also demonstrated in 4 longitudinal uterine tissues from 4 preterm animals. The results of such an experiment in one of these longitudinal strips is shown in Figure 28. In the intact strip prior to cutting, the burst discharge frequency was about .38 ± .10 cycles/min with the ovarian end of the strip near electrode "1" having phase lead (Figure 28A).

After cutting through the strip between electrodes "4" and "5", the burst activity in the isolated segment containing electrodes "5" and "6" became out of phase with that in the intact portion of the strip and decreased in frequency to about .23 $\pm$ .06 cycles/min (Figure 28B). Further partitioning of the strip between electrodes "2" and "3" caused uncoupling of the burst activities in these segments, phase lead being maintained by the ovarian end of the strip containing electrodes "1" and "2" (Figure 28C). The discharge frequency in the segment containing electrodes "3" and "4" decreased slightly to about .35 $\pm$ .06 cycles/min after cutting. In the 3 other preterm longitudinal strips that were studied, phase lead in the intact strip was at the cervical end in 1 strip, the ovarian end in 1 strip, and in the middle in the other strip. Phase leads after cutting were also maintained in the portions of these strips having lead prior to cutting, and the "intrinsic" discharge frequencies of the isolated segments were usually less than those of the corresponding intact strips. However, in most of the intact strips or strip segments, the spontaneous activity gradually diminished during the course of the experiment making it difficult to assess the true "intrinsic" frequencies. In one experiment, TTX (1 $\mu$g/ml) was added to the muscle bath prior to cutting to see if nerves were involved in the burst uncoupling phenomenon resulting from partitioning the strip (Figure 29). In this tissue, the burst discharge frequency prior to cutting was about .52 $\pm$ .14 cycles/min, with the ovarian end of the strip having phase lead (Figure 29A). The strip was then partitioned between electrodes "2" and "3" and then immediately after between electrodes "4" and "5". Burst activities in the isolated segments became out of phase after cutting and phase lead was maintained by the ovarian segment containing electrodes "1" and "2" (Figure

29B). The "intrinsic" burst discharge frequencies in the isolated segments were about .43 ± .11 cycles/min (electrodes "1" and "2"), .36 ± .14 cycles/min (electrodes "3" and "4") and .31 ± .03 cycles/min (electrodes "5" and "6"). Thus in the presence of TTX, the general features of uncoupling caused by partitioning the strip were similar to those of the untreated preterm strips, suggesting that nerves were not involved.

B. Transverse Axis

To test the possibility that burst propagation in the transverse axis of the uterus (i.e. circumferentially) at delivery is facilitated by the circular muscle layer, entrainment of bursts was assessed in circular uterine strips before or after selectively cutting, or otherwise damaging, the circular muscle layer. In other words, if the circular muscle provides a (low-resistance) pathway for current flow between longitudinal muscle bundles in the transverse direction, then burst coupling should be impaired in circular strips in which the circular muscle has been cut or damaged but with the longitudinal muscle left intact. To selectively cut the circular muscle, the circular strips were pinned out (mucosal side down) onto Sylgard blocks in which a razor blade was embedded across the block (see "Materials and Methods"). Cutting was attempted by gently pressing down on the serosal surface of the portion of the strip that lay over the blade. For these experiments the 6 electrodes were arranged in 2 groups of 3 electrodes each (inter-electrode distance, 3 mm) such the groups were separated by a 6 mm distance. The array was then positioned on the strip such that a group of electrodes was on either side of the region of the strip overlaying the razor blade. As illustrated in Figure 30A, the bursts were entrained over the entire recording distance of 18 mm in the intact strip. In

this record, the burst discharge frequency was about .93 ± .24 cycles/min. Although there was often some small amplitude membrane oscillations at the beginning of the bursts recorded in the region of the strip under electrode "1" that preceded activity recorded at the other electrode sites, faster speed traces of the beginnings of the bursts showed that the portion of the strip near electrode "6" usually had phase lead of the larger amplitude triphasic shaped spikes. However, the burst that was discharged just prior to cutting the strip had phase lead at the opposite end of the strip, near electrode "1" (Figure 30B). Immediately after cutting, the bursts became uncoupled at the region of the strip over the razor blade (Figure 30B). The arrows in this figure show where the dynograph recorder was momentarily turned to "standby" while the strip over the razor blade was compressed to cut the circular muscle. Phase lead after cutting was retained in the portion of the strip containing the group of electrodes "4", "5" and "6" (burst discharge frequency, .97 ± .17 cycles/min) while that portion containing electrodes "1", "2" and "3" fell out of phase, the burst discharge frequency in that segment decreasing to about .74 ± .10 cycles/min. Similar observations were made in 4 other circular strips from 3 horns (3 delivering animals). Phase lead in these strips was usually retained in the strip portion having phase lead prior to cutting. Thus, propagation of bursts in the transverse axis of the uterus at delivery seemed to require an intact circular muscle. Histological examination of semi-thin (.5 $\mu$m) sections, made in cross-section through the cut at the sides and middle portions of the strips, revealed that while the endometrium was compressed and partially cut in all strips, both the longitudinal and circular muscle layers were intact (Figure 31A). However, when the sections were examined at higher magnification the

circular muscle layer appeared damaged in the area just above the compressed area of the endometrium, as evidenced by the poor staining of the muscle bundles and their lack of a well-defined bundle like structure. (Figure 31B).

## DISCUSSION

The purpose of this study (and that in the following Chapter) was to determine the functional consequences of the enhanced cell-to-cell coupling (i.e. the increased spread of electrotonic current) that is associated with gap junction development in the longitudinal myometrium of the delivering rat uterus (see Sims et al., 1982). An improved propagation of spontaneous burst discharges along the longitudinal and transverse axes of the rat myometrium at delivery as compared to 5 days before (day 17) was demonstrated in this study. At both stages of gestation, bursts appeared to represent a system of coupled electrical relaxation oscillators (Daniel and Sarna, 1978; see below).

Since propagation is enhanced at the time when large numbers of gap junctions appear in the longitudinal and circular muscle layers, these results support the view that current flow in the parturient rat uterus is facilitated by the formation of low-resistance (gap junction) contacts between myometrial smooth muscle cells.

### Gap Junctions in the Myometrium

Thin section electron microscopy of samples from some of the uterine strips used for electrical recordings (fixed before or after experimentation), showed that gap junctions were present in the longitudinal or circular muscle layers in all delivering tissues (Table I). In contrast, no gap junctions were

observed in either muscle layers of preterm strips fixed before experimentation, and only a few junctions were observed in preterm tissues fixed after the electrical recordings. These gap junctions may have developed in vitro during the course of electrical recordings in the muscle bath (Garfield et al., 1978). In parturient tissues, the mean-values of gap junction frequency and fractional area, while not significantly different between longitudinal and circular layers, were markedly and significantly higher than in the preterm tissues (Table I). In addition, the mean gap junction sizes in delivering tissues were larger than those of the few junctions found in the preterm tissues. These values (i.e. frequency, fractional area and size) are similar to those values previously reported for preterm and delivering rat myometria (see Chapter 1). The gap junction frequencies in the preterm tissues fixed after in vitro electrical recording were slightly less than (but comparable to) those previously reported for midterm pregnant rat myometria incubated for a comparable time (i.e. 1-2 hrs) in vitro (see Garfield et al., 1980a). Thus, the preterm and delivering tissues used for experimentation represented two different groups of myometria with respect to the incidence of gap junctions.

The formation of low-resistance gap junction contacts between uterine smooth muscle cells at delivery (and their absence before) may account for the improved propagation of spike bursts observed at that time (see "Excitable Region" and "Mechanism of Burst Coupling", below). However, there are other structural changes in the myometrium between late pregnancy and parturition that could affect burst propagation. For example, the uterus increases in size (e.g. weight) during the second half of gestation to accomodate the growing fetus. In pregnant rat, the maximum uterine weight is achieved

about one day prior to parturition (Vasilenko, 1981). The weight of the myometrium (which displays a growth pattern similar to that of the whole uterus) is larger at delivery than at gestation day 17, and this increase is contributed equally by hyperplasia and hypertrophy of its smooth muscle and connective tissue cells (Afting and Elce, 1978; Vasilenko et al., 1981). Therefore, the average myometrial smooth muscle cell increases slightly in size from day 17 of pregnancy to term. The myometrium at term is also thinner and more flattened than at gestation day 17, due to a marked increase in fetal weight (Knox and Lister-Rosenoer, 1978) and a change in fetal shape (Carsten, 1968), indicating an increased stretch on the muscle fibers of both the longitudinal and circular layers.

Spontaneous Electrical Activity

All uterine strips (longitudinal and circular) were spontaneously active and discharged bursts of action potentials (spikes) alternating with quiescent periods. As studied in detail in the longitudinal strips only, the frequency of burst discharging increased significantly from early pregnancy to delivery, while the burst durations were significantly longer, and the spike discharge frequency within bursts significantly higher at preterm than at delivery (Table II). Previous studies have also shown changes in the frequency of spontaneous electrical or mechanical activity in the pregnant rat uterus between day 17 of pregnancy and parturition (in vivo: Fuchs, 1969; Fuchs and Poblete, 1970; de Paiva and Csapo, 1973; in vitro: Osa and Katase, 1975; Kuriyama and Suzuki, 1976a; Anderson et al., 1981; Bengtsson et al., 1984b). The origin of this in vitro spontaneous activity (and hence the basis of the differences in activity between late pregnancy and delivery) was not

investigated in this study. However, it was not due to release of a transmitter from intrinsic nerves in the tissues, since addition of high concentrations of tetrodotoxin to the bathing solution appeared to have little effect on the spontaneous activity at either stage of gestation. This finding is similar to those from previous studies showing that TTX doesn't affect spontaneous electrical activity in longitudinal rat myometrium excised at midpregnancy to term (Kuriyama and Suzuki, 1976a; Mironneau et al., 1982). It is well known that the rhythmic discharges of rat uterine strips persist in the presence of a variety of nerve and ganglionic blocking agents (Marshall, 1962). On the other hand, it is commonly accepted that rat uterine spontaneous activity in vitro depends on endogenous prostaglandin synthesis (Aiken, 1972; Vane and Williams, 1973; Dubin et al., 1979; 1982; Gimeno et al., 1979; Phillips and Poysey, 1981). For example, uterine prostanoid production and release into the bathing medium increases as pregnancy progresses and peaks at parturition, and the increase in spontaneous activity parallels their production (Harney et al., 1974; Anderson et al., 1981; Dubin et al., 1982). Factors such as the stress of isolating the uterus, cutting the strips and bathing them in an artificial salt solution, stretching and pinning out the tissue, hypoxia and gradual deterioration of the strips with time in the muscle bath, are thought to initiate this prostaglandin generation and release (Gimeno et al., 1981; de Barioglio and Lacuara, 1985). Thus, it is possible that the differences in frequency of spontaneous bursting that I observed were partly due to a differential prostaglandin release at preterm compared to that at delivery (Dubin et al., 1982). However, it is not clear that the differences in burst duration and spike frequency within bursts are due to differential prostaglandin production between late pregnancy and

parturition (see Anderson et al., 1981). For example, exogenously added prostaglandins are well known to increase the within burst spike frequencies in pregnant and parturient rat myometria (Kuriyama and Suzuki, 1976b; Reiner and Marshall, 1976; Grossett and Mironneau, 1977) and therefore it is difficult to reconcile a higher prostaglandin production at delivery causing a decreased spike frequency. It is likely that at least some of the changes in spontaneous electrical activity with progression of pregnancy are due to changes in the myogenic properties of the muscle cells (Casteels and Kuriyama, 1965; Kuriyama and Suzuki, 1976a). The basis for these changes in myogenic properties (which serve to control the frequency and intensity of phasic uterine contractions) is little known, despite their importance for the onset of parturition (Tomita and Watanabe, 1973; Anderson, 1978).

The finding that the frequency of spike discharge within spike bursts in the longitudinal myometrium was higher preterm than at delivery supports the results of previous studies (Thiersch et al., 1959; Kuriyama and Suzuki, 1976a; Anderson et al., 1981; Kishikawa, 1981) and has important implications regarding the control of uterine contractions. It is well known for example, that the intensity of contraction of the longitudinal myometrium is potentiated when the within burst spike discharge frequency increases (Kuriyama and Csapo, 1961; Marshall, 1973; Kao, 1977a). However, the contractile force of the longitudinal myometrium is greater at delivery than in late pregnancy, despite a considerable decrease in spike discharge frequency, suggesting a more effective coupling of excitation with contraction at term (Anderson et al., 1981). Since the $Ca^{2+}$ handling properties of neither the longitudinal nor circular muscle (and hence their ability to maximally contract) are significantly different between late

pregnancy and parturition (Bengtsson et al., 1984a,b), the greater contractile force of the myometrium at term is likely the result of an increased cell-to-cell electrical coupling (see Chapter 1).

Burst Propagation

I have demonstrated that spontaneously discharged spike bursts were entrained over much longer distances in the longitudinal than in the transverse axis of the late pregnant rat myometrium, and that at delivery, there was a marked and significant increase in transverse (but not longitudinal) propagation, so that the distances of propagation were similar in both axes at delivery (Table III). In the transverse axis at preterm, bursts were sometimes only entrained over distances as small as 3 mm, while at delivery they were always entrained in the axis over the available distance of 15 mm. Ohkawa (1975) similarly showed a much longer burst propagation distance in the longitudinal (20 mm) as compared to the circular (2 to 5 mm) direction, in uterine strips from midpregnant (12-15 days) rats. Similarly in the intact uterine horn of the day 18 pregnant rat, bursts propagate over a longer distance in the longitudinal as compared to the transverse axis (see Figure 2, Csapo, 1969). Since I recorded spontaneous activity over maximum distances of only about 15-21 mm, I have no evidence whether this represents a maximum or minimum distance, and hence whether the longitudinal burst coupling distance (if measured over a larger area of the myometrium) is greater at delivery than before. However, chronic in vivo recordings of electrical activity at more widely separated (e.g. 30 mm) sites along the pregnant rat uterus, show that the distance of apparent burst propagation in the longitudinal axis is shorter at gestation day 17 than at term (de Paiva and Csapo, 1973). Similarly, it is not known from the present

studies whether or not the entrainment distance at delivery (if measured over a larger area of the myometrium) is greater in one axis than the other.

Propagation of spike bursts over large areas of the uterus is associated with high amplitude intrauterine pressure cycles in rat (Csapo, 1969; de Paiva and Csapo, 1973) and other species (e.g. rabbit: Csapo and Takeda, 1965; pig: Taverne et al., 1979a; human: Wolfs and van Leeuwen, 1979). The longer entrainment distance in the transverse axis of the myometrium at delivery than at preterm, and the better coordination of spike discharge at the beginning of the bursts in both axes at delivery than at preterm (see "Excitable Region", below) may also partly be the basis of the enhanced uterine contractility during delivery.

The observation that the burst entrainment distance in neither axis of the myometrium, at preterm or at delivery, was altered by TTX treatment suggests that propagation was not mediated by intrinsic nerves, and thus supports previous structural studies showing a relatively low density of intrinsic nerves to nonvascular myometrial smooth muscle in the body of the rat uterus (Silva, 1967; Adham and Schenk, 1969). The low nerve density, lack of discrete relations between the nerve endings and muscle cells (Silva, 1967), and the decrease in nerve density at the end of pregnancy (Thorbert, 1979; Marshall, 1981; Arkinstall and Jones, 1985) implies the necessity of myogenic spread of excitation from cell to cell to provide electrical continuity through the pregnant myometrium (Daniel and Lodge, 1973).

Generally speaking, in smooth muscle from the uterus or other visceral organs, electrical conduction is better along the long axis of the muscle fibers than transversely between fibers in the same or different bundles

(Landa et al., 1959; Kuriyama, 1961; Prosser, 1962; Nagai and Prosser, 1963; Zelcer and Daniel, 1979). In the circular strips that I used to measure burst propagation, the longitudinal muscle bundles were oriented at right angles to the strip's long axis while the underlying circular muscle bundles were aligned parallel to the long axis of the tissue. Electrical activity was recorded from the longitudinal muscle surface with the electrodes aligned transversely to long axes of the longitudinal fibers. Thus, the poorer propagation (i.e. shorter distance over which bursts were entrained) in the transverse axis at preterm and the improved propagation in the axis at delivery, may reflect the at term development of gap junctions in the underlying circular muscle or an improved coupling between the longitudinal and circular muscle layers at delivery or both. The change in configuration of the spike complex from preterm to delivery (e.g. see Osa and Fujino, 1978; Anderson et al., 1981; Bengtsson et al., 1984b) may also play a role. Given that the longitudinal and circular layers interact electrically (see below), enhanced propagation in the transverse axis of the longitudinal myometrium at term could be achieved by an increased electrical coupling in the circular muscle at that time. Low-resistance gap junction contacts between circular uterine smooth muscle cells are absent or present in very small numbers in the preterm pregnant rat uterus but develop in large numbers at term (Table I; and see Garfield et al., 1977; 1982). However, while previous studies demonstrated that gap junction formation in the longitudinal muscle of the rat myometrium is associated with an increased spread of electronic current (Sims et al., 1982), no information is available about the functional consequences of gap junction formation in the circular muscle. In the circular muscle of the sheep uterus, the spread of electronic current (i.e.

length constant) is greatest at delivery (Thorburn et al., 1984; Parkington, 1985), the time when gap junctions develop in large numbers between the smooth muscle cells in the longitudinal (and presumably also the circular) myometrium of this species (Garfield et al., 1979). Regarding the electrical coupling between the longitudinal and circular muscle layers of the uterus, previous studies showed that in the rat or mouse uterus at mid to late pregnancy and at term, electrical activity generated in one layer is conducted into the other layer (Osa, 1974; Ohkawa, 1975; Osa and Katase, 1975). However, there is no direct evidence showing an improved coupling between muscle layers at delivery. Some indirect evidence though, suggests that coupling between the muscle layers is better at delivery than before. For example, when spontaneous electrical activity from the longitudinal muscle layer and the mechanical activity from the circular layer are recorded in circular uterine strips from midpregnant (12-15 days) rats, contractions not corresponding with burst activity are often seen (Ohkawa, 1975). Conversely, in a few circular strips that I studied from delivering rats, contractions of the circular muscle always corresponded to burst activity recorded from the longitudinal muscle. Of the possible intervening processes of transmission from one muscle layer to the other, nervous mediation or mechanical interference are not involved (Osa, 1974; Ohkawa, 1975; Osa and Katase, 1975), suggesting that the interaction is electrical. However, the structural basis for this electrical coupling is unknown. In certain regions of the rat myometrium, the longitudinal and circular muscles inter-twine and come into close contact (Finn and Porter, 1975; Garfield, 1979), and some electrophysiological evidence suggests the existence of smooth muscle cells interconnecting the longitudinal and circular muscle

layers (Osa and Katase, 1975). To my knowledge, low-resistance contacts (e.g. gap junctions) connecting the muscle layers in these regions have not been observed. It is also possible that gap junctions between interstitial cells and myometrial smooth muscle cells could provide a low-resistance pathway connecting the muscle layers (Daniel et al., 1978), but I am not aware of the presence of such contacts in the pregnant rat uterus. Garfield and Daniel (1974) reported that gap junctions are found consistently between fibrocytes surrounding bundles of smooth muscle cells in rat myometrium at all stages of pregnancy, but there are no reports of gap junctions between fibrocytes and smooth muscle cells.

It is claimed that the pregnant rat uterus *in situ* has a localized pacemaker area such that at preterm, activity originates at the cervical end while at parturition it originates from the ovarian end (see Fuchs, 1978). However, I was unable to demonstrate a fixed location of pacemaker activity in myometrial tissues from late pregnant or delivering animals. In other words, spontaneous burst acitivity originated at different sites in the longitudinal strips and was not always localized to a given portion (e.g. ovarian or cervical) of the strips studied *in vitro*. Osa et al. (1983) found similar results in longitudinal muscle strips from the uteri of late and term pregnant (days 20 or 22) rats. As Marshall (1974) pointed out, uterine pacemakers are labile and thus their localization is extremely difficult, especially in isolated muscle segments. Removal of the uterus, bathing it in an artificial salt solution and cutting it into small segments may cause the pacemaker activities to become random.

"Excitable" Region

Discoordination in the onset of spike discharges in bursts recorded at multiple sites along the longitudinal axis of the myometrium at preterm (and

their coordination at term) is direct evidence that the bursts are not as well propagated in the axis preterm as at delivery, even though at preterm the bursts occurred at similar, overlapping times (i.e. were entrained) along the tissue. The much shorter "excitable" region before delivery (Table IV) suggests a failure of spike propagation at that time. Landa et al. (1959) and Daniel (1960) previously reported an initial failure of action potential propagation at the onset of bursts recorded by two electrodes (over distances of 5 to 20 mm, respectively) in the longitudinal axis of uterine segments from preterm pregnant rats. However, they didn't elucidate the processes responsible for the conduction failure. The conduction failure was most likely a myogenic and not a neurogenic (i.e. due to the presence of intrinsic inhibitory nerves) phenomenon, as TTX treatment did not alter the length of the "excitable" region in the preterm longitudinal strips.

The conducting unit (i.e. pathway) for excitation in visceral smooth muscle consists of many parallel muscle fibers which interact electrically to provide a front of depolarization (Bulbring et al., 1958; Burnstock and Prosser, 1960; Prosser, 1962; Nagai and Prosser, 1963; Melton and Saldivar, 1964; Kobayashi et al., 1967). Conduction distance is increased when more conduction paths (i.e. fiber bundles) are simultaneously depolarized providing a larger current sink (Prosser, 1962; Nagai and Prosser, 1963). Thus, the longer "excitable" region in the longitudinal axis of the myometrium at delivery may be due to the formation of a larger (i.e. wider and longer) conducting pathway than that which exists before delivery. This may be the result of increased interaction between parallel muscle fibers within longitudinal bundles and at branching points between bundles, due to the at term development of gap

junctions between the longitudinal muscle fibers. The number (i.e. width) of inter-locking longitudinal muscle bundles in the transverse direction would also be increased as a result of improved electrical coupling (i.e. gap junction formation) in the underlying circular muscle layer, given that the layers are electrically coupled to each other. An enhanced electrical coupling between longitudinal and circular muscle layers at delivery (see below), would further increase the size (width) of the conducting pathway, and hence would increase the conduction distance in the longitudinal myometrium at delivery. Conversely, at preterm the absence of low-resistance gap junction contacts between uterine smooth muscle cells in the longitudinal and circular muscle layers, would result in a smaller conducting pathway and hence a smaller conduction distance. The failed propagation of only the initial spikes (and sometimes those at the ends of the spike bursts), suggests that the "excitable" region is not stationary but moves down the strip (see "Mechanism of Burst Propagation", below).

The length of the "excitable" region in the transverse axis of the longitudinal myometrium was also much shorter preterm than that in the axis at delivery (Table IV). This is expected since bursts were entrained over shorter distances in this axis at preterm than at delivery (Table III). However, even when bursts were entrained over distances of 6 to 15 mm in the transverse axis, the length of the "excitable" region was only about 3 mm. In contrast, the "excitable" region in this axis at delivery was usually 6 to 9 mm in length. TTX-treatment at either stage of pregnancy had no effect on the length of the "excitable" region in the transverse axis. Therefore, as discussed for the longitudinal axis, the longer propagation distance (i.e. "excitable" region) in the transverse axis of the myometrium at delivery, is probably due to the

existence of a larger conducting pathway at that time. In other words, since the direction of propagation in the transverse axis of the longitudinal myometrium is in the direction of the long axes of the underlying circular muscle fibers, gap junction formation between circular muscle fibers (within bundles and at branch points between the bundles) at delivery, would provide this larger conducting pathway. Given that the longitudinal and circular muscle layers are electrically coupled, the width of the conducting pathway (i.e. the transverse coupling of parallel circular muscle bundles), would be also increased as a result of an enhanced electrical coupling in the overlying longitudinal muscle layer. An increased electrical interaction between the muscle layers at delivery (see below) would further increase the width of the circular muscle conducting pathway.

At both stages of gestation, the "excitable" region was about 2 times longer in the longitudinal than in the transverse axis of the myometrium (Table IV). These results are consistent with previous studies on pregnant rat myometrium which showed that current spread in the longitudinal layer is poorer in the transverse as compared to the in the longitudinal axis of the cells (Landa et al., 1959; Zelcer and Daniel, 1979). The difference in conduction between the two axes is most likely related to the greater numbers of cell-to-cell junctions (e.g. greater resistance per unit length of tissue) in the transverse axis than in the long axis of the cells. However, if the propagation pathway is also through the underlying circular muscle layer, the axial difference in propagation in the longitudinal myometrium may be also be due to a poorer electronic current spread in the long axis of the circular muscle as compared to in the long axis of the longitudinal layer. For example, the length

constant is much shorter in the circular muscle than in the longitudinal muscle from midpregnant rat uterus (Abe, 1971; Kawarabayashi, 1978). On the other hand, it is not known if the length constant of the circular muscle is shorter than that of the longitudinal muscle at delivery. Parkington (1985) found that the length constant of the circular muscle of the sheep myometrium is much longer at parturition than at preterm, but in this species the passive electrical properties of the longitudinal muscle have not been determined for comparison.

Mechanism of Burst Propagation

A. Longitudinal Axis

The effect of partitioning upon burst entrainment and burst discharge frequency suggests that spike bursts in the longitudinal myometrium represent the operation of a system of coupled electrical relaxation oscillators, as in the gastrointestinal tract (Daniel and Sarna, 1978). At delivery, the intrinsic frequencies of the isolated uterine segments were about 15-40% less than the coupled frequencies in the intact strips. In the preterm longitudinal strips, it was more difficult to ascertain the intrinsic frequencies because of the tendancy of the pacemakers (in both intact and partitioned strips) to decrease their activity and become quiescent within a relatively short time in the muscle bath. However, in all the preterm strips, the frequency immediately following partition was less than in the intact strip just prior to cutting. This decrease in frequency following partition is almost certainly myogenic, as it was also observed in preterm strips that were treated with the neuronal blocking agent, TTX. Thus, both at preterm and delivery the oscillations of the higher intrinsic frequency pacemakers appeared to drive (i.e. "pull up") the lower intrinsic frequency oscillators resulting in entrainment and phase-locking of the

oscillators (Daniel and Sarma, 1978). In this way, local pacemakers can become entrained to one another, resulting in the coordination of electrical (and hence contractile) events over a large region of the myometrium. Takeda (1965) similarly found that the pacemaker with the highest "rhythm" drives the burst activity in the intact horn of the parturient rabbit uterus.

The direction of spread of bursts across a chain of coupled relaxation oscillators is away from the oscillator with the highest intrinsic frequency which is the pacemaker (dominant oscillator) for the chain. I was unable to find a fixed anatomical location (e.g. at the ovarian or cervical ends of the strip) of the dominant oscillator in either preterm or delivering strips: the driving pacemaker was found at the ovarian ends of some strips and at the cervical ends of others. I was also unable to find a gradient of intrinsic frequencies along the strips in one direction (ovarian) or the other (cervical). This may in part be due to changes in conduction patterns as a result of tissue preparation (e.g. excising the strips from the uterus may have caused the formation of new pacemaker areas), or because I studied burst conduction only over relatively short distances (up to 21 mm) as compared to the total length of the uterine horn. For example, that distance is approximately the length (in the longitudinal axis) of the uterus over only one fetal compartment at preterm, but only about one-half of the longitudinal length over a fetal compartment at delivery. Thus, it is not certain from these results how the polarity of uterine movement, which is generally thought to be "adovarian" at delivery and in the opposite direction preterm (see Fuchs, 1978), is influenced by the polarity (phase-lead relationships) of the oscillators. Problems of regional phase lead of activity and intrinsic frequency gradients along the uterus would be better

studied in much longer uterine segments covering several fetal compartments, or in the intact uterus using chronically implanted electrodes placed over wide areas.

A single uterine oscillator is presumably a group of smooth muscle cells (see Lodge and Sproat, 1981) which oscillate in phase to form a functional unit (Sarna, 1975). Entrainment of oscillators (a prerequisite of the relaxation oscillator model) probably involves the flow of a local depolarizing current through low-resistance junctions between the cells or across the extracellular space between them, or a combination of both (Daniel and Sarna, 1978). Entrainment is explained as follows: the earlier depolarization of higher intrinsic frequency oscillators results in current flow to neighbouring lower intrinsic frequency oscillators which have not yet depolarized, thus bringing them to an earlier threshold and depolarization (Sarna, 1975). In uterine and some other visceral smooth muscles, electrical coupling has been shown to be correlated with the existence of gap junctions between the muscle cells (see Daniel et al., 1976; Sims et al., 1982). Thus, entrainment of bursts in the longitudinal myometrium at delivery may be due to the presence of gap junctions at this time (Garfield et al., 1977; Table I). Entrainment of bursts in preterm longitudinal strips may be due to the presence of small numbers of gap junctions which formed <u>in vitro</u> (Table I) or to other types of cell-to-cell contacts, e.g. close or intermediate contacts (see Daniel et al., 1976; Daniel and Sarna, 1978).

The results of the present study do not provide much information as to the strength or the extent of coupling between oscillators and thus whether the oscillators are more tightly coupled at delivery than at preterm. Detailed measurements of the size of the oscillators, their intrinsic frequencies, the

maximum distances over which oscillators are coupled, and the phase lags between oscillators are therefore needed to determine whether coupling is stronger at delivery than at preterm. However, if the length of the "excitable" region (see above) is taken into account, it seems that the bursts are more tightly coupled at delivery than at preterm. At preterm, the bursts propagated a longer distance than the intitial spikes in the bursts. In other words, these spikes failed to propagate, except over much shorter distances than the bursts, although subsequently they propagated over the region of the strip that was in the excitable phase of an oscillation. As Daniel and Sarna (1978) pointed out, this may imply that at preterm the bursts are propagated by a different mechanism than that of the spikes, since the same circuitry is available for spread of both spikes and bursts. Alternately, the spike discharge frequency at preterm (about 4 Hz) may be higher than the maximum frequency which the intrinsic burst oscillator can follow (see Sarna, 1975). If this is so, then the improved coordination of spike discharge between oscillators at delivery may be partly due to the lower spike frequency (about 2 Hz) at this time.

Mechanical coupling (i.e. transmission of strain) may also be involved in entraining active regions along the uterus. For example, Takeda (1965) and Osa et al. (1983) found that isolation by ligation of a portion of the uterine horn or a muscle strip excised from the uterine horn respectively, caused each part to independently generate spontaneous activity. In the detailed study by Takeda (1965), uncoupling of electrical activity between fetal compartments could be produced by either ligation or cutting of the uterine muscle, except when the lumens of the fetal compartments were mechanically coupled by hydrodynamic contact. However, in my studies the effect of mechanical coupling

(i.e. transmission of strain) was diminished by using flat muscle strips that were carefully pinned out to avoid movement of the strip or changes in its length as a result of partitioning.

B). Transverse Axis

The observation that spike bursts recorded from the longitudinal myometrium at delivery were not entrained in the transverse axis across a segment of the tissue where the underlying circular was damaged, suggests that the circular muscle provides a path for current flow transversely between the longitudinal muscle fibers. It is well established that at delivery, the muscle cells of both the longitudinal (see Kuriyama and Suzuki, 1976a) and circular (Osa and Fujino, 1978; Kishikawa, 1981; Anderson et al., 1981) layers can spontaneously discharge spike bursts. Thus, it is possible that the oscillators in the underlying circular muscle could provide some of the depolarizing current necessary for transverse entrainment of the oscillators located in the longitudinal layer, providing that the muscle layers are electrically coupled to each other. In other words, as suggested by Connor et al. (1979) for the entrainment of slow waves in the cat intestine, the circular muscle of the uterus may act as an amplifier in a positive feedback circuit with the longitudinal muscle. In this type of system, a depolarizing current generated in the longitudinal muscle would supply a depolarizing current to initiate an active response in the underlying circular layer, which in turn would be conducted back into the longitudinal layer to reinforce its depolarization. Since the effectiveness of an oscillator to influence its neighbours depends on the length of the "gap" between them (Sarna, 1975), circumferential entrainment of oscillators in the longitudinal myometrium may require a strong current because

of the relatively large intercellular distance between the longitudinal fibers in the transverse axis. "Regenerative amplification" of the output of the longitudinal oscillators by oscillators located in the underlying circular muscle might provide this stronger current. Such a scheme would imply that the oscillators in the longitudinal layer drive those in the circular muscle. Whether the activity of one muscle layer has phase-lead (and hence drives) the activity of the other layer at delivery is not known. Simultaneous recording of the electrical activities from both sides of circular uterine strips might provide such information. Alternately, the circular muscle might only provide a low-resistance pathway in the transverse direction for current originating in the longitudinal muscle oscillators. At any rate, effective contractions of the uterine wall, necessary to expel the fetus at delivery, probably requires the spread of bursts in both axes of the uterus, and an intact circular muscle layer seems necessary for spread in the transverse axis.

Simultaneous recordings of electrical activity from the longitudinal muscle and contractions from the circular muscle in 2 circular uterine strips from delivering rats in the present study, revealed that the activities of the longitudinal and circular layers were well synchronized. This is direct evidence that the two layers are coupled (electrically) to each other. However, the identity of the connecting link between the muscle layers has not been determined. In most areas of the myometrium, the muscle layers are rather widely separated by connective tissue (e.g. interstitial cells, fibroblasts) and blood vessels, although there are some regions where the layers come into closer contact (see "Burst Propagation", above). Whether low-resistance gap junction contacts occur between longitudinal and circular smooth muscle cells in

these regions of the myometrium is not known. On the other hand, it is unlikely that gap junctions form at term between muscle cells within the longitudinal and circular layers, but not between muscle cells connecting the layers. Taylor et al. (1977) suggested that the coupling current between longitudinal and circular smooth muscle cells of the cat intestine was carried by the intervening connective tissue cells which form gap junctions with the muscle cells. To my knowledge such structural contacts have not been documented for the muscle layers of the myometrium. In any event, entrainment of oscillators between the longitudinal and circular muscle layers of the rat myometrium may not require an extensive network of low-resistance contacts connecting them, since the active (e.g. burst and spike frequencies) and resting (e.g. membrane potential) membrane properties of the layers are similar at delivery (Anderson et al., 1981; Bengtsson et al., 1984b).

## CONCLUSIONS

The results described in this chapter demonstrate a change in spontaneous electrical activity, and accompanying changes in propagation of excitation in rat myometrium between late pregnancy and parturition: 1) burst frequency increased (spike discharge frequency within bursts decreased) in the longitudinal myometrium and 2) burst propagation was enhanced in the longitudinal axis (e.g. the "excitable" region increased) and in the transverse axis (e.g. increased distance over which bursts were entrained). These changes may be the basis of the enhanced contractility of the uterus during labour.

At both stages of pregnancy, burst oscillators (pacemakers) appeared to interact as a system of coupled electrical relaxation oscillators. At

delivery, entrainment of bursts in the transverse axis of the longitudinal myometrium required an intact (i.e. undamaged) circular muscle layer, suggesting that the muscle layers were electrically coupled to each other.

Propagation of excitation in the myometrium was enhanced at a time when large numbers of low-resistance cell-to-cell contacts (gap junctions) appeared in the myometrium. I interpret this enhanced propagation to be the result of an improved cell-to-cell electrical coupling due to the presence of an increased number of gap junctions in the longitudinal and circular muscle layers, and to an increased electrical coupling between muscle layers. However, other factors such as the altered pattern of action potentials in the circular muscle (as noted by others), or possible changes in the size or arrangement of muscle bundles (due to increased uterine stretch) during pregnancy, may also have contributed to the change.

Therefore, the results of this study support the hypothesis that gap junction formation in the myometrium at term results in improved cell-to-cell coupling, in agreement with previous studies. In the following chapter, using a different measure of electrical coupling, I provide supporting evidence for this hypothesis.

TABLE I. Frequency, size and fractional area of gap junctions (GJs) in preterm pregnant (day 17) and delivering tissues fixed before and following completion of electrical recordings. "n" is the number of uterine horns examined, one per animal. Three tissues from each uterine horn were examined: one (longitudinal) tissue fixed before experimentation (i.e. immediately after removal of the uterus from the animal) and the other two (i.e. one longitudinal and one circular) tissues fixed after experimentation. The number in brackets is the number of tissues in which GJs were identified. The number of GJs is the total number of all 5 or 7 lined junctions identified in 18-22 non-overlapping micrographs of each tissue. The frequency of GJs is expressed as the number of GJs per 1000 $\mu$m of plasma membrane surveyed. The fractional area of GJs was calculated by doubling the length of GJ membrane and dividing by the total length of plasma membrane. Values are means $\pm$ SD. Those with the same superscript are significantly different ($p < .05$) as determined by the Wilcoxon Rank Sum Test.

Tissues were fixed after 1 hr to 3 hrs following removal of the uterus from the animal.

TABLE I.

GAP JUNCTIONS IN MYOMETRIUM

| Treatment | No. of Tissues, n | No. of GJs | Length of Membrane Surveyed, $\mu$m | No. of GJs/ 1000 $\mu$m Membrane | Mean Size GJs, nm | Fractional Area of GJs, % |
|---|---|---|---|---|---|---|
| Day 17 | | | | | | |
| a. Fixed immediately | 4(0) | 0 | 4,404 | 0 $\pm$ 0[a] | 0 $\pm$ 0[d] | 0 $\pm$ 0[g] |
| b. After recording (longitudinal) | 4(3) | 4 | 4,615 | .87 $\pm$ .76[b] | 74 $\pm$ 11[e] | .011 $\pm$ .008[h] |
| c. After recording (circular) | 4(1) | 2 | 4,594 | .48 $\pm$ .96[c] | 104 $\pm$ 23 | .010 $\pm$ .020[i] |
| Delivering | | | | | | |
| a. Fixed immediately | 4(4) | 35 | 4,728 | 7.46 $\pm$ 2.44[a] | 165 $\pm$ 95[d] | .245 $\pm$ .113[g] |
| b. After recording (longitudinal) | 4(4) | 35 | 4,468 | 7.94 $\pm$ 3.34[b] | 166 $\pm$ 73[e] | .264 $\pm$ .163[h] |
| c. After recording (circular) | 4(4) | 26 | 4,536 | 5.64 $\pm$ 1.32[c] | 193 $\pm$ 98 | .217 $\pm$ .106[i] |

## TABLE II

### SPONTANEOUS ELECTRICAL ACTIVITY OF PREGNANT MYOMETRIUM BEFORE TERM AND AT DELIVERY

| | Before Term (n = 10) | Delivering (n = 10) | P |
|---|---|---|---|
| Burst frequency (cycles/min) | .45 ± 0.06 | 1.19 ± 0.12 | $p<.001$ |
| Burst duration (sec) | 32.20 ± 7.93 | 21.52 ± 4.38 | $p<.001$ |
| Spike frequency (spikes/sec) | 3.99 ± 0.59 | 1.49 ± 0.33 | $p<.001$ |

TABLE II. Summary of spontaneous electrical activities of the longitudinal myometrium, recorded extracellularly, in longitudinal uterine strips from 5 animals before term (day 17) and from 5 animals at delivery. Two strips from one uterine per animal were analyzed. Electrical activities simultaneously recorded at 3 adjacent electrodes were used for analysis. Three sets of bursts per uterine strip were analyzed to determine the mean burst duration and mean spike frequency. All values are means ± SE. P values were determined using a one-way analysis of variance.

## TABLE III

### BURST ENTRAINMENT DISTANCE IN THE LONGITUDINAL AND TRANSVERSE AXES OF THE MYOMETRIUM BEFORE TERM AND AT DELIVERY

| Axis | Before Term | Delivery |
|---|---|---|
| Longitudinal | $\geq 15$ mm[a] | $\geq 15$ mm |
| No. of tissues | 14 (9) | 13 (8) |
| Circular | $5.01 \pm 4.02$ mm[a,b] | $\geq 15$ mm[a,b] |
| No. of tissues | 7 (6) | 7 (7) |

TABLE III. Summary of the distances over which spontaneous burst discharges were entrained in longitudinal and circular uterine strips from pregnant animals before term (day 17) and during delivery. "n" is the number of uterine strips analyzed, usually one strip per uterine horn. The numbers in brackets are the number of uterine horns examined, one per animal. All values are means $\pm$ SD. P values were determined using the Student's t test for independent samples. Those with the same superscript are significantly different ($p < .001$).

TABLE IV

LENGTH OF THE "EXCITABLE" REGION IN THE LONGITUDINAL AND TRANSVERSE AXES OF THE MYOMETRIUM BEFORE TERM AND AT DELIVERY

| Axis | Before term | Delivering |
|---|---|---|
| Longitudinal | 6.10 ± 3.48 mm[a] | 14.80 ± 0.76 mm[a] |
| No. of tissues | 10 (5) | 10 (5) |
| Circular | 3.00 ± 1.77 mm[a,b] | 6.60 ± 1.23 mm[a,b] |
| No. of tissues | 6 (5) | 5 (4) |

TABLE IV. Summary of the lengths of the "excitable" regions of spontaneous bursts discharges in longitudinal and circular uterine strips from pregnant animals before term (day 17) and at delivery. "n" is the number of uterine strips analyzed, usually one per uterine horn. The number in brackets is the number of uterine horns examined, one per animal. Three sets of bursts were analyzed per longitudinal strip and four sets of bursts were analyzed per circular strip. All values are means ± SD. P values were determined using the Student's t test for independent samples. Those with the same superscript are significantly different ($p < .001$).

FIGURE 1. Schematic drawings of A) the muscle bath used to record spontaneous myogenic electrical activity and B) the electrode holder and its alignment with the uterine strip. A). The uterine strip was pinned out (serosal side up) to the Sylgard floor of the recording chamber (30 ml capacity) and six glass pore surface electrodes were uniformly placed over the long axis of the strip. (Figure modified from Holman and Neild, 1979). B). Six glass pore electrodes were clamped vertically (3 mm apart) between the serrated and smooth faces of two Plexiglas blocks which were held together by screws. The holder was rigidly mounted to the base of a microscope stand. (Figure modified from Christensen and Hauser, 1971).

A

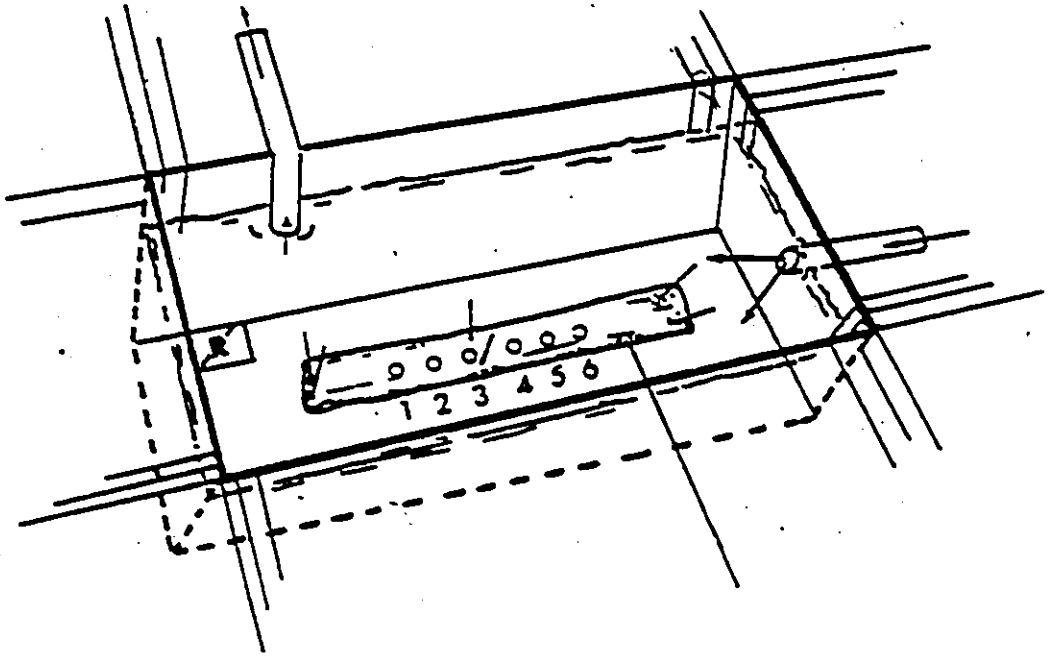


B

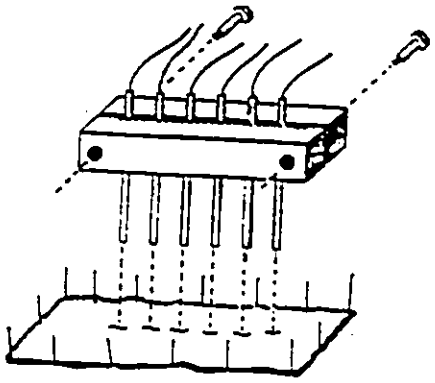

FIGURE 2. Spontaneous electrical activity recorded extracellularly by a glass pore surface electrode on a longitudinal uterine strip (delivering rat). An upward deflection is positive with respect to ground in this and all other records. A). Burst discharges, chart speed = 1 mm/sec. Burst frequency for each consecutive burst was determined by measuring the inter-burst intervals (T) and taking their reciprocals. The burst duration (d) was calculated as the time interval between the appearance of the first and last spikes comprising the spike burst. B). Individual spikes comprising a spike burst, chart speed = 50 mm/sec. The instantaneous spike frequencies were determined using computer programs that measured the inter-spike intervals (t) between negative peaks and calculated their reciprocals. Negative peaks were used because they were usually 2-3 times the amplitude of the positive peaks, thus facilitating peak detection.

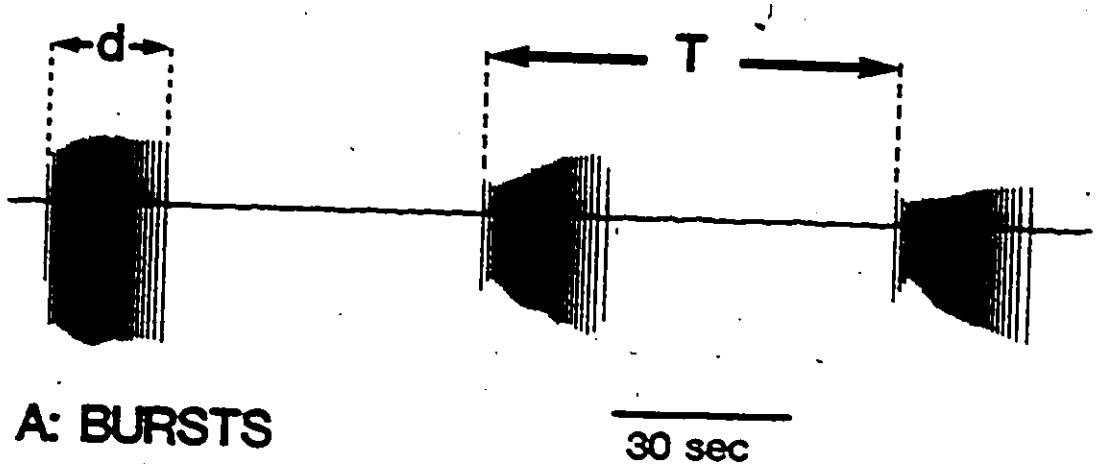
d
T
A: BURSTS
30 sec

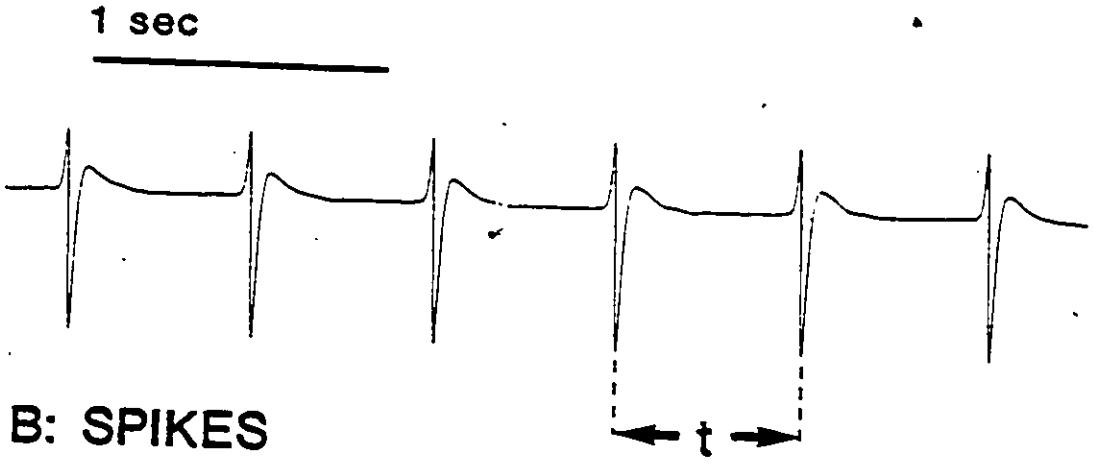
1 sec
B: SPIKES
t

FIGURE 3. Low power electron micrograph of the uterine wall, fixed *in situ*, from a late pregnant (day 17) rat. The lumen, which is surrounded by the endometrium (ENDO), is to the bottom of the field. The inner circular (CIRC) and outer longitudinal (LONG) muscle layers are shown respectively, in longitudinal and transverse orientation. Total uterine wall thickness is approximately 70 $\mu$m. Bar, 10 $\mu$m. X 1,900.

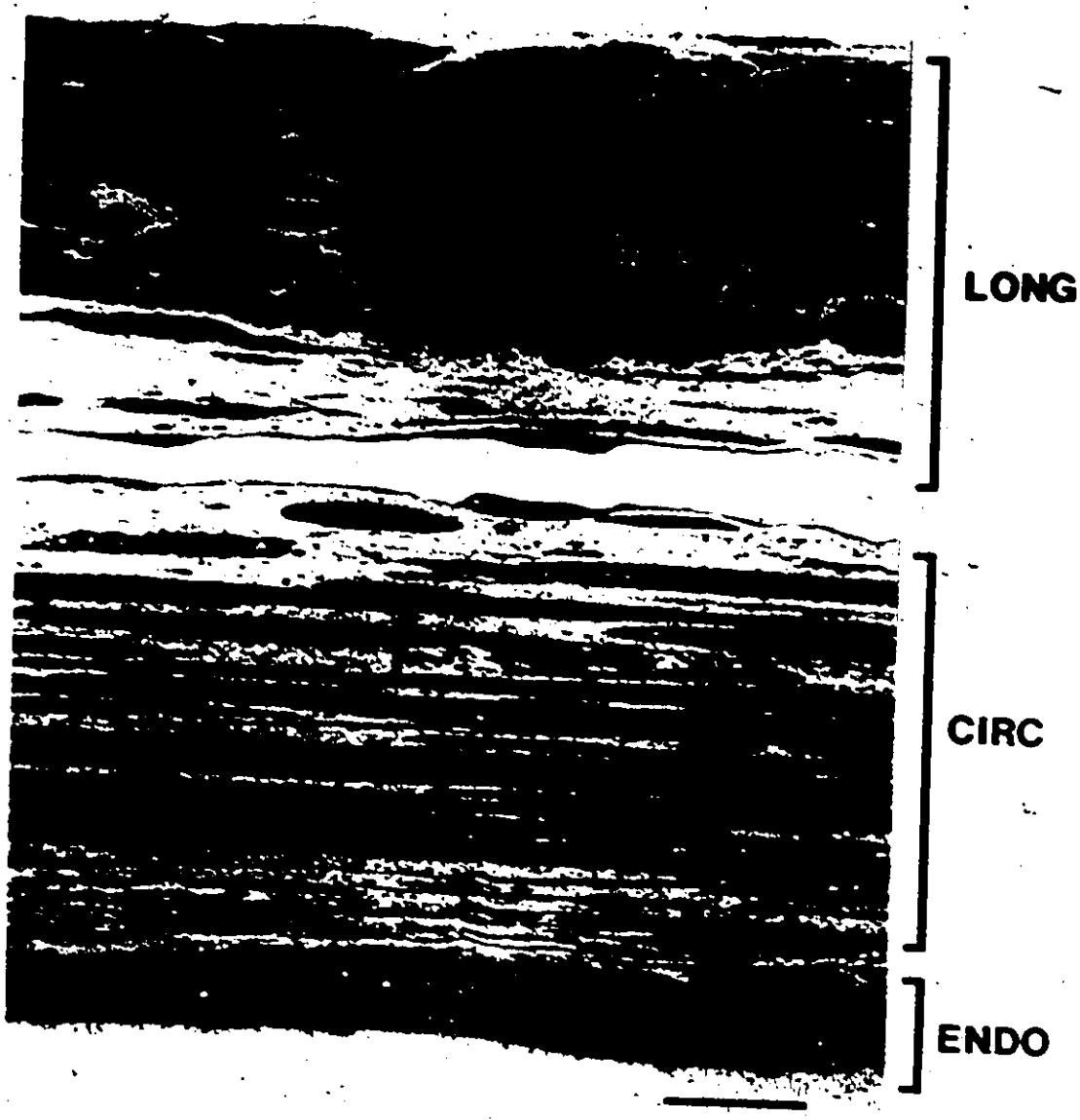
LONG
CIRC
ENDO

FIGURE 4. Longitudinal muscle bundles from pregnant rat uterus. A). Low power photomicrograph of a "whole mount" of isolated longitudinal muscle (endometrium and circular muscle removed) from the uterus of a delivering rat. Uterine wall was fixed in situ and then stained with trypan blue. The bundles of muscle fibers are approximately 100-200 $\mu$m in diameter and are arranged in an interlacing network. Bar, 200 $\mu$m. X 90. B). Low power electron micrograph of a portion of a bundle of muscle fibers in the longitudinal muscle layer from day 17 pregnant rat uterus fixed in vitro. The muscle cells are shown in transverse section, indicating that are oriented in the long axis of the bundle. Bar, 10 $\mu$m. X 2,500.


A

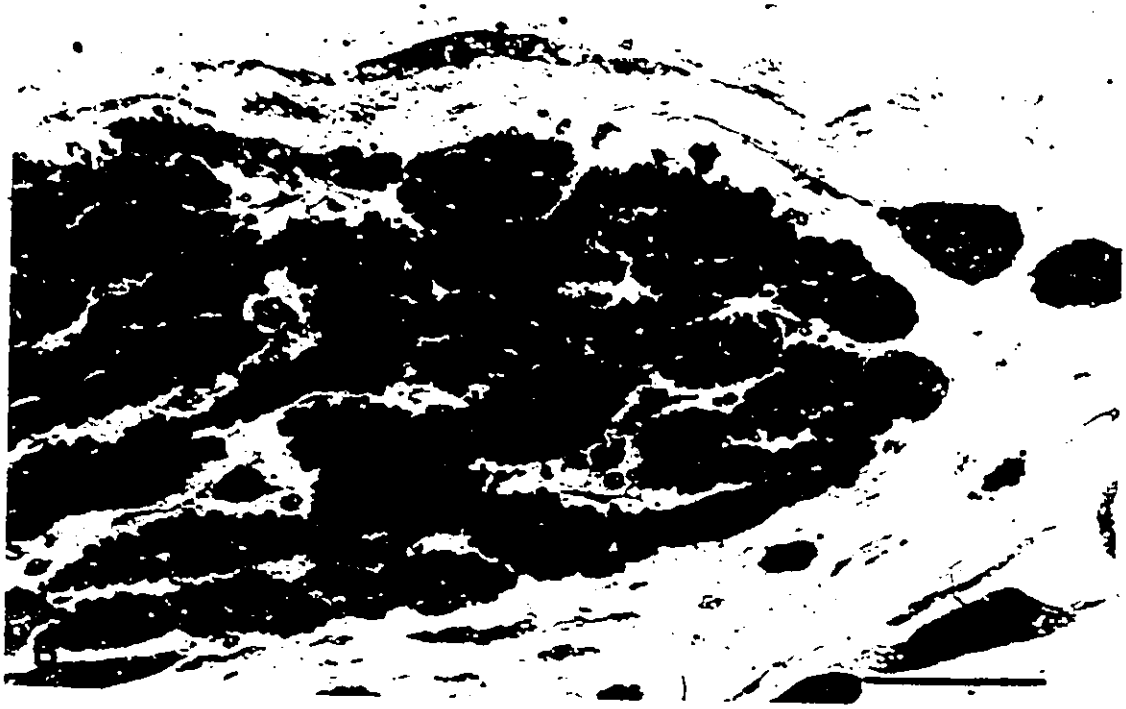

FIGURE 5. An electron micrograph of longitudinal muscle in myometrium fixed immediately after removal of the uterus from a day 17 pregnant rat. Several ultrastructural features of the uterine smooth muscle cells are shown, including the nucleus (N), mitochondria (M) and caveolae (C). Close contacts and interdigitations are apparent, but gap junctions are absent. Bar, 1 $\mu$m. X 33,000.

FIGURE 6. An electron micrograph of longitudinal muscle in myometrium fixed immediately after removal from a delivering rat, showing the presence of gap junctions (arrows) between the uterine smooth muscle cells. Bar, 1 $\mu$m. X 33,000. In the inset, a higher power electron micrograph illustrates the 7 lined structure of a gap junction (arrows). Bar, .1 $\mu$m. X 102,000.

FIGURE 7. Electron micrograph of a small gap junction (arrow) in a sample of preterm (day 17) pregnant myometrium (longitudinal muscle) fixed after *in vitro* electrical recording for about 1 hr. Bar, 1 $\mu$m. X 33,000. In the inset, a higher power micrograph illustrates the 5 lined structure of a gap junction. Bar, .1 $\mu$m. X 102,000.

FIGURE 8. Spontaneous electrical activity of preterm pregnant and delivering rat uterus. Extracellular electrical activity was recorded simultaneously at 3 sites in the long axis of a longitudinal uterine strip (inter-electrode distance = 3 mm). A). Bursts. Burst frequencies and burst durations from the 3 sites were averaged to give a mean value. B). Individual spikes within bursts. Records are fast speed (50 mm/sec) traces of portions of the spike bursts in (A). Spike frequencies from the 3 electrode sites were averaged to a mean value.

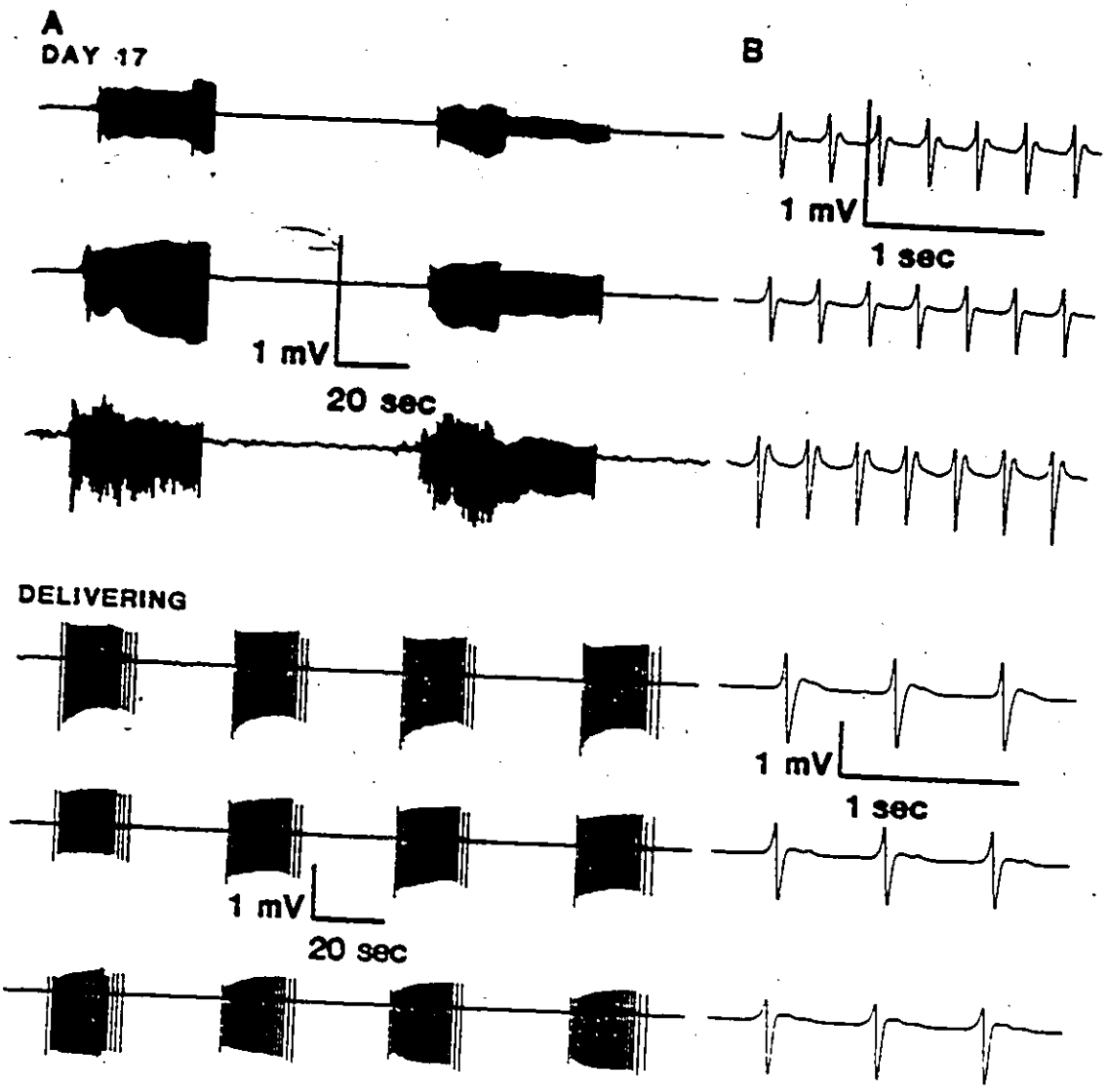
A
DAY 17
B
1 mV
1 sec
1 mV
20 sec
DELIVERING
1 mV
1 sec
1 mV
20 sec

FIGURE 9. Entrainment of spontaneous burst discharges in the longitudinal axis of the preterm (day 17) pregnant rat uterus. Extracellular electrical activity was recorded simultaneously at 6 sites in the long axis of a longitudinal uterine strip. Inter-electrode distance = 3 mm. Entrainment distance = 15 mm.

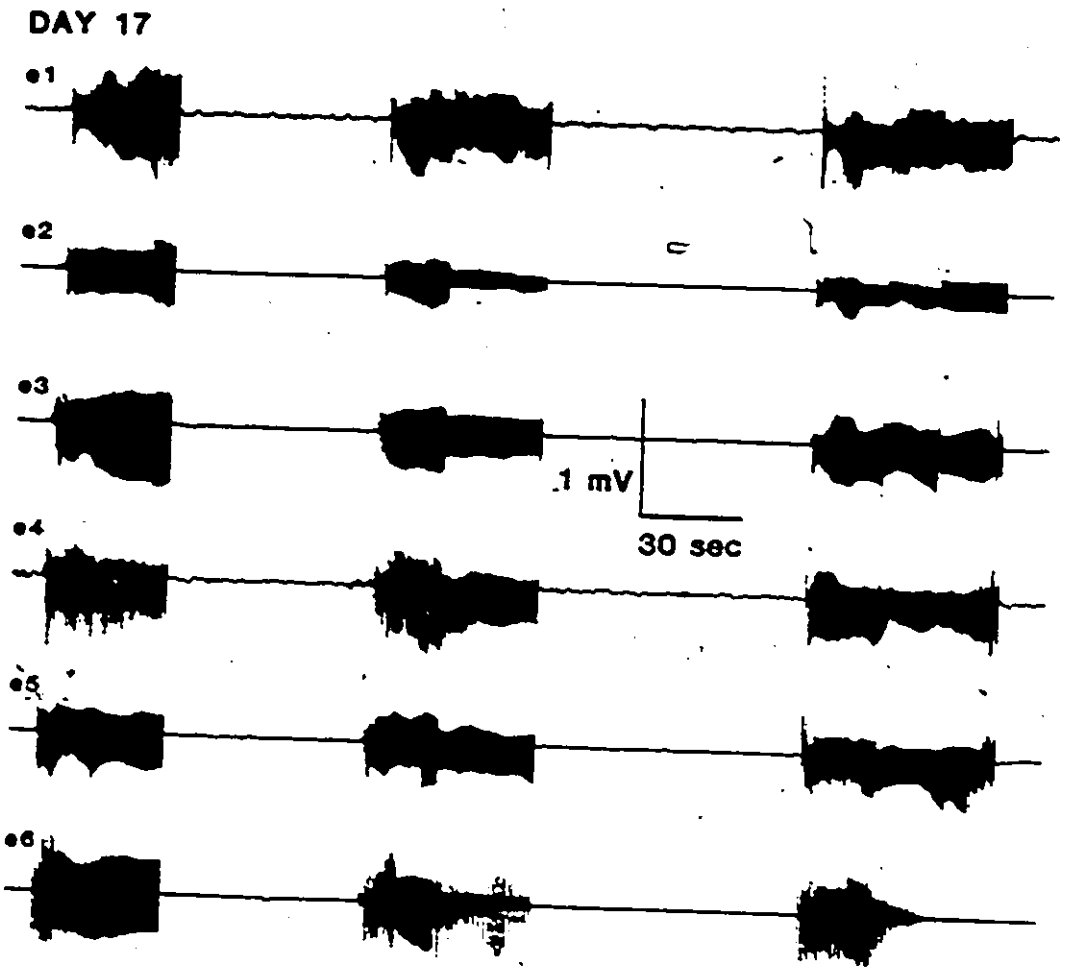
DAY 17
e1
e2
e3
.1 mV
30 sec
e4
e5
e6

FIGURE 10. Entrainment of spontaneous burst discharges in the delivering rat uterus. Extracellular electrical activity was recorded simultaneously at 6 sites in the long axis of a longitudinal uterine strip. Inter-electrode distance = 3 mm. Entrainment distance = 15 mm.

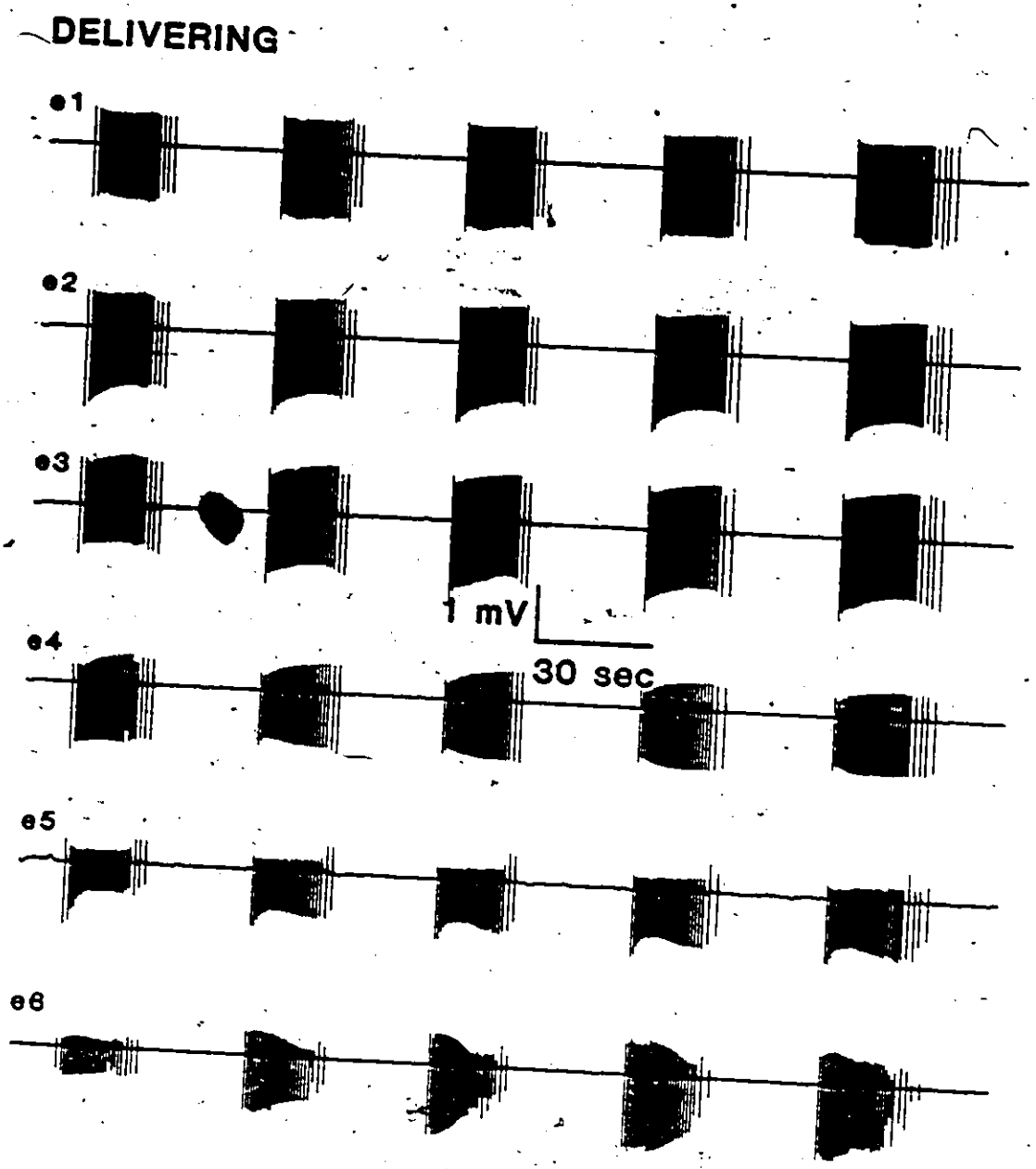
DELIVERING
e1
e2
e3
1 mV
30 sec
e4
e5
e6

FIGURE 11. Entrainment of spontaneous burst discharges in the transverse axis of the preterm pregnant (day 17) rat uterus. Extracellular electrical activity was recorded simultaneously at 6 sites in the long axis of a circular uterine strip. Inter-electrode distance = 3 mm. Variable entrainment distances of 3 mm, 6 mm and 3 mm (left to right) can be seen in this record. The mean entrainment distance from 7 strips was 5.01 $\pm$ 4.02 mm (median distance, 6 mm) (Table III).

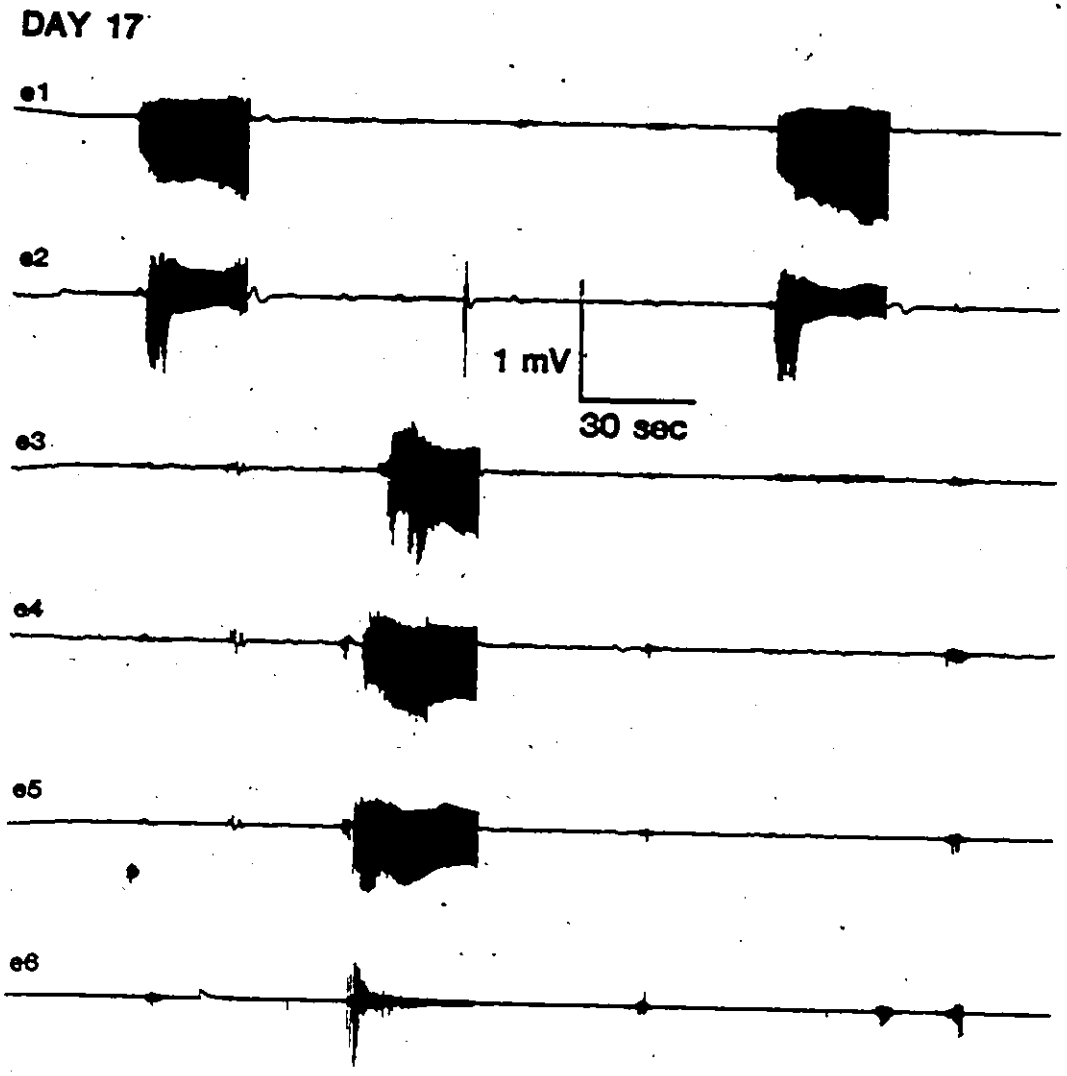
DAY 17
e1
e2
1 mV
30 sec
e3
e4
e5
e6

FIGURE 12. Entrainment of spontaneous burst discharges in the transverse axis of the delivering rat uterus. Extracellular electrical activity was recorded simultaneously at 6 sites in the long axis of a circular uterine strip. Inter-electrode distance = 3 mm. Distance of entrainment = 15 mm.

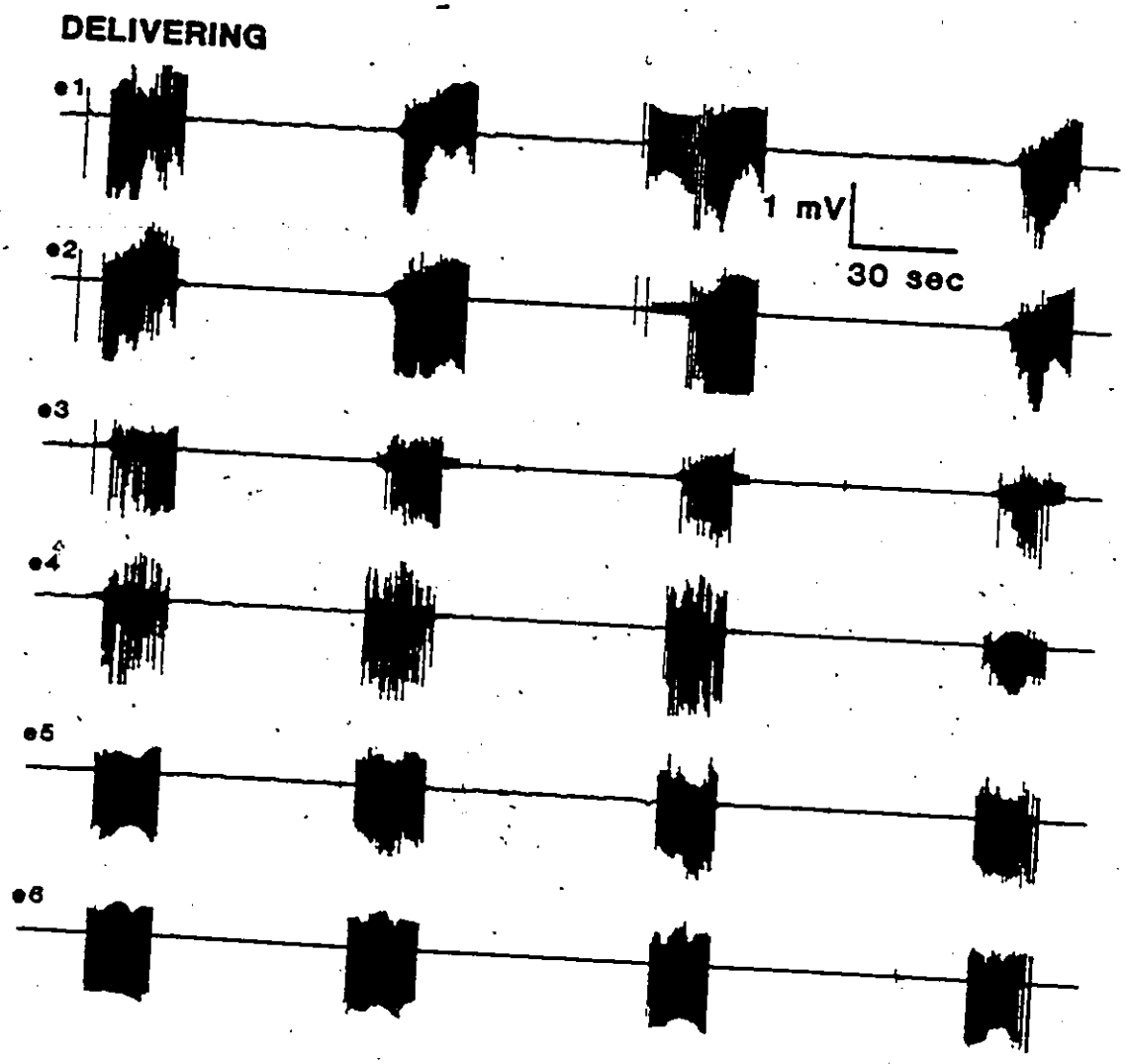
DELIVERING
1
2
3
4
5
6
1 mV
30 sec

FIGURE 13. Entrainment of spontaneous spike bursts in the longitudinal and transverse axes of the same uterine horn from a preterm pregnant (day 17) rat. Extracellular electrical activity was recorded simultaneously at 6 sites in the long axes of the uterine strips after treatment with 1 $\mu$g/ml of TTX. Inter-electrode distance = 3 mm. A). Longitudinal uterine strip. Entrainment distance = 15 mm. B). Circular uterine strip. Variable entrainment distances of 9 mm, 3 mm and 0 mm (left to right) can be seen in this record. From 3 TTX-treated circular strips, a mean entrainment distance of 4.71 $\pm$ 4.22 mm (median distance, 6 mm) was obtained.

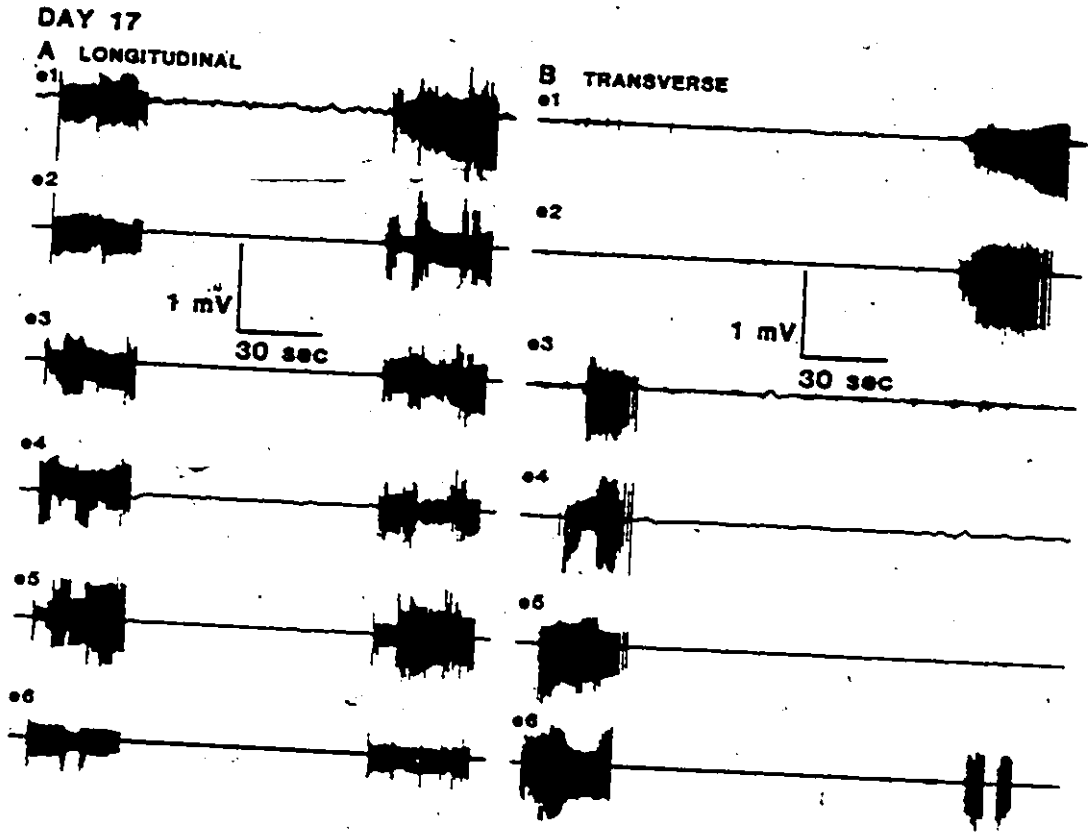
DAY 17
A LONGITUDINAL
B TRANSVERSE
e1
e2
e3
e4
e5
e6
1 mV
30 sec
1 mV
30 sec

FIGURE 14. Entrainment of spontaneous spike bursts in the longitudinal and transverse axes of the same uterine horn from a delivering rat. Extracellular electrical activity was recorded simultaneously at 6 sites in the long axes of the uterine strips, after treatment with 1 $\mu$g/ml of TTX. A). Longitudinal uterine strip. Entrainment distance = 15 mm. B). Circular uterine strip. Entrainment distance = 15 mm.

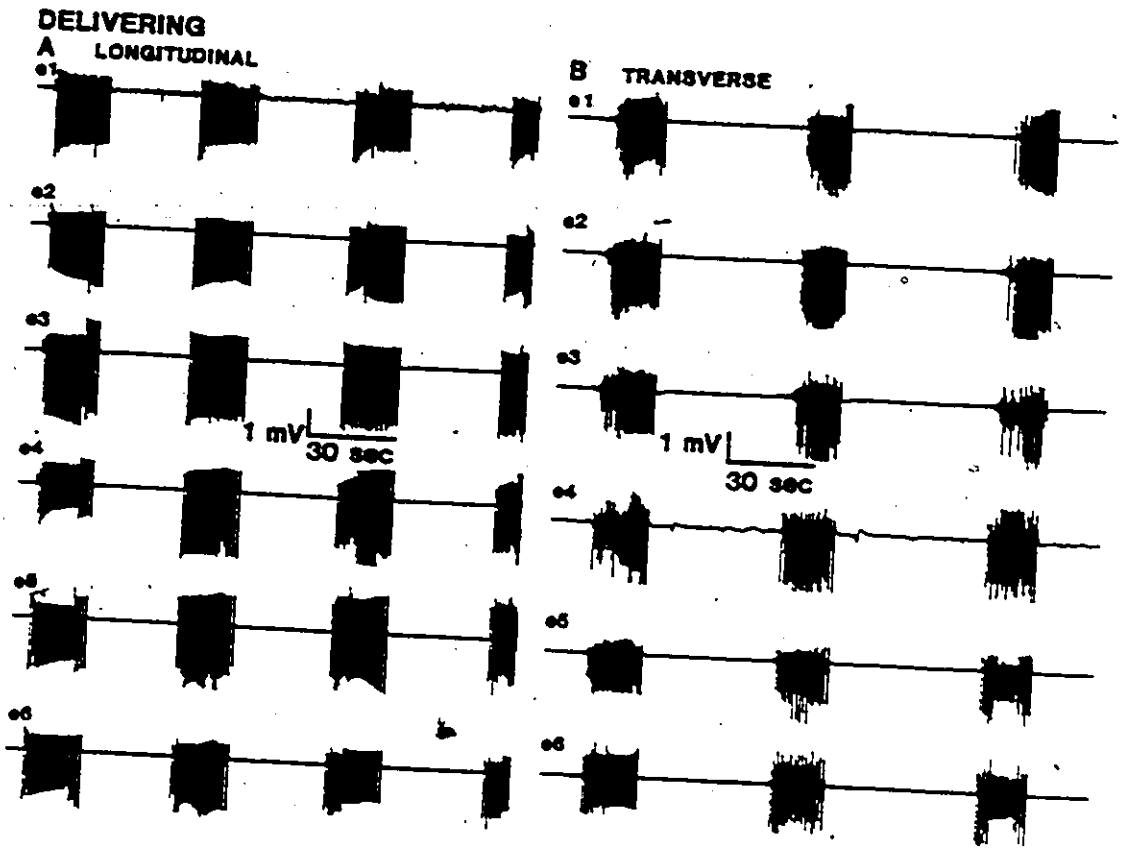
DELIVERING
A LONGITUDINAL
e1
e2
e3
1 mV
30 sec
e4
e5
e6
B TRANSVERSE
e1
e2
e3
1 mV
30 sec
e4
e5
e6

FIGURE 15. "Excitable" region in the longitudinal axis of the preterm pregnant (day 17) rat uterus. Records are fast speed (10 mm/sec) traces of the individual spikes comprising the beginnings (A) and ends (B) of spike bursts simultaneously recorded at 6 sites in the long axis of a longitudinal uterine strip. Inter-electrode distance = 3 mm. Unequal spike numbers are seen at the beginnings (A), while equal spike numbers are seen at the ends (B) of the spike bursts. Arrows indicate where spikes recorded at an electrode site are either not conducted into or are conducted into but not past (i.e. monophasic shape) the adjacent electrode site. Dotted lines indicate the time when the bursts become completely coupled at adjacent electrode sites. In this record, only electrodes "5" and "6" are in the same "excitable" region at the onset of the bursts: "excitable" region = 3 mm.

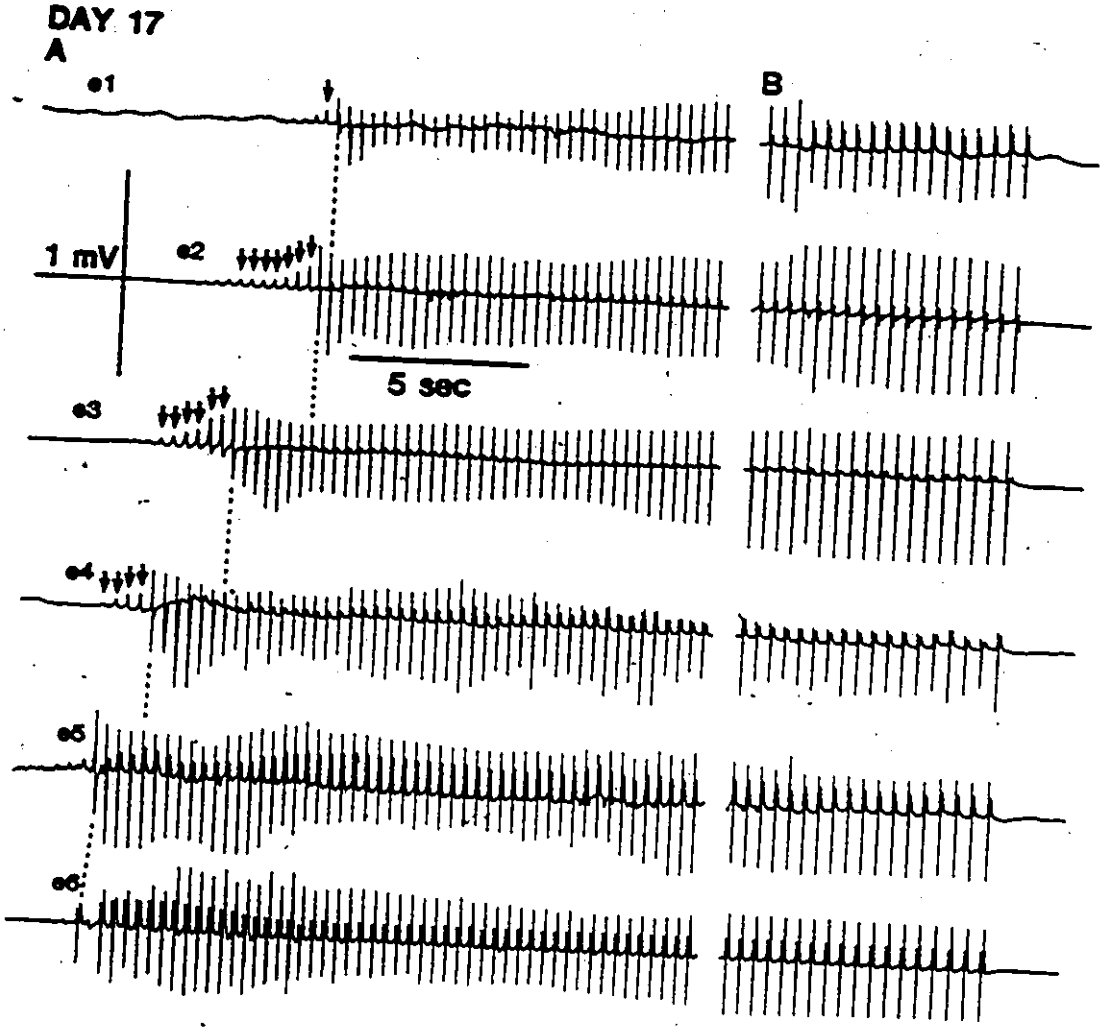
DAY 17
A
B
e1
1 mV
e2
5 sec
e3
e4
e5
e6

FIGURE 16. Variable lengths of the "excitable" region in the longitudinal axis of a preterm pregnant (day 17) rat uterus. Records are fast speed (10 mm/sec) traces of the individual spikes comprising the beginnings of bursts simultaneously recorded at 6 sites in the same longitudinal strip. Inter-electrode distance = 3 mm. Dotted lines connect electrode sites that are in the same "excitable" region. Lengths are (A) 3 mm, (B) 3 mm, 6 mm and (C) 9 mm. The mean length of the "excitable" region in 30 sets of bursts from 5 uterine horns was $6.10 \pm 3.48$ mm.

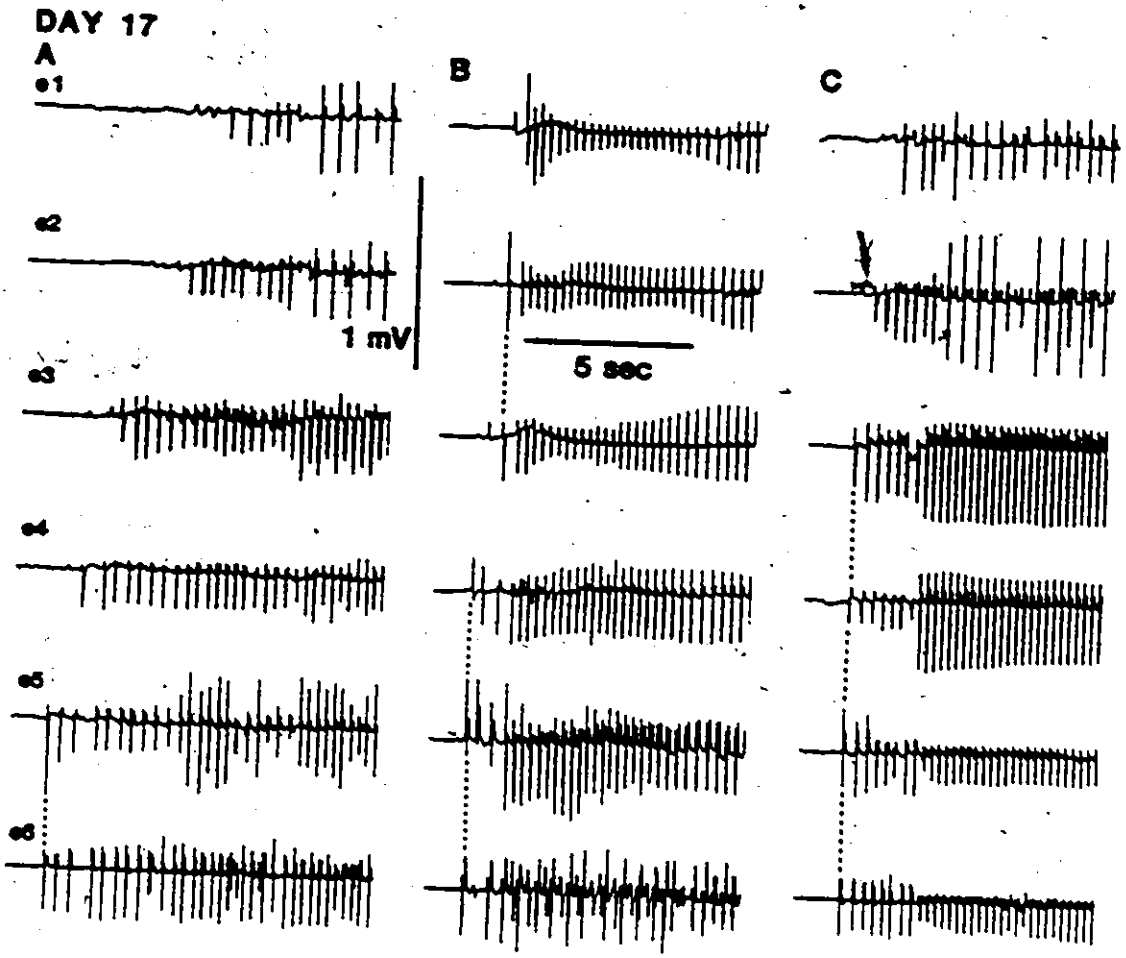
DAY 17
A
B
C
e1
e2
e3
e4
e5
e6
1 mV
5 sec

FIGURE 17. Long (15 mm) "excitable" region in the longitudinal axis of preterm pregnant (day 17) rat uterus. Records are fast speed (10 mm/sec) traces of the individual spikes comprising the beginnings (A) and ends (B) of spike bursts simultaneously recorded at 6 sites along a longitudinal uterine strip (same strip as in Fig. 16). Inter-electrode distance = 3 mm. Of 30 sets of bursts, only 2 sets showed "excitable" regions of 15 mm.

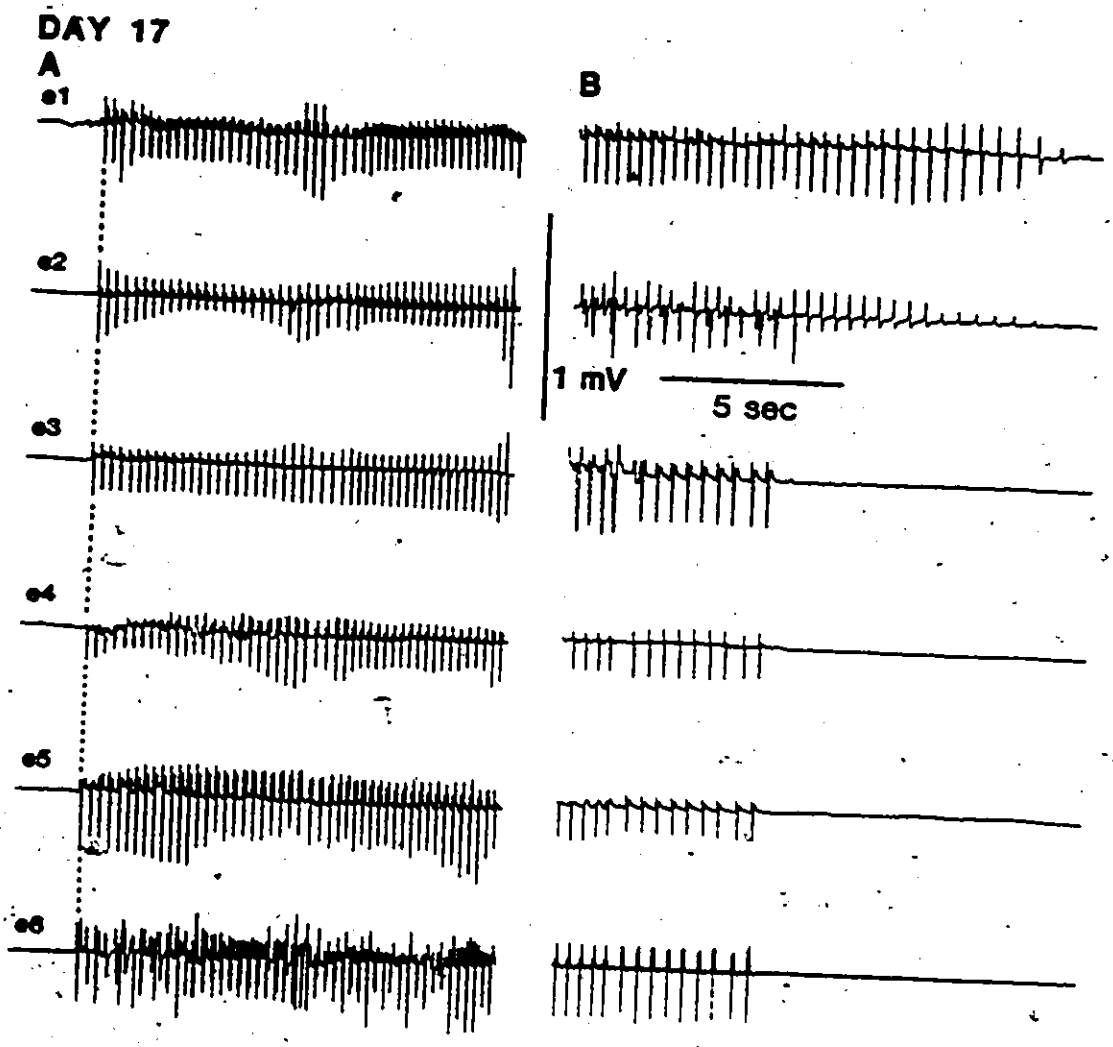
DAY 17
A
B
e1
e2
e3
e4
e5
e6
1 mV
5 sec

FIGURE 18. Effect of TTX on the "excitable" region in the longitudinal axis of preterm pregnant (day 17) rat uterus. Records are fast speed (10 mm/sec) traces of the beginnings of spike bursts simultaneously recorded at 6 sites in the long axes of 3 different longitudinal uterine strips treated with 1 $\mu$g/ml of TTX. Inter-electrode distance = 3 mm. The mean length of the "excitable" regions in 15 sets of bursts from these strips ($6.40 \pm 3.56$ mm) was not significantly different ($p = .8$) from the mean length in the untreated strips.

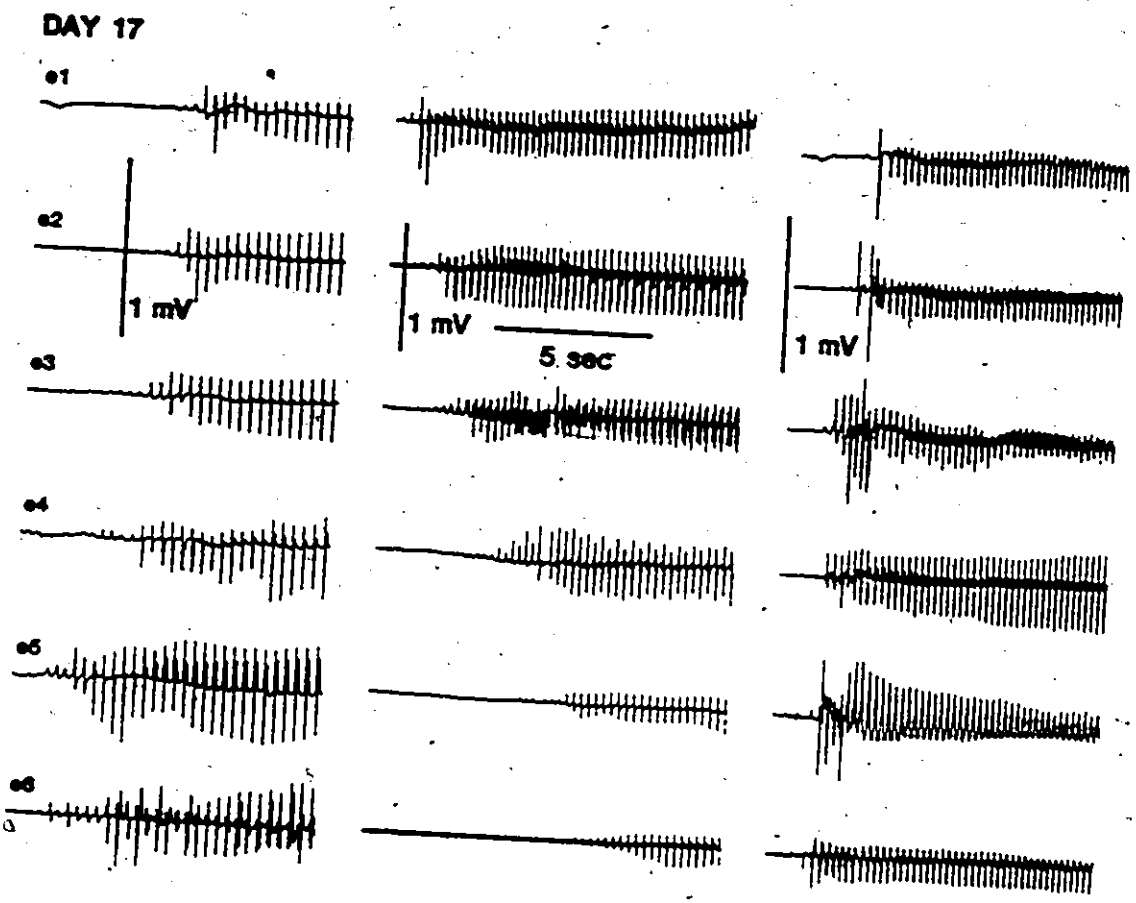
DAY 17
e1
e2
1 mV
1 mV
5 sec
1 mV
e3
e4
e5
e6

FIGURE 19. "Excitable" region in the longitudinal axis of the delivering rat uterus. Records are fast speed (10 mm/sec) traces of the individual spikes comprising the (entire) bursts simultaneously recorded at 6 sites in the long axis of a longitudinal uterine strip. Inter-electrode distance = 3 mm. Equal spike numbers are seen throughout the entire burst. "Excitable" region = 15 mm.

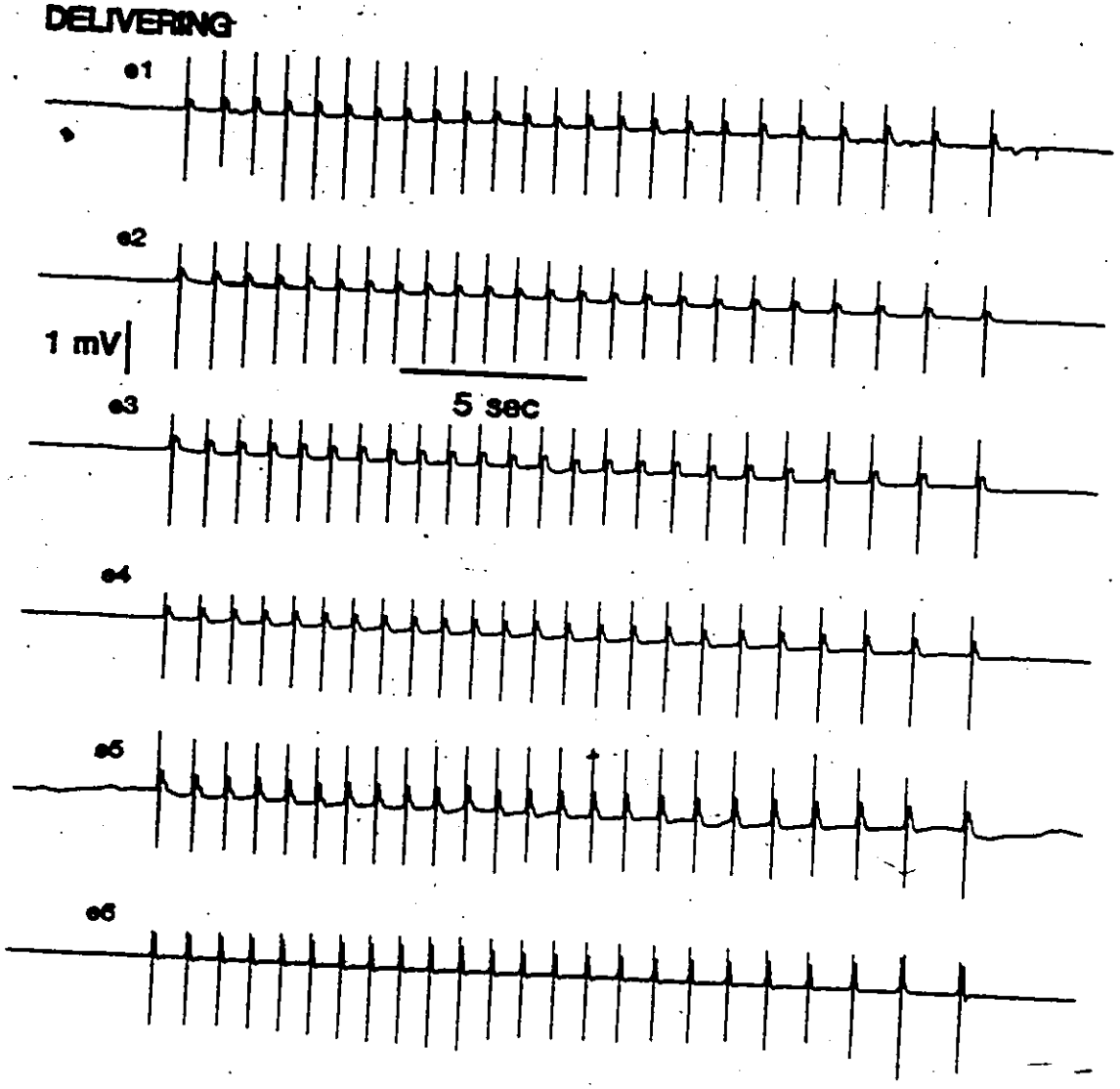
DELIVERING
e1
e2
1 mV
5 sec
e3
e4
e5
e6

FIGURE 20. "Excitable" region shorter than 15 mm, in the longitudinal axis of the delivering rat uterus. Electrical activity was recorded simultaneously at 6 sites in the long axis of a longitudinal uterine strip. Inter-electrode distance = 3 mm. Arrow indicates a low amplitude (monophasic shaped) spike that was presumably conducted into but not past the area of the tissue under electrode "1", i.e. the "excitable" region = 12 mm. Of 30 sets of bursts from 5 uterine horns, only 3 sets (from the same uterine horn) showed "excitable" regions that were shorter than 15 mm. The mean length of the "excitable" region in the delivering longitudinal strips was 14.80 $\pm$ .76 mm.

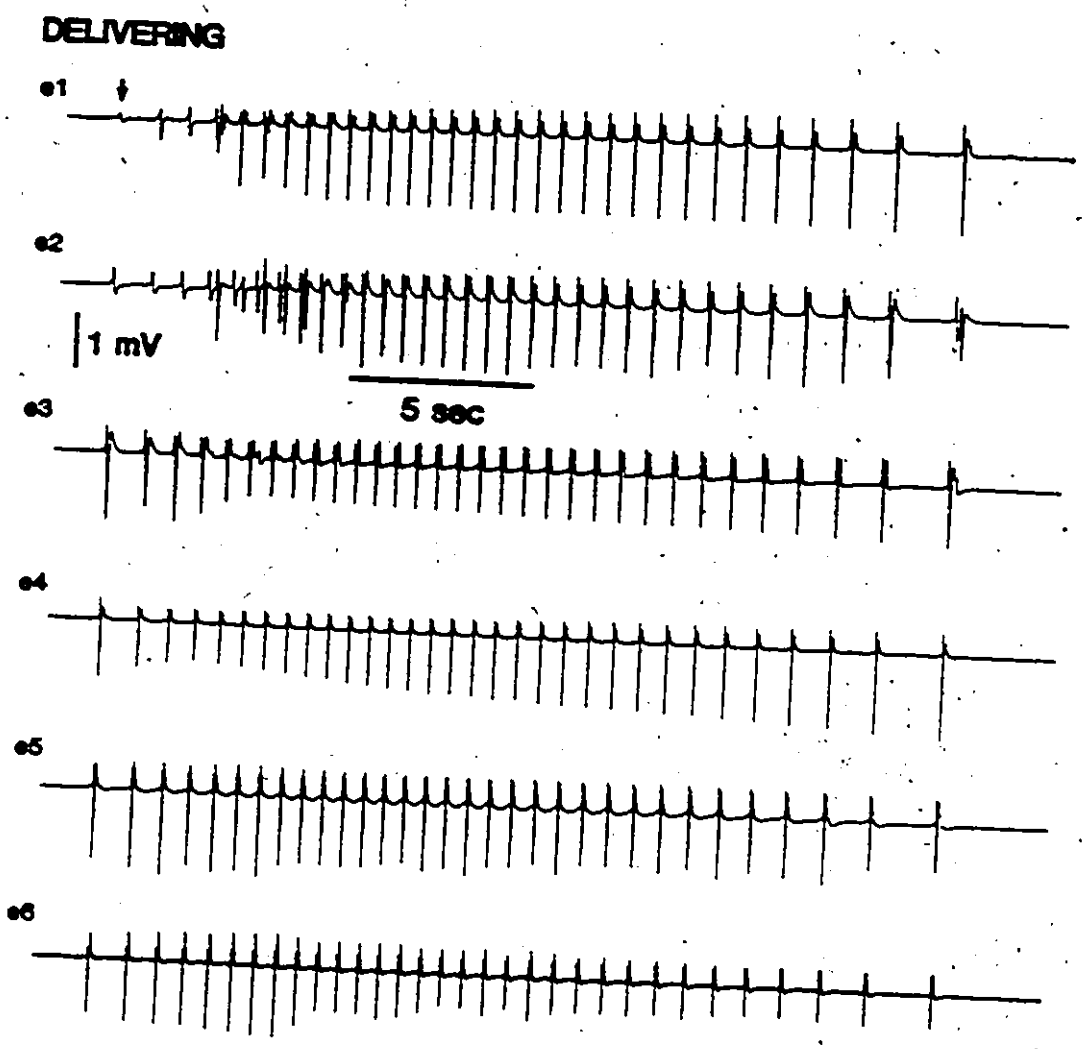
DELIVERING
e1
e2
1 mV
5 sec
e3
e4
e5
e6

FIGURE 21. Effect of TTX on the "excitable" region in the longitudinal axis of the delivering rat uterus. Records are fast speed (10 mm/sec) traces of spike bursts recorded simultaneously at 6 sites in the long axis of a longitudinal strip treated with 1 μg/ml TTX. Inter-electrode distance = 3 mm. Equal spike numbers are seen throughout the entire burst. The mean length of the "excitable" region (15 ± 0 mm) was similar to the mean length in the untreated strips.

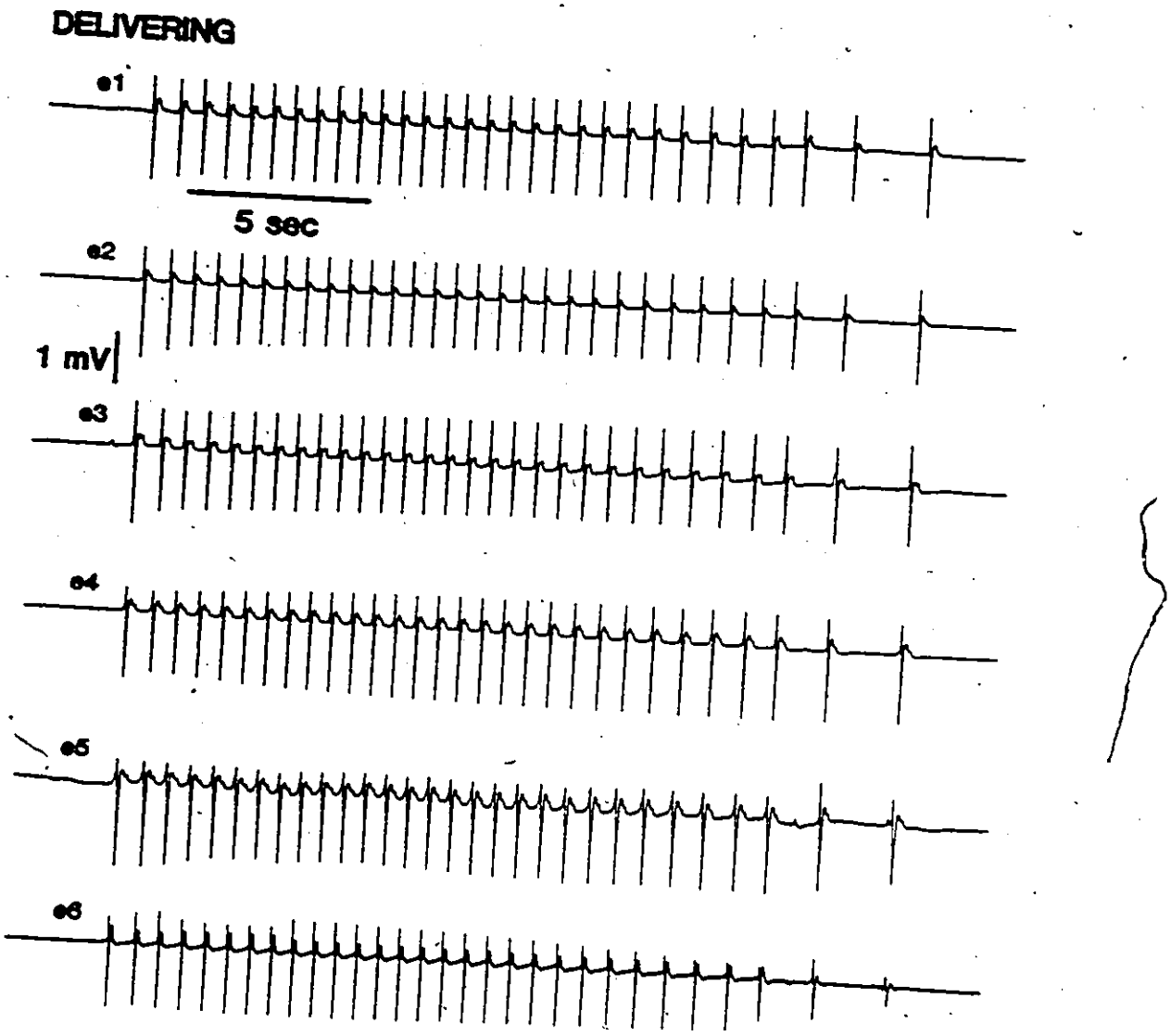
DELIVERING
e1
5 sec
e2
1 mV
e3
e4
e5
e6

FIGURES 22-23. "Excitable" regions in the transverse axis of preterm pregnant (day 17) rat uterus. Records are traces of the spike bursts (A) and the individual spikes comprising the beginnings of the bursts (B) simultaneously recorded at 6 sites in the long axis of a circular uterine strip. Inter-electrode distance = 3 mm.

FIGURE 22. A). Burst entrainment distance = 9 mm. B). "Excitable" region < 3 mm.

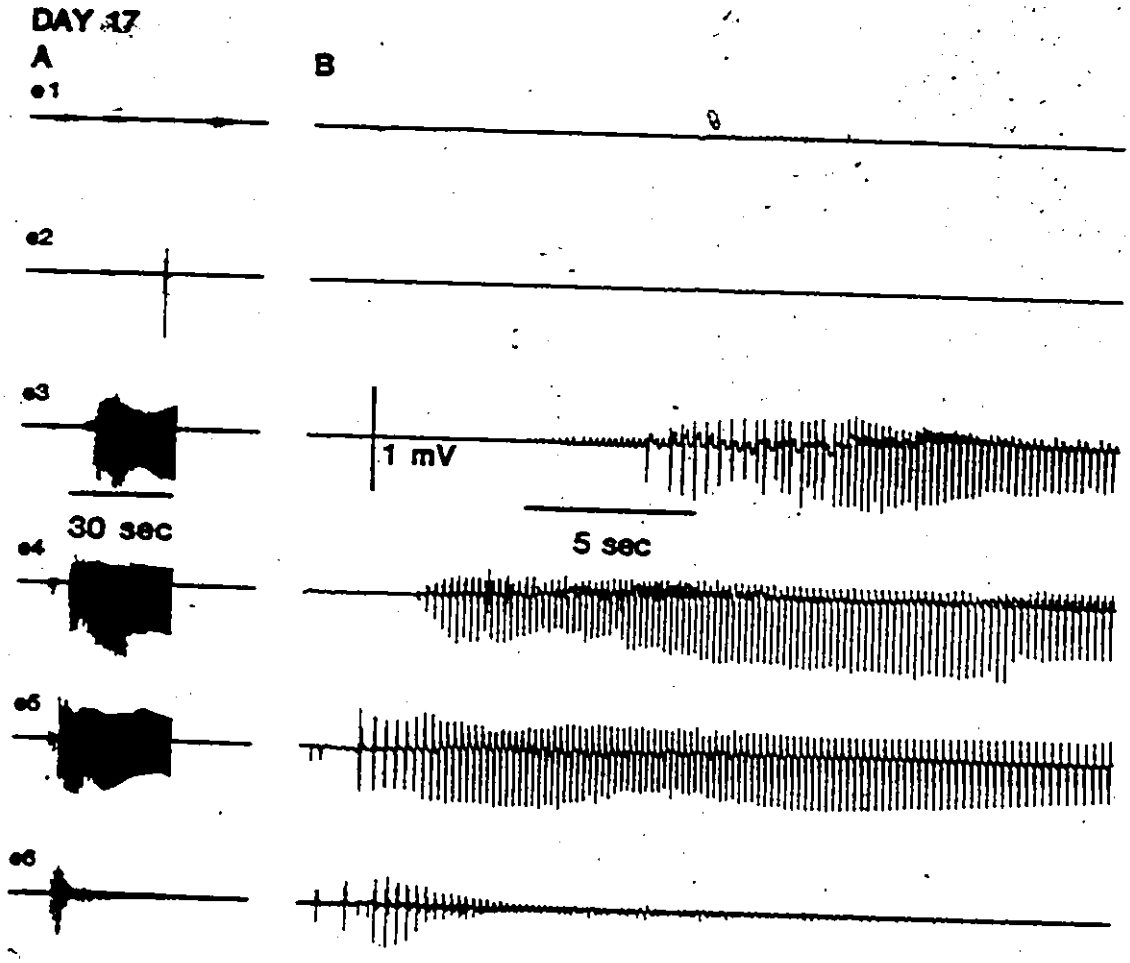
DAY 17
A
B
e1
e2
e3
1 mV
30 sec
5 sec
e4
e5
e6

FIGURE 23. A). Burst entrainment distance = 15 mm.

B). "Excitable" region = 3 mm. Of 24 sets of bursts from 6 circular strips (5 uterine horns), the mean length of the "excitable" region was 3.00 ± 1.77 mm.

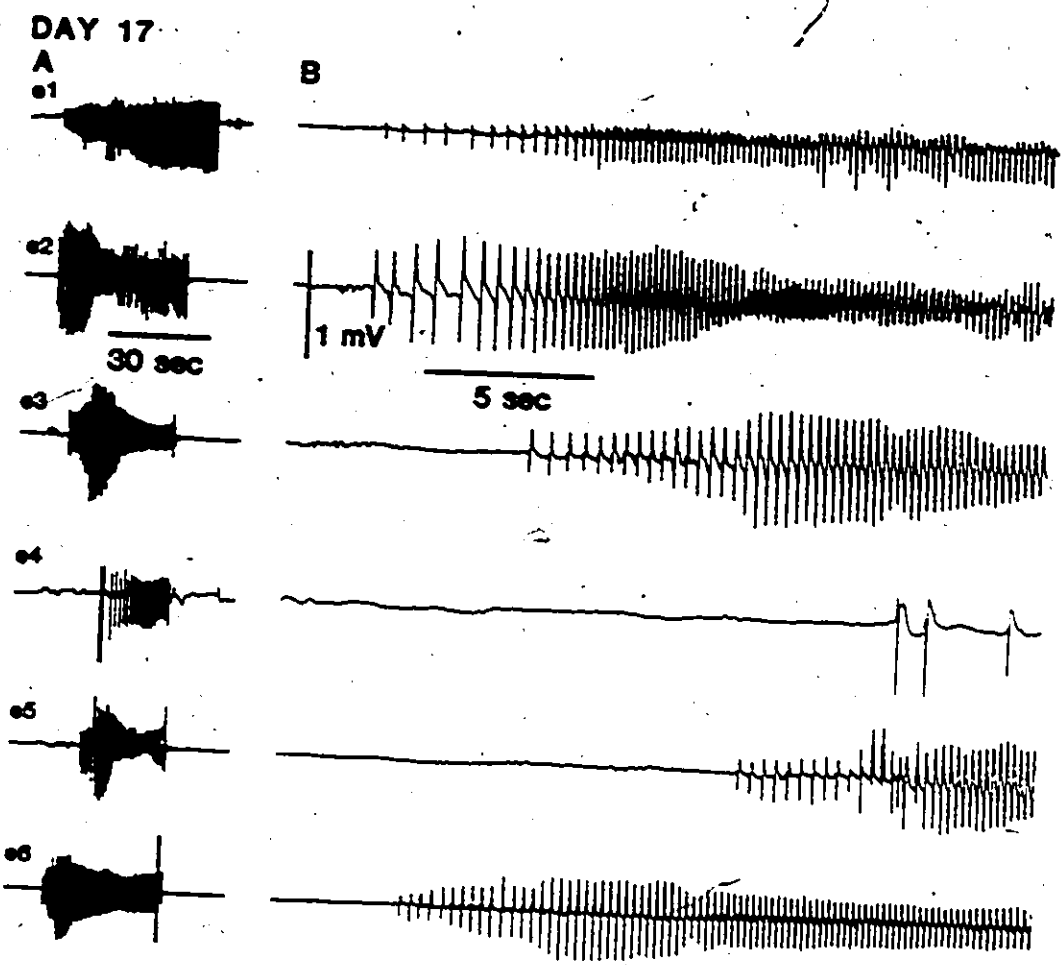
DAY 17
A
B
e1
e2
e3
e4
e5
e6
30 sec
1 mV
5 sec

FIGURE 24. Effect of TTX on the "excitable" region in the transverse axis of preterm pregnant (day 17) rat uterus. Records are traces of the spike bursts (A) and the individual spikes comprising the beginnings of the bursts (B) simultaneously recorded at 6 sites in the long axis of a circular uterine strip treated with 1 μg/ml of TTX. Inter-electrode distance = 3 mm. A). Burst entrainment distance = 9 mm. B). "Excitable" region < 3 mm. In 2 preterm circular strips treated with tetrodotoxin, the "excitable" regions were ≤ 3 mm.

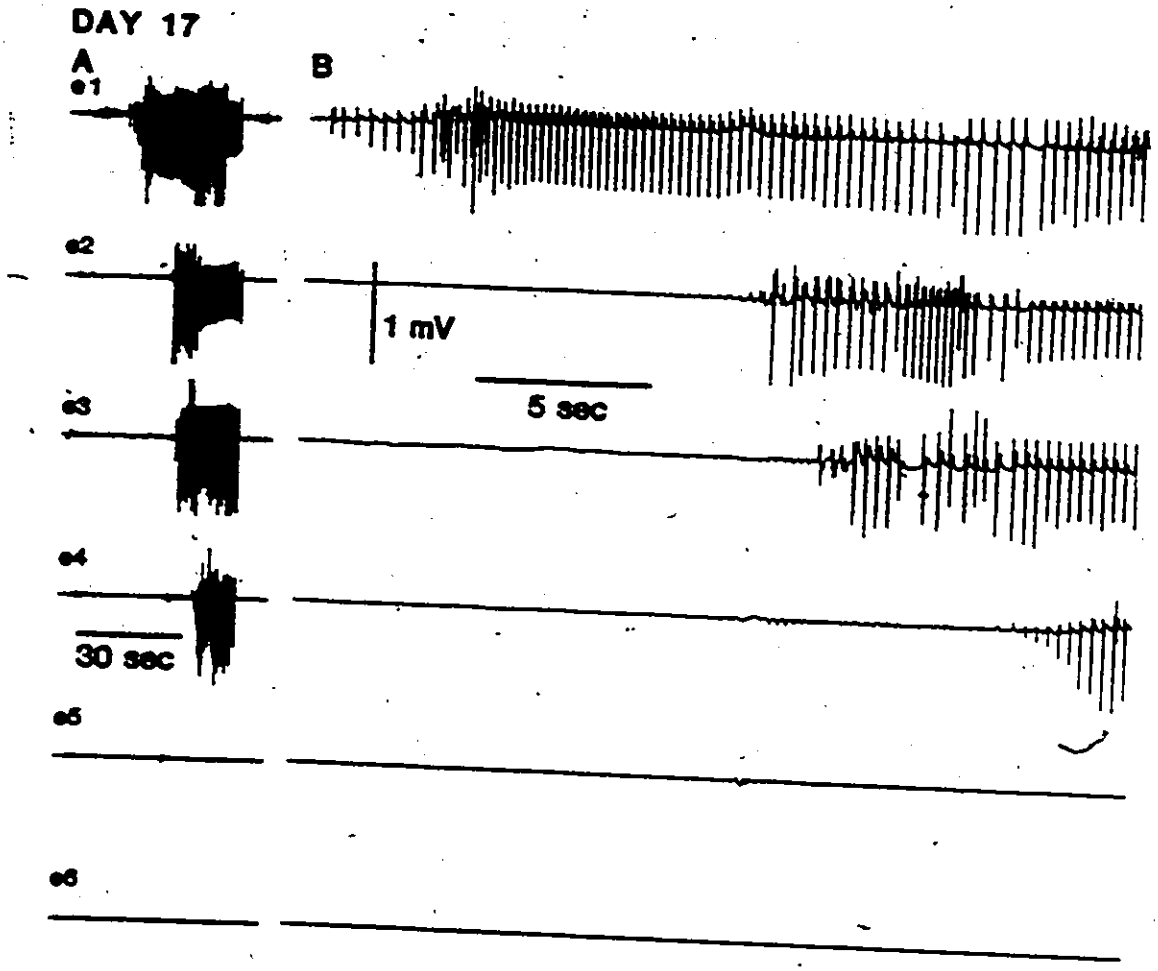
DAY 17
A
B
e1
e2
1 mV
5 sec
e3
e4
30 sec
e5
e6

FIGURE 25. "Excitable" region in the transverse axis of a delivering rat uterus. Records are fast speed (10 mm/sec) traces of spike bursts simultaneously recorded at 6 sites in the long axis of a circular uterine strip. Inter-electrode distance = 3 mm. "Excitable" region = 6 mm. Of 20 sets of bursts from 5 circular strips (4 uterine horns), the mean length of the "excitable" region was 6.60 $\pm$ 1.23 mm.

DELIVERING

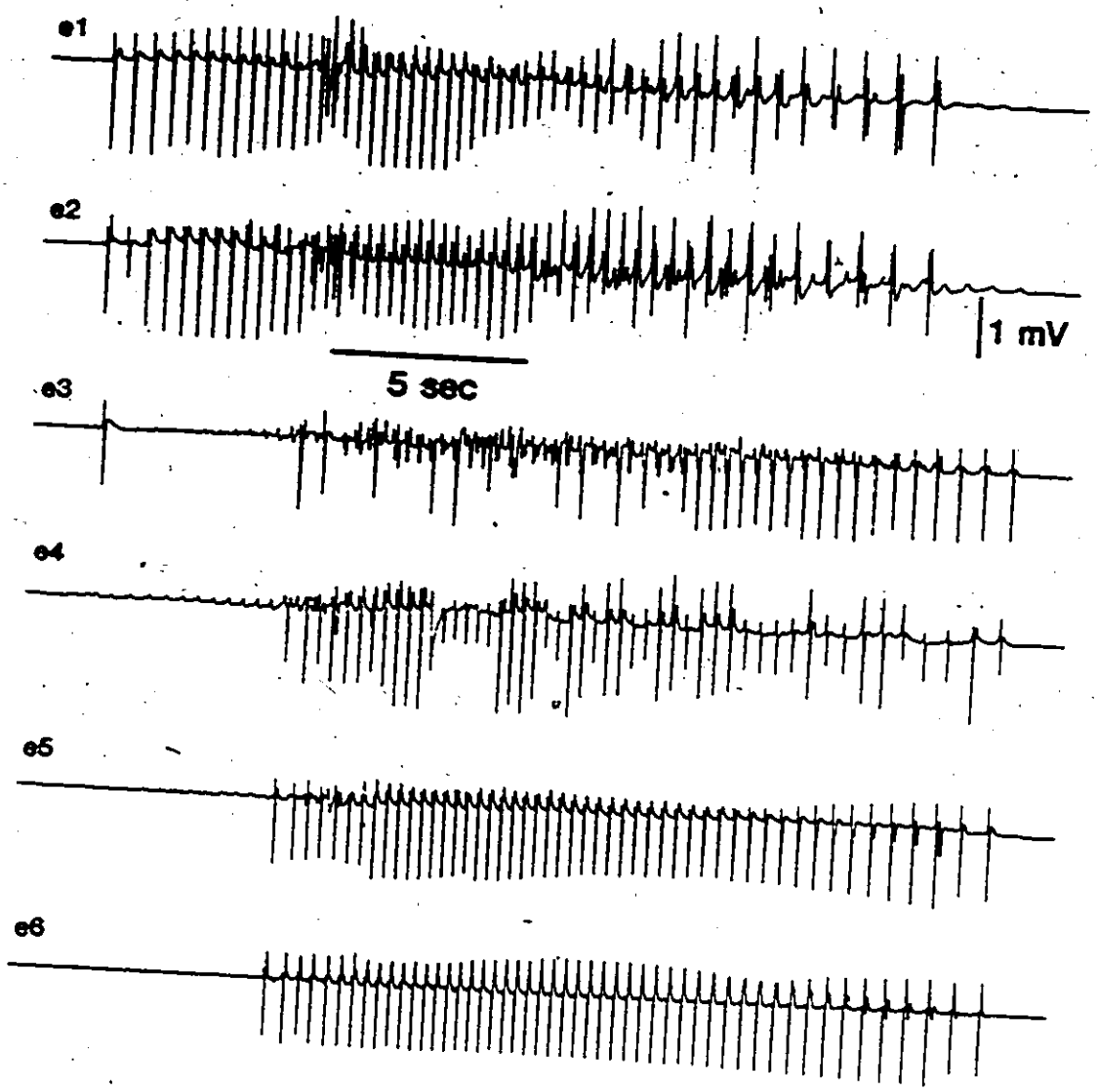

FIGURE 26. Effect of TTX on the "excitable" region in the transverse axis of a delivering rat uterus. Records are fast speed (10 mm/sec) traces of spike bursts simultaneously recorded at 6 sites in the long axis of circular uterine strip treated with 1 μg/ml of TTX. Inter-electrode distance = 3 mm. "Excitable" region = 6 mm. In 2 delivering circular strips (2 uterine horns) treated with tetrodotoxin, the "excitable" regions were 6 mm.

DELIVERING

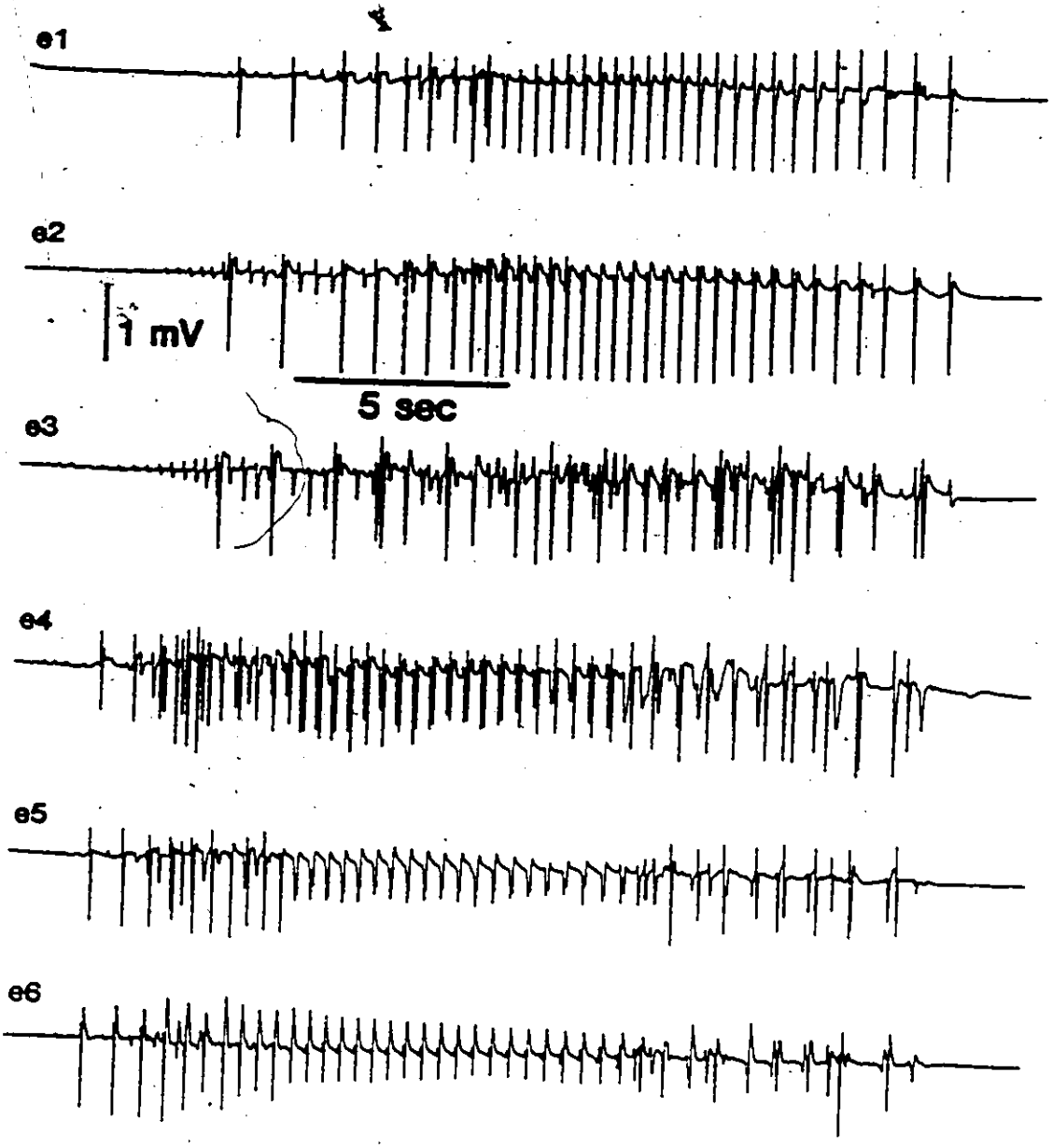

FIGURE 27. Entrainment of bursts before and after partitioning a longitudinal strip from a delivering rat uterus into 3 segments. The 6 electrodes were placed in 3 pairs (6 mm apart) along the long axis of the strip. Inter-electrode distance = 3 mm. A). In the intact strip, bursts were entrained over the 21 mm recording distance. Arrows indicate where small pins were placed across the strip prior to cutting. B)-C). The strip was sectioned between electrodes "4" and "5". Arrows indicate the time of cutting in (B). Cutting uncoupled the spike bursts and altered their discharge frequencies, as described in the text. D)-E). Ten minutes later, the strip was sectioned between electrodes "2" and "3". Arrows indicate the time of cutting. Cutting uncoupled the spike bursts and altered their discharge frequencies, as described in the text.

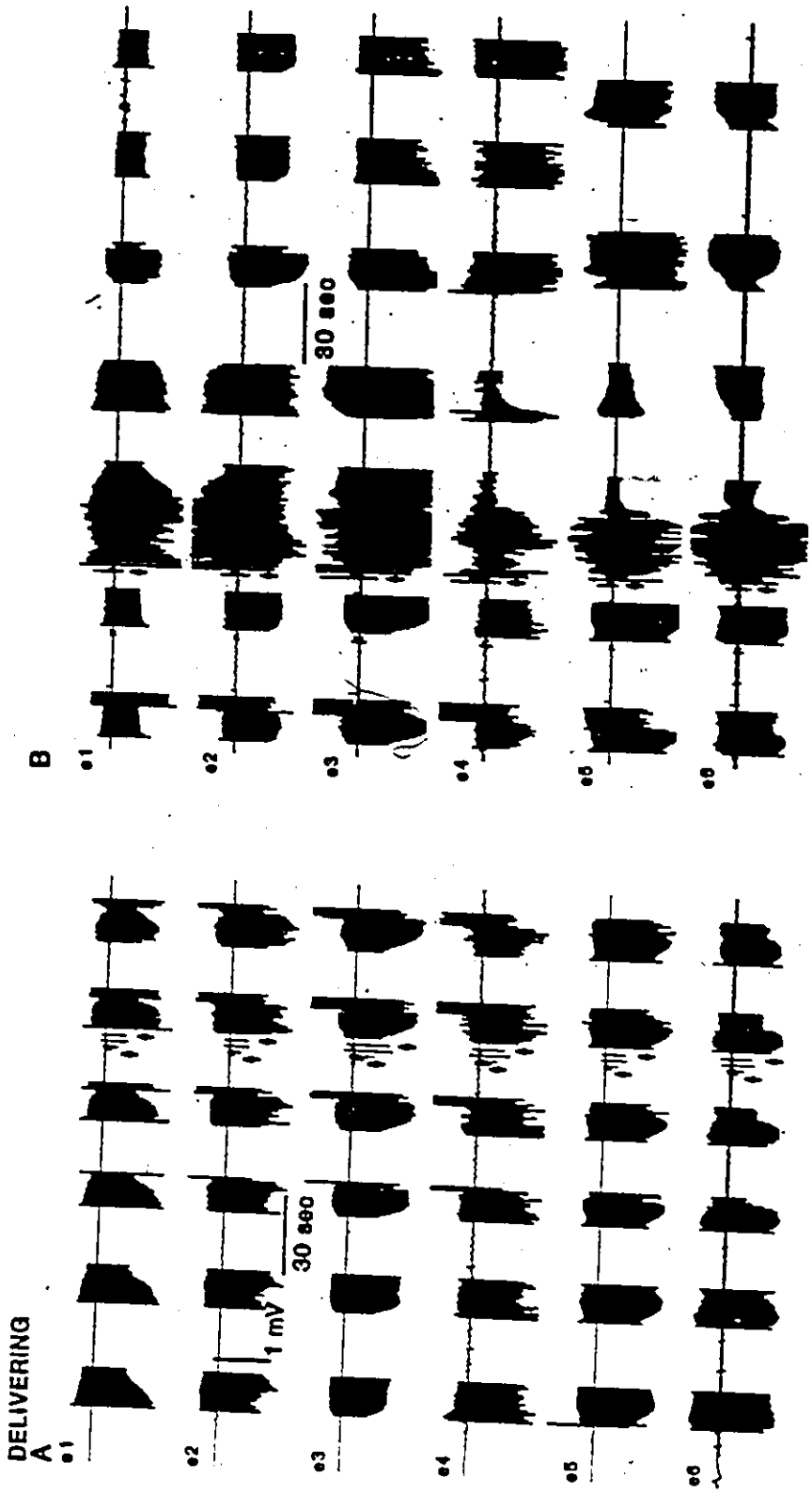
B
DELIVERING
A
30 sec
1 mV
30 sec

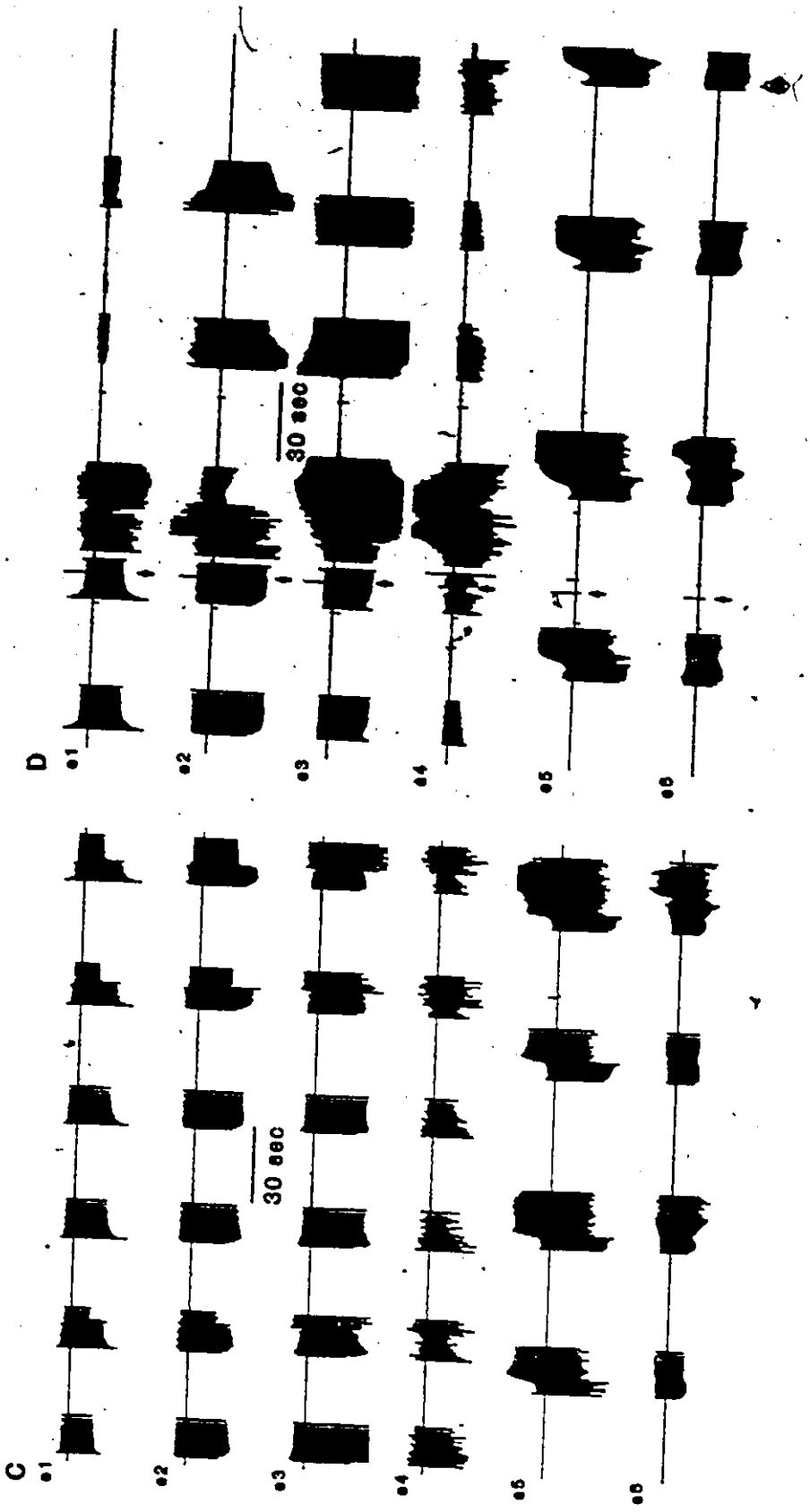
D
C
30 sec
30 sec
1
2
3
4
5
6

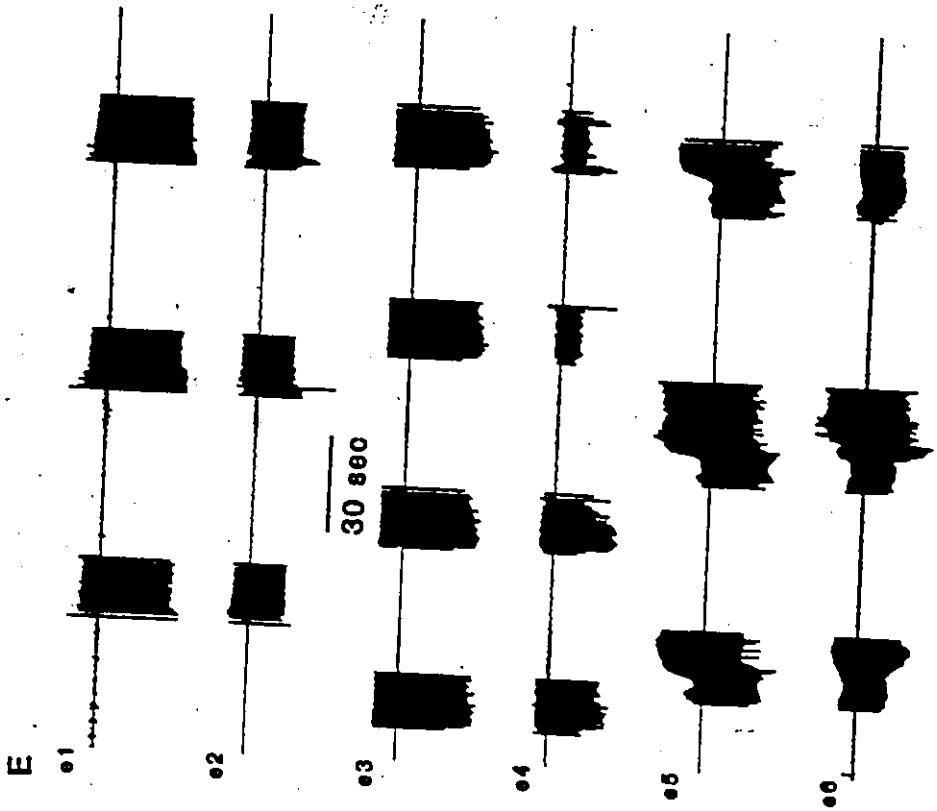
E
e1
e2
e3
e4
e5
e6
30 sec

FIGURE 28. Entrainment of bursts before and after partitioning into 3 segments a longitudinal strip from a preterm pregnant (day 17) rat uterus. The 6 electrodes were arranged in 3 pairs (6 mm apart) along the long axis of the strip. Inter-electrode distance = 3 mm. A). Intact strip. Bursts were entrained over the 21 mm recording distance. B). The strip was sectioned between electrodes "4" and "5" and then 10 minutes later (C) between electrodes "2" and "3". Cutting uncoupled the burst oscillators and altered their discharge frequencies, as described in the text.

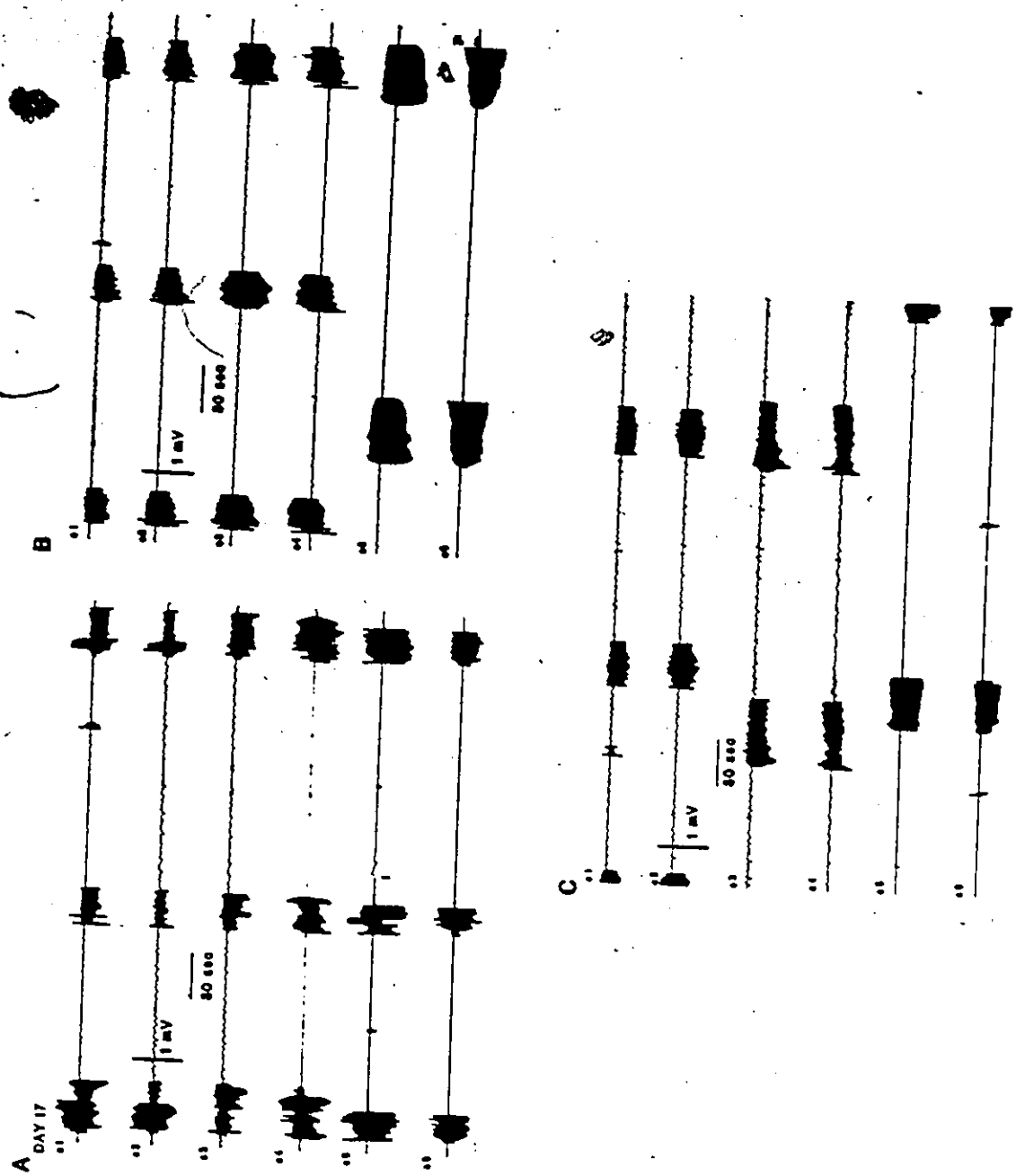
A
DAY 17
B
C
1 mV
50 sec

FIGURE 29. Effect of TTX on the uncoupling of spike bursts caused by partitioning into segments a longitudinal uterine strip from a preterm pregnant (day 17) rat. The 6 electrodes were arranged in 3 pairs (6 mm apart). Inter-electrode distance = 3 mm. A). Intact strip, pretreated with 1 $\mu$g/ml of TTX. Bursts were entrained over the 21 mm recording distance. B). Partitioning the strip between electrodes "2" and "3" and then between electrodes "4" and "5" uncoupled the bursts and altered their discharge frequencies, as in the untreated strips (see text).

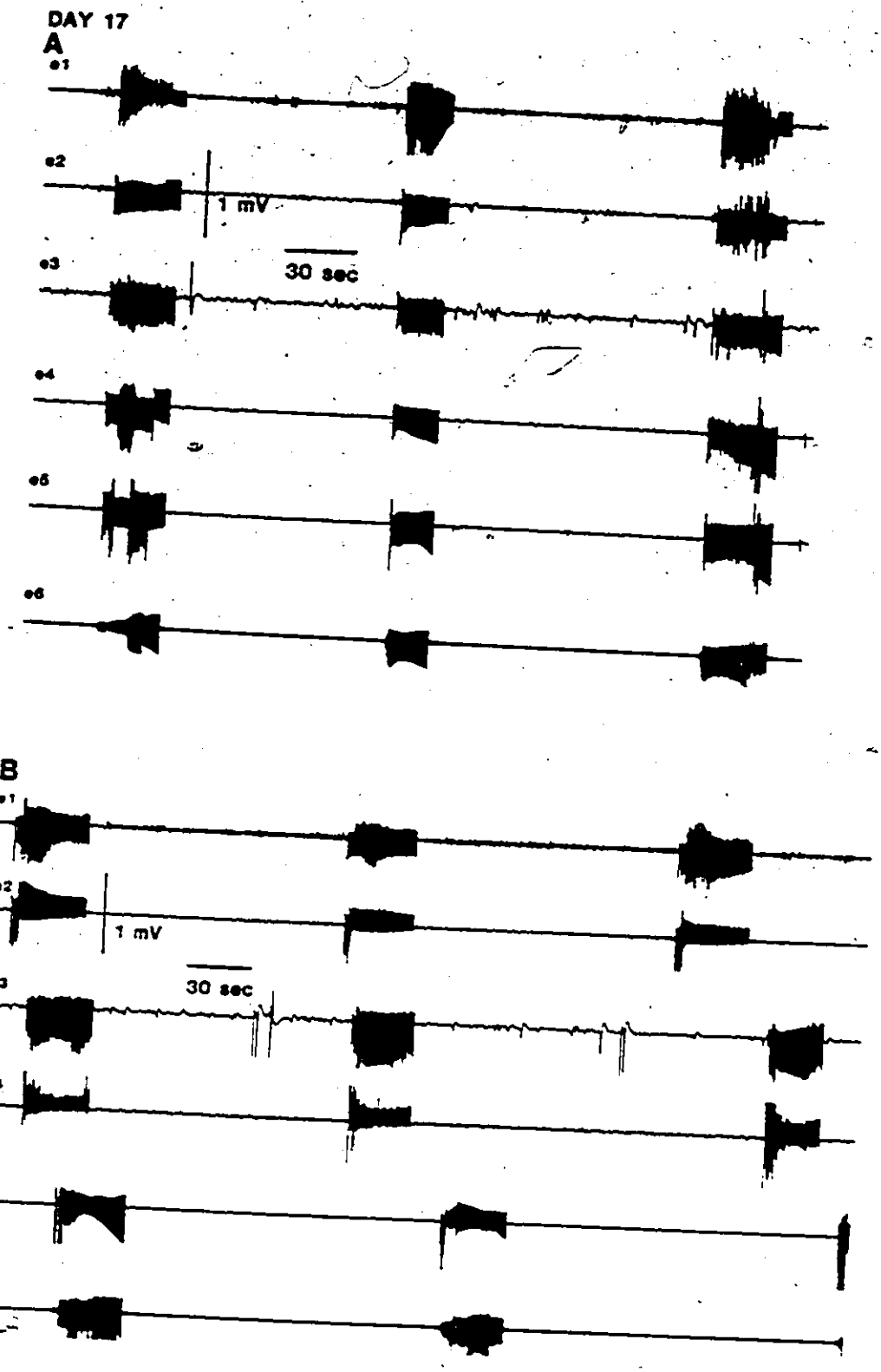
DAY 17
A
e1
e2
1 mV
30 sec
e3
e4
e5
e6
B
e1
e2
1 mV
30 sec
e3
e4
e5
e6

FIGURE 30. Entrainment of bursts in the transverse axis of the myometrium (delivering rat uterus) before (A) and after (B) damaging the circular muscle. The 6 electrodes were arranged in 2 groups (6 mm apart) of 3 electrodes along the long axis of a circular uterine strip. Inter-electrode distance = 3 mm. A). Intact strip. Bursts were entrained across the 18 mm recording distance. B). The endometrium and circular muscle in the portion of the strip between electrodes "3" and "4" were damaged by compressing that portion of the strip over a razor blade that was embedded in the floor of the muscle bath, as described in the text. Arrows indicate the time when the strip was compressed onto the razor blade. Bursts became uncoupled and their discharge frequencies altered on either side of the damaged tissue, as described in the text.

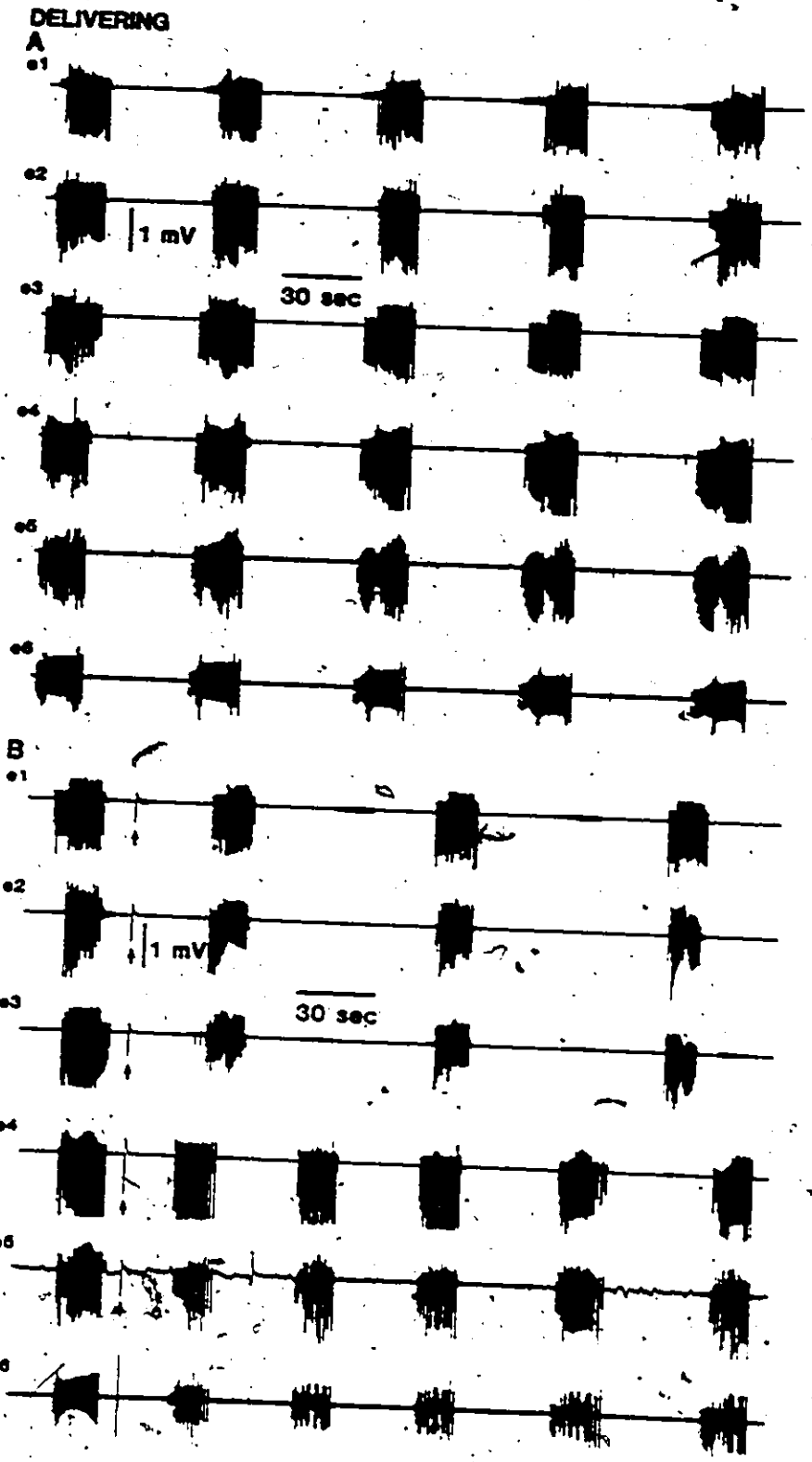
DELIVERING
A
e1
e2
1 mV
30 sec
e3
e4
e5
e6
B
e1
e2
1 mV
30 sec
e3
e4
e5
e6

FIGURE 31. Photomicrograph of a longitudinal section through a segment of the circular uterine strip used in the experiment of Figure 30. Tissue was fixed, embedded in Spurr resin and then sectioned so that the compressed area could be viewed in cross section. Sections were cut at .5 $\mu$m and then stained with trypan blue. A). Note that while cut (see arrow) extends partially into the endometrium (E), the circular (C) and longitudinal (L) muscle layers are intact. Bar, 100 $\mu$m. X 100. B). Higher power photograph reveals that the circular muscle above the compressed endometrium (between arrows) is damaged, as the muscle is poorly stained and the cell contours are altered. Bar, 40 $\mu$m. X 240.

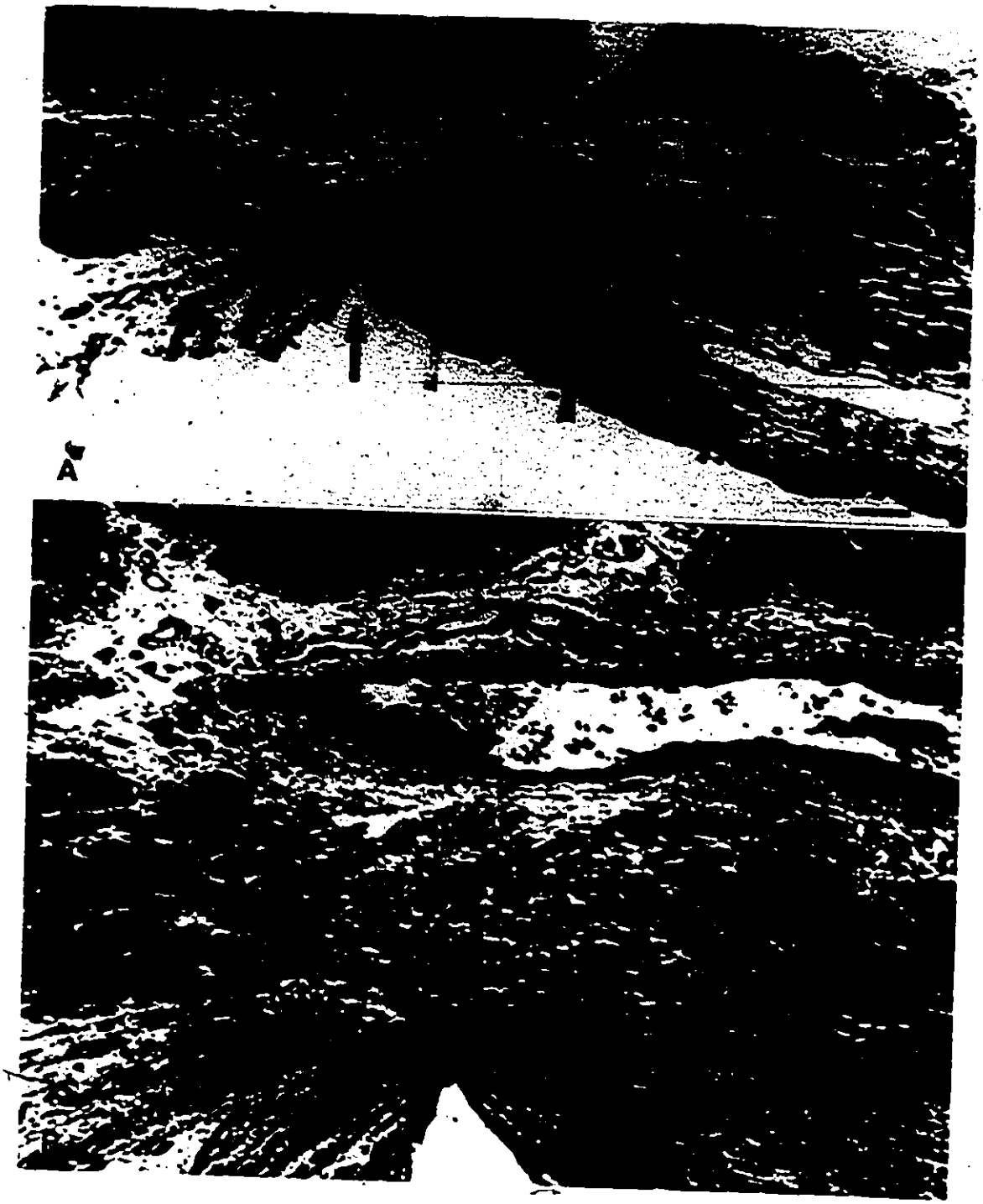
A

# CHAPTER 3

## Changes in Spike Propagation Associated With the Formation of Gap Junctions in the Myometrium at Parturition

## INTRODUCTION

It is widely believed that electrical and mechanical asynchrony of the uterine musculature allows maintenance of pregnancy, while synchronous activity promotes the onset and progress of labour, thereby terminating pregnancy (Csapo, 1981). Uterine contractions are initiated by action potentials which originate in pacemaker regions and propagate to neighbouring inactive cells (Kuriyama, 1961; Csapo, 1962; Marshall, 1962). During the progression of pregnancy, the amounts of humoral (e.g. estrogen and oxytocin) and local (e.g. prostaglandins) myometrial stimulants increase, as does the stimulation due to stretch caused by the growing uterine contents (see reviews of Csapo, 1971; Marshall, 1973; Fuchs, 1978; and Thorburn and Challis, 1979; Kawarabayashi and Marshall, 1981). Yet, despite the full potential of the uterus for generating sufficient wall tension to expel its contents, the fetus(es) are retained because propagation from pacemaker cells is relatively limited, until just before delivery (Csapo, 1981). Gap junctions, which develop in the myometrium of rats (Garfield et al., 1977; Puri and Garfield, 1982) and other species (see review of Garfield, 1985) immediately before and during parturition, are thought to provide low-resistance pathways for current flow between muscle cells, thus promoting action potential propagation through the myometrium and hence synchronous contractile activity (Garfield et al., 1977; 1978). Previous studies (Sims et al., 1982; Cole et al., 1985) demonstrated that gap junction formation in the longitudinal muscle of rat myometrium is associated with improved electrical coupling (i.e. the space constant, measured by extracellular current injection,

increased and junctional impedance, based on an assumed equivalent circuit, decreased) and metabolic coupling (i.e. increased diffusion of an intracellularly confined glucose analogue) between myometrial cells. This enhanced intercellular coupling may facilitate contractile synchrony in the uterine wall. However, there have been no studies on whether action potential propagation in the longitudinal myometrium is enhanced at delivery when gap junctions are present in large numbers.

Recordings in vivo, of electrical or contractile (intrauterine pressure) activities or both in the uteri of various species (e.g. rabbit: Csapo and Takeda, 1965; rat: Fuchs and Poblete, 1970; de Paiva and Csapo, 1973; sheep: Harding et al., 1982; Verhoeff et al., 1985; human: Wolfs and van Leeuwen, 1979) have shown putative qualitative changes in myometrial electrical coupling during gestation: i.e. at preterm, electrical and mechanical activities are asynchronous as compared to more synchronous activity at delivery. In the study of Verhoeff et al. (1985) these changes were related to an increase in gap junction area in the myometrium. However, the in vivo studies provide little quantitative information on the changes in extent or velocity of propagation of individual action potentials in the myometrium at term. Attempts to more accurately measure propagation of impulses through the myometrium in vivo (e.g. by electrically stimulating one part of the uterine horn and following the conduction of the evoked response) have provided little quantitative information (see Thorburn et al., 1984).

There are few detailed in vitro studies on gestational changes in action potential propagation in the isolated uterine horn or in excised uterine strips, despite the suitability of such preparations for studying action

potential propagation (e.g. see Melton, 1956; Daniel, 1960; Melton and Saldivar, 1964; Talo and Csapo, 1970). While Talo and Csapo (1970) reported a higher velocity and distance of propagation of action potentials evoked at the ovarian ends of parturient as compared to preterm pregnant (day 25) rabbit uterine strips, they provided no statistical analysis of their data and did not show very convincing records of propagation. Kanda and Kuriyama (1980) evoked action potentials in small stips of longitudinal myometrium from pregnant rat uteri and found that propagation velocity increased during the progression of pregnancy up to term. However, the measurements were made over very small distances (less than 1.5 mm) and thus little information was provided on the extent of propagation at any stage of pregnancy. Few studies have been done regarding action potential propagation in the transverse axis of the myometrium (see Landa et al., 1959; Goto et al., 1961; Osa, 1974) and no studies have addressed the question of whether there are gestational changes in velocity or extent of propagation in this axis, despite the importance of conduction in the transverse axis for development of intrauterine pressure (see Mosler, 1968). In addition, measurements of action potential propagation in the transverse axis of the myometrium during the progression of pregnancy may also provide information about the functional consequences (as yet undetermined) of gap junction formation in the circular layer.

In this chapter, the spread of spontaneously discharged and evoked spikes along the myometrium from late pregnant (day 17) and parturient rat myometrium was studied using extracellular recording. With these measurements, which yield indirect measurements of the extent of intercellular electrical coupling (Kao, 1977a), I examined the question of whether improved propagation

and electrical coupling in the myometrium was evident at delivery, a time when gap junctions are present in large numbers (Garfield et al., 1977). The results show an enhanced propagation of action potentials in both the longitudinal and transverse axes of the uterus at delivery, when presumed low-resistance cell-to-cell contacts (gap junctions) were present in large numbers. These data thus add to the previous evidence implicating gap junctions as the structural basis for intercellular coupling in the parturient uterus.

## MATERIALS AND METHODS

### A) Tissue Preparation

Timed pregnant white Wistar rats were used at delivery (gestation day 22) and at preterm (day 17). Uterine tissues (longitudinal and circular strips) were obtained from these animals and prepared for experimentation, as described in Chapter 2. In brief, the procedure was as follows. Each excised uterine horn (with intact fetal contents) was transferred to a dissecting tray (filled with warm Krebs solution gassed with 95% $O_2$-5% $CO_2$, pH 7.4) and then pinned out at its *in situ* length. The circumference of the horn around several fetal compartments was measured with a piece of thread and then a longitudinal cut was made along the mesometrial attachment to remove the fetuses and placentae. The emptied uterine horn was pinned out flat (endometrial side up) to its original length and width (i.e. circumference). Longitudinal and circular uterine strips were cut over nonplacental regions from this sheet.

### B) Electrical Recording

For measurement of the electrical properties of spontaneously discharged spikes, longitudinal uterine strips (3 cm long and 5-10 mm wide) were

transferred to an organ bath of 30 ml capacity (described in Chapter 2) and pinned out (serosal side up) at their in situ length and width. Electrical events within the muscle were recorded extracellularly by glass pore surface electrodes and were made in reference to an Ag-AgCl bath electrode, as described in Chapter 2. Six electrodes were used to simultaneously monitor electrical events at six sites (3 mm apart) along the serosal surface of the muscle. Signals were amplified by standard AC (.1-200 Hz) preamplifiers (Beckman Type 481B) and couplers (Beckman Type 9806A) and were simultaneously recorded by pen recorder and FM tape (for later computer analysis).

To measure conduction velocity of evoked spikes, longitudinal and circular uterine strips (3 cm long and 3-5 mm wide) were transferred to a modified Abe and Tomita type bath (Abe and Tomita, 1968) of about 10 ml capacity (see Figure 32) and pinned out (serosal side up) at their in situ lengths. This muscle bath is divided into two compartments, one for electrical stimulation (stimulating chamber) and the other for recording (recording chamber), by a chlorided-silver plate (hereafter called the "stimulating partition") of dimensions 1 cm x 1 cm which was insulated on the side facing the recording chamber. A second chlorided-silver plate of similar dimensions was placed approximately 1.2 cm from the partition and formed the back of the stimulating chamber. Both compartments were perfused with prewarmed, preoxygenated (95% $CO_2$-5% $O_2$) Krebs solution at a rate of about 5 ml/min and were maintained at a constant temperature of 37 $\pm$ 1 °C. One end of the strip was threaded through a small oval-shaped hole at the bottom of the partition such that approximately 1 cm of the strip was pinned in the stimulating chamber, with the remaining 2 cm portion of the strip pinned in the recording chamber. In both compartments, the

strip width was the same. The longitudinal uterine strips were always arranged such that their ovarian ends were placed in the stimulating chamber between the electrode plates. Action potentials ("spikes") were evoked in the uterine strip, near its entrance into the recording chamber, by applying rectangular electrical pulses (6-8 V in amplitude and 50-400 msec in duration) between the electrode plates. The polarity of the stimulating current was such that the cathode was at the partitioning plate while the other plate was the anode. A Grass S-88 stimulator was used to generate the stimulus. Although the amount of current flowing into the tissue is not known, it is assumed to be proportional to the applied current. Electrical activity was simultaneously monitored at six sites along the serosal surface of the muscle, and the signals amplified and recorded by pen recorder and FM tape, as described above. The first recording electrode was positioned about 3 mm from the cathode.

C) Analysis of Electrical Activity

Spontaneous Spikes

Electrical signals were retrieved from storage on FM tape and then played back into the computer with simultaneous monitoring on an 8 channel oscilloscope (Beckman Type E-018). The signals were digitized (100 samples/sec) and then further processed by a NOVA 830 minicomputer, using computer programs written in Fortran IV. At this sampling rate, the temporal resolution in each electrode was 10 msec. Peaks in the digitized signals at the electrode sites were detected using an algorithm based on local maxima and minima (see Dumpala et al., 1982). Negative peaks of the the triphasic shaped action potentials were used for peak detection because they were usually 2-3 times the amplitude of the positive peaks and were always much greater in amplitude than the

background baseline voltage. Arbitrarily chosen threshold amplitude (i.e. .1-.5 of maximum peak) and duration (i.e. 100 msec) criteria were used to eliminate spurious peaks. The duration threshold of 100 msec was chosen on the basis of the maximum spike discharge frequency of about 5 spikes/sec that was estimated from chart records of several bursts. In other words, this duration corresponds to the time interval between spikes discharged at two times the maximum spike discharge frequency, i.e. 10 spikes/sec, and is about 2-3 times longer than the duration of the negative peak of the action potential (see "Results"). The following is a more detailed procedure of the analysis. For each uterine strip, three sets of spike bursts (viz. spike bursts simultaneously recorded at 6 sites along the tissue) were selected for analysis from the original chart paper recordings, as described in Chapter 2. These bursts were retrieved from storage on FM tape and then played back into the chart recorder to obtain fast speed (25 mm/sec) hard copies. At this paper speed, the individual spikes comprising the burst discharges were readily visualized. Thus, the number of spikes in each burst could be manually counted and later used as a check for the number of peaks identified by the peak detection analysis, to verify that all of the spikes within the burst were detected by the computer. The electrical activities of 3 out of the 6 electrodes were subjected to peak detection analysis. These were chosen on the basis of the shape and amplitude of their spikes as visualized in the fast speed chart records (see above). In other words, only good records were analyzed, i.e. the 3 adjacent electrode sites whose spike bursts were comprised of mostly triphasic shaped spikes of amplitude greater than twice the baseline voltage.

The temporal positions of the spikes (peaks) were automatically recorded by the computer and used in algorithms to compute instanteous spike

frequency, latency, phase shift and time shift (Reddy et al., 1984; see Figure 33). The instantaneous spike frequency is the reciprocal of the time interval between successive spikes and was determined for each spike comprising the burst at an electrode site. The mean spike frequency for the burst was then calculated from the instantaneous spike frequencies of the individual spikes comprising the burst. For each set of bursts at the 3 electrode sites, the mean spike frequency at each electrode was determined and these 3 mean values were averaged to give a mean value for that set of bursts. The latency is the delay ($\triangle t$) in milliseconds between the peaks (negative peaks) of "entrained" spikes from paired electrodes. Entrainment means that the spikes from the paired electrodes were synchronized with a fixed or slowly changing latency. For a set of bursts recorded at 3 adjacent electrode sites (i.e. 2 electrode pairs), the latency for each spike in the burst was determined and these were used for calculation of phase shift. Phase shift by definition is $(\triangle t_{i,i+1} \times 360^{\circ}/T_i)$, where $\triangle t$ is the latency of the electrical event between paired electrodes and T is the period of the preceding oscillation of the spike (see Figure 33). Zero phase shift would mean that the spike occurred simultaneously at the 2 electrode sites, possibly because the spike was initiated between the electrode sites. Positive phase values indicate propagation from one electrode of the pair to the other, while negative phase values indicate propagation in the opposite direction. Phase shifts were calculated for each spike comprising the bursts at an electrode pair. Time shifts (lags) are the absolute values (i.e. ignoring direction of phase lead/lag) of the latencies. The time shift for each spike in the burst was determined and these were averaged to give a mean time shift for the burst. Mean time shifts for the 2 electrode pairs were averaged

to give a mean value for the set of bursts.

Evoked Spikes

Peak detection of evoked spikes was also computer-assisted, as described above for spontaneous spikes, except that the evoked spikes were digitized at 400 samples per second. At this sampling rate, the temporal resolution at each electrode site was 2.5 msec, which is less than 10% of the latency of the most rapidly conducted spikes. Latencies were usually measured between positive peaks, unless otherwise indicated. Positive peaks were used for analysis because they were often sharper than the negative peaks. However, the positive peaks were sometimes not very well resolved, particularly in transverse strips, and in these cases velocity was measured between negative peaks. The electrical activity at all 6 electrode sites was analyzed and propagation (conduction) velocities were calculated manually, by dividing the latencies into the known inter-electrode distances, and were expressed as centimeters per second.

D) Electron Microscopy

Samples of longitudinal and circular uterine strips were obtained prior to and following completion of some experiments, processed for thin section electron microscopy, sectioned and then quantitatively analyzed for gap junctions, as described in detail in Chapter 2.. Gap junctions were identified as distinct 5 or 7 lined structures at the points of membrane fusion between opposing cells.

E) Statistical Analysis

For the morphological data, all results were expressed as mean values $\pm$ SD. A Wilcoxon Rank Sum Test was used to compare these values. For the electrophysiological measurements of spontaneous spikes, the spike discharge

frequencies and time shifts are mean values ± SE. Differences between preterm and delivering tissues were compared using a one-way analysis of variance. The propagation velocity and distance values of evoked spikes are mean values ± SD. The Student's t test was used to test for differences between preterm and delivering tissues.

## RESULTS

### Electron Microscopy

Samples from some of the longitudinal and circular strips used for electrical recording were examined by thin section electron microscopy for the presence of gap junctions. Table V shows the results of gap junction quantitation in uterine tissues that were used to measure propagation of evoked spikes. Preterm myometrial tissues, fixed either before or after experimentation, showed few or no gap junctions (Figures 34 and 35a). In 2 of the 4 tissues fixed immediately after removal of the uterus from the animal, two gap junctions (.47/1000 $\mu$m), occupying a small percentage (.012%) of the total cell membrane, were identified (Figure 34). A similar number of gap junctions (.24-.74/1000 $\mu$m) occupying a small percentage (.006-.011%) of the total cell membrane were also observed in some of the preterm myometrial tissues fixed after electrical recording. In contrast, myometrial tissues obtained from delivering animals and fixed before or after electrical recording showed large numbers of gap junctions (Figure 35b). The frequency of gap junctions (7.46-8.50/1000 $\mu$m), as well as the fractional area of cell membrane occupied by the junctions (.214-.249%) in these tissues were markedly (20-40 fold higher) and

significantly ($p < .05$) higher than in the preterm tissues. The values of gap junction frequency and fractional area are comparable to those from the tissues used to assess the electrical properties of spontaneously discharged spikes (see Table I, Chapter 2).

Electrical Properties

I. Spontaneously Discharged Spikes

Spontaneous electrical activity was recorded from the serosal surface (in longitudinal strips only) simultaneously at 6 sites (3 mm apart) along the tissue. The spike-shaped action potentials ("spikes") recorded from preterm pregnant and delivering tissues consisted of an initial positive deflection followed by a larger negative deflection and then by recovery to baseline (Figure 36a,b). The initial positive deflections were about one-third or less of the amplitude of the large negative deflections, the latter being complete in about 30-60 msec. Peak to peak duration was about 20-30 msec, while peak amplitudes were 1 mV or less in preterm pregnant and 1-2 mV in delivering tissues. However, in the preterm tissues, more complex spike configurations were frequently observed. For example, "notches" on the positive and negative deflections were often seen, giving the appearance of multiple peaks (Figure 36c-h). In the delivering tissues, spikes recorded at a given electrode site were generally of uniform shape and amplitude (Figure 37b) while at preterm, in contrast, both spike shape and amplitude usually varied during the burst (Figures 37a and 38).

In the longitudinal axis of the myometrium at delivery, individual spikes within spike bursts were entrained one-to-one between all 6 electrode sites (Figure 37b), usually for the entire burst duration (also see Figures 19

and 20, Chapter 2). In this axis at preterm, however, spikes were not usually entrained across all 6 electrode sites, particularly at the onset of a burst (Figure 37a; also see "Excitable Region", Chapter 2), but they became entrained over variable distances (6-15 mm) once the bursts had commenced at all electrode sites. This phenomenon is illustrated in Figure 37a which shows the beginning, middle and end portions of a set of bursts simultaneously recorded at 6 sites in a preterm pregnant tissue. Initially, the spikes were uncoordinated (i.e. occurred independently) across the 6 electrode sites, although some spikes at a given electrode site produced small depolarizations (see arrows) at its neighbouring electrode site. As the burst progressed the spikes became entrained across all 6 electrode sites, but by the end of the burst they were entrained across only 5 electrodes. At this latter stage, some spikes at electrode "5" produced small depolarizations (see arrows) at the neighbouring electrode "6". Similarly, the increase in entrainment distance following the onset of bursting was observed in tissues treated with 1 $\mu$g/ml of tetrodotoxin (Figure 38). As illustrated in this Figure, the intitial spikes at the beginning of the bursts were entrained across only 2 electrode sites ("e5" and "e6"), but the distance of entrainment subsequently increased to include 4 electrode sites by the middle of the burst, and this was maintained until the bursts ended.

To provide some evidence for a possible interaction (i.e. electrical conduction) of entrained spikes between electrode sites, the instantaneous spike discharge frequencies, phase shifts and time shifts of successive spikes in bursts recorded at adjacent electrode sites were determined. Of the 6 recording electrodes per tissue, the signals at only 3 adjacent sites were analyzed. This was partly to save computing time but also because in the preterm tissues it was

difficult to find more than 3 adjacent electrodes at which the bursts had component spikes of a "simple" shape (e.g. Figure 36b–e) which provided reliable detection of the action potential peak. This problem is illustrated in Figure 37a for a set of bursts recorded from a preterm pregnant tissue. At the end of the bursts of this record, only electrodes "3", "4" and "5" recorded spikes whose negative peaks would be reliably detected by the peak detection programs.

Instantaneous Spike Frequency

At both preterm and delivery, the within burst instantaneous spike discharge frequencies of entrained spikes were well coordinated across adjacent electrode sites, i.e. they had the same or similar instantaneous spike frequencies (e.g. see Figure 41a). The record in this figure shows the change in spike discharge frequency during the progression of a burst simultaneously recorded at 3 adjacent electrode sites in a longitudinal uterine strip from a preterm pregnant animal (see bursts in Figure 39a). Instantaneous spike frequencies at adjacent electrodes were highly correlated ($r = .9$ and .95, for electrode pairs 1,2 and 2,3, respectively). The mean spike discharge frequency of 3.2 spikes/sec was the same at each electrode site. The change in spike discharge frequency during bursts simultaneously recorded at 3 adjacent electrodes in the myometrium from a delivering animal (see bursts in Figure 40a) is shown in Figure 41b. Instantaneous spike frequencies at adjacent electrodes were also highly correlated ($r = 1.0$ for both electrode pairs) in this tissue. The mean spike discharge frequency at each electrode was 1.28 spikes/sec. For 30 sets of 3 bursts each from 10 preterm and 10 delivering longitudinal strips, the instantaneous spike frequencies of entrained were highly correlated ($r > .9$) at adjacent electrode sites. While the spike frequency within a given burst was

not constant at either stage of gestation, the spike discharge was less stable (i.e. more "erratic") at preterm than at delivery (see Figure 41). The grand mean spike discharge frequency at preterm (3.99 $\pm$ .59 spikes/sec) was significantly higher ($p < .001$) than the frequency of 1.49 $\pm$ .33 spikes/sec at delivery (Table VI).

The maximum spike discharge frequency within a burst can be used as a "rough" estimate of the maximum relative (functional) refractory period of the membrane for spiking (Daniel, 1960; Goto et al., 1961; Bortoff, 1976). The grand mean of the maximum discharge frequencies in the preterm tissues (5.24 $\pm$ .82 spikes/sec) was about 3 times greater than the maximum frequency of 1.83 $\pm$ .48 spikes/sec in the delivering tissues (Table VI). Maximum relative refractory periods of about 200 msec and 500 msec, respectively were estimated from these maximum spike frequencies. These are similar to the values previously reported of about 200 msec and 200-400 msec for refractory periods in pregnant rat (Daniel, 1960; Casteels and Kuriyama, 1965) and mouse (Goto et al., 1961; Kuriyama, 1961) longitudinal myometrium, respectively.

Phase Shift

Phase shifts for entrained spikes in a set of bursts simultaneously recorded at 3 adjacent electrode sites in a preterm tissue (see bursts in Figure 39a) and a delivering tissue (see bursts in Figure 40a) are shown in Figure 42. In the preterm tissue, the phase shift varied and phase lead changed direction during the burst (Figure 42a). For electrode pair "2-3", the spikes at electrode "3" had phase lead initially and spikes apparently propagated in the ovarian direction from electrode "3" to electrode "2" (i.e. positive phase shifts). Similarly at electrode pair "1-2", the initial spikes apparently propagated in

the ovarian direction, i.e. electrode "2" had phase lead. Later during the burst (see Figure 39b), the phase lead changed direction twice more, i.e. the spikes propagated in the cervical and then finally in the ovarian direction. For this set of bursts, the mean phase shifts in the ovarian direction were about 80° (maximum = 160°) and 60° (maximum = 120°) for electrode pairs "2-3" and "1-2", respectively, while those in the cervical direction were about 70° (maximum = 90° ) and 50° (maxiumum = 60°) for the respective pairs. Phase shift values at both electrode pairs were clustered around "+" or "-" 50-60°, as observed in most preterm tissues. In the delivering tissue, the phase shifts also varied within the bursts but the direction of phase lead was constant (i.e. in the ovarian direction) throughout the burst (Figure 42b). The mean phase shifts were about 10° and 14° for electrode pairs "2-3" and "1-2", respectively. The maximum phase shift of about 16° was the same at both electrode pairs. Phase shifts were studied in 30 sets of 3 bursts from 10 delivering tissues and in 30 sets of 3 bursts from 10 preterm tissues. The grand mean phase shift (absolute values, i.e. ignoring direction of phase lead) of $12.3 \pm 5.4^{\circ}$ in the delivering tissues was much smaller ($p < .001$) than the value of $57.8 \pm 21.4^{\circ}$ in the preterm tissues (Table VI). Unidirectionality of phase lead throughout the entire burst was observed in about 90% of the bursts from delivering tissues as compared to only about 30% of the bursts from preterm pregnant tissues. There did not appear to be a preferred direction of phase lead at delivery (i.e. the proportion of bursts with ovarian phase lead was about equal to the proportion with cervical phase lead). Phase shifts were similar in both directions (i.e. $12.3 \pm 5.6^{\circ}$ in the ovarian as compared to $12.2 \pm 5.5^{\circ}$ in the cervical direction). In summary, while the phase shifts were not constant at either stage of gestation, at preterm they

were larger with phase lead changing direction during the burst, as compared to at delivery where phase shifts were smaller and generally unidirectional. It was clear from the similarity of phase shifts irrespective of the direction of apparent spike propagation that the mechanism of propagation did not show a directional preference.

Time Shifts

It was desirable to determine whether the smaller phase shifts observed at delivery as compared to at preterm were due solely to the lower spike discharge frequency at delivery (which might allow less refractoriness in these tissues), or whether there was also a gestational change in the propagation velocity (i.e. latency or time shift) of entrained spikes. The time shifts (lags) of entrained spikes within a given burst were rather widely scattered, particularly in the preterm tissues. For example, in the set of 3 bursts from a preterm tissue (see bursts in Figure 39a), the time shifts ranged from 10-80 msec at electrode pair "2-3" and from 0-80 msec at electrode pair "1-2" (Figure 43a). In contrast, the time shifts were less widely scattered, i.e. 20-30 msec at electrode pair "2-3" and 20-40 msec at electrode pair "1-2" (Figure 43b), in the set of 3 bursts from a delivering tissue (see bursts in Figure 40a). In bursts from preterm tissues, spikes frequently (but not more than about 20% of the spikes within a given burst) occurred simultaneously at adjacent electrode sites (i.e. latency = 0 msec at the resolution of 10 msec for peak detection, see "Materials and Methods"). These values were not included in the calculations of the mean time shift for a burst. For 30 sets of 3 bursts from 10 preterm tissues, the mean time shifts (absolute values of latencies, i.e. ignoring direction of apparent propagation) ranged from 21 msec to 59 msec,

with a grand mean value of 38.9 $\pm$ 12.6 msec. For 30 sets of 3 bursts from 10 delivering tissues, the mean time shifts ranged from about 12 msec to 45 msec, with a grand mean value of 22.9 $\pm$ 9.4 msec, significantly smaller ($p < .001$) than the grand mean value at preterm (Table VI). These grand mean time shifts correspond to mean apparent conduction velocities (inter-electrode distance = 3 mm) of 7.9 $\pm$ 3.0 cm/sec and 13.5 $\pm$ 4.2 cm/sec at preterm and delivery, respectively (Table VI).

It is possible that the higher latencies of entrained spikes at preterm as compared to at delivery were due to the higher spike discharge frequency at preterm. In other words, the higher the spike discharge frequency, the more refractory might be the tissue which the spike propagates through and hence the greater the latency (i.e. slower propagation velocity) of the spike (see Bortoff, 1976). To determine if the latencies of entrained spikes at either gestational state were limited by the relative refractoriness of the membrane, the relationship between time shift (lag) and spike frequency was studied for each of the 30 sets of 3 bursts from the 10 preterm and 10 delivering tissues. For all bursts, the plots of time shift against instantaneous spike frequencies did not reveal a constant relationship. In other words, at either stage of gestation, the time shifts within bursts were positively associated with spike frequency in some bursts and negatively associated with it in other bursts. Sometimes opposite associations were observed at the two electrode pairs from the same set of 3 bursts. In any event, the correlations between time shift and spike frequency, although sometimes significantly different from 0, were not strong (i.e. $|r| < .5$). These features are illustrated in Figure 43a for plots of time shift against instantaneous spike frequency for a set of 3 bursts from a

preterm tissue (see bursts in Figure 39a) and in Figure 43b for a delivering tissue (see bursts in Figure 40a). In the preterm tissue, the time shifts of spikes at electrode pair "2-3" showed a weak positive ($r = .15$) but not significant ($p > .05$) correlation with the spike frequency while those at electrode pair "1-2" showed a weak negative ($r = -.28$) but significant ($p < .01$) correlation with spike frequency (Figure 43a). For the delivering tissue, the time shifts of the spikes at electrode pair "2-3" were not correlated ($r = .06$) with spike frequency while those at electrode "1-2" showed a moderate negative ($r = -.48$) and significant ($p < .01$) correlation with the spike frequency (Figure 43b). When the mean spike frequencies for the 30 sets of bursts from preterm and delivering tissues were plotted against the respective mean time shifts, the slope of the regression line was not significantly different from 0. Thus, at neither stage of gestation was the time shift (i.e. apparent propagation velocity) of spikes that were entrained in the longitudinal axis, affected by the spike discharge frequency (i.e. the presumably maximum duration of membrane refractoriness).

The apparent propagation velocity of spontaneous spikes in the transverse axis was not determined. Spikes in this axis were entrained over distances of only about 3 mm at preterm and 6 mm at delivery (Table IV, Chapter 2). Moreover, the usually complex shape of the spikes from bursts in these tissues precluded the reliable measurement of the latency.

II. Evoked Spikes

The rather wide scatter of latencies between entrained spontaneously discharged spikes within a given burst, particularly in the preterm tissues, may be partly due to a shifting pacemaker location. In other words, if the spike

originated somewhere between the recording electrodes, the latency would be less than when the spike originated outside the electrode pair, i.e. when it propagated over the whole of the 3 mm distance from one electrode to the other. Those lower time shifts would give erroneous values for apparent propagation velocity if the conduction distance was assumed to be 3 mm. A more accurate means of assessing propagation velocity is to evoke a spike at a known location (e.g. at one end of the tissue) and follow its conduction down the strip. In this way, both the velocity and extent of propagation can be obtained from the same experiment. Propagation velocity and distance of evoked spikes were measured in the longitudinal and transverse axes of the myometrium at delivery and 5 days before (gestation day 17), as described below.

A) Longitudinal Axis

All longitudinal strips were spontaneously active, discharging spike bursts between quiescent periods. Because of the difficulty in identifying an evoked spike from one that is spontaneously discharged, it is necessary to stimulate the tissue during the silent period between spike bursts (Melton, 1956; Tomita, 1970). Single spikes were evoked in the longitudinal strips by applying single square wave electrical pulses at their ovarian ends. In the delivering tissues, propagating spikes were readily evoked in the silent period in response to 6-7 V depolarizing pulses of about 50 msec duration (Figure 44). The records in this figure show the shape of several evoked spikes recorded at 2 electrode sites, located 3 mm ("e1") and 6 mm ("e2") from the stimulating partition, when the stimulus duration was increased from 50 msec up to 150 msec (Figure 44b-d). Although the shape of the spike recorded by the electrode closest to the partition (i.e. 3 mm away) was somewhat distorted by the stimulus artifact, it is

apparent that the spikes were evoked after about 50 msec of depolarization. There was no velocity change with increasing stimulus duration in the 50- 150 msec range studied. Hyperpolarizing pulses did not evoke spikes (Figure 44e). The shape of the evoked spike at the second recording electrode (i.e. 6 mm away from the partition), although slightly distorted by the stimulus artifact, was similar to that of the spontaneously discharged spikes (Figure 44a).

The excitability of the uterine smooth muscle cell membrane to electrical stimulation fluctuates during the silent period between bursts, as does the input (e.g. transmembrane) resistance (Casteels and Kuriyama, 1965; Kuriyama and Suzuki, 1976a; Kanda and Kuriyama, 1960). These fluctuations might alter spike propagation, depending on the time during the silent period when spikes are evoked. It was therefore necessary to determine whether there was a difference in propagation velocity of spikes that were evoked at different times during the quiescent period between spontaneous bursts. An example of such an experiment on a delivering longitudinal uterine strip is shown in Figure 45. Seven spikes were evoked by repetitive stimulation (6V x 50 msec) at .5 Hz in the 20 second silent period between 2 spontaneously discharged bursts (see arrows in Figure 45a). The respective propagation velocities were 11.8, 11.5, 11.5, 11.8, 12.0, 12.0 and 12.2 cm/sec (latencies measured between positive peaks of signals at "e2-e6", see below) and all were conducted over the 15 mm recording distance (Figure 45b). The shape of the spike recorded at electrode "1" closest to the partition was somewhat distorted by the stimulus artifact and therefore latencies were measured between electrodes "2-6". (In this and several other records from different parturient tissues, there was no difference in the propagation velocity with latencies calculated between "positive" as

compared to "negative" peaks). Thus, there was only a slight increase in the conduction velocity of spikes evoked just prior to the onset of a burst as compared to those evoked earlier in the quiescent period. Similar results were obtained for a set of 10 spikes evoked in the silent period between bursts in this tissue and for a set of 8 evoked spikes in another delivering tissue. The propagation velocity and distance in delivering longitudinal strips was therefore determined by evoking spikes during at least 4 different silent periods between bursts (over a 10-15 min period) using repetitive stimuli (6-7 V x 40-70 msec) applied at a .5 Hz rate, and 10 of these evoked spikes were randomly selected for analysis. In 11 longitudinal strips from 8 delivering animals (n = 110 measurements), the mean propagation velocity of the evoked spikes was 10.5 $\pm$ 1.3 cm/sec (Table VII). Individual values ranged from a minimum of 8.8 cm/sec to a maximum of 14.0 cm/sec (median value 10.5 cm/sec). All evoked spikes propagated over the entire 15 mm recording distance (Table VII). Although not studied in detail for every burst, the propagation velocity of spontaneously discharged spikes in these tissues were of similar magnitude (about 11-13 cm/sec) to that of the evoked spikes propagating in the same direction (e.g. see Figure 46). In 5 longitudinal uterine strips from 4 delivering animals, spikes were evoked before and after addition of the nerve blocker TTX (1 $\mu$g/ml) to the bath. The mean propagation velocity (n = 50 measurements) of 10.5 $\pm$ 1.5 cm/sec in the presence of TTX was similar to the mean velocity of 10.5 $\pm$ 1.1 cm/sec in its absence. The propagation distance of 15 $\pm$ 0 mm was the same with or without TTX (Figure 47). In the tissue whose record is shown in this figure, the mean conduction velocity of 10 evoked spikes was 10.9 $\pm$ .7 cm/sec before, and 11.6 $\pm$ .7 cm/sec after addition of TTX.

In contrast to the delivering tissues, longitudinal uterine strips from preterm pregnant animals required stimuli (6-8 V) of about 3 times longer duration (i.e. 150-250 msec) to evoke a spike. Voltages of amplitude greater than 8 V were not usually used because the stimulus artifact became too large at the recording electrodes near the stimulating plate, thereby obliterating the evoked spike. However, increasing the stimulus up to 10 V did not decrease the duration required to evoke the spike (see below). Thus, if the duration of a shock evoking a propagated spike is used as a measure of membrane excitability (Casteels and Kuriyama, 1965), the myometrium was about 3 times less excitable at preterm (gestation day 17) than at delivery. Moreover, unlike the delivering tissues in which spikes were readily evoked throughout the silent period between bursts, only those stimuli applied immediately before or immediately after the generation of a burst usually evoked a spike in the preterm tissues (Figure 48). As shown in the record of this figure, when 4 stimuli (8V x 250 msec) were successively applied at 2 second intervals (i.e. at .5 Hz) following the cessation of the burst, only the first 2 stimuli evoked a propagating spike. In other words, the membrane quickly became refractory to stimulation following the spontaneous generation of a burst. During this refractory period, stimuli (6-10 V) of prolonged durations (i.e. up to 700 msec) did not evoke spikes. In 2 of 8 preterm tissues studied, a few spikes were sometimes evoked in the quiescent period between bursts. However, these spikes seldom propagated past the first recording electrode 3 mm from the stimulating partition. In 8 longitudinal strips from 7 preterm animals (n = 74 measurements), the mean propagation velocity of 9.2 $\pm$ .8 cm/sec was significantly slower ($p < .001$) than at delivery (Table VII). Individual values ranged from a minimum of 7.5 cm/sec

to a maximum of 10.7 cm/sec (median value = 9.2 cm/sec). Spontaneously discharged spikes in these tissues propagated at similar velocities to the evoked spikes (Figure 49). For example, Figure 49b shows the last 2 spikes in the spontaneous burst that preceded an evoked spike (Figure 49a). The propagation velocities of the spontaneous spikes (about 8 cm/sec) were only slightly less than the velocity (8.6 cm/sec) of the evoked spike. Conduction distances of the evoked spikes were variable (6-15 mm) and most spikes propagated just part way down the strip (Figure 49a). Only 30% of the evoked spikes propagated over the entire 15 mm recording distance. Propagation distance was not significantly ($p = .4$) correlated ($r = -.1$) with velocity. The mean propagation distance of $11.8 \pm 2.8$ mm (median = 12 mm) was significantly shorter ($p < .001$) than at delivery (Table VII).

In 2 longitudinal uterine strips from 2 preterm pregnant animals, spikes were evoked before and after addition of TTX (1 $\mu$g/ml). The mean propagation velocity of $9.6 \pm .5$ cm/sec (n = 20 measurements) in the absence of TTX was similar to the velocity of $9.5 \pm .7$ cm/sec (n = 18 measurements) in the presence of TTX (Figure 50). The mean propagation distance of $12.8 \pm 2.1$ mm in the absence of TTX was similar to the distance of $12.0 \pm 2.6$ mm in its presence.

B) Transverse Axis

All transverse strips were spontaneously active, discharging spike bursts between quiescent periods. Repetitive stimuli (6-8 V x 300-400 msec) were successively applied at a rate of about .5 Hz, in the silent period between spontaneous bursts. In delivering tissues, spikes were evoked only by stimuli applied immediately before or immediately after the generation of a burst. The membrane quickly became refractory to stimulation after the generation of a

burst as shown in Figure 51a. In the record shown in this figure, the membrane became refractory after the third stimulus was applied. The propagation velocity of 3.6 cm/sec for the spike evoked just after cessation of the burst (Figure 51b) was similar to the propagation velocity of 3.5 cm/sec for the last spontaneously discharged spike in the preceding burst (Figure 51c). The spontaneous spikes in this strip originated between electrodes "5" and "6" and travelled in the opposite direction to that of the evoked spike. In 5 transverse strips from 4 delivering animals, the mean propagation velocity of evoked spikes (n = 49 measurements) was 4.0 $\pm$ .8 cm/sec. Individual values ranged from a minimum of 2.3 cm/sec to a maximum of 6.4 cm/sec (median = 4.0 cm/sec). The mean propagation velocity in the transverse axis at delivery was less than one-half the mean velocity in the longitudinal axis (Figure 52; Table VII). Propagation distances in the transverse strips were variable (6-15 mm) and most spikes travelled only part way down the strip. The distance of propagation was weakly ($r = .4$) but significantly ($p < .01$) correlated with the velocity. The mean propagation distance of 10.4 $\pm$ 2.3 mm (median = 9 mm) was significantly less ($p < .001$) than the 15 mm propagation distance in the longitudinal axis at delivery (Figure 52; Table VII).

In transverse strips from preterm pregnant animals, spikes were difficult to evoke. Of 7 tissues studied (from 4 animals), spikes were evoked in only 4 of the strips. Burst discharge frequencies were low (i.e. < .5 cycles/min) and erratic in these tissues. It was therefore difficult to time the stimuli such that they were applied just before the generation of a burst. Instead, successive stimuli were applied just after the generation of a burst and stimulation was stopped when the membrane became refractory. Stimuli (6-8 V x

300-400 msec) applied immediately after spontaneous generation of a burst were usually successful in evoking a spike, however the membrane quickly became refractory to stimulation (Figure 53a-c). As shown in this figure, the membrane became refractory after the second stimulus was applied. In the 4 transverse tissues where spikes were successfully evoked, the mean propagation velocity (n = 40 measurements) was 2.3 $\pm$ .7 cm/sec, significantly less ($p < .001$) than the velocity in this axis at delivery (Table VII). Individual values ranged from a minimum of 1.9 cm/sec to a maximum of 3.5 cm/sec (median = 2.1 cm/sec). In the preterm pregnant myometrium, the mean propagation velocity in the transverse axis was less than one-third of the mean velocity in the longitudinal axis (Table VII). Propagation distances were variable (3-9 mm) in the transverse axis at preterm and were not correlated ($r = -.01$) with velocity. The mean propagation distance of 7.4 $\pm$ 1.7 mm (median = 6.0 mm) in the transverse axis at preterm was significantly less ($p < .001$) than the propagation distance in this axis at delivery (Table VII). At preterm, the propagation distance in the transverse axis was also significantly ($p < .001$) shorter than that in the longitudinal axis (Table VII). These results are similar to the distances for spontaneous spikes in the transverse and longitudinal axes of the preterm and delivering myometrium (see Table IV, Chapter 2).

In 2 preterm transverse tissues, TTX (1 $\mu$g/ml) was added to the muscle bath at the beginning of the experiment. The mean propagation velocity and distance (n = 20 measurements) of 2.2 $\pm$ .3 cm/sec and 8.2 $\pm$ 1.6 mm, respectively in these tissues were similar to those of the untreated strips (see Figures 53a; 54a). In the TTX-treated strips, the evoked spikes propagated with similar velocity (i.e. 2.2-2.3 cm/sec) to spontaneously discharged spikes (i.e. 2.5-2.6 cm/sec) travelling in the opposite direction (Figure 54b).

## DISCUSSION

In the previous chapter, I demonstrated that entrainment of spontaneous spike burst discharges was enhanced in both axes of the myometrium at delivery, when large numbers of gap junctions were present between uterine smooth muscle cells, suggesting that gap junction formation at term facilitates current flow in the myometrium. My aim in the present chapter was to further investigate the role of gap junction formation in myometrial electrical coupling by assessing the entrainment of spontaneously discharged spikes as well as the velocity and extent of propagation of evoked spikes. The major findings of this chapter are as follows:

1). Spontaneously discharged spikes were better entrained in the longitudinal axis of the myometrium at delivery, since i) entrainment distance was longer, ii) phase leads/lags of entrained spikes were smaller, more stable and more unidirectional, and iii) latencies between entrained spikes were less, than at preterm.

2). Accompanying these changes were changes in the electrical properties of the muscle cell membrane such that at delivery: i) spike discharge frequencies were lower and less erratic within a given burst, ii) spike shapes were simpler and iii) spike amplitude higher, than at preterm.

3). Velocity and extent of propagation of electrically evoked spikes were greater in the longitudinal and transverse axes of the myometrium at delivery than at preterm. At both stages of gestation, propagation was greater in the longitudinal than in the transverse axis.

4). Accompanying these propagation changes were changes in the electrical properties of the membrane such that the excitability of the muscle to electrical stimulation was greater at delivery than at preterm.

5). The incidence of gap junctions was markedly higher in parturient as compared to preterm pregnant myometrium.

Since the degree of action potential entrainment and the extent and velocity of action potential propagation in the myometrium are thought to depend on the degree of cell-to-cell electrical coupling between uterine smooth muscle cells, the results are consistent with the hypothesis that increased numbers of gap junction contacts between uterine smooth muscle cells facilitates intercellular current flow in the myometrium.

Gap Junctions in the Myometrium

Thin section electron microscopy of samples from some of the tissues used for in vitro electrophysiological studies confirmed that gap junctions were present in large numbers in all delivering tissues, as compared to preterm tissues where only a few or no gap junctions were present (Table V). The values of gap junction frequency, fractional area and size are similar to the values previously found for delivering and preterm tissues (see Table I in Chapter 2) and to values for the incidence of gap junctions in pregnant and parturient rat myometrium, previously reported in the literature (e.g. Garfield et al., 1977; Puri and Garfield, 1982; and see "Gap Junctions", Chapter 1).

In parturient tissues, the mean values of gap junction frequency and fractional area (in both longitudinal and circular muscle layers) were markedly (e.g. 20-40 times higher) and significantly higher than in the respective preterm tissues (Table V). Thus, the ultrastructural evidence showed that two distinct

groups of myometrium, with respect to the incidence of gap junctions, were studied. Although a small number of gap junctions was identified in some of the preterm tissues fixed after completion of electrical recording, it is of considerable importance that gap junctions did not develop in large numbers (if at all) in preterm (or delivering) tissues during the course of experimentation. Assuming that the junctions at both stages of gestation are functional and that the much greater incidence of gap junctions at delivery is the basis for the observed changes in electrical properties, then junctions in the preterm tissues should only tend to conceal the differences in electrical properties (e.g. action potential propagation) of the muscle at the two stages of gestation. Thus, the presence of large numbers of gap junctions between uterine smooth muscle cells at delivery, by providing low-resistance pathways for current flow between muscle cells, probably accounts for the enhanced entrainment and propagation of action potentials observed in the delivering tissues (see Sims et al., 1982). However, other structural changes in the myometrium from gestation day 17 to delivery, e.g. increase in smooth muscle cell size (Afting and Elce, 1978; Vasilenko et al., 1981) and possible changes in the packing of muscle cells into bundles (and hence the size and geometry of the extracellular space within the bundles) or arrangement (e.g. overlapping of muscle bundles), might also affect current flow and hence contribute to the observed differences (see below).

## Changes in Electrical Properties

### Spontaneous Spikes

Extracellular recordings at multiple sites along the longitudinal axis of the myometrium showed coordination of spontaneous activity (e.g. action potentials) between widely separated groups of cells at both preterm and

delivery, indicating that uterine smooth muscle cells were electrically coupled. However, at delivery coupling of myometrial cells was apparently enhanced because 1) spike shape, amplitude and discharge rate within bursts were more regular at delivery than at preterm, 2) at delivery the distance available for propagation (15 mm), over which virtually all of the spikes within bursts were entrained one-to-one, was longer than the variable entrainment distances (e.g. 6-15 mm) within bursts in preterm tissues and 3) entrained action potentials exhibited more stable phase shifts (e.g. smaller deviation from zero, and unidirectionality) and smaller latencies, at delivery than at preterm. These results are consistent with some previous reports on the electrophysiology of pregnant rat longitudinal myometrium. For example, the higher and more regular spike discharge rate and variable spike amplitude in preterm as compared to delivering longitudinal myometrium are well known (e.g. see Thiersch et al., 1959; Casteels and Kuriyama, 1965; Kuriyama and Suzuki, 1976a; Kanda and Kuriyama, 1980; Anderson et al., 1981).

Osa et al. (1983) similarly reported a more complicated spike shape recorded extracellularly in preterm pregnant (day 20) as compared to term pregnant (day 22) rat longitudinal myometrium, consistent with the present results. Surface electrodes measure the combined activity of many cells (Kao, 1977a); the pore size (200-300 $\mu$m) of the electrodes used in the present study would record the activities of about 20-60 cells, assuming a uterine smooth cell diameter of 5-10 $\mu$m (see Marshall, 1973). The amplitude of the extracellular signal is a rough indication of the number of active cells under the electrode (although, it is also affected by leak currents, e.g. by the "tightness" of the seal between the electrode and the tissue surface), while its shape is

determined by the temporal dispersion of the individual spikes (Kao, 1977a). Therefore, the gestational change in action potential amplitude and shape observed in this study probably reflected changes during pregnancy in the spread of action potentials between myometrial cells. In other words, the higher amplitude and simpler shaped signals recorded at delivery imply a more synchronized spike activity (i.e. electrical coupling) among individual cells at delivery than at preterm. It is unlikely that the complex spikes recorded from preterm tissues resulted from mechanical injury by the electrode (e.g. excess pressure of the electrode on the tissue), because even within the same burst action potential shape was variable. Moreover, the occurrence of complex spikes did not increase with time of recording as would be expected if they resulted from injury caused by the electrode. However, the difference in shape of the extracellular signal may be due to tissue contraction pushing more or less hard against the recording electrode. On the other hand, it is possible that the underlying circular muscle layer, which shows a different type of action potential (i.e. spike followed by a plateau potential) than the longitudinal muscle at preterm (see Osa and Fujino, 1978; Anderson et al., 1981; Osa and Ogasawara, 1983; Bengtsson et al., 1984b), contributed to the serosal surface electromyogram at preterm producing a complex-shaped spike. (See Ohkawa, 1975; Osa and Katase, 1975 for evidence of an electrical interaction between longitudinal and circular muscle layers of preterm pregnant rat myometrium). At delivery in contrast, the shape of the spike is similar in both muscle layers (e.g. Anderson et al., 1981; Bengtsson et al., 1984b). Asynchronous activity of longitudinal myometrial cells at preterm (and their synchrony at delivery) may alternately reflect a gestational change in coupling of the longitudinal to the

circular muscle layer. In other words, if longitudinal muscle bundles are poorly coupled to each other in the transverse direction at preterm, an enhanced coupling to the underlying circular muscle at delivery might faciliate current flow in the transverse axis between the longitudinal muscle bundles (see below).

The longer distance over which spikes were entrained one-to-one in the myometrium at delivery than at preterm is consistent with the results of Osa (1974) who found one-to-one entrainment of spontaneous spikes over a 10 mm distance in longitudinal myometrium from immediately postpartum but not preterm (15-20 days) pregnant mouse uterus. Daniel (1960) recorded spontaneous spike burst discharges simultaneously at 2 sites (5 mm apart) from the longitudinal axis of pregnant rat uterine strips and found that the individual spikes within bursts occurred independently at the two electrodes but subsequently became entrained one-to-one as the burst progressed, consistent with the results for preterm pregnant myometrium in the present study. Similarly, Landa et al. (1959) found coordination of individual spikes within spontaneous bursts recorded over distances of 1-7 mm from the longitudinal axis of preterm pregnant (day 21) rat myometrium, but discoordination over longer distances, consistent with the short entrainment distances observed at preterm in the present study. The large within burst scatter of latencies for entrained spikes between adjacent sites, characteristic of the preterm tissues, is consistent with previous results for spontaneous spike conduction in the longitudinal axis of preterm pregnant rat myometrium (e.g. see Landa et al., 1959; Daniel, 1960). The mean apparent propagation velocity of about 8 cm/sec obtained in this study is similar to the velocities for propagation of spontaneous spikes previously reported for preterm pregnant rat, rabbit and cat longitudinal myometrium (Daniel and Singh,

1958; Daniel, 1960; Daniel and Renner, 1960). There are no previous reports on the propagation velocity of spontaneously discharged spikes from delivering myometrium of rat or any other species. Thus, this is the first study showing that the apparent propagation velocity of spontaneously discharged spikes is higher at delivery than at preterm.

Osa et al. (1983) studied the polarity of individual spikes comprising spontaneous bursts in preterm (day 20) and term pregnant rat longitudinal myometrium, and found that while there was no preferential direction of propagation at either stage of pregnancy, the direction changed more frequently before term. Assuming that the behaviour of the uterus during parturition would be an extension of these changes from day 20 to term, their results are consistent with the results of the present study, i.e. bidirectionality of phase for spike propagation within bursts at preterm and unidirectionality (but with no preferred direction) at delivery. The less stable and bidirectional phase shifts within bursts at preterm indicate that pacemaker areas are more labile in preterm pregnant as compared to delivering myometrium (Marshall, 1962; Osa et al., 1983). It has been reported for pregnant mouse myometrium that impulses propagate with greater velocity from the tubal to the cervical end, than in the reverse direction (Kuriyama, 1961). The results of the present study indicate that the mechanism of propagation in the longitudinal axis of pregnant rat myometrium does not show a directional preference (e.g. at both preterm and delivery, phase shifts were similar irrespective of direction of apparent spike propagation), consistent with the results of Melton and Saldivar (1964) for impulse propagation in the longitudinal axis of estrogen-treated nonpregnant rat myometrium.

Entrainment of action potentials between pacemaking regions (i.e. electrode sites) presumably depends on current flow crossing the junctional resistance between them (DeHaan and Hirakow, 1972; Jalife, 1984). Since the latency between entrained action potentials is directly related to the junctional resistance between pacemakers (Ypey et al., 1979; Clapham et al., 1980; Joyner et al., 1983), the shorter action potential latencies in the myometrium at delivery than at preterm indicate enhanced electrical coupling of myometrial cells at delivery. Its basis may be an increased electrotonic propagation resulting from a combination of several factors, including a decreased junctional resistance between uterine smooth muscle cells (Sims et al., 1982), an increased membrane resistance of individual cells (Kuriyama and Suzuki, 1976a; Sims et al., 1982), and an improved extracellular coupling (i.e. change in the clefts between cells), at term. It is difficult to assess the importance of either factor in enhancing propagation in the myometrium from before term to delivery. In cardiac tissue, entrainment of spontaneous discharges (action potentials) generated by pacemaker cells is more sensitive to alterations in longitudinal internal resistance (i.e. intercellular resistance) than to alterations in membrane resistance (see Delmar et al., 1986). The longer latencies at preterm were not due to other gestational changes in membrane properties, such as the higher spike discharge frequency at preterm which might slow propagation (i.e. through more refractory membrane) in these tissues (see Bortoff, 1976), since there was usually no dependance of latency on spike frequency. In bursts where there was a dependence, the latencies (time shifts) were most often negatively correlated with the spike frequency (i.e. shorter latencies with higher spike frequencies) which is opposite to that expected if propagation was slowed by more refractoriness (Bortoff, 1976).

These results provide electrophysiological evidence for a closer cell-to-cell coupling of myometrial cells at delivery than at preterm, which taken together with the ultrastructural data showing a much higher number of gap junction contacts between uterine smooth muscle cells at delivery than at preterm, suggest but do not prove that gap junction formation caused an improvement in electrical coupling in the parturient myometrium. These data are consistent with the generally accepted view of the importance of electrical transmission through gap junctions for cell-to-cell coupling of pacemaker cells in other tissues (De Mello, 1982; Jalife, 1984).

Evoked Spikes

The increased velocity and extent of spike propagation in the longitudinal axis of the myometrium at delivery as compared to at preterm (day 17) was verified using an independent procedure, namely that of evoking a spike at a known location in the tissue (i.e. at the ovarian end of the strip) and measuring its propagation along the strip. The mean propagation velocities of 10.5 cm/sec at delivery and 9.2 cm/sec at preterm are similar to the propagation velocities of spontaneously discharged spikes at their respective stages of pregnancy (Table VII). They are also similar in magnitude to previously reported velocities for propagation of evoked spikes in the longitudinal axis of rat myometrium: 1-10 cm/sec in untreated or estrogen- or estrogen plus progesterone-treated, nonpregnant (Melton, 1956; Melton and Saldivar, 1964; 1965; 1967; 1970; Saldivar and Melton, 1966), 7-33 cm/sec in pregnant (Kanda and Kuriyama, 1980) and 9.6 cm/sec in postpartum (Csapo and Kuriyama, 1963) animals. There have been no previous studies on evoked spike propagation in parturient

rat myometrium. This is the first study to demonstrate an increased spike propagation velocity in the longitudinal axis of rat myometrium during delivery and supports the results of Talo and Csapo (1970) who reported that evoked spikes propagated with higher velocity in the longitudinal axis of rabbit myometrium at delivery than at late (25 days) pregnancy. However, their report showed only a few slow speed traces of supposed evoked spikes (i.e. it is not clear from the traces whether they measured propagation of the stimulus artifact or of the evoked spike), and although they claimed that a large number of strips were studied, there was no statistical analysis of the data. Kanda and Kuriyama (1980) reported for the longitudinal myometrium from pregnant rats, that the velocity of propagation of evoked spikes (measured over very short, e.g. < 1.5 mm. distances), increased during the progression of pregnancy (from day 7 to term), but they did not study propagation during delivery.

The higher excitability (lower threshold) of the membrane to electrical stimulation at delivery than at preterm (as judged by the duration of a depolarizing pulse at a constant voltage required to evoke a spike), supports the previous results of Casteels and Kuriyama (1965). They similarly found the duration of stimulus (at constant voltage) required to trigger a spike was longer at late pregnancy (18-20 days) than just after (6-8 hrs) delivery. The excitability of a tissue is more properly described in terms of a strength-duration curve, but these were not determined for preterm or parturient tissues in the present study. The larger stimulus strength required to trigger a spike in the preterm as compared to parturient longitudinal strips is probably related to the level of the membrane potential (i.e. at preterm, the resting membrane is more hyperpolarized and hence further from threshold), as well as to the size

(diameter) of the individual smooth muscle fibers (i.e. at preterm, fiber diameter is smaller hence the threshold for stimulation by external electrodes is larger than at delivery; see Kuffler et al., 1984). During the silent period between spontaneous bursts in preterm tissues, a constant stimulus could not trigger a spike until just shortly before or immediately after bursts, consistent with previous studies on late pregnant rat uterus (Kuriyama, 1964; Casteels and Kuriyama, 1965; Abe, 1970). This periodical change of membrane excitability is probably due a change in membrane resistance: membrane resistance is increased just before the generation of a burst (presumably due to a reduction in $K^+$ conductance) and decreases (presumbably due to increase in $K^+$ conductance) following the burst (Kuriyama and Suzuki, 1976a; Kanda and Kuriyama, 1980).

Evoked spikes propagated further in the longitudinal axis of the myometrium at delivery as compared to at preterm (Table VII). The mean propagation distances of approximately 12 mm at preterm and 15 mm at delivery are similar to those of spontaneously discharged spikes in the longitudinal axis at the respective times during pregnancy (see "Excitable Region", Chapter 2). Talo and Csapo (1970) similarly reported that for rabbit myometrium studied in vitro, evoked spikes propagated further in the longitudinal axis at delivery than at late pregnancy. The present results do not provide information on the actual distance of spread of action potentials in the longitudinal axis of the parturient myometrium. In other words, the 15 mm distance over which all spikes propagated at delivery may be only a lower limit of the actual extent of impulse spread. At preterm, in contrast, the conduction distance was variable, with most spikes stopping before reaching the farthest recording electrode. The mean propagation distance of about 12 mm at preterm is probably the upper limit of

the extent of actual spread at that time of pregnancy. Individual distances of propagation in the longitudinal axis at preterm were not correlated with the indivudual propagation velocities, consistent with the results of previous studies on spread of evoked spikes in isolated uterine (Melton and Saldivar, 1964) and other visceral (Burnstock and Prosser, 1960) smooth muscles. The shorter propagation distances at preterm were not due to the effects of inhibitory nerves in the myometrium as tetrodotoxin, which selectively blocks most (but not smooth muscle) $Na^+$ channels (Kao, 1966), did not affect impulse spread in the preterm tissues. This might be expected because of the relatively low density of innervation in rat myometrium and the probable degeneration myometrial nerves during pregnancy (Thorbert, 1979; Marshall, 1981; Garfield, 1986). Therefore, the increased distance of impulse spread at delivery is probably due to a change in morphological or electrical properties (or both) of the uterine smooth muscle at term (see below).

An increased velocity and extent of impulse propagation was also observed for evoked spikes in the transverse axis of the myometrium during delivery as compared to at preterm (Table VII). However, at both stages of pregnancy, velocity and distance of propagation in this axis were only about 25-40% and 60-70%, respectively, of the corresponding values in the longitudinal axis. These results support those from the preceding chapter that showed an increased extent of spontaneous spike burst propagation in the transverse axis of the myometrium during pregnancy (see "Excitable Region" and Table IV, Chapter 2). There have been no other previous reports on spike propagation in this axis during pregnancy for myometrium from rat or any other species. Assuming that the propagation pathway of the electrical activity

recorded from the serosal surface of the tissue is through the longitudinal muscle layer at both stages of gestation (but see below), the differences in spike propagation between the longitudinal and transverse axes is probably related to the difference in tissue resistances between the two axes. For example, the smooth muscle cells are much longer than they are wide and thus a greater number of cell-to-cell junctions per unit distance will be encountered by the spike propagationg in the transverse, as compared to in the long axis of the cells. Hence the internal resistance of the longitudinal layer would be greater in the transverse than in the longitudinal axis. The tissue extracellular space is also anisotropic, so the resistance of the extracellular space is higher in the transverse than in the longitudinal axis (Sperelakis, 1979). Thus, propagation would be impeded to a greater extent in the former than in the latter axis. Zelcer and Daniel (1979) have previously shown that passive current spread is less in the transverse than in the longitudinal axis of longitudinal muscle from preterm pregnant and parturient rat uteri. However, for the uterine tissues used in the present study (which contained both longitudinal and circular muscles), the question remains whether the primary propagation pathway for excitation (recorded from the serosal surface of the longitudinal muscle along its transverse axis), is through the longitudinal or circular layer (see below).

What is the basis for the observed propagation changes in the myometrium from before term to delivery? Propagation in uterine, as in other visceral smooth muscles, occurs along bundles (composed of many muscle fibers connected in series and in parallel) of relatively large (200-300 $\mu$m) size and several millimeters in length (Burnstock and Prosser, 1960; Prosser et al., 1960;

Nagai and Prosser, 1963; Melton and Saldivar, 1964; Csapo, 1971). These bundles have cable-like electrical properties, analogous to those of nerve fibers (Abe, 1970; Tomita, 1970; 1975; Kuriyama and Suzuki, 1976a; Sims et al., 1982). According to Huxley (cf. Tomita, 1970; Weingart, 1977), propagation velocity ($v$) in a cable-like structure under different conditions can be compared according to the relation:

$$v \propto \sqrt{\frac{(dV/dt_{max})}{c_m V_p (r_i+r_o)}}$$

where $(dV/dt)_{max}$ is the maximum rate of rise of the action potential; $c_m$, the membrane capacity; $V_p$, the amplitude of the action potential; $(r_i+r_o)$, the sum, respectively, of the inside and outside (external) longitudinal resistance per unit length. Impulse velocity thus depends on both the size and rate of change of excitatory currents in the active membrane region, and on the cable characteristics of the tissue (principally its membrane capacity and internal and external longitudinal resistances). Changes during pregnancy in one or more of these parameters of the myometrium might alter propagation velocity. In longitudinal rat myometrium, spikes (recorded intracellularly) have higher amplitudes, greater overshoots and greater maximum rates of rise at late (17-20 days) pregnancy than at delivery or shortly postpartum (Kuriyama, 1964; Casteels and Kuriyama, 1965; Kuriyama and Suzuki, 1976a; Kanda and Kuriyama, 1980; Anderson et al., 1981). These changes would tend to cause an opposite conduction velocity change to the one observed in this study. On the other hand, the membrane capacitance is similar at late pregnancy and delivery (Sims et al., 1982). Of the possible factors which might increase propagation velocity, any change(s) leading to a decreased longitudinal resistance (myoplasmic and

junctional resistances) at term should lead to an increase in electrotonically mediated interactions, and hence to an increased propagation velocity during delivery, provided that its influence is not masked by some other effect. Sims et al. (1982) reported a decrease of about 30% in the internal longitudinal resistance (measured by extracellular current injection) of rat myometrium from before term to delivery. Contributing to this change (based on an assumed equivalent circuit) was a decreased junctional resistance between muscle cells, whereas there was no change in the myoplasmic resistance of individual cells. If gap junctions provide the only pathways for low-resistance coupling between uterine smooth muscle cells, their presence in much larger numbers in the longitudinal muscle layer in parturient as compared to preterm tissues (Table V; Table I, Chapter 2; Garfield et al., 1977; Sims et al., 1982) would result in better electrical coupling within this layer at delivery than at preterm. This improvement in coupling should result in a decrease in the longitudinal internal resistance of the tissue and hence to an increased velocity of spike propagation (see Weingart, 1977). If gap junctions are distributed more-or-less evenly over the smooth muscle surface (see Gabella and Blundell, 1979; 1981), the resistance to radial current flow within and between longitudinal muscle bundles would also be reduced at term, resulting in an increased propagation velocity in the transverse axis (and see below). On the other hand, a change in cable radius (i.e. radius of the individual smooth muscle fibers) would also affect the longitudinal internal resistance of the myometrium (Sims et al., 1982). However, the cable radius is probably similar at day 17 of pregnancy and delivery: the slight increase in uterine smooth muscle cell size (length and diameter) from day 17 to delivery (i.e. increased weight of myometrium due in part to

hypertrophy of the cells; see Afting and Elce, 1978; Vasilenko et al., 1981) is offset by an increased stretch on the myometrium caused by an increase in fetal weight (Knox and Lister-Rosenoer, 1978) and change in fetal shape (Carsten, 1968) which would tend to decrease the cable radius. Care was taken in the present study to maintain the muscle strips at their in situ lengths and thus to avoid over- or understretching the tissues which might influence their cable properties (see Sims et al., 1982) and hence impulse propagation. Whether there are changes during pregnancy in the configuration of myometrial cells (e.g. decreased cleft resistances between cells) or other properties of the extracellular space (see below) resulting in a decreased resistance to extracellular flow in the myometrium and contributing to the higher propagation velocity observed at delivery (see Tomita, 1967 and Cranefield, 1983 for discussion of action potential propagation in visceral smooth muscle and cardiac muscle, respectively), is not known. Comparative studies of action potential propagation in visceral smooth muscles have revealed that for smooth muscles which conduct the fastest, the extracellular space is smaller, the fibers are longer and more closely packed, than in slow conducting muscle (Burnstock and Prosser, 1960; Prosser et al., 1960). The size of the extracellular space in rat longitudinal myometrium does not change between late pregnancy (18-20 days) and 6-8 hrs postpartum (Casteels and Kuriyama, 1965). On the other hand, the longer uterine smooth muscle cell length at term (Csapo, 1971; and see above) may contribute to the increased propagation velocity during delivery: the longer the individual muscle cells, the fewer number of cell junctions (and hence the shorter the delay in propagation) per unit length of myometrium (i.e. conduction velocity along a single cell is almost instantaneous whereas a delay occurs at

its junction with another cell). Whether the individual smooth muscle fibers are more closely packed into bundles at delivery than at preterm, to account for the higher velocity of propagation during delivery, is not known.

If propagation in the transverse axis of the longitudinal muscle is partly through the underlying circular muscle layer (see above), then the increased propagation velocity in this direction of the myometrium from preterm to delivery may be partly due to an improved coupling between the muscle layers at delivery, or to an improved spike propagation of the circular muscle in its own axis, or to a combination of both. Ohkawa (1975) and Osa and Katase (1975) provided evidence suggesting that the longitudinal and circular muscle layers of preterm pregnant rat myometrium are electrically coupled (e.g. electrical activity generated in one muscle layer was conducted into the other layer). The extent of this coupling must be weak, at least at preterm, since there are marked differences in electrical properties of the muscle layers which make it unlikely that electrical activity spreads readily from one layer to the other (Bengtsson et al., 1984b). However, coupling between layers may be enhanced at delivery when their electrical activities are similar. In the previous chapter (see "Results", Chapter 2), evidence was presented to suggest that the longitudinal and circular muscle layers were electrically coupled during delivery (e.g. in circular strips: 1) electrical activity recorded from the longitudinal muscle occurred simultaneously with contractions of the circular layer and 2) entrainment of spike bursts was abolished over a portion of the strip where the circular muscle (but not the longitudinal muscle) was damaged. On the other hand, the shape of the circular muscle action potential changes from plateau-type at preterm to spike-shaped at term (Osa and Katase, 1975; Osa

and Fujino, 1978; Anderson et al., 1981; Bengtsson et al., 1984b). The prolonged depolarization of the plateau component at preterm may slow action potential propagation. On the other hand, the amplitudes and maximum rates of rise of the circular muscle action potentials are higher at delivery than at late (16-17 days) pregnancy (Bengtsson et al., 1984b). This would result in an increased velocity of propagation, if not masked by some other change. An increased electrical coupling of the circular muscle in its own axis at delivery should also enhance propagation between longitudinal muscle bundles in the transverse direction. Gap junctions were present in large numbers between uterine smooth cells in the circular muscle layer at delivery (Table V; and see Garfield et al., 1977), and their presence should result in a decreased longitudinal internal resistance in the circular layer. Studies on passive current spread for circular muscle from pregnant sheep myometrium have indicated an improved electrical coupling (i.e. length constant increased) between uterine smooth muscle cells in the circular muscle at delivery (Thorburn et al., 1984; Parkington, 1985), a time when gap junctions appear in large numbers in the longitudinal (and presumably the circular) muscle layer of the myometrium of this species (Garfield et al., 1979). Measurements of intercellular coupling (e.g. length constant) have not been made for circular muscle of pregnant rat myometrium at delivery. However, the results of the present study, showing a higher velocity of spike propagation in the transverse axis of the myometrium (i.e. in the direction of the long axis of the circular muscle cells), provide indirect evidence of an improved electrical coupling between uterine smooth muscle cells in the circular muscle of rat myometrium at delivery.

What is the basis for the further spread of impulses in the myometrium during delivery as compared to at preterm? As previously mentioned,

spikes in uterine smooth muscle propagate along functional bundles. These bundles branch out and join other bundles forming a mesh or network (see "General Anatomy", Chapter 1; Figure 4, Chapter 2). Propagation may be blocked at a branching point of a bundle due to a low safety factor, i.e. the local circuit current of the spike must excite a larger membrane area at the branching point and hence the safety factor would be low (Tomita, 1967; 1970; 1975). Thus, the geometrical factor of branching is an important determinant affecting the propagation distance. If the amount of branching changed during pregnancy, the propagation distance might be altered. If this is the basis for the further spread of spikes in the myometrium during delivery, then there must be more branching at preterm than at term. However, whether the arrangement of the bundles and hence their branching changes during pregnancy has not been studied. The increased length of the individual smooth muscle fibers at term than at preterm (see above) may result in a longer bundle length and hence fewer branches per length of muscle at delivery. The safety factor for propagation may be lower at preterm (day 17) than at delivery (because the membrane potential is more hyperpolarized, i.e further from threshold, at preterm than at delivery) making it more likely than propagation would be blocked at a branching point (Tomita, 1967). On the other hand, since propagation in the smooth muscle bundles requires the simultaneous generation of spikes in many fibers, the interaction of smooth muscle fibers, both within and between bundles, may also be important in determining the extent of conduction (Burnstock and Prosser, 1960; Nagai and Prosser, 1963; Tomita, 1967). The presence of gap junction contacts between uterine smooth muscle fibers at delivery would enhance fiber interactions (within and between bundles), thereby increasing the

width and length of the conduction path and hence the extent of conduction. As for the change in extent of propagation in the transverse of the myometrium from preterm to delivery, a decreased resistance to radial current flow within and between longitudinal muscle bundles (e.g. due to gap junction formation), an improved coupling of the underlying circular muscle in its own axis (e.g. due to gap junction formation), and an enhanced coupling between muscle layers would increase the width and length of the conduction path (and hence the distance of impulse spread) in the transverse axis of the longitudinal layer at delivery.

Despite its superficial resemblance to a core-conductor (Prosser, 1962; Barr and Dewey, 1968), the flow of current through such a complex syncitium as the myometrium with its three-dimensional intercellular connections within branching and overlapping fiber bundles, must be very complicated. It would be a formidable task to predict the effect of any one factor on impulse propagation through such a structure (Cranefield, 1983). However, the results showing an increased velocity and extent of propagation of evoked spikes in the myometrium at delivery as compared to at preterm provides indirect electrophysiological evidence for a closer electrical coupling of myometrial cells during delivery, consistent with the results for apparent propagation of spontaneous bursts and spikes in the myometrium during pregnancy, and they support the results of previous studies using different techniques of assessing electrical coupling in the myometrium (Sims et al., 1982). Taken together with the ultrastructural evidence (Table V; Table I, Chapter 2), these data support but do not prove the hypothesis that gap junction formation in the longitudinal and circular muscle layers causes an improvement in electrical coupling in parturient myometrium (Garfield et al, 1977; 1978).

On the other hand, relatively good electrical coupling existed at preterm (e.g. spontaneous action potentials were entrained, and evoked spikes propagated, over distances many times the length (300-800 $\mu$m, see Csapo, 1962; Marshall, 1973) of individual uterine smooth muscle cells (and see "General Discusion", Chapter 4). Since the gap junction is widely held as the anatomical correlate of functional electrical coupling between many cell types (Dewey and Barr, 1968; Gabella, 1981; Loewenstein, 1981; De Mello, 1982), the basis of the coupling in the myometrium before term is uncertain. Perhaps the few gap junctions observed in preterm tissues are sufficient for coupling. Although we have no idea of how many gap junctions must be present in the myometrium for a change in coupling (and hence impulse propagation) to be detected, it is logical to suppose that an increased frequency of gap junctions at term would further reduce junctional resistance and hence improve electrical coupling between cells. Alternately, very small gap junctions, undetected by thin section electron microscopy, may be present in the myometrium at preterm, and these may be sufficient for coupling. For example, Williams and DeHaan (1981) reported for heart cell aggregates that spontaneously discharged action potentials remain synchronized in the absence of ultrastructurally defined gap junctions (caused by treatment of the tissue with protein synthesis inhibitors). These data may also suggest that gap junctions are not necessary for coupling the heart cells. On the other hand, gap junctions may not be the only route for current to spread between cells (Sperelakis, 1969). Other coupling mechanisms could play a role, including capacitative (Sperelakis and Mann, 1977) and electric field (Sperelakis et al., 1983) coupling. These modes of coupling imply that current spreads between cells by way of the extracellular space in regions of close contact between them. Close or intermediate contacts are numerous in the

myometrium at preterm (see Garfield and Daniel, 1974) and these structures may facilitate current flow through the extracellular space in the myometrium (Zelcer and Daniel, 1979). At any event, the nature of the intercellular current flow (and of cell-to-cell conduction of the action potential) are debatable, as is the general question of whether gap junctions are necessary for cell-to-cell coupling in smooth muscle (Daniel et al., 1976; Gabella, 1981). However, the results of the present study add to the previous evidence (e.g. Sims et al., 1982) and suggest that gap junctions are sufficient for electrical coupling of uterine smooth muscle cells.

In summary, these results which show an enhanced velocity and extent of action potential propagation in the myometrium at delivery, suggest an improved electrical coupling of myometrial cells associated with gap junction formation between uterine smooth muscle cells at term. In this regard, the development of gap junctions in the term pregnant myometrium may be one factor promoting synchronous contractile activity in the uterine wall and hence expulsion of the fetus(es). The widespread occurrence of gap junctions at parturition (and their virtual absence at preterm) in all species studied (mice: Dahl and Berger, 1978; rabbit: Demianczuk et al., 1984; guinea pig, sheep, baboon and human: see review of Garfield et al., 1985; Verhoeff et al., 1985) suggests their fundamental importance in promoting labour. However, as pointed out by Liggins (1979), the initiation of parturition is a complex event, involving the inter-play of several factors including hormones (e.g. estrogen, progesterone, oxytocin, relaxin) and locally produced stimulants (e.g. prostaglandins), as well as the physical factor of stretch imposed on the uterus by its fetal contents, which together alter the excitability and contractility of the uterine smooth muscle cells (see Marshall, 1973). Gap junction formation (and the resulting

coordinated activities of the uterine smooth muscle cells) would aid in the conversion of these excitability and contractility changes into the powerful contractions of the uterine wall necessary to expel the fetus(es).

## CONCLUSIONS

Spike propagation and gap junction frequency in the myometrium were measured at preterm and at delivery to test the hypothesis that gap junction formation at parturition results in improved electrical coupling between uterine smooth muscle cells. Spontaneously discharged spikes were entrained over longer distances and with shorter latencies (i.e. higher apparent propagation velocities) in the longitudinal axis of the myometrium at delivery than at preterm. The improved spike propagation in the myometrium at delivery was confirmed by measuring the spread of spikes evoked by electrical stimulation. Evoked spikes similarly propagated with higher velocity and over longer distances in both the longitudinal and transverse axes of the myometrium at delivery as compared to at preterm. Structural studies confirmed that gap junctions were present in large numbers between uterine smooth muscle cells at delivery, whereas few if any junctions were found in preterm tissues. Since the velocity and extent of action potential propagation through a network of multicellular muscle bundles depends in part on the cell-to-cell coupling resistances of the muscle cells, these results provide indirect evidence for an improved cell-to-cell electrical coupling associated with gap junction formation at the end of gestation. This improved electrical coupling between myometrial cells may be the basis for development of synchronous contractile activity in the uterine wall at parturition.

TABLE V. Frequency, size and fractional area of gap junctions (GJs) in preterm pregnant (day 17) and delivering tissues fixed before and after electrical stimulation and recording. "n" is the number of uterine horns examined, one per animal. Three tissues from each uterine horn were examined: one (longitudinal) tissue fixed before experimentation (i.e. immediately after removal of the uterus from the animal) and the other two (one longitudinal and one circular) tissues fixed after experimentation. The number of GJs is the total number of all 5 or 7 lined junctions identified in 18-22 nonoverlapping micrographs of each tissue. The frequency of GJs is expressed as the number of GJs per 1000 $\mu$m plasma membrane surveyed. The fractional area of GJs was calculated by doubling the length of GJ membrane and dividing by the total length of plasma membrane. Values are means $\pm$ SD. Those with the same superscript are significantly different ($p < .05$) as determined by the Wilcoxon Rank Sum Test. Tissues were fixed after 1 hr to 3 hrs following removal of the uterus from the animal.

TABLE V.

GAP JUNCTIONS IN MYOMETRIUM

| Treatment | No. of Tissues, n | No. of GJs | Length of Membrane Surveyed, $\mu$m | No. of GJs/ 1000 $\mu$m Membrane | Mean Size GJs, nm | Fractional Area of GJs, % |
|---|---|---|---|---|---|---|
| Day 17 | | | | | | |
| a. Fixed immediately | 4(2) | 2 | 4,313 | .47 ± .54[a] | 122 ± 38 | .012 ± .014[e] |
| b. After recording (longitudinal) | 4(3) | 3 | 3,802 | .74 ± .50[b] | 78 ± 10[d] | .011 ± .008[f] |
| c. After recording (circular) | 4(1) | 1 | 3,952 | .24 ± .48[c] | 119 ± 0 | .006 ± .011[g] |
| Delivering | | | | | | |
| a. Fixed immediately | 4(4) | 42 | 4,897 | 8.50 ± 1.54[a] | 127 ± 66 | .214 ± .041[e] |
| b. After recording (longitudinal) | 4(4) | 29 | 3,918 | 7.46 ± 1.51[b] | 150 ± 54[d] | .224 ± .053[f] |
| c. After recording (circular) | 4(4) | 36 | 4,424 | 8.22 ± .67[c] | 158 ± 80 | .249 ± .084[g] |

TABLE VI

CHARACTERISTICS OF ENTRAINED SPONTANEOUS SPIKES IN THE LONGITUDINAL AXIS OF THE MYOMETRIUM DURING PREGNANCY

| | Before Term (n = 10) | Delivering (n = 10) | P |
|---|---|---|---|
| Spike Discharge Frequency (spikes/sec) | 3.99 ± .59 | 1.49 ± .33 | $p < .001$ |
| Maximum Spike Discharge Frequency (spikes/sec) | 5.24 ± .82 | 1.83 ± .48 | $p < .001$ |
| Phase Shift (degrees) | 57.8 ± 21.4 | 12.3 ± 5.4 | $p < .001$ |
| Time Shift (msec) | 38.9 ± 12.6 | 22.9 ± 9.4 | $p < .001$ |
| Mean Apparent Conduction Velocity (cm/sec) | 7.9 ± 3.0 | 13.5 ± 4.2 | $p < .001$ |

TABLE VI. Summary of characteristics of entrained spontaneous spikes in the longitudinal axis of the pregnant myometrium from 5 animals before term and 5 animals during delivery. "n" is the number of tissues, 2 per uterine horn. Electrical activities were simultaneously recorded at 6 adjacent electrodes (3 mm apart): activities at 3 electrode sites were analyzed (see "Materials and Methods"). All values are means ± SE. P values were determined using a one-way analysis of variance.

TABLE VII

PROPAGATION VELOCITY AND DISTANCE OF EVOKED SPIKES IN RAT MYOMETRIUM DURING PREGNANCY

| | Before Term | Delivering | P |
|---|---|---|---|
| LONGITUDINAL AXIS | (n = 8) | (n = 11) | |
| Propagation velocity, cm/sec. | 9.2 ± .8 | 10.5 ± 1.3 | $p < .001$ |
| Propagation distance, mm. | 11.8 ± 2.8 | ≥15 | $p < .001$ |
| TRANSVERSE AXIS | (n = 4) | (n = 5) | |
| Propagation velocity, cm/sec. | 2.3 ± .7 | 4.0 ± .8 | $p < .001$ |
| Propagation distance, mm. | 7.4 ± 1.7 | 10.4 ± 2.3 | $p < .001$ |

TABLE VII. Summary of gestational changes in propagation of evoked spikes in the longitudinal and transverse axes of the pregnant rat myometrium. "n" is the number of tissues examined, usually only one per uterine horn. Spikes were evoked at the ends of the strips and their propagation down the strips was followed using 6 glass pore surface electrodes, as described in "Materials and Methods". Approximately 10 measurements were made per tissue (see text). All values are means ± SD. P values were determined by the Student's t test for independent samples.

FIGURE 32. Schematic representation of the modified Abe and Tomita (1968) type bath of about 10 ml capacity (5 cm x 1.5 cm x 1.5 cm) that was used for evoking and recording electrical activity. A uterine strip (3 cm long x .3-.5 cm wide) was pinned out at its in situ length (serosal side up) to the Sylgard floor of the bath such that 1 cm of the strip (ovarian end) was pinned between the 2 stimulating electrodes that formed the ends of the stimulating chamber, while the other 2 cm portion of the strip protruded into the recording compartment. To record electrical activity, 6 glass pore extracellular electrodes (only 2 are shown in figure) were rigidly mounted (3 mm apart) in a holder that was attached to the base of a microscope stand, and the electrode array was placed on the serosal surface of the strip in the direction of the strip's long axis (modified from Specht and Bortoff, 1972).

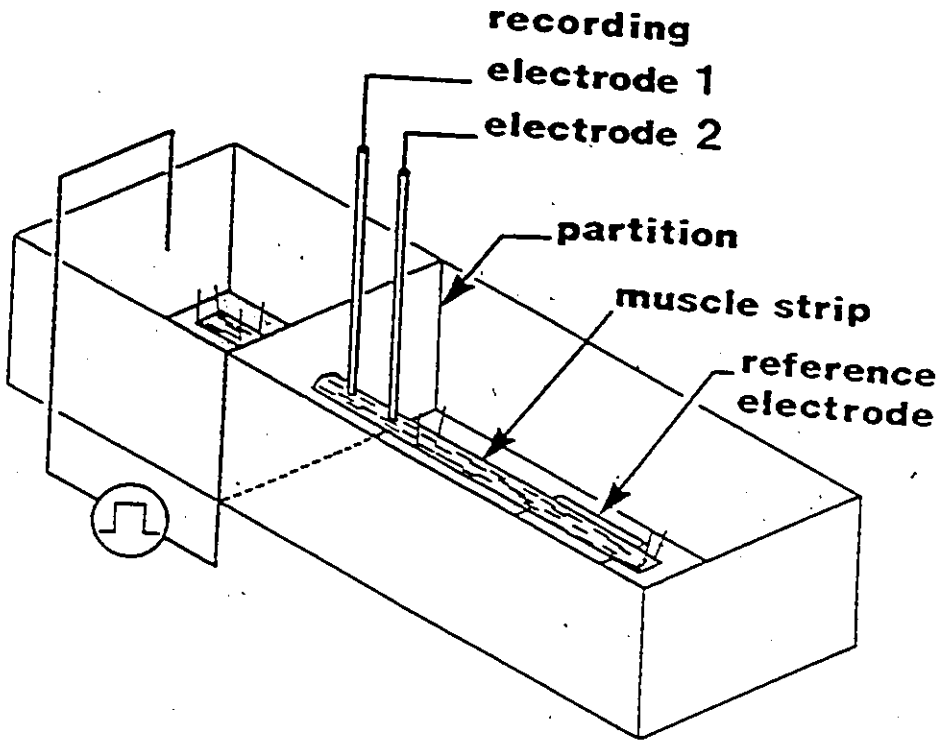
recording
electrode 1
electrode 2
partition
muscle strip
reference
electrode

FIGURE 33. Determination of the instantaneous spike frequency, phase shift and time shift of spontaneously discharged spikes. The activities of 3 adjacent electrodes ("e") were digitized, and the temporal positions of the spikes determined using computerized peak detection analysis, as described in "Materials and Methods". The instantaneous spike frequency is the reciprocal of the time interval ($T_i$) between successive spikes in the burst. The latency ($\Delta t_{i,\ i+1}$) for the occurrence of corresponding entrained spikes at an electrode pair was calculated for each entrained spike in the burst. Phase shifts of entrained spikes were calculated as $\Delta t_{i,\ i+1}/T_i \times 360^{\circ}$. Time shifts (lags) are the absolute values (i.e. direction of apparent propagation ignored) of the latencies.

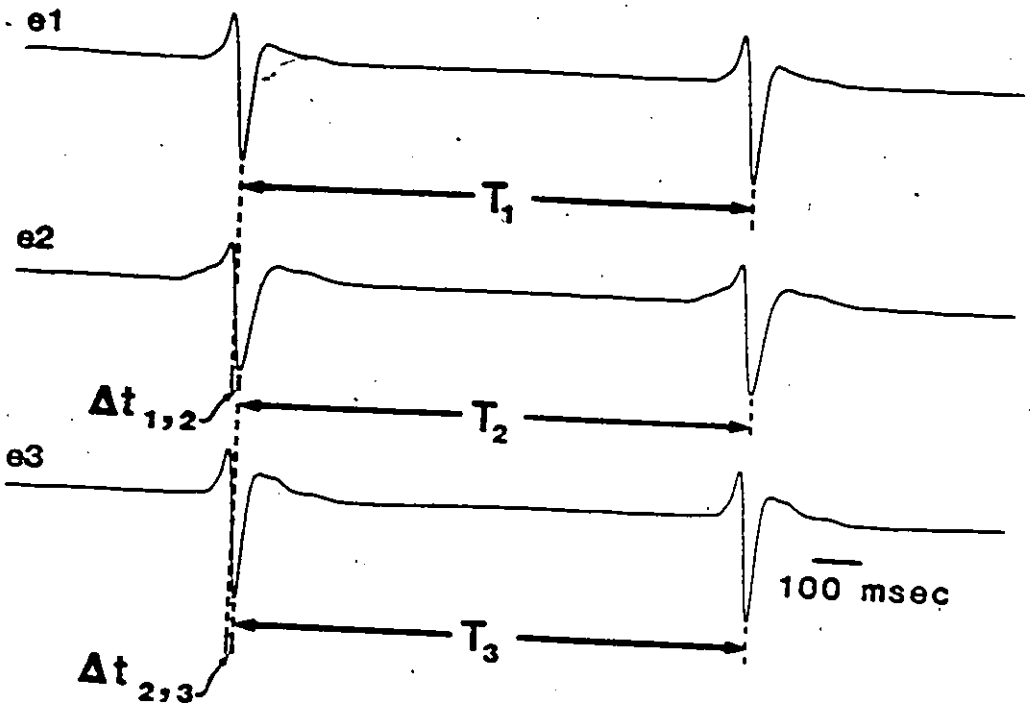
e1
e2
e3
$T_1$
$T_2$
$T_3$
$\Delta t_{1,2}$
$\Delta t_{2,3}$
100 msec

FIGURE 34. Electron micrograph of a small gap junction between uterine smooth muscle cells of preterm pregnant (day 17) rat myometrium fixed immediately after removal of the uterus from the animal. Bar, 1 $\mu$m. X 33,000. Inset. Bar, .5 $\mu$m. X 63,000.

FIGURE 35. Electron micrographs of myometrium fixed following *in vitro* electrical recordings (tissue in the muscle bath for about 1 hour). A). Preterm pregnant (day 17) myometrium showing no gap junctions but some intermediate contacts (see arrows) between uterine smooth muscle cells. Bar, 1 $\mu$m. X 33,000. B). Gap junctions in delivering myometrium. Bar, .5 $\mu$m. X 61,000.

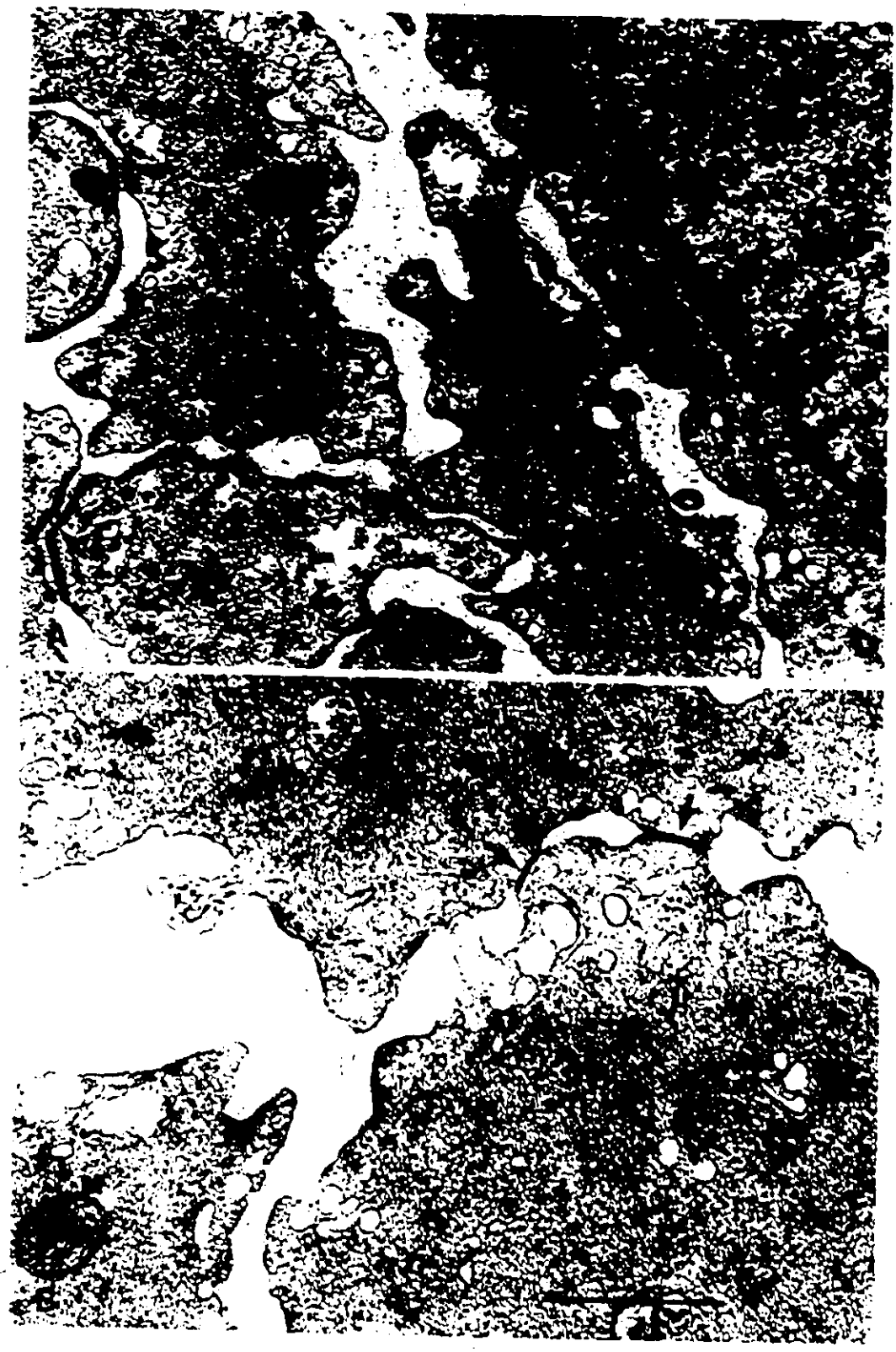

FIGURE 36. Shapes of spontaneously discharged spikes recorded extracellularly from the pregnant rat myometrium. An upwards deflection indicates relative positivity with respect to ground. A). Delivering myometrium. B-H). Preterm pregnant (day 17) myometrium. These action potentials were from bursts in the same tissue. This variation in action potential shape was sometimes observed within the same burst at a given electrode site.

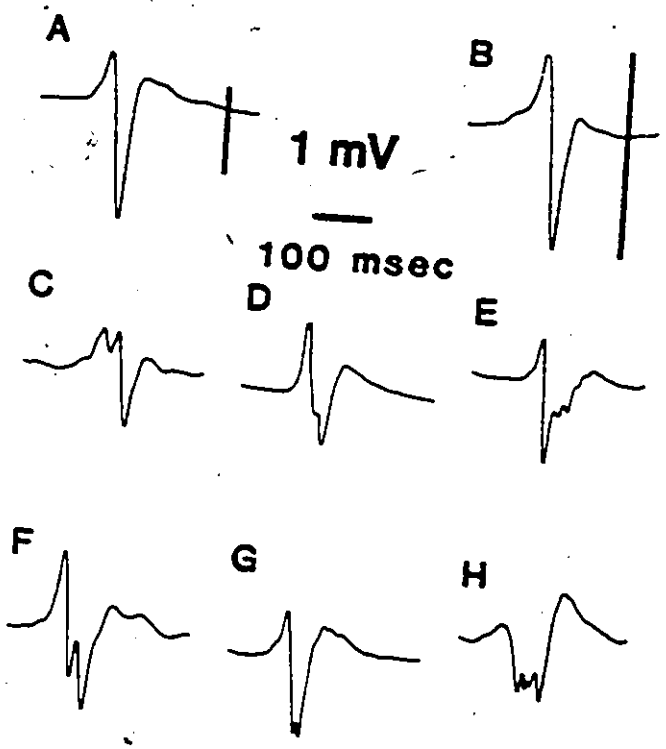
A
B
1 mV
100 msec
C
D
E
F
G
H

FIGURE 37. Entrainment of spontaneously discharged spikes in the longitudinal axis of the pregnant myometrium. Records are fast speed traces (50 mm/sec) of portions (e.g. onset, middle and end) of spike bursts simultaneously recorded at 6 sites in a longitudinal uterine strip. Inter-electrode distance = 3 mm. A). Preterm (day 17). Entrainment distance increased from 3 mm at the onset of the burst to 15 mm at the middle, and then decreased to 12 mm at the end of the burst. Arrows indicate where spikes at an electrode site produced only small depolarizations at its adjacent electrode site. B). Delivering. Entrainment distance = 15 mm throughout the entire burst.

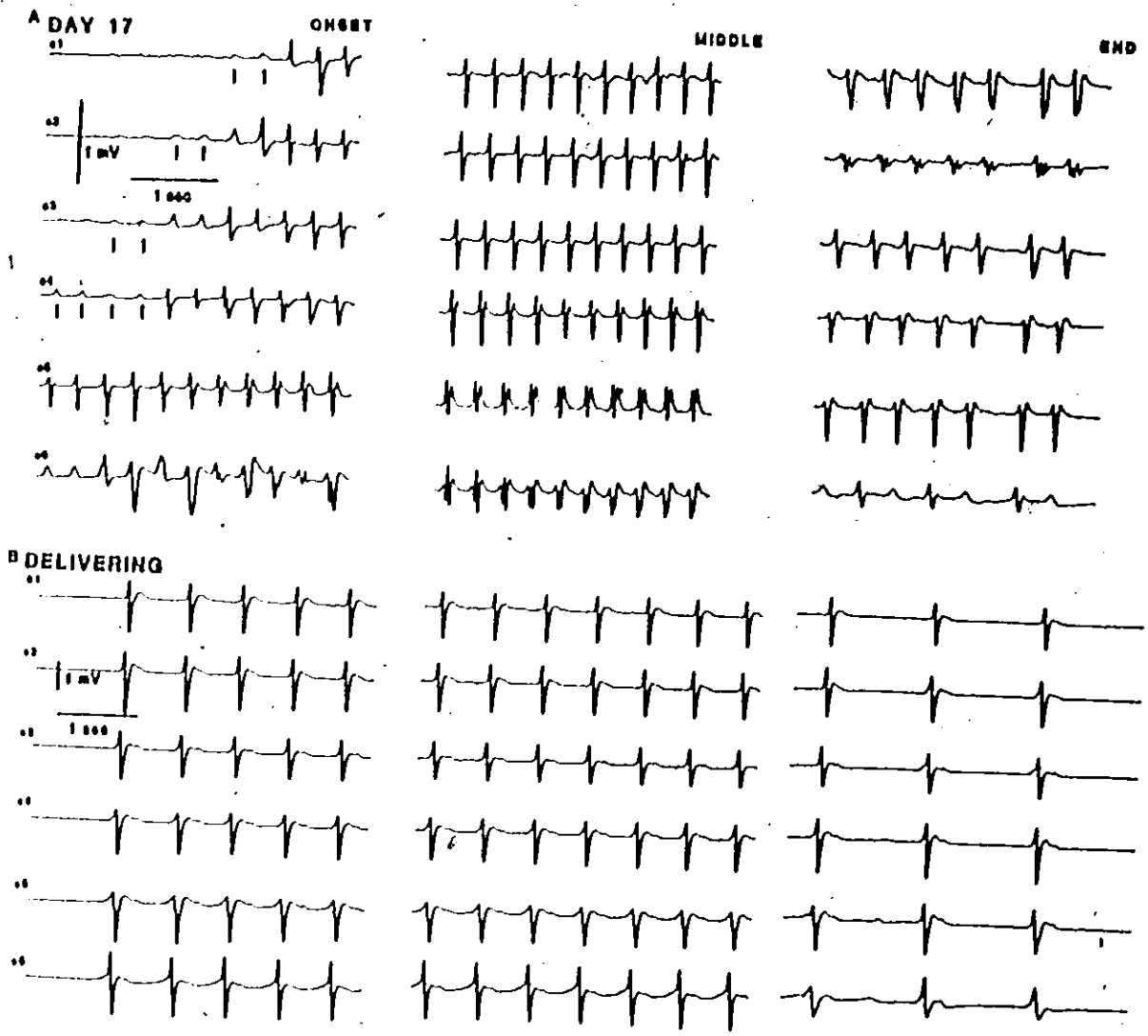
A DAY 17
ONSET
MIDDLE
END
1 mV
1 sec
B DELIVERING
1 mV
1 sec

FIGURE 38. Entrainment of spontaneously discharged spikes in TTX-treated preterm pregnant (day 17) myometrium. Records are fast speed (50 mm/sec) traces of the onset, middle and end portions of bursts simultaneously recorded at 6 sites in the long axis of a longitudinal uterine strip after treatment with 1 $\mu$g/ml of tetrodotoxin. Inter-electrode distance = 3 mm. Entrainment distance increased from 3 mm at the onset of the burst to 12 mm at the middle and end of the bursts.

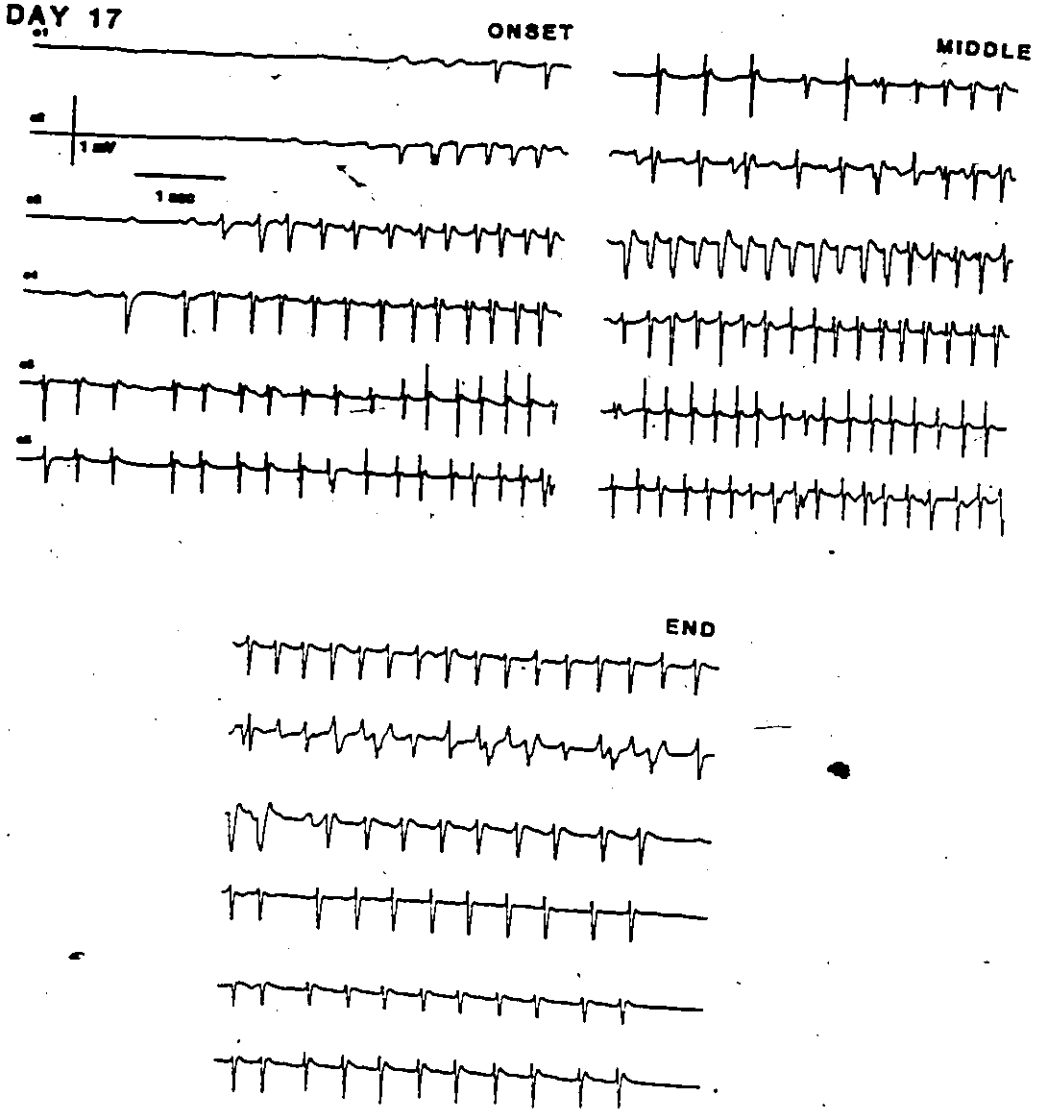
DAY 17
ONSET
MIDDLE
END

FIGURE 39. Individual spikes comprising bursts simultaneously recorded at 3 adjacent electrode sites in the longitudinal axis of preterm pregnant myometrium. A). Entire bursts. Short arrows indicate portions of the bursts shown in (B). B). Fast speed (50 mm/sec) traces of portions of bursts in (A) showing entrained spikes. Long arrows indicate the times during the bursts when the phase lead of spike propagation changed direction at both electrode pairs. Inter-electrode distance = 3 mm. The electrical characteristics of entrained spikes were quantitated for this set of bursts, as shown in Figures 41A, 42A and 43A.

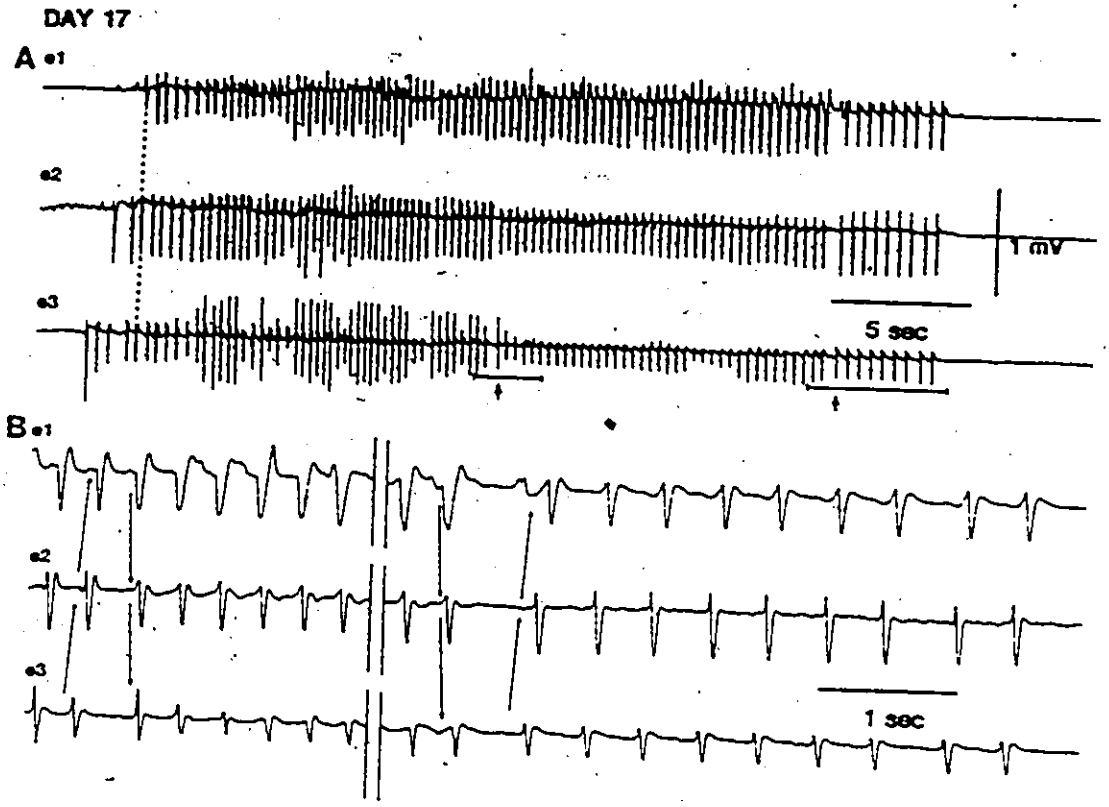
DAY 17
A
e1
e2
e3
1 mV
5 sec
B
e1
e2
e3
1 sec

FIGURE 40. Individual spikes comprising bursts simultaneously recorded at 3 adjacent electrode sites in the longitudinal axis of delivering myometrium. A). Entire bursts. The portions of these bursts (see short arrow and bar) are shown in (B) below. B). Fast speed (50 mm/sec) traces of portions of bursts in (A) showing entrained spikes. Long arrows indicate the direction of phase lead of spike propagation. Inter-electrode distance = 3 mm. The electrical characteristics of entrained spikes in this set of bursts were quantitated, as shown in Figures 41B, 42B and 43B.

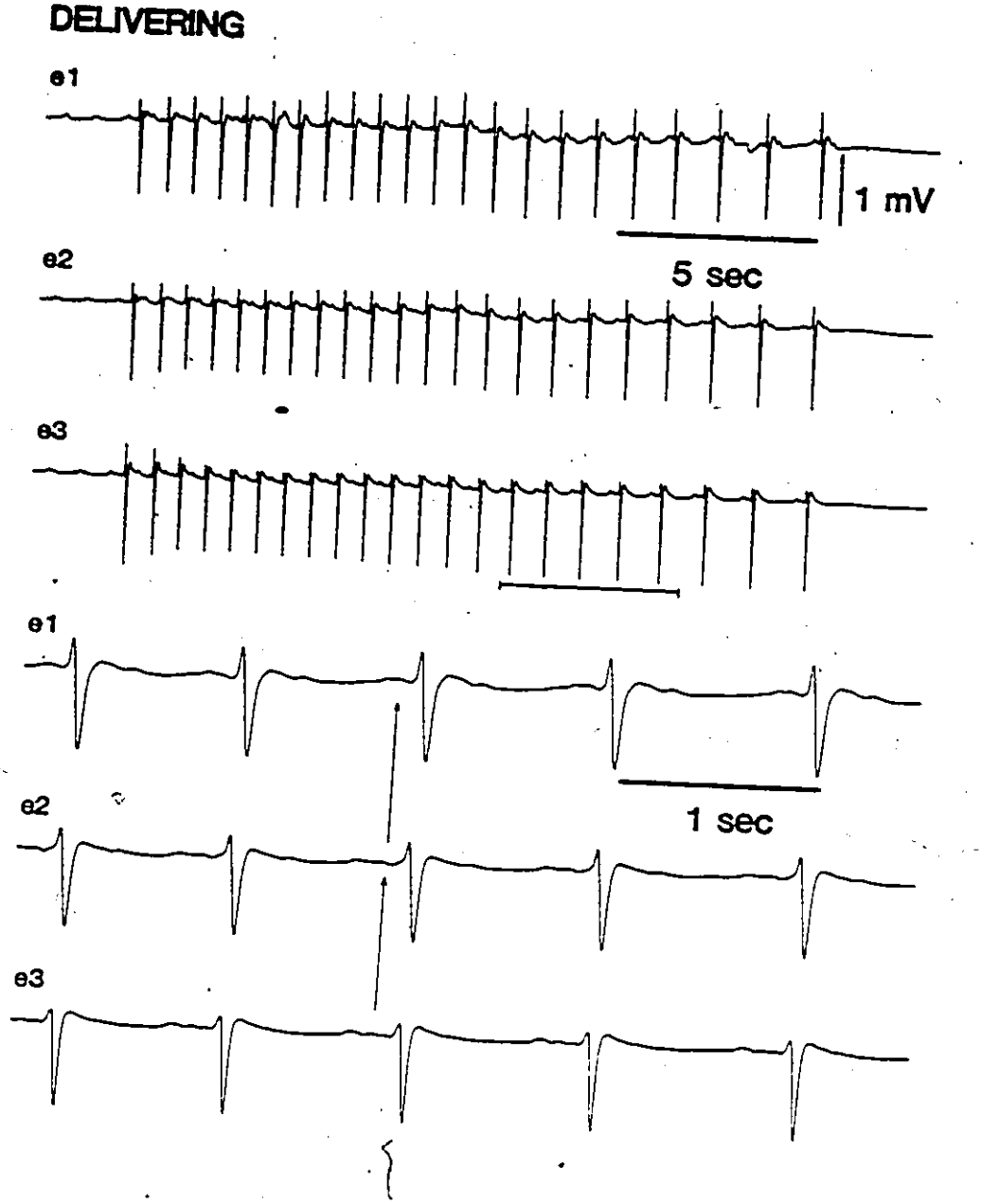
DELIVERING
e1
1 mV
5 sec
e2
e3
e1
1 sec
e2
e3

FIGURE 41. Spike discharge frequency during the progression of a burst of action potentials in the pregnant myometrium. A). Preterm (see bursts in Figure 39). B). Delivering (see bursts in Figure 40). Instantaneous spike frequencies of successive entrained action potentials in bursts simultaneously recorded at 3 adjacent electrode sites ("e1", "e2" and "e3") were calculated from the time intervals between successive action potentials, as described in "Materials and Methods".

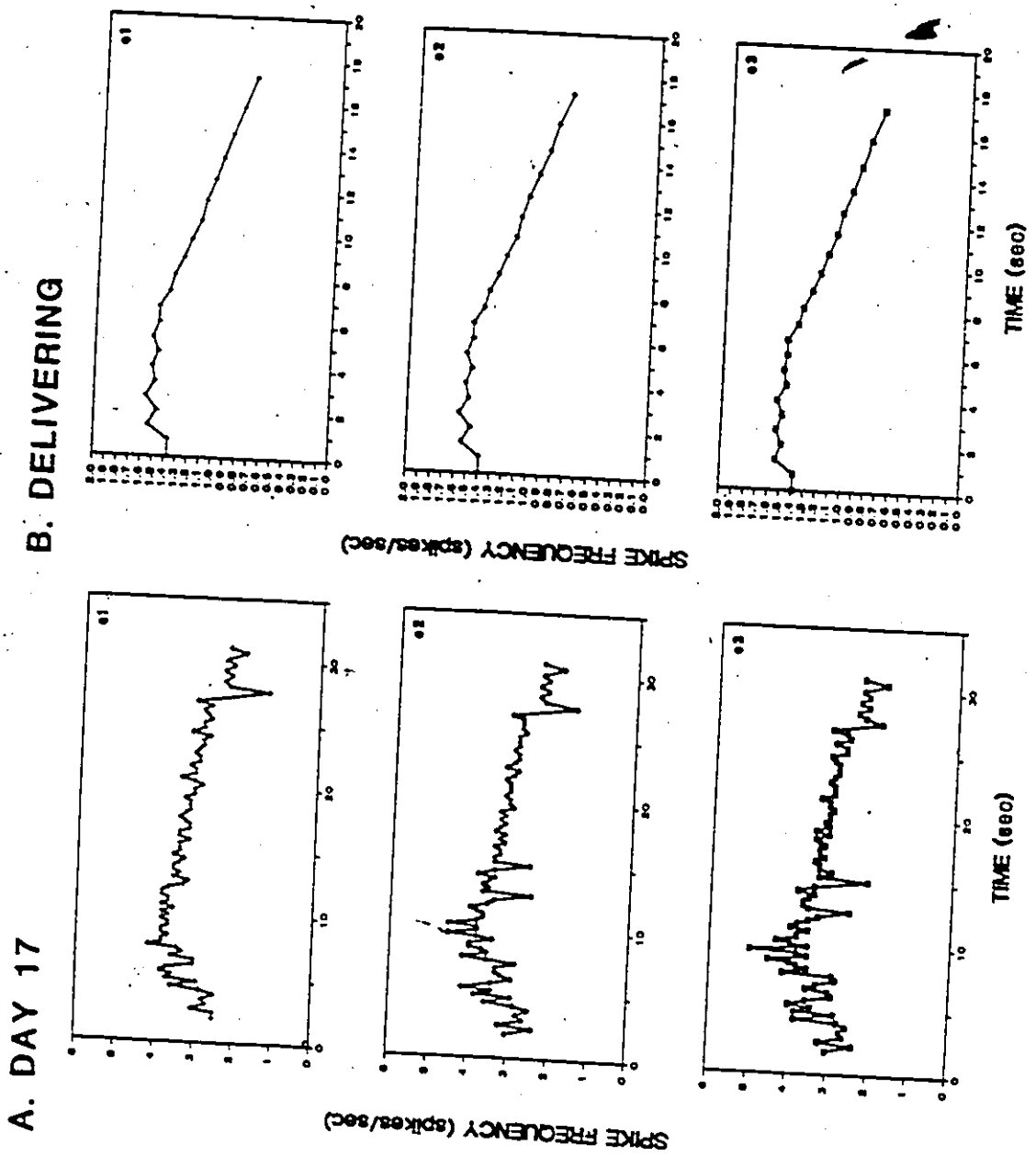
A. DAY 17
B. DELIVERING
SPIKE FREQUENCY (spikes/sec)
TIME (sec)

FIGURE 42. Phase shifts of successive entrained spikes during the progression of bursts simultaneously recorded at 3 adjacent electrodes in the pregnant myometrium. A). Preterm (see bursts in Figure 39). B). Delivering (see bursts in Figure 40). Phase shifts ($\triangle t_{i,\ i+1}/T_i$ X $360^{o}$) between adjacent electrodes (pairs 2→1 and 3→2) were calculated as described in "Materials and Methods".

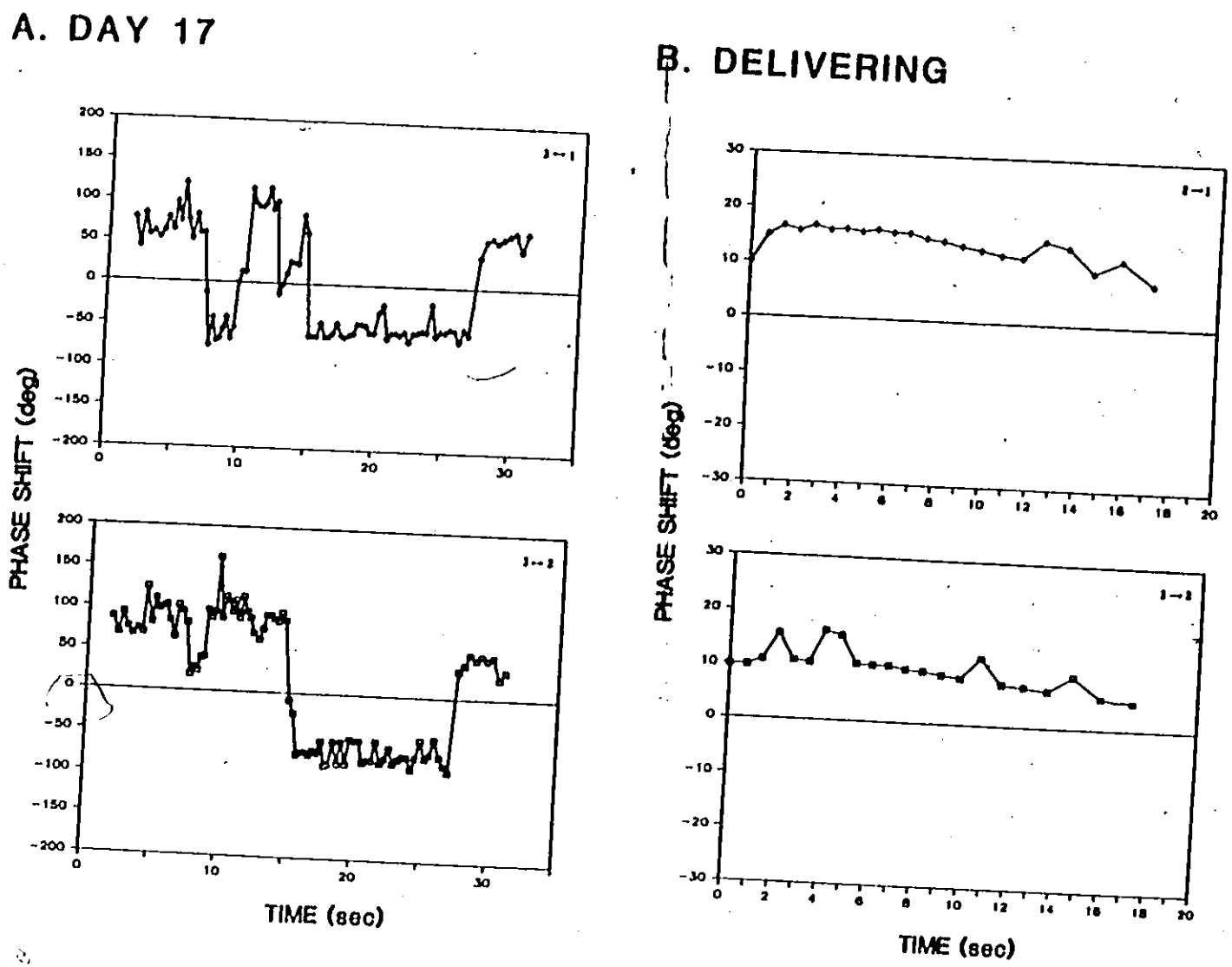
A. DAY 17
B. DELIVERING
PHASE SHIFT (deg)
TIME (sec)
3→1
3→2
1→1
1→2

FIGURE 43. Time shifts (lags) plotted against instantaneous spike frequencies of successive entrained spikes during the progression of bursts simultaneously recorded at 3 adjacent electrodes in pregnant myometrium. Time shifts (msec) were calculated as described in "Materials and Methods". A). Preterm (see bursts in Figure 39). Time shifts were only weakly ($r=-.28$) but significantly ($p < .01$) correlated with spike frequency at electrode pair "2→1", while at electrode pair "3→2", the correlation ($r=.15$) was not significant ($p > .05$).
B). Delivering (see bursts in Figure 40). Time shifts were moderately ($r=-.48$) and significantly ($p < .01$) correlated with spike frequency at electrode pair "2→1", while at electrode pair "3→2" time shifts were not correlated ($r=.06$) with spike frequency.

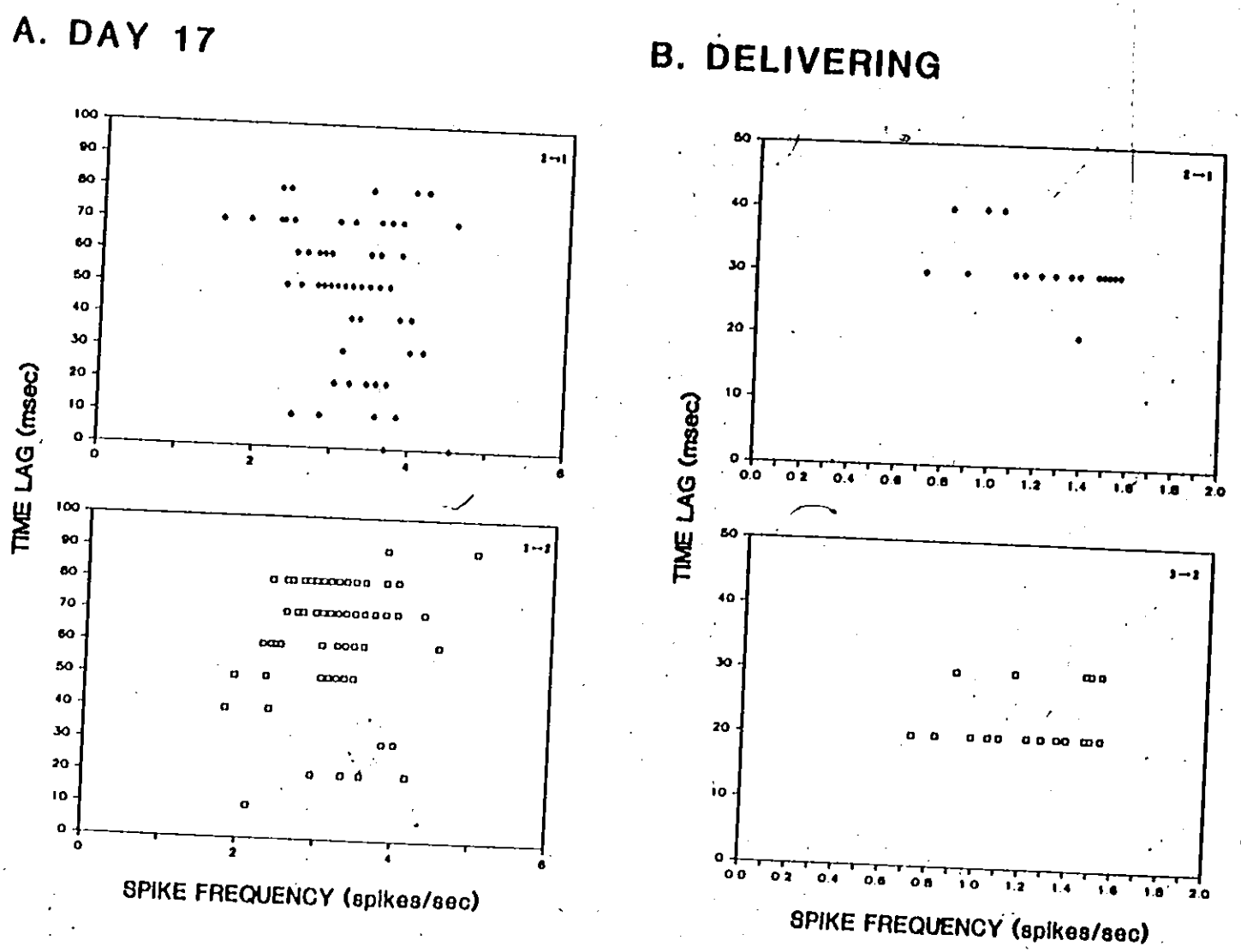
A. DAY 17
B. DELIVERING
TIME LAG (msec)
SPIKE FREQUENCY (spikes/sec)
TIME LAG (msec)
SPIKE FREQUENCY (spikes/sec)

FIGURE 44. Effect of varying the stimulus duration on the generation and shape of the evoked spikes recorded extracellularly near the cathodal stimulating partition. Spikes were evoked at the ovarian end of a delivering longitudinal uterine strip by applying square wave electrical pulses (6-7 V) between 2 chlorided-silver plates (described in "Materials and Methods) and were simultaneously recorded at 2 electrodes, "e1" and "e2", located 3 mm and 6 mm, respectively, from the cathode. In this and subsequent records, "e1" is at the ovarian end of the strip, closest to the partition. An upwards deflection indicates relative positivity with respect to ground.
A). Spontaneously discharged spike. B)-D). Evoked spikes to depolarizing pulses of 50 msec, 100 msec and 150 msec, respectively. E). 50 msec hyperpolarizing pulse.
Arrows indicate when stimulus was applied. Note the distortion of the action potential recorded at e1, closest to the stimulating plate.

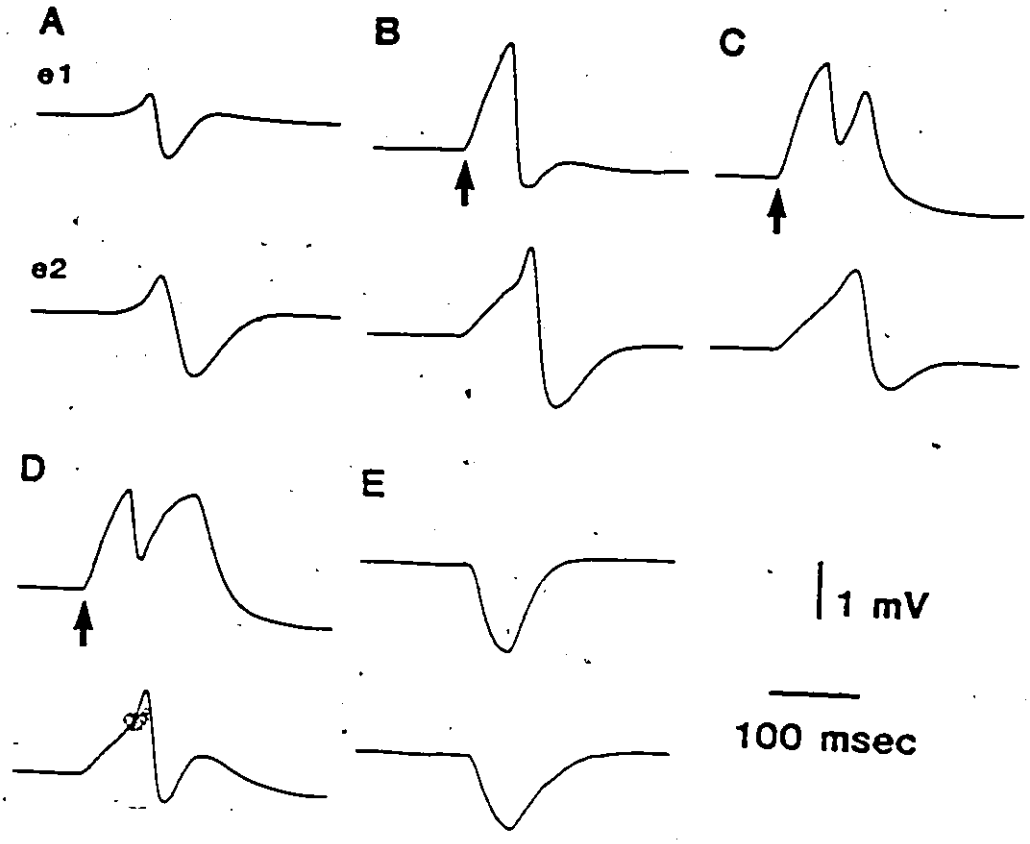
A
e1
e2
B
C
D
E
1 mV
100 msec

FIGURE 45. Stimulation of delivering myometrium during the quiescent period between spontaneous burst discharges. Spikes were simultaneously recorded at 6 electrode sites in the long axis of a longitudinal uterine strip. Inter-electrode distance = 3 mm. A). Seven spikes (see arrows) were evoked by repetitive (e.g. at .5 Hz) application of depolarizing pulses (6V X 40 msec). B). Fast speed (200 mm/sec) traces of the 1st, 4th and 7th evoked spikes. Propagation velocities were 11.8 cm/sec, 11.8 cm/sec and 12.2 cm/sec, respectively, measured between positive peaks of electrodes "e2"-"e6" (stimulus artifact obscured peak at "e1" . In subsequent records, propagation velocities of evoked spikes were measured between positive peaks unless otherwise indicated.

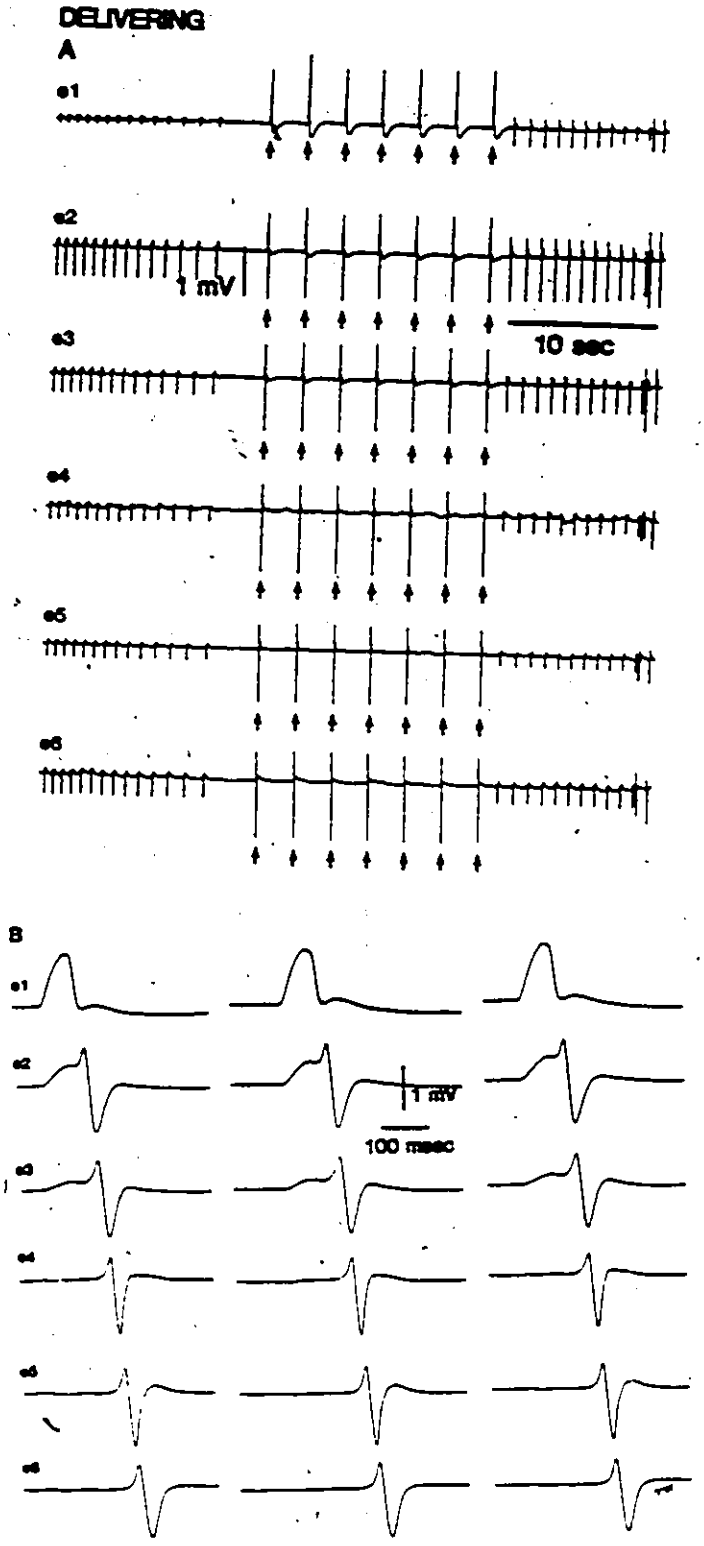
DELIVERING
A
e1
e2
1 mV
10 sec
e3
e4
e5
e6
B
e1
e2
1 mV
100 msec
e3
e4
e5
e6

FIGURE 46. Propagation velocity of spontaneously discharged spikes in delivering myometrium. Records are fast speed (200 mm/sec) traces of the last 3 spikes in the burst just preceding the evoked spikes in the longitudinal uterine strip of Figure 45. Activity was recorded simultaneously at 6 electrode sites. Inter-electrode distance = 3 mm. Propagation velocities were 13 cm/sec.

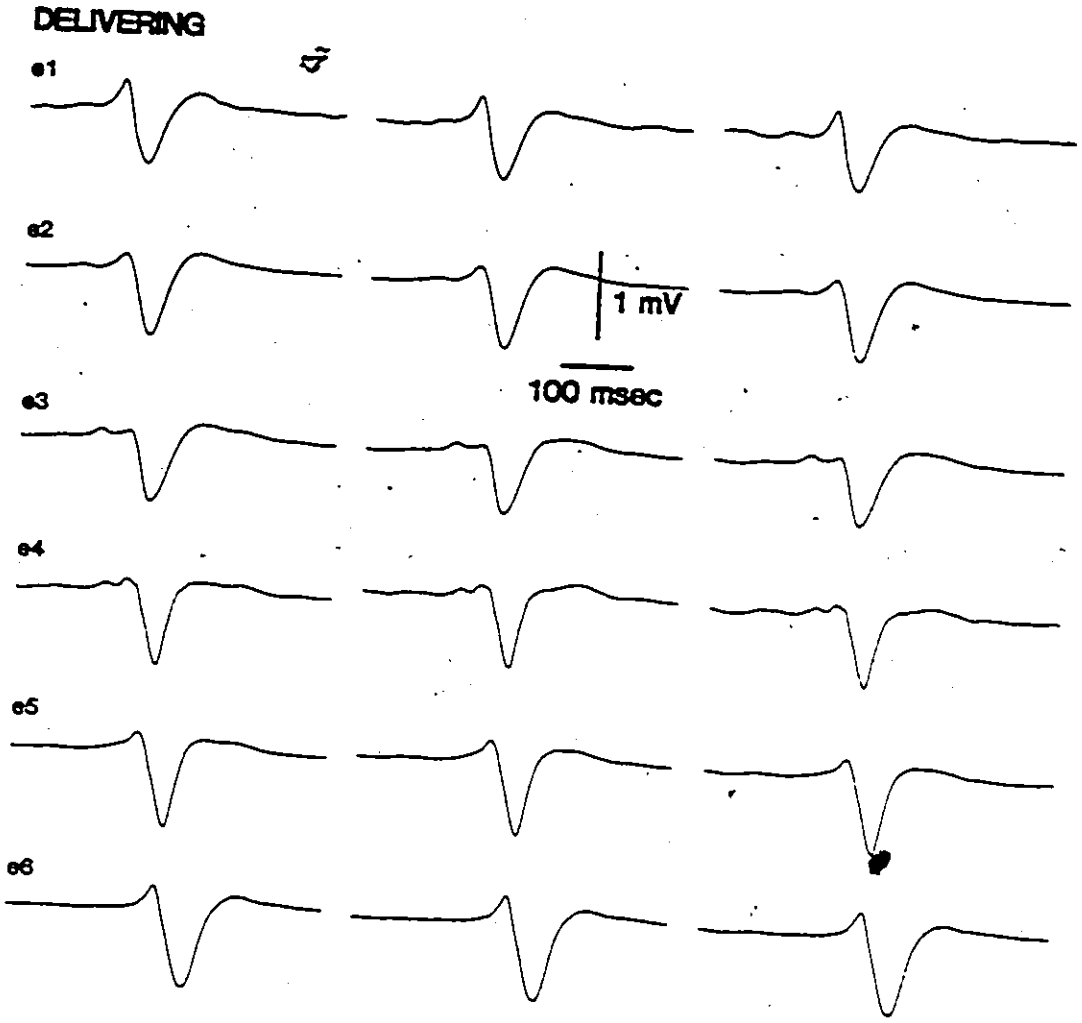
DELIVERING
e1
e2
1 mV
100 msec
e3
e4
e5
e6

FIGURE 47. Effect of TTX on propagation of evoked spikes in the delivering myometrium. Spikes were evoked by single square wave pulses (6V X 50 msec) and simultaneously recorded at 6 electrodes (3 mm apart) in the long axis of a longitudinal uterine strip. A). Without TTX. Propagation velocity, 10.9 cm/sec. B). With TTX (1 μg/ml). Propagation velocity, 11.1 cm/sec.

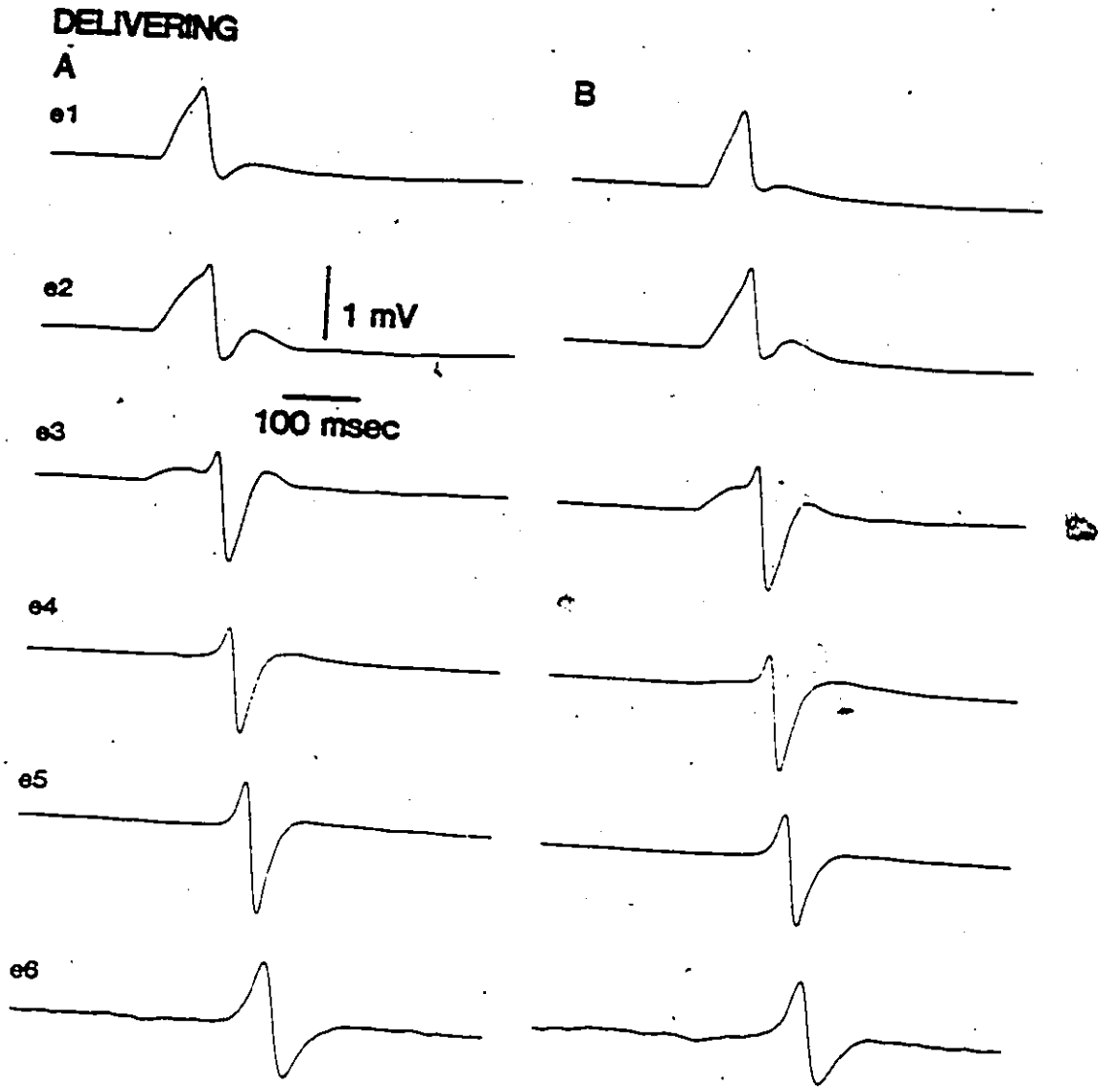
DELIVERING
A
B
e1
e2
1 mV
100 msec
e3
e4
e5
e6

FIGURE 48. Refractoriness to stimulation of preterm pregnant myometrium in the quiescent period following the cessation of a spontaneous burst. Electrical activity was simultaneously recorded at 6 sites (3 mm apart) in the long axis of a longitudinal uterine strip. Four stimuli (8V X 250 msec) were successively applied at 2 second intervals immediately after the burst ended. Arrows indicate stimuli that evoked spikes. The second spike appeared to be evoked at a location distal to "e1".

DAY 17

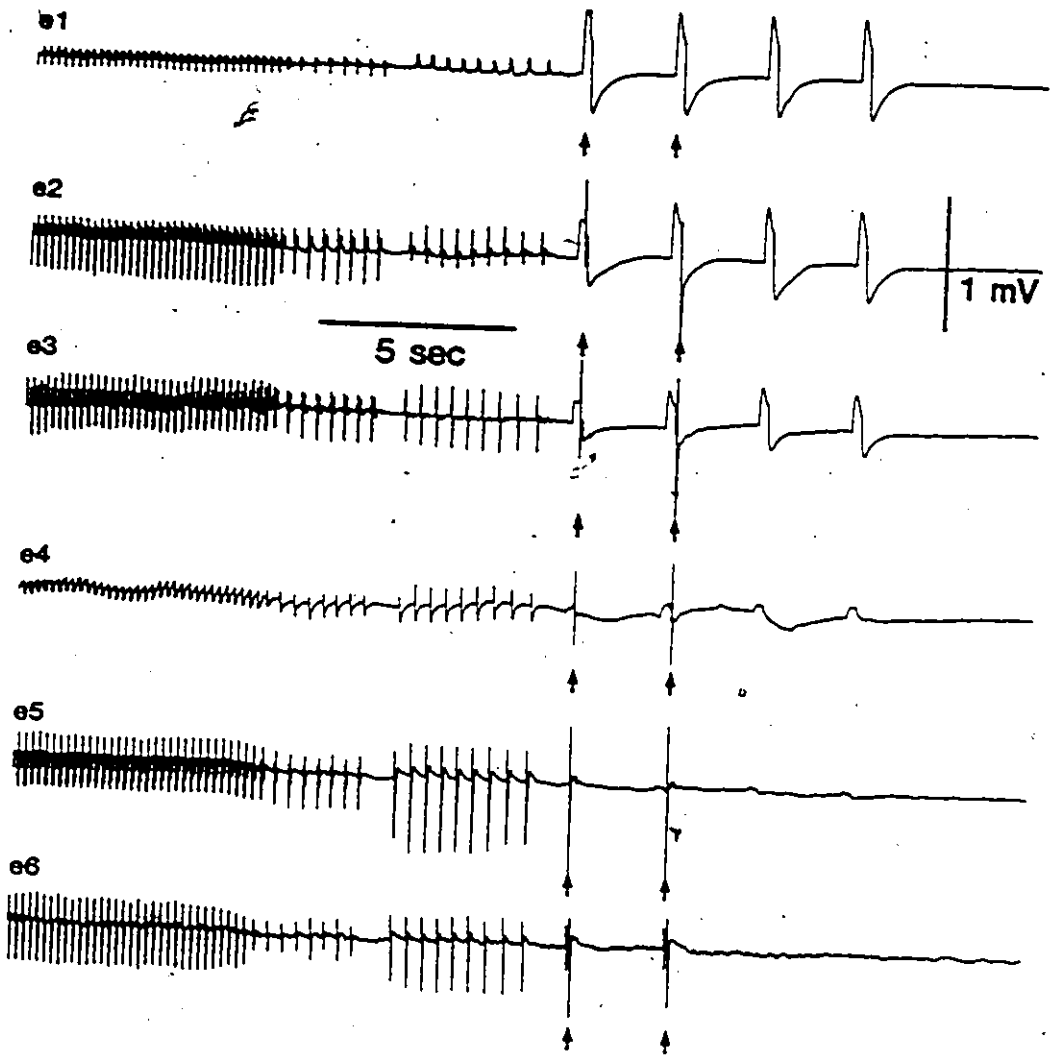

FIGURE 49. Propagation of evoked and spontaneously discharged spikes in preterm pregnant (day 17) myometrium. Electrical activity was simultaneously recorded at 6 electrodes (3 mm apart) in the long axis of a longitudinal uterine strip. A). Spike evoked by a single pulse (7V X 200 msec) applied immediately after (about 2 sec) after the end of a spontaneous burst. Propagation velocity, 8.6 cm/sec (determined between electrodes "2-5"). B). Spontaneously discharged spikes in the burst preceding the evoked spike in (A). The spontaneous spikes were initiated between electrodes "e2" and "e3" and propagated at velocities of 7.9 cm/sec and 8.2 cm/sec, respectively (determined between positive peaks of "e3-e5".

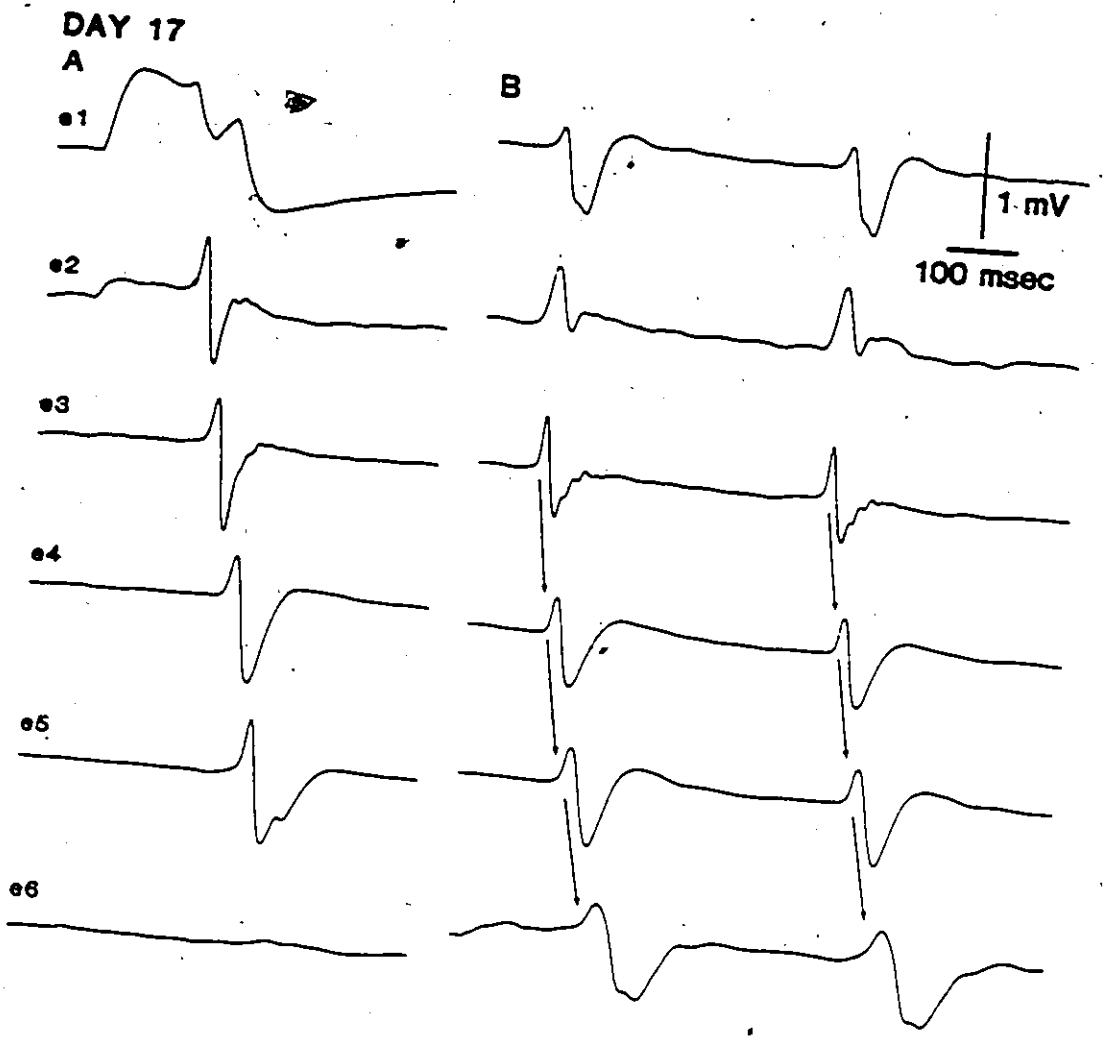
DAY 17
A
B
e1
e2
e3
e4
e5
e6
1 mV
100 msec

FIGURE 50. Effect of tetrodotoxin on propagation of evoked spikes in preterm pregnant (day 17) myometrium. Spikes were evoked by single pulses (7V X 200 msec) and simultaneously recorded at 6 electrodes (3 mm apart) in the long axis of a longitudinal uterine strip. A). Without TTX. Propagation velocity, 9.2 cm/sec (determined between "e2-e5"). B). With TTX (1 μg/ml). Propagation velocity, 8.9 cm/sec (determined between "e2-e5").

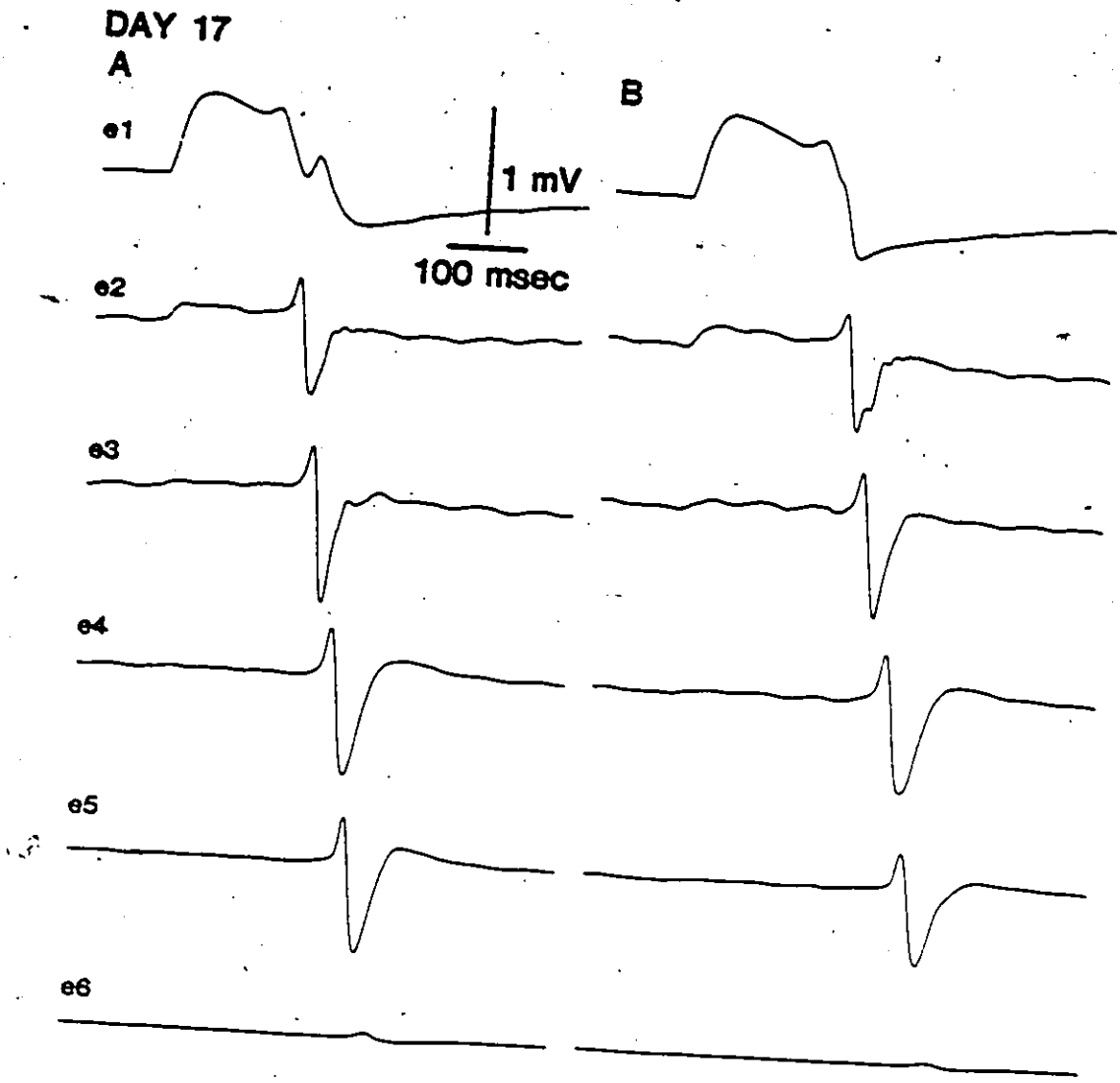
DAY 17
A
B
e1
1 mV
100 msec
e2
e3
e4
e5
e6

FIGURE 51. Propagation in the transverse axis of delivering myometrium. Electrical activity was simultaneously recorded at 6 electrodes (3 mm apart) in the long axis of a circular uterine strip. A). Five successive pulses (7V X 300 msec) were applied at 2 second intervals, immediately after the end of the burst. Small arrow indicates first stimulus. B). Evoked spike to the first stimulus. Propagation velocity, 3.6 cm/sec (determined between "e3-e6"). C). Last spontaneously discharged spike in the burst preceding the evoked spikes (see large arrow in A). This spontaneous spike was initiated between electrodes "e5" and "e6" and propagated in the direction opposite to the evoked spikes. Propagation velocity, 3.5 cm/sec (determined between "e3-e5").

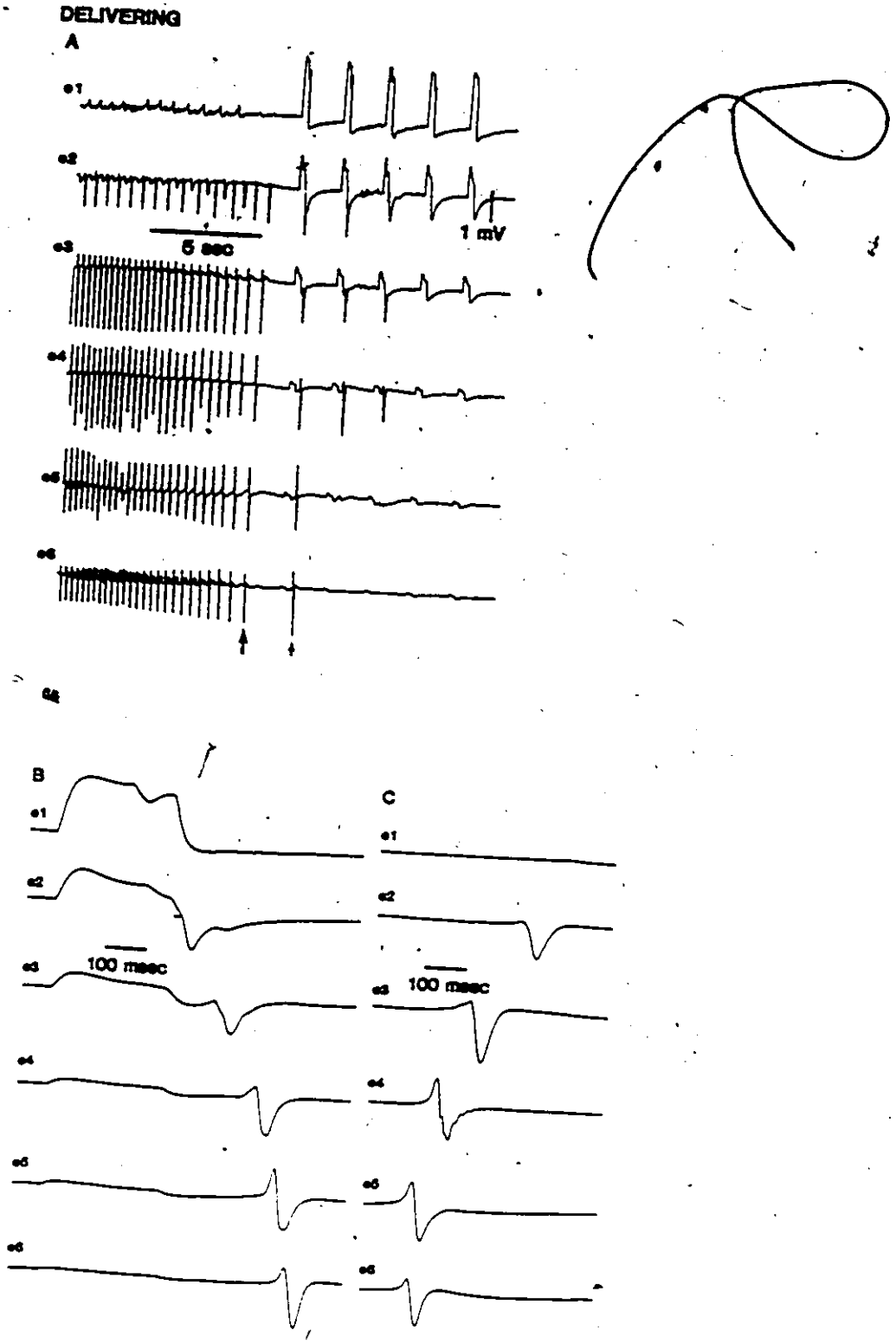
DELIVERING
A
e1
e2
5 sec
1 mV
e3
e4
e5
e6
B
C
100 msec
100 msec

FIGURE 52. Propagation of evoked spikes in the longitudinal and transverse axes of delivering myometrium from the same uterine horn. Electrical activity was simultaneously recorded at 6 electrodes (3 mm apart) in the long axis of the uterine strips. Longitudinal strip: evoked spike to single pulse (6V X 70 msec). Propagation velocity, 10.3 cm/sec (determined between "e2-e6"). Circular strip: evoked spike to single pulse (7V X 350 msec). Propagation velocity, 3.1 cm/sec (determined between negative peaks of "e1-e4").

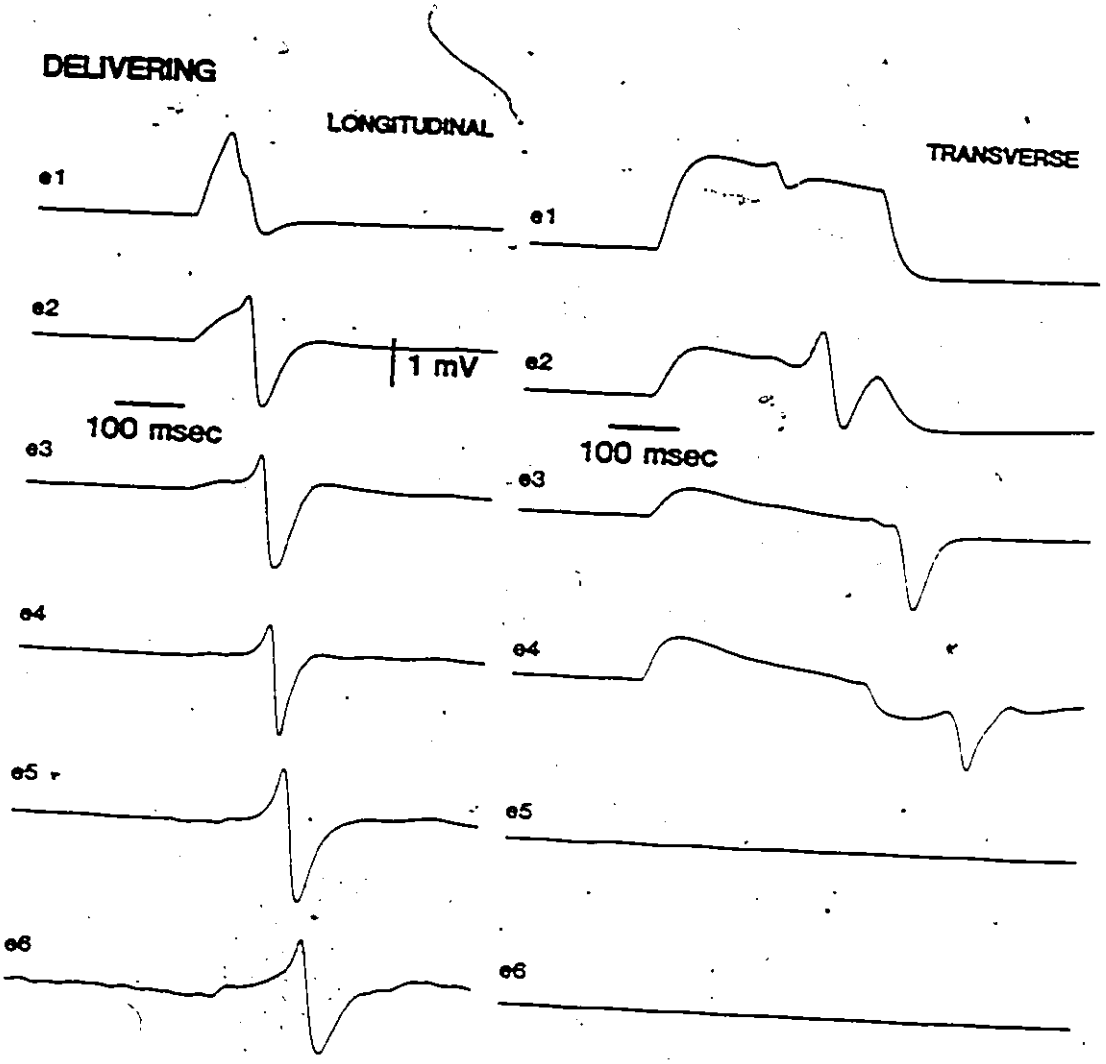
DELIVERING
LONGITUDINAL
TRANSVERSE
e1
e2
e3
e4
e5
e6
1 mV
100 msec
100 msec

FIGURE 53. Propagation of evoked spikes in the transverse axis of preterm pregnant (day 17) myometrium. Electrical activity was simultaneously recorded at 6 electrodes (3 mm apart) in the long axis of a circular uterine strip. A). Three pulses (7V X 300 msec) were applied at 2 second intervals (see arrows) immediately after the end of a spontaneous burst. Propagation velocity of the first evoked spike, 1.8 cm/sec (measured between negative peaks of "e2-e4"). B). Propagation velocity of the second evoked spike, 1.9 cm/sec (measured between negative peaks of "e2-e3").

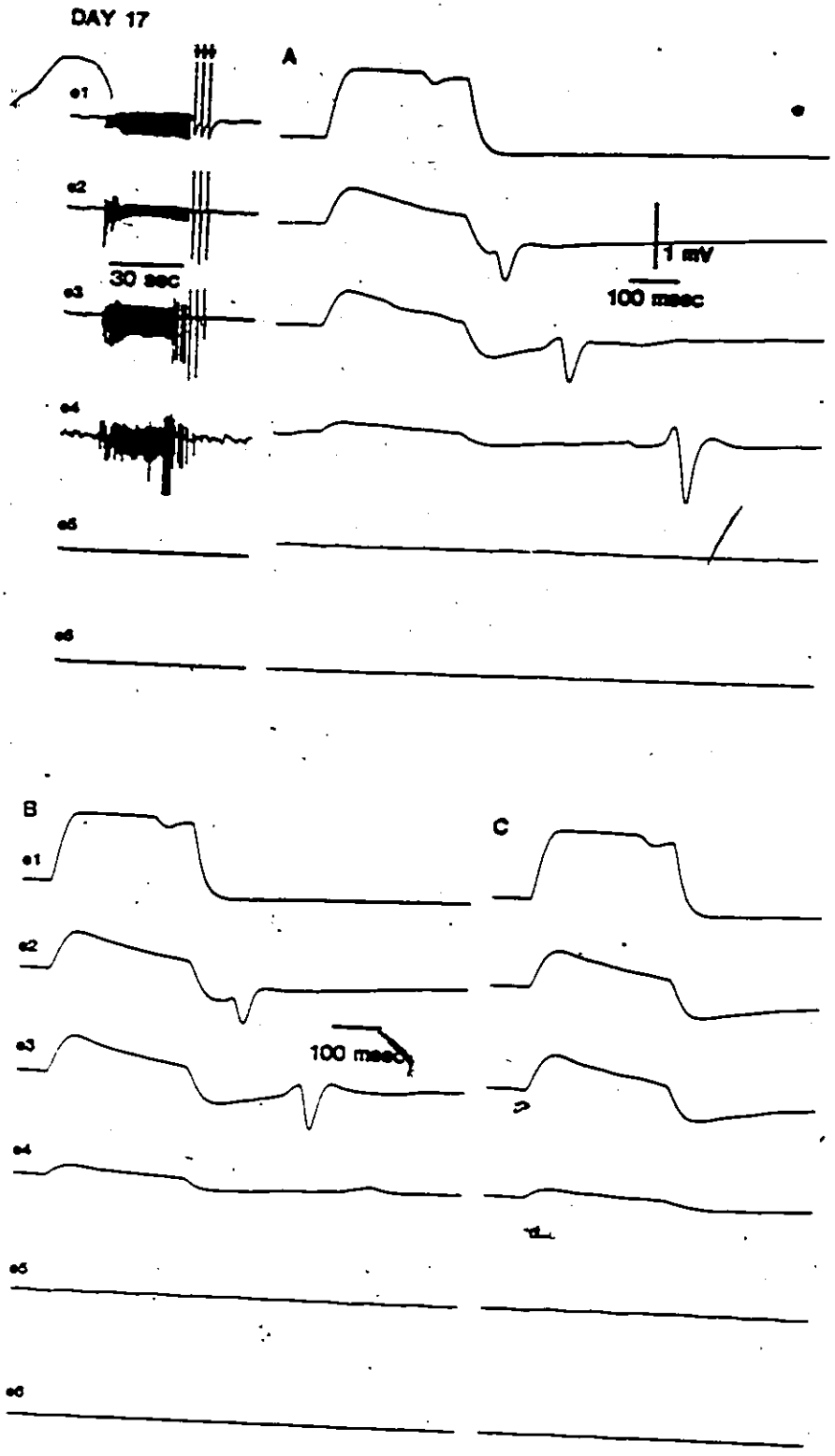
DAY 17
A
e1
e2
e3
e4
e5
e6
30 sec
1 mV
100 msec
B
C
100 msec

FIGURE 54. Effect of tetrodotoxin on propagation of evoked spikes in the transverse axis of preterm pregnant (day 17) myometrium. Electrical activity was simultaneously recorded at 6 electrodes (3 mm apart) in the long axis of a circular uterine treated with 1 μg/ml of TTX. A. Evoked spikes to electrical pulses (7V X 300 msec) applied after the end of a spontaneous burst. Propagation velocity of second evoked spike, 2.3 cm/sec (measured between negative peaks of "e2-e4"). B). Spontaneous spikes in the same strip. Propagation velocities (in direction opposite to the evoked spikes), 2.4 cm/sec and 2.6 cm/sec.

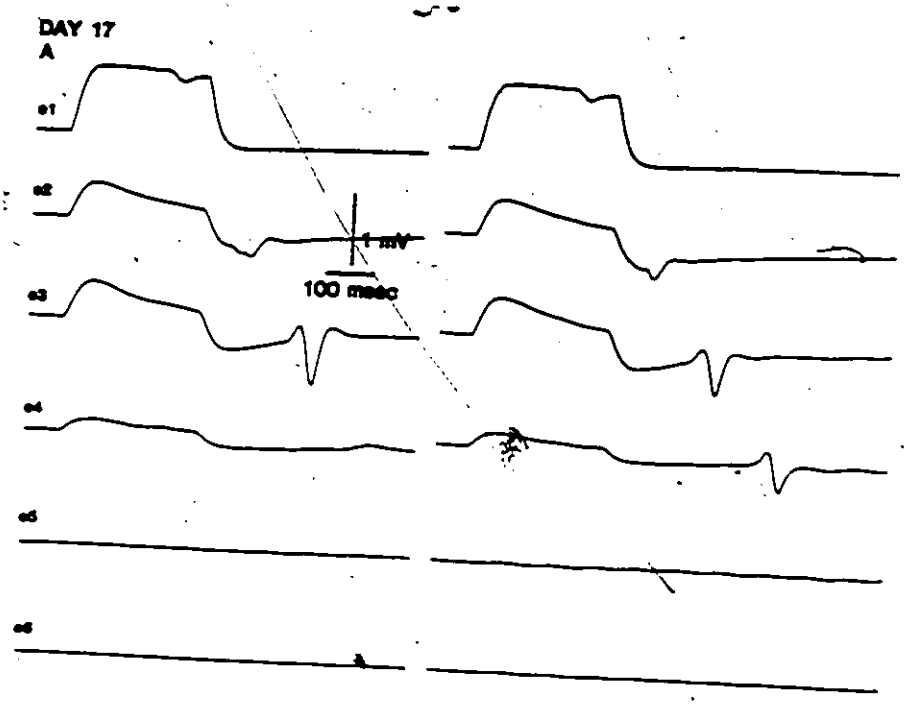
DAY 17
A
e1
e2
1 mV
100 msec
e3
e4
e5
e6

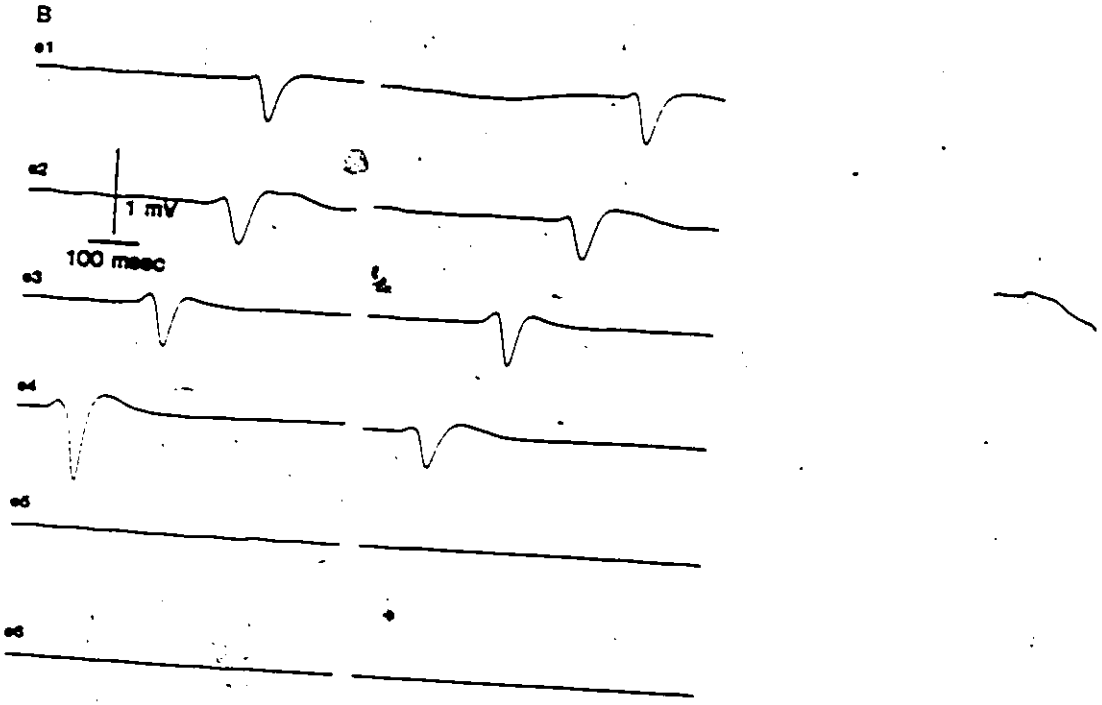
B
e1
e2
1 mV
100 msec
e3
e4
e5
e6

# CHAPTER 4

## General Discussion

Distinctive Nature of This Research

The objective of my thesis was to examine the functional consequence (specifically, the effects on propagation of electrical excitation) of gap junction formation in the myometrium at parturition. I demonstrated an enhanced propagation of spike bursts and individual spikes in delivering tissues, where gap junctions were found in significant numbers, as compared to preterm tissues which had few if any gap junctions. Since the spread of excitation along a uterine strip is an indirect measure of electrical coupling between the uterine smooth muscle cells (Kao, 1977a), the results imply that improved intercellular coupling of myometrial cells is associated with an increased area of gap junction contact between them. Therefore, these results support the general hypothesis that gap junction formation at the end of gestation improves coupling between uterine smooth muscle cells (Garfield et al., 1978). According to the generally accepted mechanism of current flow through a physiological syncytium such as uterine smooth muscle, formation of gap junction contacts between uterine smooth muscle cells would decrease junctional resistance (i.e. decrease internal resistance to local circuit current flow) between cells, thereby facilitating propagation of excitation throughout the myometrium (Barr and Dewey, 1968; Bortoff, 1976; Kao, 1977a). My results are the first to quantitatively show an enhanced propagation of electrical activity (spike bursts and individual spikes) in the rat myometrium at delivery, and support the previous studies showing enhanced electrical (Sims et al., 1982) and metabolic (Cole et al., 1985) coupling associated with gap junction formation in rat longitudinal myometrium at delivery. The improved spread of excitation in the

transverse axis of the myometrium at delivery has not previously been documented for rat or any other species, nor has the role of the underlying circular muscle for the spread of bursts in the transverse direction between longitudinal muscle bundles, been previously demonstrated. If the improved spread of activity in this axis of the myometrium at term is partly due to an improved electrical coupling between circular muscle cells in their own axis, the above results are the first to provide evidence of the functional consequence of gap junction formation in the circular muscle layer at term. As discussed below, these results provide a plausible explanation for the evolution of contractile synchrony in the uterine wall at delivery.

Spontaneous Activity

Contractions of the myometrium are physiologically achieved by a sequence of processes: spike initiation, spike propagation, excitation-contraction coupling and contraction, any one of which may change during gestation (Abe, 1970). The frequency of burst discharge determines the frequency (rate) of myometrial contractions, while the spike discharge rate and spike number within bursts determines the intensity and duration, respectively of the contraction (Marshall, 1973; Kao, 1977a). The observations in the present study showing that the burst discharge rate was markedly higher at delivery than at preterm, is similar to previous reports of the spontaneous activity of isolated longitudinal muscle from pregnant rats (e.g. Anderson et al., 1981) and suggest that uterine contractions are more frequent at delivery than at preterm, which is confirmed by *in vivo* recording of uterine activity in the rat at preterm and during delivery (e.g. see Fuchs, 1969; de Paiva and Csapo, 1973).

However, the *in vitro* frequencies at both stages of gestation are considerably higher than those *in vivo*, probably due to removal of some *in vivo* regulatory influence or to tissue trauma caused by cutting the strips, stretch, bathing them in an artificial medium, etc., (which probably causes prostaglandin release; see Harney et al., 1974; Gimeno et al., 1981), thereby altering the pacemaker discharge frequencies (Kuriyama and Suzuki, 1976b; Reiner and Marshall, 1976; Grossett and Mironneau, 1977). While it is obvious that an enhanced contraction rate at delivery is needed for expulsion of the fetus(es), a moderate rate of contraction may be required at preterm to stimulate the uterine vasculature to provide nutrition to the myometrium and fetus (Abe, 1970).

The observed decrease in spike discharge rate within bursts in the longitudinal myometrium from late pregnancy to delivery, has been previously noted by others (Thiersch et al., 1959; Kuriyama, 1961; Casteels and Kuriyama, 1965; Kuriyama and Suzuki, 1976a; Anderson et al., 1981). The spike frequency within each burst is well known to determine the force (amplitude) of the longitudinal muscle contraction (see review of Marshall, 1973). However, the amplitude of spontaneous longitudinal muscle contractions from pregnant rat uterus is greater at term than at preterm (day 18), despite the higher spike discharge frequency in bursts accompanying the contractions at preterm (e.g. see Anderson et al., 1981). In other words, the increment of tension per spike is much greater at term than at preterm, suggesting a more effective coupling of excitation with contraction at term (Anderson et al., 1981). The uterus acquires its maximum working capacity by midterm due to an increase in actomyosin content during pregnancy (Csapo, 1962). The overall ability of the isolated longitudinal muscle to contract (e.g. when the muscle cell membrane is

depolarized by $K^+$) is not significantly different at term as compared to at preterm; nor are there large differences in the $Ca^{2+}$ handling properties of the muscle, $Ca^{2+}$ sensitivity of the contractile proteins, or $Ca^{2+}$ release from intracellular storage sites (Anderson et al., 1981; Bengtsson et al., 1984a,b; Izumi, 1985). These observations (taken together with those showing a change in spike discharge frequency from preterm to term) suggest that improved cell-to-cell conduction in the longitudinal muscle at term is the basis for its enhanced contractile force during delivery compared to at preterm (Anderson et al., 1981). The results of the present study confirm that propagation is enhanced in the myometrium at delivery as compared to before term.

I was unable to demonstrate a preferred direction of burst or spike propagation at either stage of gestation. As pointed out by Marshall (1973), the lability of uterine pacemakers, particularly in isolated muscle strips where tissue trauma often causes pacing to become random, makes their localization difficult. Fuchs (1973) claims that contractile activity in the delivering rat uterus (studied in vivo) originates at the ovarian end of the horn. However, detailed in vivo studies of electrical activity in other animal species show that spontaneous activity may start at any point along the uterine horn and propagate tubocervically or cervicotubically (Kao, 1959; see review of Taverne et al., 1979b). Often, cervicotubal propagation dominates before and during expulsion of the fetuses. It may be argued that application of surface electrodes or introduction of pressure balloons into the uterine lumen to measure spontaneous activity may disrupt physiological pacemaker organization (Marshall, 1973). Thus, whether the uterus in vivo has a localized pacemaker has not been satisfactorily determined. Taverne et al. (1979b) provide a plausible

explanation for cervicotubally directed propagation at delivery. They suggest that such contractions would prevent "untimely interruption of the fetal-placental-maternal connections of the fetuses that are not yet due to be expelled". This idea is consistent with the observations of Mosler (1968) which suggest that in the rat (and presumably other polytoccus species), the fetuses are expelled by uterine contractions propagating in the direction opposite to the expulsion direction.

Burst Propagation

Synchronous electrical activity in the uterus is associated with parturition in many species (rat: de Paiva and Csapo, 1973; rabbit: Csapo et al., 1963; Csapo and Takeda, 1965; sow: Taverne et al., 1979a; sheep: Thorburn et al., 1984; Verhoeff et al., 1985; human: Wolfs and van Leeuwen, 1979). It is widely believed that this synchronicity results from propagation of excitation throughout the uterine horn, although with in vivo studies it is not certain that the recorded electrical activity at one electrode site represents propagated activity from another (Taverne et al., 1979b). On the other hand, the fact that the frequencies of burst activity are similar (e.g. the periods of activity and inactivity are synchronous) at various locations in the uterus, implies that electrical activity is propagated through it (Taverne et al., 1979b; Germain et al., 1982). At any rate, there has been little quantitative information on the extent or velocity of propagation (and possible gestational changes in these parameters), in the pregnant uterus. The results of this thesis provide good evidence that bursts at both stages of gestation propagated between electrode sites, as the bursts were not entrained after cutting through the tissue between

them. These results are consistent with those of previous studies which showed that ligation or cutting of the uterine wall uncouples synchronic burst activity in the isolated uterus of the parturient rabbit (Takeda, 1965), and in isolated longitudinal muscle from term pregnant rat uterus (Osa et al., 1983). However, synchronic burst activity in vivo may also be facilitated by the mechanical stretching effect of the active portion on the passive region and by the stretching effect of the movement of uterine contents (see Takeda, 1965).

Cutting through the strip between electrode sites also revealed that the spontaneous burst activities (pacemakers) showed some of the characteristics of a system of coupled relaxation oscillators (see Daniel and Sarna, 1978): each isolated uterine segment had an intrinsic frequency which was less than that of the intact strip, and the highest frequency of bursting was retained in the segment which had phase lead prior to cutting. In such a system, propagation is brought about by entraining different pacemakers whose "natural" (i.e. intrinsic) frequencies are different. This type of pacemaker organization could result in integrated contractile activity over large areas of the uterus at delivery, providing that the pacemakers become well coupled at term (see below). Moreover, according to this model, a frequency gradient of pacemaker activity along the uterine horn could provide directionality of contractions, i.e. away from the pacemakers with the highest intrinsic frequency. However, whether such a gradient exists is not yet determined. Local hormone effects, local stretch or other local factors in vivo may alter the frequency of pacemaker discharge at a specific uterine region, which in turn may alter (drive) neighbouring cells to initiate a propagated contraction. Thus, there is no requirement for a fixed anatomical location (e.g. the ovarian end of the uterus; see Fuchs, 1973) from which contractions are initiated.

The relaxation oscillator model assumes electrical coupling among adjacent oscillators or pacemakers (Daniel and Sarna, 1978). Presumably local depolarizing current flow through low-resistance junctions connecting cells is the basis for coupling (but see Daniel and Sarna, 1978). This raises the question of how the burst oscillators in the longitudinal axis at preterm are entrained as a system of coupled relaxation oscillators prior to the in vivo development of gap junctions. Perhaps the few gap junctions that developed in vitro before or during recording were sufficient for coupling. If so, then in vitro studies of electrical coupling in the myometrium must be interprated with caution when extrapolated to the muscle in vivo (Garfield, 1985). Studies on the relationship between gap junctions and in vivo electrical properties of the myometrium (e.g. see Verhoeff et al., 1985) may circumvent this problem. If current flow through the extracellular space between cells is sufficient for coupling of the burst oscillators (Daniel and Sarna, 1978), then close apposition contacts, which are found between uterine smooth muscle cells in rat myometrium (Garfield and Daniel, 1974) may facilitate this mode of coupling as they would provide a lower resistance pathway between cells relative to the higher resistance extracellular space (Daniel and Sarna, 1978). These contacts may also facilitate "electric field" coupling through the extracellular space between cells, according to the model of Sperelakis et al. (1983). On the other hand, it has been suggested for other visceral smooth muscles (e.g. see Fry et al., 1977) and embryonic heart cells (e.g. see Williams and DeHaan, 1981) that small aggregations of membrane particles (visible by freeze-fracture but invisible by thin section electron microscopy), may provide coupling via low circuit current flow between cells. Whether such cell-to-cell channels exist in the membrane of

uterine smooth muscle cells at preterm and facilitate electrical coupling, is not known.

At both stages of gestation, bursts were entrained over a 15 mm distance in the longitudinal axis. It would be informative to determine whether the maximum burst propagation distance is longer at delivery than at preterm, as would be expected if current flow in the myometrium was enhanced by gap junction formation at term. Perhaps the 15 mm distance at preterm represents a near maximum length over which bursts propagate when few or no gap junctions are present. Gap junction formation at delivery should increase current flow between cells, thereby increasing the extent of burst propagation. On the other hand, perhaps coupling of burst oscillators does not require gap junctions, i.e. coupling may be via the extracellular space in the junctional clefts between myometrial cells. Further studies should be done to determine the maximum distances over bursts are entrained in the longitudinal axis at preterm and at delivery.

Bursts appeared to be more completely propagated over the 15 mm recording distance in the longitudinal axis at delivery than at preterm because the length of the "excitable" region in the axis was much longer at delivery than at preterm. The longer "excitable" region at delivery may be the result of an improved synchronization of the excitatory cycles of the burst oscillators which in turn might facilitate spike propagation between them (Kuriyama, 1964). On the other hand, the increased length of the "excitable" region at delivery may reflect changes in spike propagation not related to the changes in burst propagation. A more reliable assessment of whether coupling of burst oscillators is improved at delivery would be to measure the phase lag between

bursts at both stages of gestation. With improved coupling at delivery, the phase lag should be less than at preterm. Alternately, it may be possible to drive (e.g. by electrotonic pulses) the burst frequency and observe changes in phase lag or phase-locking. If the oscillators are better coupled at delivery, due to low-resistance gap junction contacts between muscle cells, then electrotonically driving the oscillators to higher than intrinsic frequencies should result in smaller increases in phase lag than in electrotonically driven preterm tissues, and bursts should remain phase-locked to higher frequencies at delivery than at preterm, according to relaxation oscillator theory (Daniel and Sarna, 1978).

Bursts at preterm spread over shorter distances in the transverse than in the longitudinal axis, consistent with the results of Csapo (1969) who recorded electrical activity from the intact uterine horn of the preterm pregnant (day 18) rat. The finding in the present study that bursts in the transverse axis at delivery were not entrained over a region of the tissue where the underlying circular muscle was damaged, implies a role of the circular muscle in circumferential coupling between longitudinal muscle bundles. Presumably, the bundles of longitudinal muscle lack (or have only limited) transverse coupling but become coupled in the axis at delivery as a result of enhanced coupling to the underlying circular muscle, or improved coupling of the circular muscle in its own axis, or a combination of both. There have been no studies on gestational changes of current spread in rat uterine circular muscle, although Parkington (1985; and see Thorburn et al., 1984) has shown that cell-to-cell coupling of isolated circular muscle from sheep myometrium is markedly improved (i.e. the space constant is much larger) at delivery than at

preterm. Gap junctions are present in large numbers in the myometrium (i.e. in longitudinal muscle and presumably also in the circular layer) of this species immediately before and during parturition (Garfield et al., 1979): these may be the structural basis for the enhanced electrical coupling in the circular muscle at delivery. It is likely that gap junction formation in the circular muscle of the rat myometrium at term would also result in enhanced cell-to-cell coupling in its own axis. This should result in an improved flow of current transversely between longitudinal muscle bundles, providing that the longitudinal and circular muscle layers of the rat myometrium are coupled to each other. Conversely, gap junction formation in the longitudinal layer should improve conduction in its own axis, and if coupled to the underlying circular layer, might enhance current flow between circular muscle bundles in the direction transverse to their long axis. The spread of excitation in both axes of each muscle layer is undoubtedly required for coordinated contraction of the uterus during labour.

Several other studies have provided evidence for an interaction between the longitudinal and circular muscle layers of the pregnant uterus (mouse: Osa, 1974; rat: Ohkawa, 1975; Osa and Katase, 1975). In the present study, additional evidence was obtained for an interaction of the layers: in some circular strips in which electrical activity from the serosal (longitudinal muscle) surface and contractions of the underlying circular muscle (assuming that contractions in the circular strips are predominantly those of the circular muscle fibers which are oriented in the long axis of the strips; see Osa, 1974) were simultaneously recorded, contractions of the circular muscle were always preceded by and synchronous with the serosal surface electrical activities.

These results further suggest that electrical activity was initiated in the longitudinal layer and then conducted into the circular layer. However, in such large strips, it is also possible that the electrical activity originated in the circular layer and was conducted into the longitudinal layer in the period of latency between excitation and contraction of the circular layer. Further studies of the possible role of circular muscle in the circumferential coupling of longitudinal muscle bundles (and of longitudinal muscle in coupling of circular muscle bundles in the uterine long axis) are required, particularly the uncoupling effects of various complete or incomplete cuts in one or both muscle layers. It is also important to determine whether or not the contractions of one muscle layer drive those of the other layer, and in which layer, longitudinal or circular, the burst pacemaker (i.e. the high frequency oscillator) is located.

The nature or extent of interaction between the muscle layers of the myometrium is not clear and requires further study. It is claimed that bundles of muscle connect the outer longitudinal to the underlying circular layer in the rat myometrium (Mosler, 1968; Garfield, 1979). Gap junction formation between uterine smooth muscle cells at term (which presumably also form between the muscle cells of the bundles connecting the layers) would therefore provide a low-resistance pathway for current flow between the layers. However, it is not known how extensive these connections are, nor have they been identified or studied by electron microscopy. In any event, most of the region between the muscle layers seems to be composed of connective tissue cells and blood vessels (Finn and Porter, 1975). While it has been suggested for some other visceral smooth muscle that coupling of the longitudinal and circular muscle layers may occur via the connective tissue cells in the interlayer space (e.g. see Taylor

et al., 1977; Gabella and Blundell, 1981), "heterocellular" gap junction contacts (or other membrane junctions) connecting uterine smooth muscle cells to connective tissue cells have not been observed in the rat myometrium (Garfield and Daniel, 1974).

What are the functional roles of the longitudinal and circular muscles of the uterus? The importance of the circular layer has been emphasized because it undergoes more marked changes in electrophysiological (e.g. resting membrane potential, action potential shape, but not frequency of spontaneous activity) and contractile (e.g. amplitude of spontaneous contraction) properties than does the longitudinal layer (Anderson et al., 1981; Kawarabayashi and Marshall, 1981; Bengtsson et al., 1984b). Mosler (1968) has shown for isolated pregnant rat uterus, that contractions of the circular but not the longitudinal muscle increases intrauterine pressure. He postulates that constriction of the circular muscle exerts force on the fetus which is then expelled by a contraction of the longitudinal muscle which shortens over the fetus and thus frees it. Others (Bengtsson et al., 1984b) acknowledge the importance of large regular contractions of the circular muscle (aided by longitudinal muscle contractions) in pushing the fetuses toward the cervix at delivery, but also postulate a role of weak and irregular circular muscle contractions at preterm, in producing a tonic constriction of the uterine lumen to prevent fetal movement toward the cervix. In any event, enhanced interaction between uterine muscle layers at delivery would facilitate circumferential and longitudinal spread of contractions, and thus expulsion of the fetuses.

Spike Propagation

According to Csapo (1962; 1981), the number of myometrial cells simultaneously activated is of critical importance to the development of uterine wall tension, since it is the ratio of active to inactive cells that controls the magnitude of the uterine contraction. In other words, labour-like contractions of the uterine wall are thought to be promoted by propagating action potentials of high velocity that allow the simultaneous activation of many muscle cells. In contrast, local activity restricted to pacemaker areas does not promote development of significant uterine wall tension, since contractions of these cells is dissipated by elastic lengthening of neighbouring inactive cells (Csapo, 1981). However, few detailed studies have determined whether action potential propagation is improved in the myometrium at delivery, despite the importance of that information to our understanding of the control of uterine function. Talo and Csapo (1970) made measurements of the extent and velocity of impulse propagation on strips of late pregnant and parturient rabbit myometrium. Although they reported that propagation of evoked spikes was enhanced at delivery as compared to at preterm, the recordings shown in their paper are not convincing because the traces are at too slow a speed to resolve the action potential from the stimulus artifact. In the present study, the extent and velocity of impulse propagation was more convincingly shown to be greater (in both axes of the myometrium) at delivery than at preterm. The similar magnitudes (at both stages of gestation) of velocity and distance of propagation of spontaneous spikes compared to those evoked by electrical stimulation, reassures me of the existence of a conduction change in the myometrium at preterm. Tetrodotoxin did not affect propagation in either axis, suggesting

that the propagation change was due to alterations in the electrical or structural properties of the uterine smooth muscle (i.e. inhibitory nerves did not impede spike propagation at preterm). Since velocity was highest and distance of spread farthest at delivery, when gap junctions were present in large numbers between muscle cells, the results support but do not prove the hypothesis that the presence of gap junctions lowered the junctional resistance between myometrial cells and hence facilitated current flow between them. Sims et al. (1982) observed an aproximately 30% decrease in internal resistance (e.g. junctional impedance decreased but myoplasmic resistance was constant) associated with gap junction formation in isolated rat longitudinal myometrium from before term to delivery. In the present study, an approximately 10% increase in propagation velocity was observed from before term to delivery for spikes in the longitudinal axis of the myometrium (Table VII). If propagation velocity is proportional to the square root of the longitudinal internal resistance (assuming a uniform fiber diameter and a uniform resistance per unit length), the decreased internal resistance observed by Sims et al. (1982) could account for the increased propagation velocity during delivery observed in the present study. In other multicellular excitable tissues (e.g. cardiac muscle), propagation velocity of the action potential is quantitatively related to the longitudinal internal resistance (e.g. Weingart, 1977; Wojtczak, 1979; and see "Role of Gap Junctions in Regulating Uterine Smooth Muscle Activity", below). Further studies are needed to study the correlations between the cable properties and the velocity of impulse propagation in both the longitudinal and circular muscle layers of the myometrium. If both the cable properties and propagation velocity were determined on the same strip, and correlated with

structural studies (e.g. gap junction quantitation) of the tissues, important information on the mechanisms of current flow in smooth muscle might be obtained (Daniel and Lodge, 1973). Alternately, use of more simplified cell systems (e.g. isolated myometrial cells) may provide better access to the gap junction for detailed functional analysis (see Weingart, 1986 for electrophysiological studies of the gap junction membrane between isolated cardiac cell pairs).

The amount of stretch placed on the muscle strips in vitro is an important factor which could also affect spike propagation, e.g. by altering the passive or active properties of the tissue (Kuriyama, 1961; Tomita, 1975; Sims et al., 1982). In the present study, I tried to ensure that the strips were maintained at their in situ lengths in the muscle bath, but I acknowledge that it is difficult to be certain that the amount of stretch imposed on the strips was consistent. However, I am confident that the strips were not over- or understretched because the burst frequencies and spike discharge frequencies within bursts were similar to those reported in other careful studies of spontaneous activity of the pregnant rat myometrium (e.g. see reviews of Kuriyama, 1961 and 1964; Casteels and Kuriyama, 1965; Kuriyama and Suzuki, 1976a; Kanda and Kuriyama, 1980; Anderson et al., 1981). The effects of stretch on membrane activity of the myometrium are well known: overstretching causes a continuous spike discharge while marked understretching results in a low spike and burst discharge frequency with few spikes per burst (Kuriyama, 1961; Marshall, 1962; Csapo et al., 1963). On the other hand, a careful quantitative study of the effect of stretch on impulse propagation in isolated uterine strips is needed. Csapo et al. (1963) previously observed that propagation of

spontaneous bursts in intact uterine horns of parturient rabbit was improved by moderate increases in intrauterine volume.

Further evidence for a role of myometrial gap junction formation in the enhancement of intercellular electrical coupling would be provided by experiments in which spike (and burst) propagation were measured before and after treatment of the tissues with agents that are known to uncouple gap junctions. For example, it is well known that junctional permeability can be modulated (i.e. junctions functionally uncoupled) in other excitable tissues by altering intracellular levels of $Ca^{2+}$, $H^{+}$ or cAMP (e.g. see De Mello, 1983; Spray and Bennett, 1985). In cardiac tissue, entrainment of action potentials between pacemakers is lost when cell-to-cell coupling is abolished by pharmacological manipulation (Jalife, 1984; Delmar et al., 1986). Recent studies (Cole and Garfield, 1985) have also provided evidence suggesting that cell-to-cell coupling (measured as the diffusion of glucose analogues) in isolated longitudinal myometrium from delivering rats is altered by agents which are known to alter intracellular levels of $Ca^{2+}$, $H^{+}$ and cAMP in this tissue. However, many of these agents probably also alter the membrane properties (e.g. excitability or membrane resistance) of the uterine smooth muscle cells, which must be taken into account in assessing their affect on impulse propagation (see Delmar et al., 1986).

At this point it is worth considering the possible physiological significance of the propagation changes in the myometrium observed at delivery. The uterus is a tubular organ that expels its contents by a squeezing contraction (Mosler, 1968). For this to be effective, all the uterine muscle fibers must be contracting more or less simultaneously (Csapo, 1981). Assuming

an average length of the rat uterine horn of about 20 cm at term, i.e. 5 fetuses per unit horn (see "Materials and Methods", Chapter 2) and a 4 cm fetal crown-rump length (see Anderson et al., 1981; Kawarabayashi and Marshall, 1981), it would take about 2 seconds for the spike to propagate over the length of the uterine horn at delivery. This is well within the time it takes the uterus to develop maximum tension following electrical stimulation (cf. Talo and Csapo, 1970). On the other hand, the uterine wall portion enclosing each fetus may be the functional unit for expelling the fetus at delivery (Mosler, 1968). The length of this "compartment" is only about 4 cm at delivery (i.e. fetal crown-rump length is 4 cm at delivery; see above). At preterm, contractile synchrony is prevented (despite the high velocity of spike propagation) because the spike usually propagates over only a limited distance (about 1 cm; see Table VII, Chapter 3). At delivery, in contrast spikes always propagated over distances of at least 1.5 cm (Table VII, Chapter 3) and probably further. In parturient rabbit myometrium evoked spikes propagate over distances of at least 4.5 cm (Talo and Csapo, 1970). It is likely that spikes can also propagate over distances similar in magnitude to the 4 cm length of the uterine wall enclosing a fetus (rat, see above). However, the present study does not provide information about the maximum distance of impulse spread in the rat myometrium. It is often assumed in discussions on uterine physiology (e.g. see Kao, 1977a; Csapo, 1981) that at delivery, impulses initiated at one end of the uterine horn are propagated along its entire length. This remains to be determined. At any rate, the higher velocity and extent of impulse propagation in the longitudinal axis of the myometrium at delivery than at preterm, may be the basis for the development of the higher amplitude (and faster rate of rise) intrauterine pressure cycles

characteristic of the parturient uterus (Csapo and Takeda, 1965; Wolfs and van Leeuwen, 1979; Verhoeff et al., 1985).

Intrauterine pressure development presumably also depends on the extent and velocity of impulse spread in the transverse axis of the myometrium (e.g. see Mosler, 1968: in isolated rat uterine horns, contraction of the circular muscle alone results in development of intrauterine pressure). In the present study, the spike propagation velocity in the transverse axis was almost 2 times higher at delivery than at preterm. However at both times during pregnancy, the distances of spread were much less than the circumferences (e.g. about 5 cm; see "Materials and Methods", Chapter 2) around the uterine horn. Therefore, how contractions are synchronized circumferentially at delivery is unclear. Perhaps contractile synchrony is achieved by propagation of spike bursts, instead of individual spikes. Bursts were entrained over longer distances (at least 15 mm) in this axis at delivery than before (Table III, Chapter 2). It remains to be determined whether or not bursts are entrained over the entire circumference of the uterine horn at term.

Role of Gap Junctions in Regulating Uterine Smooth Muscle Activity

The results of the present study suggest that at term, a functional transformation of the rat myometrium occurs such that propagation of electrical excitation is enhanced. It is widely believed that this transition is a prerequisite for inducing normal labour in all species (Csapo, 1971). Its basis may be due to the formation of gap junction contacts between uterine smooth muscle cells at term, which would generate low-resistance pathways for current flow between cells and thus promote propagation of electrical discharges

(Garfield et al., 1978). In myometrium (Sims et al., 1982) and other muscle synctia (e.g. cardiac muscle, see Ypey et al., 1979; Clapham et al., 1980), electrical coupling is improved by gap junction formation, and coupling can be altered by modulation of the junctional resistance (Weingart, 1977; Jalife, 1984; Delmar et al., 1986).

In most species of animals, labour is thought to be controlled by changes in plasma or uterine tissue levels of steroid hormones and prostaglandins (Thorburn and Challis, 1979; Csapo, 1981). In the pregnant rat, circulating and myometrial levels of progesterone are high at gestation day 17 and fall towards towards term, while the opposite is true for estrogens and prostaglandins (e.g. Csapo and Wiest, 1969; Puri and Garfield, 1982). Extensive studies by Garfield and associates (summarized in the review of Garfield, 1985) suggest that the changes in steroid hormones and prostaglandins preceding labour, control gap junction formation in the rat myometrium: progesterone may inhibit whereas estrogen may stimulate gap junction formation. Gap junction regulation by prostaglandins, although experimentally demonstrated, is less well defined, i.e. some prostaglandins may stimulate while others may inhibit junction formation (see Mackenzie et al., 1983; Garfield, 1985; MacKenzie and Garfield, 1985). Distension of the uterus by the growing uterine contents may also stimulate gap junction formation in the rat myometrium (Wathes and Porter, 1982).

Estrogen administration to nonpregnant animals results in a decreased junctional resistance between myometrial cells (i.e. length constant is increased, see Kuriyama and Suzuki, 1976a), whereas progesterone administration increases junctional resistance between myometrial cells (Bortoff and Gilloteaux, 1980). Whether the occurrence of gap junctions was also altered by the hormone

treatments given these tissues is not known. It is known that large doses of estrogen induce gap junction formation in nonpregnant and pregnant myometrium (e.g. see Dahl and Berger, 1978; MacKenzie and Garfield, 1985). Steroid hormone treatment also causes other changes in myometrial electrical properties (e.g. resting membrane potential, rate of rise, amplitude and shape of the spike) in longitudinal (see reviews of Marshall, 1962 and Kao, 1977a) and circular (Kawarabayashi and Marshall, 1981) muscles. However, it is not clear how these latter changes by themselves would affect impulse propagation (e.g. see Marshall, 1962 and Kao, 1977a). On the other, the regulation by the steroid hormones of gap junction formation (and hence intercellular current flow) in the myometrium during pregnancy, provides a more plausible explanation of control of impulse propagation in the myometrium. Hence, the contractile activity of the uterus is asynchronic (and pregnancy is maintained) until gap junction formation at term allows synchronic activity and termination of pregnancy.

Another important role for gap junctions in the rat myometrium at term may be to provide pathways for direct exchange of metabolites (e.g. "metabolic coupling") between myometrial cells (see Cole et al., 1985). However, the nature of the metabolite or intracellular "signal" that is transferred, and its importance in synchronizing uterine metabolism during labour are unknown.

In all other species studied to date, including mice (Dahl and Berger, 1978), rabbit (Demianzuck et al., 1984), guinea pig, sheep, baboon and human (Garfield, 1985), gap junctions are present between uterine smooth muscle cells only immediately before, during and immediately following normal parturition. They are also present in the myometrium of some species (e.g. rat, baboon and human) during preterm labour, but are absent or present in reduced numbers in

tissues from similar animals when labour is prevented experimentally (see review of Garfield, 1985). Thus, myometrial gap junctions generally appear to be necessary for parturition. However, other factors besides the formation of gap junctions, are also likely involved in the initiation and progression of labour (Liggins, 1979; Csapo, 1981; Garfield, 1985). For example, stimulants such as oxytocin and prostaglandins which act to directly excite the uterine muscle cells, may be needed to trigger parturition, once the gap junctions have formed.

## REFERENCES


Abe, Y. 1970. The hormonal control and the effects of drugs and ions on the electrical and mechanical activity of the uterus. In Smooth Muscle. Bulbring, E., Brading, A. F., Jones, A. W. and Tomita, T., editors. Edward Arnold, London. 396-417.

Abe, Y. 1971. Effects of changing the ionic environment on passive and active membrane properties of pregnant rat uterus. J. Physiol. (Lond.) 214:173-190.

Abe, Y. and Tomita, T. 1968. Cable properties of smooth muscle. J. Physiol. (Lond.) 196:87-100.

Adham, N. and Schenk, E. A. 1969. Autonomic innervation of the rat vagina, cervix and uterus and its cyclic variation. Am. J. Obstet. Gynecol. 104:508-516.

Afting, E.-G. and Elce, J. S. 1978. DNA in rat uterus myometrium during pregnancy and postpartum involution. Anal. Biochem. 86:90-99.

Aiken, J. W. 1972. Aspirin and indomethacin prolong parturition in rats. Evidence that prostaglandins contribute to the expulsion of the fetus. Nature 240:21-25.

Alexandrova, M. and Soloff, M. S. 1980. Oxytocin receptors and parturition. I. Control of oxytocin receptor concentration in the rat myometrium at term. Endocrinology 106:730-735.

Alm, P., Alumets, J., Hakanson, R., Owman, Ch., Sjoberg, N.-O., Sundler, F. and Walles, B. 1980. Origin and distribution of VIP (Vasoactive Intestinal Polypeptide)-nerves in the genito-urinary tract. Cell Tissue Res. 205:337-347.

Anderson, N. C. 1969. Voltage-clamp studies on uterine smooth muscle. J. Gen. Physiol. 54:145-165.

Anderson, N. C. 1978. Physiological basis of myometrial function. Semin. Perinatol. 2:211-222.

Anderson, G. F., Kawarabayashi, T. and Marshall, J. M. 1981. Effect of indomethacin and aspirin on uterine activity in pregnant rats: comparison of circular and longitudinal muscle. Biol. Reprod. 24:359-372.

Anderson, N. C. and Ramon, F. 1976. Interaction between pacemaker electrical behaviour and action potential mechanism in uterine smooth muscle. In Physiology of Smooth Muscle. Bulbring, E. and Shuba, M. F., editors. Raven Press, New York. 53-63.

Anderson, N. C., Ramon, F. and Snyder, A. 1971. Studies on calcium and sodium in uterine smooth muscle excitation under current-clamp and voltage-clamp conditions. J. Gen. Physiol. 58:322-339.

Arkinstall, S. J. and Jones, C. T. 1985. Regional changes in catecholamine content of the pregnant uterus. J. Reprod. Fert. 73:547-557.

Barioglio de, S. R. and Lacuara, J. L. 1985. Release of prostaglandins E and F from rat uterine strips incubated in depolarizing and hyperpolarizing solutions. Prostagland. Leuk. Med. 20:129-138.

Barr, L., Berger, W. and Dewey, M. M. 1968. Electrical transmission at the nexus between smooth muscle cells. J. Gen. Physiol. 51:347-368.

Barr, L. and Dewey, M. M. 1968. Electrotonus and electrical transmission in smooth muscle. In Handbook of Physiology, Section 6: Alimentary Canal, Vol. IV: Motility. Code, C. F., editor. American Physiological Society, Washington, D. C. 1733-1742.

Batra, S. 1985. Effect of oxytocin on calcium movements in uterine smooth muscle. Regul. Peptides Suppl. 4:78-81.

Bell, C. 1972. Autonomic nervous control of reproduction: circulatory and other factors. Pharmacol. Rev. 24:657-736.

Bengtsson, B. 1982. Factors of importance for regulation of uterine contractile activity. Acta Obstet. Gynecol. Scand. Suppl. 108:13-16.

Bengtsson, B., Chow, E. M. H. and Marshall, J. M. 1984a. Calcium dependency of pregnant rat myometrium: comparison of circular and longitudinal muscle. Biol. Reprod. 30:869-878.

Bengtsson, B., Chow, E. M. H. and Marshall, J. M. 1984b. Activity of circular muscle of rat uterus at different times in pregnancy. Am. J. Physiol. 246:C216-C223.

Bennett, M. V. L., Spray, D. C., Harris, A. L., Ginzberg, R. D., Campos de Carvalho, A. and White, R. L. 1984. Control of intracellular communication by way of gap junctions. In The Harvey Lectures, Series 78. Academic Press, Orlando. 23-57.

Bergman, R. A. 1968. Uterine smooth muscle fibers in castrate and estrogen-treated rats. J. Cell Biol. 36:639-648.

Bortoff, A. 1976. Myogenic control of intestinal motility. Physiol. Rev. 56:418-434.

Bortoff, A. and Gilloteaux, J. 1980. Specific tissue impedances of estrogen- and progesterone-treated rabbit myometrium. Am. J. Physiol. 238:C34-C42.

Bozler, E. 1941. Influence of estrone on the electric characteristics and motility of uterine muscle. Endocrinology 29:225-227.

Bradshaw, J. M. C., Downing, S. J., Moffatt, A., Hinton, J. C. and Porter, D. G. 1981. Demonstration of some physiological properties of rat relaxin. J. Reprod. Fert. 63:145-153.

Braun, J., Abney, J. R. and Owicki, J. C. 1984. How a gap junction maintains its structure. Nature 310:316-318.

Bulbring, E., Burnstock, G. and Holman, M. E. 1958. Excitation and conduction in the smooth muscle of the isolated taenia coli of the guinea pig. J. Physiol. (Lond.) 142:420-437.

Burnstock, G. 1970. Structure of smooth muscle and its innervation. In Smooth Muscle. Bulbring, E., Brading, A. F., Jones, A. W. and Tomita, T., editors. Edward Arnold, London. 1-69.

Burnstock, G. and Prosser, C. L. 1960. Conduction in smooth muscles: comparative electrical properties. Am. J. Physiol. 199:553-559.

Carsten, M. E. 1968. Regulation of myometrial composition, growth and activity. In Biology of the Uterus, vol. 1. Assali, N. S., editor. Academic Press, New York. 355-423.

Casteels, R. and Kuriyama, H. 1965. Membrane potential and ionic content in pregnant and nonpregnant rat myometrium. J. Physiol. (Lond.) 177:263-287.

Challis, J. R. G. 1984. Characteristics of parturition. In Maternal-Fetal Medicine. Creasy, R. K. and Resnik, R., editors. W. B. Saunders, Philadelphia. 401-414.

Chamley, W. A. and Parkington, H. C. 1984. Relaxin inhibits the plateau component of the action potential in the circular myometrium of the rat. J. Physiol. (Lond.) 353:51-65.

Chan, W. Y. 1983. Uterine and placental prostaglandins and their modulation of oxytocin sensitivity and contractility in the parturient uterus. Biol. Reprod. 29:680-688.

Cheah, S. H. and Sherwood, O. D. 1981. Effects of relaxin on in vivo uterine contractions in conscious and unrestrained estrogen-treated and steroid-untreated ovariectomized rats. Endocrinology 109:2076-2083.

Chow, E. H. M. and Marshall, J. M. 1981. Effects of catecholamines on circular and longitudinal uterine muscle. Eur. J. Pharmacol. 76:157-165.

Christensen, J. and Hauser, R. L. 1971. Longitudinal axial coupling of slow waves in cat colon. Am. J. Physiol. 221:246-250.

Clapham, D. E., Shrier, A. and DeHaan, R. L. 1980. Junctional resistance and action potential delay between embryonic heart cell aggregates. J. Gen. Physiol. 75:633-654.

Cole, W. C. and Garfield, R. E. 1985. Alterations in coupling in uterine smooth muscle. In: Cold Spring Harbor Symposium on Quantitative Biology (in press).

Cole, W. C., Garfield, R. E. and Kirkaldy, J. S. 1985. Gap junctions and direct intercellular communication between rat uterine smooth muscle cells. Am. J. Physiol. 249:C20-C31.

Connor, J., Mangel, A. and Nelson, B. 1979. Propagation and entrainment of slow waves in cat small intestine. Am. J. Physiol. 237:C237-C246.

Cranefield, P. F. 1983. Channels, cables, networks, and the conduction of the cardiac impulse. Am. J. Physiol. 245:H901-H910.

Crankshaw, D. J. 1985. Oxytocin receptors: comments on their regulation. In Oxytocin: Clinical and Laboratory Studies. Amico, J. A. and Robinson, A. G., editors. Elsevier, Amsterdam. 277-283.

Creed, K. E. 1979. Functional diversity of smooth muscle. Br. Med. Bull. 35:243-247.

Csapo, A. I. 1950. Actomyosin of the uterus. Am. J. Physiol. 160:46-52.

Csapo, A. I. 1961. Defence mechanism of pregnancy. In Progesterone and the Defence Mechanism of Pregnancy. Ciba Foundation Study Group 9. Little Brown, Boston. 1-27.

Csapo, A. I. 1962. Smooth muscle as a contractile unit. Physiol. Rev. 42 (Suppl. 5):7-33.

Csapo, A. I. 1969. The luteo-placental shift, the guardian of prenatal life. Postgrad. Med. J. 45:57-64.

Csapo, A. I. 1971. The uterus: a model for medical considerations. In Contractile Proteins and Muscle. Laki, K., editor. Marcel Dekker, New York. 413-482.

Csapo, A. I. 1977. The "see-saw" theory of parturition. In The Fetus and Birth. Knight, J. and O'Connor, M., editors. Ciba Foundation Symposium 47. Elsevier, Amsterdam. 159-195.

Csapo, A. I. 1981. Force of labor. In Principles and Practice of Obsterics and Perinatology. Iffy, L. and Kamientzky, H. A., editors. John Wiley and Sons, New York. 761-799.

Csapo, A. I. and Kuriyama, H. 1963. Effects of ions and drugs on cell membrane activity and tension in the postpartum rat myometrium. J. Physiol. (Lond.) 165:575-592.

Csapo, A. I. and Takeda, H. 1965. Effect of progesterone on the electric activity and intrauterine pressure of pregnant and parturient rabbits. Am. J. Obstet. Gynecol. 91:221-231.

Csapo, A. I., Takeda, H, and Wood, C. 1963. Volume and activity of the parturient rabbit uterus. Am. J. Obstet. Gynecol. 85:813-818.

Csapo, A. I. and Wiest, W. G. 1969. An examination of the quantitative relationship between progesterone and the maintenance of pregnancy. Endocrinology 85:735-746.

Dahl, G., Arzarnia, R. and Werner, R. 1980. De novo construction of cell to cell channels. In Vitro 16:1068-1075.

Dahl, G. and Berger, W. 1978. Nexus formation in the myometrium during parturition and induced by estrogen. Cell Biol. Int. Rep. 2:381-387.

Daniel, E. E. 1960. The activation of various types of uterine muscle during stretch-induced contraction. Can. J. Biochem. Physiol. 38:1327-1362.

Daniel, E. E., Daniel, V. P., Duchon, G., Garfield, R. E., Nichols, M., Malhotra, S. K. and Oki, M. 1976. Is the nexus necessary for cell-to-cell coupling of smooth muscle? J. Memb. Biol. 28:207-239.

Daniel, E. E., Garfield, R., Kannan, M. S., Zelcer, E. and Sims, S. 1978. The nature of the control over coupling between smooth muscle cells and layers: its contribution to the synchrony of smooth muscle contraction. Jpn. J. Smooth Muscle Res. 14:37-38.

Daniel, E. E., Grover, A. K. and Kwan, C. Y. 1983. Control of intracellular calcium in smooth muscle. In Calcium Regulation by Calcium Antagonists. Rahwan, R. G. and Witiak, D. T., editors. ACS Symposium Series, No. 201. 73-88.

Daniel, E. E. and Lodge, S. 1973. Electrophysiology of myometrium. In Uterine Contraction: Side Effects of Steroidal Contraceptives. Josimovich, J. B., editor. John Wiley and Sons, New York. 19-64.

Daniel, E. E. and Renner, S. A. 1960. Effect of the placenta on the electrical activity of the cat uterus in vivo and in vitro. Am. J. Obstet. Gynecol. 80:229-244.

Daniel, E. E. and Sarna, S. 1978. The generation and conduction of activity in smooth muscle. Ann. Rev. Pharmacol. Toxicol. 18:145-166.

Daniel, E. E. and Singh, H. 1958. The electrical properties of the smooth muscle cell membrane. Can. J. Biochem. Physiol. 36:959-975.

DeHaan, R. L. and Hirakow, R. 1972. Synchronization of pulsation rates in isolated cardiac myocytes. Exp. Cell Res. 70:214-220.

Delmar, M., Jalife, J. and Michaels, D. C. 1986. Effects of changes in excitability and intercellular coupling on synchronization in the rabbit sino-atrial node. J. Physiol. (Lond.) 370:127-150.

De Mello, W. C. 1982. Cell-to-cell communication in heart and other tissues. Prog. Biophys. Molec. Biol. 39:147-182.

De Mello, W. C. 1983. The role of cAMP and Ca on the modulation of junctional conductance: an integrated hypothesis. Cell Biol. Int. Rep. 7:1033-1040.

Demianczuk, N., Towell, M. and Garfield, R. E. 1984. Myometrial electrophysiologic activity and gap junctions in the pregnant rabbit. Am. J. Obstet. Gynecol. 149:485-491.

Dewey, M. M. and Barr, L. 1968. Structure of vertebrate intestinal smooth muscle. In Handbook of Physiology, Section 6: Alimentary Canal, Vol. IV: Motility. Code, C. F., editor. American Physiological Society, Washington, D. C. 1629-1654.

Downing, S. J., Bradshaw, J. M. C. and Porter, D. G. 1980. Relaxin improves the coordination of rat myometrial activity in vivo. Biol. Reprod. 23:899-903.

Downing, S. J. and Sherwood, O. D. 1985a. The physiological role of relaxin in the pregnant rat. I. The influence of relaxin on parturition. Endocrinology 116:1200-1205.

Downing, S. J. and Sherwood, O. D. 1985b. The physiological role of relaxin in the pregnant rat. II. The influence of relaxin on uterine contractile activity. Endocrinology 116:1206-1214.

Downing, S. J. and Sherwood, O. D. 1985c. The physiological role of relaxin in the pregnant rat. III. The influence of relaxin on cervical extensibility. Endocrinology 116:1215-1220.

Dubin, N. H., Blake, D. A., Ghodgaonkar, R. B. and Egner, P. G. 1982. Thromboxane $B_2$, 6-keto-prostaglandin $F_{1\alpha}$ and prostaglandin $F_{2\alpha}$ by contracting pregnant rat uteri in vitro. Biol. Reprod. 26:281-288.

Dubin, N. H., Ghodgaonkar, R. B. and King, T. M. 1979. Role of prostaglandin production in spontaneous and oxytocin-induced uterine contractile activity in in vitro pregnant rat uteri. Endocrinology 105:47-51.

Dumpala, S. R., Reddy, S. N. and Sarna, S. K. 1982. An algorithm for the detection of peaks in biological signals. Comput. Prog. Biomed. 14:249-256.

Fay, F. S., Cooke, P. H. and Canaday, P. G. 1976. Contractile properties of isolated smooth muscle cells. In Physiology of Smooth Muscle. Bulbring, E. and Shuba, M. F., editors. Raven Press, New York. 249-264.

Finn, C. A. and Porter, D. G. 1975. The Uterus. Elek Science, London.

Fowler, R. J. 1977. The role of prostaglandins in parturition with special reference to the rat. In The Fetus and Birth. Knight, J. and O'Connor, M., editors. Ciba Foundation Symposium 47. Elsevier, Amsterdam. 297-312.

Fozzard, H. A. 1979. Conduction of the action potential. In Handbook of Physiology, Section 2: The Cardiovascular System, Vol. I: The Heart. Berne, R. M., editor. American Physiological Society, Washington, D. C. 335-356.

Fried, G., Hokfelt, T., Terenius, L. and Goldstein, M. 1985. Neuropeptide Y (NPY)-like immunoreactivity in guinea pig uterus is reduced during pregnancy in parallel with noradrenergic nerves. Histochemistry 83:437-442.

Fry, G. N., Devine, C. E. and Burnstock, G. 1977. Freeze fracture studies of nexuses between smooth muscle cells. Close relationship to sarcoplasmic reticulum. J. Cell Biol. 72:26-34.

Fuchs, A.-R. 1969. Uterine activity in late pregnancy and during parturition in the rat. Biol. Reprod. 1:344-353.

Fuchs, A.-R. 1973. Parturition in rabbits and rats. In Endocrine Factors in Labour. Klopper, A. and Gardner, J., editors. Mem. Soc. Endocrinol. (London) 20:163-185.

Fuchs, A.-R. 1978. Hormonal control of myometrial function during pregnancy and parturition. Acta Endocrinol. Suppl. 221:1-70.

Fuchs, A.-R. 1983. The role of oxytocin in parturition. Curr. Topics Exptl. Endocrinol. 4:231-265.

Fuchs, A.-R. 1985. Oxytocin in animal parturition. In: Oxytocin: Clinical and Laboratory Studies. Amico, J. A. and Robinson, A. G., editors. Elsevier, Amsterdam. 207-235.

Fuchs, A.-R. and Poblete, V. F. 1970. Oxytocin and uterine function in pregnant and parturient rats. Biol. Reprod. 2:387-400.

Gabella, G. 1979. Smooth muscle cell junctions and structural aspects of contraction. Br. Med. Bull. 35:213-218.

Gabella, G. 1981. Structure of smooth muscles. In Smooth Muscle: an Assessment of Current Knowledge. Bulbring, E., Brading, A. F., Jones, A. W. and Tomita, T., editors. Edward Arnold, London. 1-46.

Gabella, G. 1984a. Structural apparatus for force transmission in smooth muscles. Physiol. Rev. 64:455-477.

Gabella, G. 1984b. Smooth muscle cell membrane and allied structures. In Smooth Muscle Contraction. Stephens, N. L., editor. Marcel Dekker, New York. 21-45.

Gabella, G. and Blundell, D. 1979. Nexuses between the smooth muscle cells of the guinea-pig ileum. J. Cell. Biol. 82:239-247.

Gabella, G. and Blundell, D. 1981. Gap junctions of the muscles of the small and large intestine. Cell Tissue Res. 219:469-488.

Garfield, R. E. 1979. Regeneration of smooth muscle: ultrastructure and multipotential properties of smooth muscle. In Muscle Regeneration. Mauro, A., editor. Raven Press, New York. 383-404.

Garfield, R. E. 1985. Cell-to-cell communication in smooth muscle. In Calcium and Contractility. Grover, A. K. and Daniel, E. E., editors. Humana Press, Clifton. 143-173.

Garfield, R. E. 1986. Structural studies of innervation on nonpregnant rat uterus. Am. J. Physiol. 251:C41-C56.

Garfield, R. E. and Daniel, E. E. 1974. The structural basis of electrical coupling (cell-to-cell contacts) in rat myometrium. Gynecol. Invest. 5:284-300.

Garfield, R. E., Kannan, M. S. and Daniel, E. E. 1980a. Gap junction formation in myometrium: control by estrogens, progesterone and prostaglandins. Am. J. Physiol. 238:C81-C89.

Garfield, R. E., Merrett, D. and Grover, A. K. 1980b. Gap junction formation and regulation in myometrium. Am. J. Physiol. 239:C217-C228.

Garfield, R. E., Puri, C. P. and Csapo, A. I. 1982. Endocrine, structural and functional changes in the uterus during premature labor. Am. J. Obstet. Gynecol. 142:21-27.

Garfield, R. E., Rabideau, S., Challis, J. R. G. and Daniel, E. E. 1979. Hormonal control of gap junction formation in sheep myometrium during parturition. Biol. Reprod. 21:999-1007.

Garfield, R. E., Sims, S. and Daniel, E. E. 1977. Gap junctions: their presence and necessity in myometrium during gestation. Science 198:958-960.

Garfield, R. E., Sims, S. M., Kannan, M. S. and Daniel, E. E. 1978. Possible role of gap junctions in activation of myometrium during parturition. Am. J. Physiol. 235:C168-C179.

Garfield, R. E. and Somlyo, A. P. 1985. Structure of smooth muscle. In Calcium and Contractility. Grover, A. K. and Daniel, E. E., editors. Human Press, Clifton. 1-36.

Germain, G., Cabrol, D., Visser, A. and Sureau, C. 1982. Electrical activity of the pregnant uterus in the cynomolgus monkey. Am. J. Obstet. Gynecol. 142:513-519.

Gimeno, M. F., Chaud, M., Bordia, E. S., Lazzari, M. and Gimeno, A. L. 1981. Does hypoxia selectively stimulate the generation of prostaglandin $E_1$ by the isolated rat uterus? Prostaglandins Med. 7:375-388.

Gimeno, M. F., Sterin-Speziale, N., Bonacossa, A. and Gimeno. A. L. 1979. Is the spontaneous motility of the isolated rat uterus controlled by prostaglandin E? Prostaglandins 17:673-682.

Goto, M., Kuriyama, H. and Abe, Y. 1961. Refractory period and conduction of excitation in the uterine muscle cells of the mouse. Jpn. J. Physiol. 11:369-377.

Grosset, A. and Mironneau, J. 1977. An analysis of the actions of prostaglandin $E_1$ on membrane currents and contraction in uterine smooth muscle. J. Physiol. (Lond.) 270:765-784.

Gu, J., Polak, J. M., Su, H. C., Blank, M. A., Morrison, J. F. B. and Bloom, S. R. 1984. Demonstration of paracervical ganglion origin for the vasoactive intestinal peptide-containing nerves of the rat uterus using retrograde tracing techniques combined with immunocytochemistry and denervation procedures. Neurosci. Lett. 51:377-382.

Ham, A. W. and Cormack, D. H. 1979. Histology. J. B. Lippincott, Philadelphia.

Hamoir, G. 1977. Biochemistry of the myometrium. In Biology of the Uterus. Wynn, R. M., editor. Plenum Press, New York. 377-421.

Harding, R., Poore, E. R., Bailey, A., Thorburn, G. D., Jansen, C. A. M. and Nathanielsz, P. W. 1982. Electromyographic activity of the nonpregnant and pregnant sheep uterus. Am. J. Obstet. Gynecol. 142:448-457.

Harney, P. J., Sneddon, J. M. and Williams, K. I. 1974. The influence of ovarian hormones upon the motility and prostaglandin production of the pregnant rat uterus in vitro. J. Endocrinol. 60:343-351.

Henderson, R. M. 1975. Cell-to-cell contacts. In Methods in Pharmacology. Vol. 3. Smooth Muscle. Daniel, E. E. and Paton, D. M., editors. Plenum Press, New York. 47-77.

Hertzberg, E. L. 1980. Biochemical and immunological approaches to the study of gap junctional communication. In Vitro 16:1057-1067.

Hervonen, A., Kanerva, L. and Lietzen, R. 1973. Histochemically demonstrable catecholamines and cholinesterases of the rat uterus during estrus cycle, pregnancy and after estrogen treatment. Acta Physiol. Scand. 87:283-288.

Higuchi, T., Honda, K., Fukuoka, T., Negoro, H. and Wakabayashi, K. 1985. Release of oxytocin during suckling and parturition in the rat. J. Endocrinol. 105:339-346.

Holman, M. E. 1968. Introduction to electrophysiology of visceral smooth muscle. In Handbook of Physiology, Section 6: Alimentary Canal, Vol. IV: Motility. Code, C. F., editor. American Physiological Society, Washington, D. C. 1665-1708.

Holman, M. E. and Neild, T. O. 1979. Membrane properties. Br. Med. Bull. 35:235-241.

Homma, S., Iwata, K., Kusama, T. and Nakajima, Y. 1983. Effects of electrical constants on conduction velocity of action potentials measured with unidimensional latency-topography in frog skeletal muscle fibers. Jpn. J. Physiol. 33:711-720.

Ichikawa, S. and Bortoff, A. 1970. Tissue resistance of the progesterone-dominated rabbit myometrium. Am. J. Physiol. 219:1763-1767.

Izumi, H. 1985. Changes in the mechanical properties of the longitudinal and circular muscles of the rat myometrium during gestation. Br. J. Pharmacol. 86:247-257.

Jalife, J. 1984. Mutual entrainment and electrical coupling as mechanisms for synchronous firing of rabbit sino-atrial pace-maker cells. J. Physiol. (Lond.) 356:221-243.

Joyner, R. W., Picone, J., Veenstra, R. and Rawling, D. 1983. Propagation through electrically coupled cells. Effects of regional changes in membrane properties. Circ. Res. 53:526-534.

Kanda, S. and Kuriyama, H. 1980. Specific features of smooth muscle cells recorded from the placental region of the myometrium of pregnant rats. J. Physiol. (Lond.) 299:127-144.

Kao, C. Y. 1959. Long-term observations of spontaneous electrical activity of the uterine smooth muscle. Am. J. Physiol. 196:343-350.

Kao, C. Y. 1966. Tetrodotoxin, saxitoxin and their significance in the study of excitation phenomena. Pharmacol. Rev. 18:997-1049.

Kao, C. Y. 1977a. Electrical properties of uterine smooth muscle. In Biology of the Uterus. Wynn, R. M., editor. Plenum Press, New York. 423-496.

Kao, C. Y. 1977b. Recent experiments in voltage-clamp studies on smooth muscles. In Excitation-Contraction Coupling in Smooth Muscle. Casteels, R., Godfraind, T. and Ruegg, J. C., editors. Elsevier/North-Holland, Amsterdam. 91-96.

Kao, C. Y. and McCullough, J. R. 1975. Ionic currents in the uterine smooth muscle. J. Physiol. (Lond.) 246:1-36.

Kao, C. Y. and Nishiyama, A. 1964. Ovarian hormones and resting potentials of uterine smooth muscle. Am. J. Physiol. 207:793-799.

Kawarabayashi, T. 1978. The effects of phenylephrine in various ionic environments on the circular muscle of midpregnant rat myometrium. Jpn. J. Physiol. 28:627-645.

Kawarabayashi, T. and Marshall, J. M. 1981. Factors influencing circular muscle activity in the pregnant rat uterus. Biol. Reprod. 24:373-379.

Kawarabayashi, T. and Osa, T. 1976. Comparative investigations of alpha- and beta-effects on the longitudinal and circular muscles of the pregnant rat myometrium. Jpn. J. Physiol. 26:403-416.

Kishikawa, T. 1981. Alterations in the properties of the rat myometrium during gestation and post partum. Jpn. J. Physiol. 31:515-536.

Knox, W. E. and Lister-Rosenoer, L. M. 1978. Timing of gestation in rats by fetal and maternal weights. Growth 42:43-53.

Kobayashi, M., Prosser, C. L. and Nagai, T. 1967. Electrical properties of intestinal muscle as measured intracellularly and extracellularly. Am. J. Physiol. 213:275-286.

Kuffler, S. W., Nicholls, J. G. and Martin, A. R. 1984. From Neuron To Brain. 2nd edition. Sinauer Associates Inc., Sunderland, Mass.

Kuriyama, H. 1961. Recent studies on the electrophysiology of the uterus. In Progesterone and the Defence Mechanism of Pregnancy. Ciba Foundation Study Group 9. Little Brown, Boston. 51-70.

Kuriyama, H. 1964. Effect of electrolytes on the membrane activity of the uterus. In Pharmacology of Smooth Muscle. Bulbring, E., editor. MacMillan, New York. 127-140.

Kuriyama, H. 1981. Excitation-contraction coupling in various visceral smooth muscles. In Smooth Muscle: an Assessment of Current Knowledge. Bulbring, E., Brading, A. F., Jones, A. W. and Tomita, T., editors. Edward Arnold, London.

Kuriyama, H. and Csapo, A. I. 1961. A study of the parturient uterus with the microelectrode technique. Endocrinology 68:1010-1025.

Kuriyama, H. and Suzuki, H. 1976a. Changes in electrical properties of rat myometrium during gestation and following hormonal treatments. J. Physiol. (Lond.) 260:315-333.

Kuriyama, H. and Suzuki, H. 1976b. Effects of prostaglandin $E_2$ and oxytocin on the electrical activity of hormone-treated and pregnant rat myometria. J. Physiol. (Lond.) 260:335-349.

Landa, J. F., West, T. C. and Thiersch, J. B. 1959. Relationships between contraction and membrane electrical activity in the uterus of the pregnant rat. Am. J. Physiol. 196:905-909.

Larsen, W. J. 1983. Biological implications of gap junction structure, distribution and composition: a review. Tissue and Cell 15:645-671.

Larsson, L.-I., Fahrenkrug, J. and Schaffalitzky de Muckadell, O. B. 1977. Vasoactive intestinal polypeptide occurs in nerves of the female genito-urinary tract. Science 197:1374-1375.

Liggins, G. C. 1973. Fetal influences on uterine contractility. In Uterine Contraction: Side Effects of Steroidal Contraceptives. Josimovich, J. B., editor. John Wiley and Sons, New York. 205-218.

Liggins, G. C. 1979. Initiation of parturition. Br. Med. Bull. 35:145-150.

Lodge, S. and Sproat, J. E. 1981. Resting membrane potentials of pacemaker and nonpacemaker areas in rat uterus. Life Sci. 28:2251-2256.

Loewenstein, W. R. 1981. Junctional intercellular communication in the cell-to-cell membrane channel. Physiol. Rev. 61:829-913.

MacKenzie, L. W. and Garfield, R. E. 1985. Hormonal control of gap junctions in the myometrium. Am. J. Physiol. 248:C296-C308.

MacKenzie, L. W., Puri, C. P. and Garfield, R. E. 1983. Effect of estradiol-17$\beta$ and prostaglandins on rat myometrial gap junctions. Prostaglandins 26:925-941.

Marshall, J. M. 1959. Effects of estrogen and progesterone on single uterine muscle fibers in the rat. Am. J. Physiol. 197:935-942.

Marshall, J. M. 1962. Regulation of activity in uterine smooth muscle. Physiol. Rev. 42 (Suppl. 5):213-227.

Marshall, J. M. 1970. Adrenergic innervation of the female reproductive tract: anatomy, physiology and pharmacology. Rev. Physiol. Biochem. Pharmacol. 62:6-67.

Marshall, J. M. 1973. The physiology of the uterus. In The Uterus. Norris, H. J., Hertig, A. T. and Abell, M. R., editors. Williams and Wilkins, Baltimore. 89-109.

Marshall, J. M. 1974. Effects of neurohypophysial hormones on the myometrium. In Handbook of Physiology, Section 7: Endocrinology, vol. IV: The pituitary gland, Part 1. Greep, R. O. and Astwood, E. B., editors. American Physiological Society, Washington, D. C. 469-492.

Marshall, J. M. 1981. Effects of ovarian steroids and pregnancy on adrenergic nerves of uterus and oviduct. Am. J. Physiol. 240:C165-C174.

Melton, C. E. 1956. Electrical activity in the uterus of the rat. Endocrinology 58:139-149.

Melton, C. E. and Saldivar, J. T. 1964. Impulse velocity and conduction pathways in rat myometrium. Am. J. Physiol. 207:279-285.

Melton, C. E. and Saldivar, J. T. 1965. Estrous cycle and electrical activity of rat myometrium. Life Sci. 4:593-602.

Melton, C. E. and Saldivar, J. T. 1967. The linea uteri, a conduction pathway in rat myometrium. Life Sci. 6:297-304.

Melton, C. E. and Saldivar, J. T. 1970. Activity of the rat's uterine ligament. Am. J. Physiol. 219:122-125.

Mercado-Simmen, R. C., Bryant-Greenwood, G. D. and Greenwood, F. C. 1982. Relaxin receptor in the rat myometrium: regulation by estrogen and relaxin. Endocrinology 110:220-226.

Merk, F. B., Kwan, P. W. L. and Leav, I. 1980. Gap junctions in the myometrium of hypophysectomized estrogen-treated rats. Cell Biol. Int. Rep. 4:287-294.

Michael, C. A. and Schofield, B. M. 1969. The influence of the ovarian hormones on the actomyosin content and the development of tension in uterine muscle. J. Endocrinol. 44:501-511.

Mironneau, J. 1973. Excitation-contraction coupling in voltage-clamped uterine smooth muscle. J. Physiol. (Lond.) 233:127-141.

Mironneau, J. 1976a. Relationship between contraction and transmembrane ionic current in voltage-clamped uterine smooth muscle. In Physiology of Smooth Muscle. Bulbring, E. and Shuba, M. F., editors. Raven Press, New York. 175-183.

Mironneau, J. 1976b. Effects of oxytocin on ionic currents underlying rhythmic activity and contraction in uterine smooth muscle. Pflugers Arch. 363:113-118.

Mironneau, J., Eugene, D. and Mironneau, C. 1982. Sodium action potentials induced by calcium chelation in rat uterine smooth muscle. Pflugers Arch. 395:232-238.

Mironneau, C., Mironneau, J. and Savineau, J.-P. 1984a. Maintained contractions of rat uterine smooth muscle incubated in a $Ca^{2+}$-free solution. Br. J. Pharmacol. 82:735-743.

Mironneau, J., Lalanne, C., Mironneau, C., Savineau, J.-P. and Lavie, J. L. 1984b. Comparison of pinaverium bromide, manganese chloride and D600 effects on electrical and mechanical activities in rat uterine smooth muscle. Eur. J. Pharmacol. 98:99-107.

Mironneau, J. and Savineau, J.-P. 1980. Effects of calcium fons on outward membrane currents in rat uterine smooth muscle. J. Physiol. (Lond.) 302:411-425.

Mironneau, J., Savineau, J.-P. and Mironneau, C. 1981. Fast outward current controlling electrical activity in rat uterine smooth muscle during gestation. J. Physiol. (Paris) 77:851-859.

Mitchell, M. D. 1984. The mechanism(s) of human parturition. J. Develop. Physiol. 6:107-118.

Mosler, K.-H. 1968. The dynamics of uterine muscle. Adv. Obstet. Gynecol. 35:1-88.

Mossman, H. W. 1977. Comparative anatomy. In Biology of the Uterus. Wynn, R. M., editor. Plenum Press, New York. 19-34.

Nagai, T. and Prosser, C. L. 1963. Patterns of conduction in smooth muscle. Am. J. Physiol. 204:910-914.

Nishikori, K., Weisbrodt, N. W., Sherwood, O. D. and Sanborn, B. M. 1982. Relaxin alters rat uterine myosin light chain phosphorylation and related enzyme activities. Endocrinology 111:1743-1745.

Novy, J. and Liggins, G. C. 1980. Role of prostaglandins and thromboxanes in the physiological control of the uterus and in parturition. Semin. Perinatol. 4:45-66.

O'Byrne, K. T., Ring, J. P. G. and Summerlee, A. J. S. 1986. Plasma oxytocin and oxytocin neurone activity during delivery in rabbits. J. Physiol. (Lond.) 370:501-513.

Ogasawara, T., Kato, S. and Osa, T. 1980. Effects of estradiol-17$\beta$ on the membrane response and K-contracture in the uterine longitudinal muscle of ovariectomized rats studied in combination with the Mn action. Jpn. J. Physiol. 30:271-285.

Ohkawa, H. 1975. Electrical and mechanical interaction between the muscle layers of rat uterus and different sensitivities to oxytocin. Bull. Yamaguchi Med. School 22:197-210.

Osa, T. 1974. An interaction between the electrical activities of longitudinal and circular smooth muscles of pregnant mouse uterus. Jpn. J. Physiol. 24:189-203.

Osa, T. and Fujino, T. 1978. Electrophysiological comparison between the longitudinal and circular muscles of the rat uterus during the estrous cycle and pregnancy. Jpn. J. Physiol. 28:197-209.

Osa, T. and Katase, T. 1975. Physiological comparison of the longitudinal and circular muscles of the pregnant rat uterus. Jpn. J. Physiol. 25:153-164.

Osa, T. and Kawarabayashi, T. 1977. Effects of ions and drugs on the plateau potential in the circular muscle of pregnant rat myometrium. Jpn. J. Physiol. 27:111-121.

Osa, T. and Ogasawara, T. 1983. Effects of magnesium on the membrane activity and contraction of the circular muscle of rat myometrium during late pregnancy. Jpn. J. Physiol. 33:485-495.

Osa, T. and Ogasawara, T. 1984. Effects in vitro of progesterone and estradiol-17$\beta$ on the contractile and electrical responses in rat myometrium. Jpn. J. Physiol. 34:427-441.

Osa, T., Ogasawara, T. and Kato, S. 1983. Effects of magnesium, oxytocin and prostaglandin $F_{2\alpha}$ on the generation and propagation of excitation in the longitudinal muscle of rat myometrium during late pregnancy. Jpn. J. Physiol. 33:51-67.

Osa, T. and Watanabe, M. 1978. Effects of catecholamines on the circular muscle of rat myometria at term during pregnancy. Jpn. J. Physiol. 28:647-658.

Ottesen, B. 1981. Vasoactive intestinal polypeptide (VIP): effect on rabbit uterine smooth muscle in vivo and in vitro. Acta Physiol. Scand. 113:193-199.

Ottesen, B., Gram, B. R. and Fahrenkrug, J. 1983. Neuropeptides in the female genital tract: effect on vascular and non vascular smooth muscle. Peptides 4:387-392.

Ottesen, B., Larsen, J.-J., Fahrenkrug, J., Stjernquist, M. and Sundler, F. 1981. Distribution and motor effect of VIP in female genital tract. Am. J. Physiol. 240:E32-E36.

Ottesen, B., Ulrichsen, H., Fahrenkrug, J., Larsen, J.-J., Wagner, G., Schierup, L. and Sondergaard, F. 1982. Vasoactive intestinal polypeptide and the female genital tract: relationship to reproductive phase and delivery. Am. J. Obstet. Gynecol. 143:414-420.

Paiva, C. E. N. de and Csapo, A. I. 1973. The effect of prostaglandin on the electric activity of the pregnant uterus. Prostaglandins 4:177-188.

Papka, R. E., Cotton, J. P. and Traurig, H. H. 1985. Comparative distribution of neuropeptide tyrosine-, vasoactive intestinal polypeptide-, substance P-immunoreactive, acetylcholinesterase-positive and noradrenergic nerves in the reproductive tract of the female rat. Cell Tissue Res. 242:475-490.

Parkington, H. C. 1985. Some properties of the circular myometrium of the sheep throughout pregnancy and during labour. J. Physiol. (Lond.) 359:1-15.

Paton, D. M. and Daniel, E. E. 1967. On the contractile response of the isolated rat uterus to prostaglandin $E_1$. Can. J. Physiol. Pharmacol. 45:795-804.

Phillips, C. A. and Poyser, N. L. 1981. Prostaglandins, thromboxanes and the pregnant rat uterus at term. Br. J. Pharmacol. 73:75-80.

Popescu, L. M., Nuto, O. and Panoui, C. 1985. Oxytocin contracts the human uterus at term by inhibiting the myometrial $Ca^{2+}$-extrusion pump. Bioscience Rep. 5:21-28.

Porter, D. G. 1979. The myometrium and the relaxin enigma. Anim. Reprod. Sci. 2:77-96.

Porter, D. G. 1982. Unsolved problems of relaxin's physiological role. Ann. N. Y. Acad. Sci. 380:151-162.

Porter, D. G., Downing, S. J. and Bradshaw, J. M. 1979. Relaxin inhibits spontaneous and prostaglandin-driven myometrial activity in anaesthetized rats. J. Endocrinol. 83:183-192.

Prosser, C. L. 1962. Conduction in nonstriated muscles. Physiol. Rev. 42 (Suppl. 5):193-206.

Prosser, C. L., Burnstock, G. and Kahn, J. 1960. Conduction in smooth muscle: comparative structural properties. Am. J. Physiol. 199:545-522.

Prosser, C. L. and Mangel, A. W. 1982. Mechanisms of spike and slow wave pacemaker activity in smooth muscle cells. In Cellular Pacemakers. Vol. 1. Carpenter, D. O., editor. John Wiley and Sons, New York. 273-300.

Puri, C. P. and Garfield, R. E. 1982. Changes in hormone levels and gap junctions in the rat uterus during pregnancy and parturition. Biol. Reprod. 27:967-975.

Reddy, S. N., Miller, S. M., Daniel, E. E. and Garfield, R. E. 1984. Quantification of the variability of biological oscillators. Proc. 10th Can. Med. Biol. Eng. Conf. pp. 3-4.

Reiner, O. and Marshall, J. M. 1975. Action of D-600 on spontaneous and electrically stimulated activity of the parturient rat uterus. Naunyn-Schmiedeberg's Arch. Pharmacol. 290:21-28.

Reiner, O. and Marshall, J. M. 1976. Action of prostaglandin, $PGF_{2\alpha}$, on the uterus of the pregnant rat. Naunyn-Schiedeberg's Arch. Pharmacol. 292:243-250.

Revel, J.-P., Nicholson, B. J. and Yancey, S. B. 1985. Chemistry of gap junctions. Ann. Rev. Physiol. 47:263-279.

Roche, P. J., Parkington, H. C. and Gibson, W. R. 1985. Pregnancy and parturition in rats after sympathetic denervation of the ovary, oviduct and utero-tubal junction. J. Reprod. Fert. 75:653-661.

Saito, Y., Sakamoto, H., MacLusky, N. J. and Naftolin, F. 1985. Gap junctions and myometrial steroid hormone receptors in pregnant and postpartum rats: a possible cellular basis for the progesterone withdrawal hypothesis. Am. J. Obstet. Gynecol. 151:805-812.

Sakai, K., Yamaguchi, T. and Uchida, M. 1981. Oxytocin-induced Ca-free contraction of rat uterine smooth muscle: effects of divalent cations and drugs. Arch. Int. Pharmacodyn. 250:40-54.

Saldivar, J. T. and Melton, C. E. 1966. Effects in vivo and in vitro of sex steroids on rat myometrium. Am. J. Physiol. 211:835-843.

Sarna, S. K. 1975. Models of smooth muscle electrical activity. In Methods of Pharmacology, Vol. 3, Smooth Muscle. Daniel, E. E. and Paton, D. M., editors. Plenum Press, New York. 519-540.

Sarosi, P., Schmidt, C. L., Essig, M., Steinetz, B. G. and Weiss, G. 1983. The effect of relaxin and progesterone on rat uterine contractions. Am. J. Obstet. Gynecol. 145:402-405.

Schild, H. O. 1964. Calcium and the effect of drugs on depolarized smooth muscle. In Pharmacology of Smooth Muscle. Bulbring, E., editor. Permagon Press, Oxford. 95-104.

Segal, J. S., Scher, W. and Koide, S. S. 1977. Estrogens, nucleic acids and protein synthesis in uterine metabolism. In: Biology of the Uterus. Wynn, R. M., editor. Plenum Press, New York. 139-201.

Sherwood, O. D., Crnekovic, V. E., Gordon, W. L. and Rutherford, J. E. 1980. Radioimmunoassay of relaxin throughout pregnancy and during parturition in the rat. Endocrinology 107:691-698.

Shoenberg, C. F. 1977. The contractile mechanism and ultrastructure of the myometrium. In Biology of the Uterus. Wynn, R. M., editor. Plenum Press, New York. 497-544.

Sigger, J. N., Harding, R. and Summers, R. J. 1986. Changes in the innervation and catecholamine concentrations in the myometrium of pregnant and nonpregnant sheep. Acta. Anat. 125:101-107.

Silva, D. G. 1967. The ultrastructure of the myometrium of the rat with special reference to the innervation. Anat. Rec. 158:21-34.

Sims, S. M., Daniel, E. E. and Garfield, R. G. 1982. Improved electrical coupling in uterine smooth muscle is associated with increased gap junctions at parturition. J. Gen. Physiol. 80: 353-375.

Singh, I., Sankaranarayanan, A. and Bawa, S. R. 1985. Autonomic innervation of pregnant and nonpregnant rat uterus. IRCS Med. Sci. 13:324-325.

Sjoberg, N.-O. 1968. The adrenergic transmitter of the female reproductive tract: distribution and functional changes. Acta Physiol. Scand. Suppl. 305:1-32.

Soloff, M. S. 1985. Oxytocin receptors and mechanisms of oxytocin action. In: Oxytocin: Clinical and Laboratory Studies. Amico, J. A. and Robinson, A. G., editors. Elsevier, Amsterdam. 259-276.

Soloff, M. S., Alexandrova, M. and Fernstrom, M. J. 1979. Oxytocin receptors: triggers for parturition and lactation? Science 204:1313-1315.

Soloff, M. S. and Sweet, P. 1982. Oxytocin inhibition of $(Ca^{2+} + Mg^{2+})$-ATPase activity in rat myometrial plasma membranes. J. Biol. Chem. 257:10687-10693.

Specht, P. C. and Bortoff, A. 1972. Propagation and electrical entrainment of intestinal slow waves. Am. J. Digest. Dis. 17:311-316.

Sperelakis, N. 1969. Lack of coupling between contiguous myocardial cells in vertebrate hearts. Experientia, Suppl. 15:135-165.

Sperelakis, N. 1979. Propagation mechanisms in heart. Ann. Rev. Physiol. 41:441-457.

Sperelakis, N. and Mann, J. E. 1977. Evaluation of electric field changes in the cleft between excitable cells. J. Theoret. Biol. 64:71-96.

Sperelakis, N., Marschall, R. A. and Mann, J. E. 1983. Propagation down a chain of excitable cells by electric field interactions in the junctional cleft: effect of variation in extracellular resistances, including a "sucrose gap" simulation. IEEE Trans. Biomed. Eng. 30:658-664.

Sperelakis, N. and Picone, J. 1986. Cable analysis relevant to cell coupling in cardiac muscle and smooth muscle bundles. IEEE Trans. Biomed. Eng., in press.

Spray, D. C. and Bennett, M. V. L. 1985. Physiology and pharmacology of gap junctions. Ann. Rev. Physiol. 47:281-303.

Stjernquist, M., Emson, P., Owman, Ch., Sjoberg, N.-O., Sundler, F. and Tatemoto, K. 1983. Neuropeptide Y in the female reproductive tract of the rat. Distribution of nerve fibres and motor effects. Neurosci. Lett. 39: 279-284.

Stjernquist, M., Ekblad, E., Owman, Ch. and Sundler, F. 1986. Neuronal localization and motor effects of gastrin-releasing peptide (GRP) in rat uterus. Regul. Peptides 13:197-205.

Takeda, H. 1965. Generation and propagation of uterine activity in situ. Fert. Steril. 16:113-119.

Talo, A. and Csapo, A. I. 1970. Conduction of electric activity in late pregnant and parturient rabbit uteri. Physiol. Chem. Phys. 2:489-494.

Taverne, M. A. M., Naaktgeboren, C., Elsaesser, F., Forsling, M. L., van der Weyden, G. C., Ellendorff, F. and Smidt, D. 1979a. Myometrial electrical activity and plasma concentrations of progesterone, estrogens and oxytocin during late pregnancy and parturition in the miniature pig. Biol. Reprod. 21: 1125-1134.

Taverne, M. A. M., Naaktgeboren, C. and van der Weyden, G. C. 1979b. Myometrial activity and expulsion of fetuses. Anim. Reprod. Sci. 2:117-131.

Taylor, A. B., Kreulen, D. and Prosser, C. L. 1977. Electron microscopy of the connective tissues between longitudinal and circular muscle of small intestine of cat. Am. J. Anat. 150:427-442.

Thiersch, J. B., Landa, J. F. and West, T. C. 1959. Transmembrane potentials in the rat myometrium during pregnancy. Am. J. Physiol. 196:901-904.

Thorbert, G. 1979. Regional changes in structure and function of adrenergic nerves in guinea-pig uterus during pregnancy. Acta Obstet. Gynecol. Scand. Suppl. 79:5-32.

Thorburn, G. D. and Challis, J. R. G. 1979. Endocrine control of parturition. Physiol. Rev. 59:863-918.

Thorburn, G. D., Challis, J. R. G. and Robinson, J. S. 1977. Endocrine control of parturition. In Biology of the Uterus. Wynn, R. M., editor. Plenum Press, New York. 653-732.

Thorburn, G. D., Harding, R., Jenkin, G., Parkington, H. and Sigger, J. N. 1984. Control of uterine activity in the sheep. J. Develop. Physiol. 6:31-43.

Tomita, T. 1967. Spike propagation in the smooth muscle of the guinea-pig taenia coli. J. Physiol. (Lond.) 191:517-527.

Tomita, T. 1970. Electrical properties of mammalian smooth muscle. In Smooth Muscle. Bulbring, E., Brading, A. F., Jones, A. W. and Tomita, T., editors. Edward Arnold, London. 197-243.

Tomita, T. 1975. Electrophysiology of mammalian smooth muscle. Prog. Biophys. Molec. Biol. 30:185-203.

Tomita, T. 1981. Electrical activity (spikes and slow waves) in gastrointestinal smooth muscles. In Smooth Muscle: an Assessment of Current Knowledge. Bulbring, E., Brading, A. F., Jones, A. W. and Tomita, T., editors. Edward Arnold, London. 127-156.

Tomita, T. and Watanabe, H. 1973. Factors controlling myogenic activity in smooth muscle. Phil. Trans. R. Soc. Lond. B. 265:73-85.

Tomita, T., Takai, A. and Tokuno, H. 1985. Possibility of metabolic control of membrane excitation. Experientia 41:963-970.

Vane, J. R. and Williams, K. I. 1973. The contribution of prostaglandin production to contractions of the isolated uterus of the rat. Br. J. Pharmacol. 48:629-639.

Vasilenko, P., Adams, W. C. and Frieden, E. H. 1981. Uterine size and glycogen content in cycling and pregnant rats: influence of relaxin. Biol. Reprod. 25:162-169.

Vassort, G. 1981. Ionic currents in longitudinal muscle of the uterus. In Smooth Muscle: an Assessment of Current Knowledge. Bulbring, E., Brading, A. F., Jones, A. W. and Tomita, T., editors. Edward Arnold, London. 353-366.

Verhoeff, A., Garfield, R. E., Ramondt, J. and Wallenburg, H. C. S. 1985. Electrical and mechanical uterine activity and gap junctions in peripartal sheep. Am. J. Obstet. Gynecol. 153:447-454.

Villar, A., D'Ocon, M. P. and Anselmi, E. 1985. Calcium requirement of uterine contraction induced by $PGE_1$: importance of intracellular calcium stores. Prostaglandins 30:491-496.

Wallace, B. G. 1981. Distribution of AchE in cholinergic and noncholinergic neurons. Brain Res. 219:190-195.

Wathes, D. C. and Porter, D. G. 1982. Effects of uterine distension and oestrogen treatment on gap junction formation in the myometrium of the rat. J. Reprod. Fert. 65:497-505.

Weingart, R. 1977. The action of oubain on intercellular coupling and conduction velocity in mammalian ventricular muscle. J. Physiol. (Lond.) 264:341-365.

Weingart, R. 1986. Electrical properties of the nexal membrane studied in rat ventricular cell pairs. J. Physiol. (Lond.) 370:267-284.

Weiss, G. 1984. Relaxin. Ann. Rev. Physiol. 46:43-52.

Wiest, W. G. 1970. Progesterone and 20$\alpha$-hydroxy-pregn-4-en-3-one in plasma, ovaries and uteri during pregnancy in the rat. Endocrinology 87:43-48.

Williams, L. 1983. Effects of estradiol and progesterone on uterine prostaglandin levels in pregnant rat. Prostaglandins 26:47-54.

Williams, E. H. and DeHaan, R. L. 1981. Electrical coupling among heart cells in the absence of ultrastructurally defined gap junctions. J. Membrane Biol. 60:237-248.

Williams, K. I. and El-Tahir, K. E. H. 1982. Relaxin inhibits prostacyclin release by the pregnant rat myometrium. Prostaglandins 24:129-136.

Williams, K. I., El-Tahir, K. E. H. and Marcinkiewicz, E. 1979. Dual actions of prostacyclin ($PGI_2$) on the pregnant rat uterus. Prostaglandins 17:667-672.

Wojtczak, J. 1979. Contractures and increase in internal longitudinal resistance of cow ventricular muscle induced by hypoxia. Circ. Res. 44:88-95.

Wolfs, G. M. J. A. and van Leeuwen, M. 1979. Electromyographic observations on the human uterus during labour. Acta Obstet. Gynecol. Scand. Suppl. 90:1-61.

Ypey, D. L., Clapham, D. E. and DeHaan, R. L. 1979. Development of electrical coupling and action potential synchrony between paired aggregates of embryonic heart cell aggregates. J. Membrane Biol. 51:75-96.

Zelcer, E. and Daniel, E. E. 1979. Electrical coupling in rat myometrium during pregnancy. Can. J. Physiol. Pharmacol. 57:490-495.

Zervos, A. S., Hope, J. and Evans, W. H. 1985. Preparation of a gap junction fraction from uteri of pregnant rats: the 28-kD polypeptides of uterus, liver and heart gap junctions are homologous. J. Cell Biol. 101:1363-1370.